University of Alberta

Discovery and Characterization of the Mobilization of Linker and Core Histones During Herpes Simplex Virus Type 1 (HSV-1) Infection

by

Kristen Lea Conn

A thesis submitted to the Faculty of Graduate Studies and Research in partial fulfillment of the requirements for the degree of

Doctor of Philosophy

Department of Biochemistry

Fall 2010

Edmonton, Alberta

Examining Committee

Luis Schang, Biochemistry

Michael Schultz, Biochemistry

Michael Hendzel, Experimental Oncology

Michele Barry, Medical Microbiology and Immumology

Sandra Weller, Molecular, Microbial and Structural Biology, University of Connecticut

ABSTRACT

Herpes simplex virus type 1 (HSV-1) genomes associate with histones in unstable nucleosomes during lytic infections. Nucleosome core particles are 146 base pairs of DNA wrapped around a histone octamer of two molecules of each H2A, H2B, H3, and H4. Histone H1 binds to nucleosomes at DNA entry and exit points. Association with histones is proposed to regulate HSV-1 gene expression. Consistently, HSV-1 transcription transactivators disrupt chromatin and HSV-1 strains mutant in these transactivators are replication impaired or transcriptionally inactive.

HSV-1 genomes have dynamic associations with histones. The genomes are not associated with histones in capsids, and input genomes are delivered to nuclear domains depleted of histones. Later during infection, HSV-1 genomes again occupy nuclear domains depleted of histones. Histone synthesis is inhibited during infection and the total level of nuclear histones remains relatively constant. It is therefore unlikely that the histones that first bind to HSV-1 genomes are newly synthesized. The source of the histones that associate with HSV-1 genomes has yet to be addressed.

Histones in cellular chromatin normally disassociate, diffuse through the nucleus, and re-associate at different sites. I propose that histones are mobilized from domains of cellular chromatin to those domains containing HSV-1 genomes in cellular attempts to silence HSV-1 gene expression. I additionally propose that HSV-1 further mobilizes

histones to counteract such silencing attempts. My **hypothesis** is that histones are mobilized during HSV-1 infection.

In this thesis, I show that linker and core histones are mobilized during HSV-1 infection. Such mobilization results in increases to their "free" (not bound to chromatin) pools. Linker and core histones were mobilized even when HSV-1 proteins were not expressed, mobilization that likely reflects cellular responses to infection. Histone mobilization was enhanced when HSV-1 IE or E proteins were expressed. This enhanced mobilization was independent of HSV-1 DNA replication and late proteins. Core histones H2B and H3.3 were differentially mobilized, suggesting that different mechanisms may mobilize histones during HSV-1 infection.

My discovery of histone mobilization reveals a novel consequence of cell-virus interactions that addresses a previously unexplained aspect of HSV-1 infection.

TABLE OF CONTENTS

LIST OF TABLES

CHAPTER 1:

CHAPTER 2:

CHAPTER 3:

CHAPTER 4:

CHAPTER 5:

CHAPTER 6:

CHAPTER 7:

CHAPTER 8:

APENDIX 1:

LIST OF FIGURES

CHAPTER 3:

CHAPTER 4:

CHAPTER 5:

CHAPTER 6:

CHAPTER 8:

CHAPTER 9:

APPENDIX 1:

LIST OF APPENDICES

LIST OF ABBREVIATIONS

ATM	ataxia-telangiectasia mutated gene product
ATR	ATM and Rad3-related gene product
ATRX	α-thalassemia/mental retardation syndrome protein
ASF-1	antisilencing function 1
bp	base pair
CAF-1	chromatin assembly factor 1
CBP	CREB-binding protein
CENP	centromeric protein
CTCF	CCCTC binding protein
CTD	carboxyl terminal domain
Daxx	death domain associated protein 6
DNA-PK	DNA dependent protein kinase
DNA-PKcs	DNA dependent protein kinase catalytic subunit
DR	direct repeat
DSB	double strand break
E	early
EBV	Epstein-barr virus
FACT	facilitates chromatin transcription
FRAP	fluorescence recovery after photobleaching
g	glycoprotein; ex. glycoprotein B, gB
GABP	GA-binding protein
GFP	green fluorescent protein
H	histone, as in H3
HAT	histone acetyltransferase
HIRA	histone regulator A
HCF-1	host cell factor-1
HCMV	Human cytomegalovirus
HDAC	histone deacetylase
HDE	histone downstream element
HHV	human herpesvirus
HMBA	n,n`-hexamethylene-bisacetamide
HMG	high mobility group

HMT	histone methyltransferase
hpi	hour post infection
HR	homologous recombination
HSPG	heparan sulfate proteoglycan
HSV-1	Herpes simplex virus type 1
HVEM	herpesvirus entry mediator
IAA	iodoacetic acid
ICP	infected cell protein; ex. infected cell protein 4, ICP4
IE	immediate early
IFN	interferon
INHAT	inhibitor of actyltransferases
KAT	K (lysine) acetyltransferase
KSHV	Kaposi's sarcoma-associated herpesvirus
L	late
LAP2	lamina-associated polypeptide 2
MCM	minichromosome maintenance
MCN	micrococcal nuclease
mRNA	messenger RNA
MT	microtubule
MTOC	microtubule organizing centre
NAP-1	nucleosome assembly protein-1
NASP	nuclear autoantigenic sperm protein
NBS-1	nibrin or Nijmegen breakage syndrome gene product
ND	nuclear dispersed
ND10	nuclear domain 10
NHEJ	non-homologous end joining
NOR	nucleolar organizing region
NPC	nuclear pore complex
Nup	nucleoporin
OBP	origin binding protein
OCT-1	octamer-binding protein
PAA	phosphonoacetic acid
PCAF	p300/CBP associated factor

PCNA	proliferating cell nuclear antigen
PCV	packed cell volume
PIKK	phosphatidylinositol-3-kinase-like
PML	promyelocytic leukemia
PML-NB	PML nuclear body
PTM	post translational modification
RC	replication compartment
RCC1	regulator of chromosome condensation
RNAPII	RNA polymerase II
RPA	replication protein A
rRNA	ribosomal RNA
SET	Su(var)3-9, enhancer of zeste and trithorax
SG	sacral ganglion
SLBP	stem loop binding protein
snRNP	small nuclear ribonucleoprotein
Sp100	nuclear antigen Sp100
SUMO-1	small ubiquitin-like modifier 1
TAF	TBP associated factors
TAF-1	template activating factor 1
TBP	TATA-binding protein
TFIID	transcription factor II D
TG	trigeminal ganglion
TK	thymidine kinase
TNF	tumor necrosis factor
TSA	trichostatin A
TUTase	terminal uridylyl transferase
Ub	ubiquitin
UL	unique long
US	unique short
vhs	virion host shutoff
VICE	virus enduced chaperone enriced
VP	virion protein; ex. VP16, virion protein 16
VZV	Varicella zoster virus

CHAPTER 1: LITERATURE REVIEW, RATIONAL, AND HYPOTHESIS

1.1 HERPESVIRALES.

Viruses are classified as members of the order *Herpesvirales* based on virion morphology, biological properties, and genomics. Characteristically, virions within the order *Herpesvirales* have double stranded DNA genomes contained within an icosahedral capsid. The capsid is surrounded by proteinaceous layer called the tegument, which is in turn enveloped by a lipid bilayer that contains viral glycoproteins (Knipe & Howley, 2007b). In addition to structural similarities, members of *Herpesvirales* share similar biological properties (Knipe & Howley, 2007b). These viruses mostly replicate in the nucleus with only limited functions occurring in the cytoplasm. Viral gene expression, DNA synthesis, capsid assembly, and genome encapsidation all occur in the nuclei. Viral replication is lytic and results in the destruction of the host cell. Herpesviruses also establish latent infections within their natural host. Latent infections are distinguished from chronic and abortive infections in that infectious progeny are not present but the capacity to express viral proteins and replicate viral DNA (reactivate) is maintained. Although similar in several biological properties, herpesviruses differ in the range of host-cells they infect, the length of their reproductive cycle, and the preferred sites of latent infection.

The order *Herpesvirales* is divided into three families (ICTV, 2009). *Alloherpesviridae* includes those viruses that infect fish and frogs,

Malacoherpesviridae includes that which infects bivalves, and *Herpesviridae* those that infect mammals, birds, and reptiles (Davison et al., 2009).

1.1.1 Herpesviridae.

Members of *Herpesviridae* infect mammals, birds, and reptiles. To date, 135 viruses are included in this family. Eight members, herpes simplex virus types 1 and 2 (HSV-1, HSV-2), varicella –zoster virus (VZV), human cytomegalovirus (HCMV), Epstein-Barr virus (EBV), Kaposi's sarcoma-associated virus (KSHV) and Human herpes viruses 6 and 7 (HHV6, HHV7), infect humans (Davison et al., 2009). The family *Herpesviridae* is further divided into three subfamilies, *Alphaherpesvirinae*, *Betaherpesvirinae*, and *Gammaherpesvirinae*, based on biological properties and genomics.

Alphaherpesvirinae characteristically have a faster, or shorter, reproductive cycle than the members of the other subfamilies of *Herpesviridae*. Latent infection of *Alphaherpesvirinae* is typically established in neurons of the sensory ganglia. The host-range for *Alphaherpesvirinae* is broad and not restricted to the family that the natural host belongs. *Alphaherpesvirinae* is divided into 4 genera, 2 of which include species of *Human herpesviruses* (ICTV, 2009). *Varicellovirus* includes Varicella-zoster virus (VZV; also known as *Human herpesvirus 3*, HHV3) (ICTV, 2009). *Simplexvirus* includes herpes simplex virus type 1 (HSV-1; also known as *Human herpesvirus 1*, HHV1) and herpes simplex virus type 2 (HSV-2; also known as *Human herpesvirus 2*, HHV2) (ICTV, 2009).

Betaherpesvirinae have slower replication cycles than other herpesviruses and typically establish latent infection in leukocytes. Infection with *Betaherpesvirinae* is often accompanied by cytomegalia. *Betaherpesvirinae* is divided into 4 genera, 2 of which include species of *Human herpesviruses* (ICTV, 2009). The genus *Cytomegalovirus* includes human cytomegalovirus (HCMV; also known as *Human herpesvirus 5* HHV5), and the genus *Roseolovirus* includes *Human herpesvirus 6* (HHV6) and *Human herpesvirus 7* (HHV7) (ICTV, 2009).

Gammaherpesvirinae typically infect B or T lymphocytes and establish latency in lymphoid tissue. Infection with *Gammaherpesvirinae* can be associated with tumor formation. The sub-family *Gammaherpesvirinae* is divided into 4 genera, 2 of which include species that infect humans (ICTV, 2009). Epstein-Barr virus (EBV; also known as *Human herpesvirus 4*, HHV4) in the genus *Lymphocryptovirus*, and Kaposi's sarcoma-associated herpesvirus (KHSV; also known as *Human herpesvirus 8*, HHV8) in the genus *Rhadinovirus* (ICTV, 2009).

1.2 HERPES SIMPLEX VIRUS TYPE-1, GENERAL VIRION STRUCTURE.

As all members of *Herpesvirales*, the HSV-1 virion includes a linear double stranded DNA (dsDNA) genome packaged within an icosahedral capsid. A layer of proteinaceous tegument surrounds the capsid, and the virion is enclosed by a lipid bilayer containing viral glycoproteins. Each component of the HSV-1 virion is discussed in more detail in the following sections.

1.2.1 The Genome.

The HSV-1 genome is linear dsDNA of approximately 150 kilobase pairs (kbp), depending on the strain, with approximately 68% guanosine (G) plus cytosine (C) (Kieff, Bachenheimer, & Roizman, 1971). The HSV-1 genome consists of a unique long sequence, designated U_L, and a unique short sequence, designated U_S, which are both flanked by inverted repeats, known as a sequences (Wadsworth, Jacob, & Roizman, 1975). The repeat sequences that flank the U_L sequence are designated ab and a`b` (Wadsworth et al., 1975). The number of a sequence repeats peripheral to U_L is variable. The repeats that border the U_S sequence are designated a`c` and ca (Wadsworth et al., 1975). The a sequence structure is highly conserved, but variable in size depending on the number of repeat elements. The a sequence of HSV-1 strain F is represented as:

DR1-U_b-DR2$_n$-DR4$_m$-U_c-DR1

Direct repeat 1(DR1) designates a 20bp direct repeat, U_b a unique 65bp sequence, DR2 a 12bp direct repeat present in 19 to 23 copies per a sequence. DR4 is a 37bp direct repeat present in 2 to 3 copies per a sequence, and U_c is a 58bp unique sequence (Mocarski & Roizman, 1981; Knipe & Howley, 2007a). The DR1 sequence is shared between adjacent a sequences (Mocarski & Roizman, 1981). Thus, the HSV-1 genome is represented as:

$a_L a_n b$-U_L-b`-a`$_m$c`-U_S-ca_S

a_L designates the terminal a sequence of the U_L component. In linear HSV-1 DNA, a_L consists of a truncated (18bp) DR1 with a one nucleotide 3` extension. $a_S$ designates the terminal a sequence of the $U_S$ component. In linear HSV-1 DNA, $a_S$ consists of 1bp of DR1 with one 3` overhanging nucleotide. The a sequences are unique (a_n) or repeated several times (a_m). Circularization of the HSV-1 genome joins a_L and a_S to form a complete DR1 sequence.

The a sequence repeats permit inversion of the HSV-1 genome U_L and U_S components relative to each other. Inversion produces 4 linear isomers, designated as P (prototype), I_L (inversion of U_L), I_S (inversion of U_S), and I_{SL} (inversion of U_S and U_L). In wild-type HSV-1 infections, the four isomers are produced in equimolar amounts.

The HSV-1 genome is arranged in concentric layers that fill the internal capsid space to the inner floor of the capsid wall (Zhou, Chen, Jakana, Rixon, & Chiu, 1999). This arrangement is consistent with a spool model of genome organization within the capsid.

Capsids do not contain histones, or other basic proteins, that would otherwise neutralize the negative charges of DNA to allow folding and packaging of HSV-1 genomes (Oh & Fraser, 2008). Capsids do, however, contain positively charged polyamines, spermine and spermidine (Gibson & Roizman, 1971), which can offset some of the charges of HSV-1 DNA. It is unlikely that spermidine is within the capsid. Spermidine is extracted when virions are disrupted with ionic detergents and urea (Gibson & Roizman, 1971). Spermine, on the other hand, is tightly associated with the capsid and not extracted by such

treatment. However, the virion associated spermine can not completely neutralize the negative charge of HSV-1 DNA. The ratio of spermine nitrogen to DNA phosphate is only approximately 0.6 (Gibson & Roizman, 1971).

1.2.2 The Capsid.

HSV-1 capsids are approximately 125nm in diameter. The main capsid protein, VP5 (U_L19), is organized into capsomers that have a central channel extending from outside of the capsid to the capsid internal cavity. The capsid itself is made up of 150 capsomers with hexavalent structure (hexons) and 12 with pentavalent structure (pentons) arranged on a T=16 icosahedral lattice (Newcomb et al., 1993). The icosahedron vertices are occupied by pentons, whereas the edges and faces are occupied by hexons. Triplexes, heterotrimers of VP19C (U_L38; ICP32) with two molecules of VP23 (U_L18), connect capsomers in groups of three (Newcomb et al., 1993). A dodecameric ring of U_L6 occupies one vertex of the capsid (Newcomb et al., 1993; Trus et al., 2004). This structure resembles a portal protein and is though to represent the portal for HSV-1 genome packaging within the capsid (Newcomb et al., 1993). Consistent with such a model, U_L6 is not required for capsid formation, but is essential for HSV-1 genome encapsidation (Patel, Rixon, Cunningham, & Davison, 1996).

VP5 constitutes both the hexons and pentons. Within virions, however, hexons and pentons have different protein contacts. VP26 (U_L35) is located at each hexon tip (Booy et al., 1994). Pentons, on the other hand, physically interact with tegument proteins (Zhou et al.,

1999). Tegument is not excluded from binding hexons by the presence of VP26, and even in extreme molar excess VP26 will not bind to pentons (Wingfield et al., 1997; Chen et al., 2001). Thus, the protein associations of hexons and pentons are specific and indicate that VP5 may have different conformations within each structure. Within virions, the penton channel is obstructed (Zhou et al., 1999). It is proposed that VP5 itself undergoes a conformational change to fill the channel (Zhou et al., 1999).

Three types of capsids, A, B, and C, are produced during infections. A type capsids do not contain HSV-1 genomes and lack internal scaffold proteins. B type capsids have internal scaffold proteins but do not contain HSV-1 genomes. C type capsids encapsidate HSV-1 genomes.

1.2.3. The Tegument.

The tegument is an amorphous protein layer, comprised of approximately 23 proteins, situated between the envelope and the capsid (Loret, Guay, & Lippe, 2008). Tegument proteins function in many aspects of HSV-1 infection. The specific roles of certain tegument proteins will be discussed in subsequent sections, VP1/2 [1.3.4], VP16 [1.4.2.1], ICP4 [1.4.2.1.2], ICP0 [1.4.2.1.1], VP22 [1.3.2.2], and virion host shutoff (vhs) [1.3.2.3].

Although inner tegument proteins make contacts with the capsid pentons, the bulk of the tegument layer does not maintain the icosahedral symmetry of the capsid (Zhou et al., 1999). There is some order to the tegument associations, however, as tegument can assemble

in the absence of capsids. Furthermore, tegument protein associations are initially maintained following capsid release into the host cell (Szilagyi & Cunningham, 1991; Zhang & McKnight, 1993; Maurer, Sodeik, & Grunewald, 2008). The exterior tegument proteins associate with the cytoplasmic tails of HSV-1 membrane proteins (Mettenleiter, 2006).

1.2.4 The Envelope.

The HSV-1 tegument is surrounded by a lipid bilayer embedded with non-glycosylated and glycosylated proteins. The lipids constituting the envelope are host derived. The specific host-cell membrane from which the HSV-1 envelope is derived is still debated, but generally accepted to be the Golgi membrane.

The HSV-1 envelope contains twelve glycoproteins. Four glycoproteins, gD, gB, gH, and gL, are essential for entry into host cells (Reske, Pollara, Krummenacher, Chain, & Katz, 2007; Heldwein & Krummenacher, 2008). Other non-essential glycoproteins mediate cell attachment (gC), confer protection from the immune system (virulence) (gC), or mediate cell-to-cell spread (gE, gK) (Knipe & Howley, 2007b).

1.3 HSV-1 ENTRY OF HOST CELLS.

1.3.1 Binding and fusion.

Typically, HSV-1 virions enter cells by fusion with the host cell plasma membrane. However, pH-dependent and –independent fusion following endocytosis has been reported in some cell types. Nonetheless, entry in

neurons or other cells used for the majority of experiments within this thesis (Vero) occurs via fusion with the host cell plasma membrane. Therefore, this mechanism of entry will be discussed. Membrane fusion occurs in three phases. In the first phase, the membrane bilayers are brought into close proximity. In the second phase, the outer membrane leaflets join to form a hemifusion intermediate. The third phase involves the stabilization and expansion of a fusion pore.

HSV-1 virions initially attach to host cells via interactions of HSV-1 glycoproteins with cell surface proteoglycans. gC or gB mediate attachment by binding to heparan sulfate proteoglycans (HSPGs). In the absence of gC, however, gB is sufficient to mediate attachment to HSPGs. gB is required for HSV-1 entry into host cells, although this requirement is at the stage of virion fusion rather than HSPG attachment. Virion attachment to the host cell is associated with an indentation in the cellular membrane (Maurer et al., 2008). Following cell attachment, gD binding to one of several entry receptors is required for cell entry. The HSV-1 entry receptors include the Herpesvirus entry mediator (HVEM; HveA), a member of the tumor necrosis factor (TNF) family of receptors, nectin-1 (HveC) a member of the immunoglobulin superfamily, and 3-O-sulphated moieties on heparan sulphate (3-O-HS) (Reske et al., 2007; Heldwein & Krummenacher, 2008). Binding of gD to an entry receptor is proposed to induce a conformational change that triggers activation of the core fusion machinery gB and the gH/L heterodimer (Reske et al., 2007; Heldwein & Krummenacher, 2008). gD binding to an entry receptor and the gH/L complex are sufficient to form a hemifusion

intermediate. However, gB is required for full fusion (Subramanian & Geraghty, 2007). During virion fusion with the host cell, large multisubunit complexes of HSV-1 glycoproteins and cell receptors are not formed (Maurer et al., 2008). Therefore, a small number of receptors and glycoprotein complexes are sufficient for fusion to occur.

The HSV-1 virion has polarity. The capsid is in close proximity to one pole of the virion and is surrounded by a tegument "hat" (Maurer et al., 2008). The virion pole in close proximity to the capsid has propensity for fusion (Maurer et al., 2008). Following fusion and release of the capsid, HSV-1 glycoproteins and tegument proteins remain associated at the membrane (Maurer et al., 2008). With time, the HSV-1 glycoproteins and tegument proteins diffuse from the site of fusion (Maurer et al., 2008).

1.3.2 Release of capsid and tegument into the host cell.

Visualization of HSV-1 entry by cryoelectron tomography demonstrated that the majority of tegument proteins remained associated with the viral membrane at the site of fusion (Maurer et al., 2008). No obvious tegument densities were observed associated with cytoplasmic capsids (Maurer et al., 2008). However, biochemical and indirect-immunofluorescence analysis have demonstrated that some inner tegument proteins remain closely associated with the capsids following entry [discussed in sections 1.3.3 and 1.3.4]. The tegument proteins prepare the cellular environment for, and promote, productive HSV-1 infection. Tegument proteins are involved in HSV-1 capsid transport and genome delivery to the nucleus [discussed in section 1.3.3], activating

HSV-1 transcription (such as VP16 [1.4.2.1], ICP0 [1.4.2.1.1], and ICP4 [1.4.2.1.2]), and in minimizing initial cellular antiviral responses (such as VP22 [1.3.2.2] and virion host shutoff (vhs) [1.3.2.3]).

1.3.2.1 VP22 (U_L49).

VP22 is a tegument protein released into the cytoplasm following virion entry of the host cell. VP22 binds to the cellular protein TAF-1 (template activating factor I), which is related to the histone chaperone nucleosome assembly protein-1 (NAP-1) (van Leeuwen et al., 2003). TAF-1 promotes the ordered addition of nucleosomes to naked DNA (Okuwaki & Nagata, 1998). TAF-1 is also a component of the INHAT (inhibitor of acetyltransferases) complex (Seo et al., 2001). INHAT binds to histones and prevents their acetylation by the histone acetyltransferases p300 and p300/CBP associated factors (PCAF) (Seo et al., 2001). VP22 binding to TAF-1 inhibits TAF-1 mediated histone deposition, but does not inhibit INHAT activity (van Leeuwen et al., 2003). Therefore, VP22 inhibition of TAF-1 mediated histone deposition may be important for prevention of histone deposition onto naked HSV-1 genomes.

1.3.2.2 Inhibition of cellular protein synthesis by virion host shutoff (vhs, U_L41).

The tegument protein virion host shutoff (vhs) comprises approximately 1-4% of mature virions (Loret et al., 2008). Release of vhs into the cell is associated with an increase in messenger RNA (mRNA) turnover and mRNA degradation (Schek & Bachenheimer, 1985; Strom & Frenkel, 1987; Sorenson, Hart, & Ross, 1991). HSV-1 infection promotes the

rapid degradation of pre-existing cytoplasmic mRNAs (Schek & Bachenheimer, 1985; Strom & Frenkel, 1987; Yager & Bachenheimer, 1988; Sorenson et al., 1991). Degradation of cellular transcripts early during infection may prevent expression of cellular proteins that would otherwise inhibit HSV-1 replication. Such degradation of cellular mRNA does not require de novo protein synthesis and is ascribed to the exonuclease activity of vhs. In addition to mediating the degradation of cellular mRNA transcripts, vhs also mediates the degradation of viral mRNA transcripts (Strom & Frenkel, 1987). This function of vhs is proposed to promote the transition between translation of viral genes that are sequentially expressed. Later during infection, the endoribonuclease activity of vhs is inhibited by its association with VP16 (Lam et al., 1996).

1.3.2.2.1 Inhibition of histone synthesis during HSV-1 infection.

During infection with HSV-1, pre-existing histone mRNAs are rapidly degraded (Schek & Bachenheimer, 1985; Yager & Bachenheimer, 1988; Sorenson et al., 1991). Some groups report this degradation to be due to vhs mediated mRNA degradation. Others suggest it to be due to the normal rapid half-life of histone mRNA transcripts (Schek & Bachenheimer, 1985; Yager & Bachenheimer, 1988; Sorenson et al., 1991). Although pre-existing cytoplasmic mRNAs rapidly vanish, the relative rate of transcription of histone H3 and H4 genes is increased (Yager & Bachenheimer, 1988; Latchman, Partidge, Estridge, & Kemp, 1989). However, the H3 and H4 mRNAs are retained and degraded in the nucleus (Yager & Bachenheimer, 1988). Unlike H3 and H4, transcription

of H2B is repressed during HSV-1 infection (Latchman et al., 1989). The H2B promoter contains an octamer binding sequence important for its cell-cycle regulated expression (Latchman et al., 1989). During HSV-1 infection, VP16 promotes recruitment of octamer binding protein (Oct-1) to viral TAATGARAT sequences and as a result H2B gene expression is repressed (Latchman et al., 1989). Regardless of the activation or repression of histone mRNA synthesis, the cytoplasmic levels of histone mRNAs are reduced during infection (Schek & Bachenheimer, 1985; Yager & Bachenheimer, 1988). Therefore, the rate of histone synthesis declines rapidly after infection. Yager et al. report that synthesis of all histones (H1, H2A, H2B, H3, and H4) is reduced to less than 10% of that in mock infected cells already by 3 hours after infection with HSV-1 (Yager & Bachenheimer, 1988). In spite of the inhibition of histone synthesis during HSV-1 infection, the total level of nuclear histones does not change (Kent et al., 2004; Huang et al., 2006).

1.3.3 Transport of HSV-1 capsids to the nuclear pore complex (NPC).

The capsids are transported to the nucleus along microtubules (Sodeik, Ebersold, & Helenius, 1997; Dohner et al., 2002). This transport is mediated by dynein, which attaches to the vertices of the capsids (Sodeik et al., 1997; Dohner et al., 2002). The tegument protein VP1/2 (U_L36) is suggested to bind to capsid vertices. VP1/2 is therefore thought to be the viral protein involved in dynein mediated capsid transport (Sodeik et al., 1997; Zhou et al., 1999). The HSV-1 proteins required for capsid transport, however, still remain to be identified.

The capsids are transported along microtubules to the microtubule organizing centre (MTOC) adjacent to the nucleus. The mechanisms of capsid migration from the MTOC to the nuclear pore complex (NPC) are as yet unknown. However, VP1/2 is implicated in such migration, as well as in docking at the NPC (Copeland, Newcomb, & Brown, 2009). The capsids dock approximately 50nm from the NPC, via attachment to the nucleoporin (nup) 214/nup358 complex or nucleoporin hCG1 (Copeland et al., 2009; Pasdeloup, Blondel, Isidro, & Rixon, 2009). Capsid protein U_L25, binds to the NPC, the portal protein (U_L6), and VP1/2 (Pasdeloup et al., 2009). UL25 is therefore proposed to mediate NPC attachment and trigger genome release (Pasdeloup et al., 2009).

1.3.4 Nuclear entry of the genome.

The HSV-1 genome is extruded from a single vertex (Newcomb, Booy, & Brown, 2007). Genome extrusion requires U_L25 and VP1/2. Capsids from mutant strains with temperature sensitive lesions in U_L25 or VP1/2 dock at NPC at non-permissive temperatures but fail to release their genomes (Batterson, Furlong, & Roizman, 1983; Preston, Murray, Preston, McDougall, & Stow, 2008). Extrusion of HSV-1 genomes requires proteolytic cleavage of VP1/2 (Jovasevic, Liang, & Roizman, 2008). In vitro analysis show HSV-1 genomes to extrude from the capsid as a single double helix strand of DNA or as a condensed rod-like structure (Shahin et al., 2006; Newcomb et al., 2007). Capsids are not disassembled during genome extrusion (Batterson et al., 1983; Sodeik et al., 1997; Preston et al., 2008). Empty capsids even remain associated

on the cytoplasmic face of the NPC following genome release (Batterson et al., 1983; Sodeik et al., 1997; Preston et al., 2008).

HSV-1 genomes are rapidly circularized in the nucleus (Strang & Stow, 2005). Circularization does not require protein synthesis or DNA replication, but it does require the cellular protein regulator of chromosome condensation 1(RCC1) (Umene & Nishimoto, 1996; Strang & Stow, 2005). Circularization of input HSV-1 genomes is proposed to occur through homologous recombination of the terminal a sequence repeats, or by direct ligation of the genomic termini (Yao, Matecic, & Elias, 1997; Strang & Stow, 2005). The circularization of HSV-1 genomes is important for viral replication. Under conditions in which genomes are not circularized, for example during infections of cells that express mutant RCC1, HSV-1 DNA is not replicated, and consequently progeny virions are not produced (Umene & Nishimoto, 1996).

Input HSV-1 genomes migrate to nuclear domains adjacent to nuclear ND10 (nuclear dot 10, also called promyelocytic leukemia (PML) nuclear domains (PML-ND)s). Alternatively, it has been reported that ND10 proteins are recruited to domains adjacent to HSV-1 genomes where they form novel ND10-like structures (Everett et. al., 2004). Localization of HSV-1 genomes adjacent to ND10 structures requires an HSV-1 ori_S sequence, ICP4, and ICP27, and is facilitated by the cellular ND10 protein hDaxx (death domain associated protein 6) (Tang et al., 2003). RNA or protein synthesis are not required, which suggests that the HSV-1 proteins required, ICP4 and ICP27, are components of

infecting virions (Ishov & Maul, 1996). However, only ICP4, but not ICP27, has been shown to be a component of virions (Loret et al., 2008).

Not all input genomes are functionally equivalent and not all associate with ND10. The genomes that do localize adjacent to ND10, however, have a higher propensity to replicate (Sourvinos & Everett, 2002). The localization of HSV-1 genomes to nuclear domains adjacent to ND10 is increased by viral transcription (Sourvinos & Everett, 2002). Thus, HSV-1 genomes that are transcriptionally active are more likely to localize adjacent to ND10 and are therefore more likely to replicate.

1.4 HSV-1 REPLICATION.

HSV-1 establishes lytic and latent infections. Lytic infections are characterized by transcriptionally active HSV-1 genomes, expression of all HSV-1 proteins, viral DNA replication, and formation of progeny virions. Lytic infections typically occur in the vermillion border, oral mucosa, or facial skin. Latent infections are characterized by repression of HSV-1 transcription. Only one family of HSV-1 transcripts, the latency associated transcripts (LATs), is detected at high levels in some latently infected neurons. During latency, HSV-1 genomes are not replicated. Latent infections are typically established in sensory neurons of the trigeminal ganglia (TG) or sacral ganglia (SG). Latent HSV-1 genomes are maintained as nuclear episomes. The ability to reactivate and express viral proteins and replicate HSV-1 DNA is maintained.

1.4.1 Latent HSV-1 infection.

Latency is described in three phases, establishment, maintenance, and reactivation. The viral and cellular factors required for each phase, or for switching between them, are still not fully known. It is proposed, however, that the repression of HSV-1 gene expression during latency is associated with epigenetic modifications to chromatin proteins bound to HSV-1 genomes. Reactivation and expression of lytic HSV-1 genes is concomitantly proposed to involve remodeling of the repressive chromatin structure associated with latent genomes.

1.4.1.1 Establishment of latency.

Progeny virions released by primary lytic infection infect the sensory nerves that innervate the sites of primary infection. HSV-1 virions fuse with the axon terminus. The HSV-1 capsid and associated tegument proteins are then carried by retrograde axonal transport to the nucleus in the cell body (Knipe & Howley, 2007a). Following primary infections of neurons, low levels of HSV-1 lytic genes are expressed and HSV-1 genomes are replicated (Valyi-Nagy et al., 1991). Although latently infected neurons typically harbor from one to many HSV-1 genomes, HSV-1 DNA replication is not required to establish latency (Valyi-Nagy et al., 1991). During the establishment of latency, histones become associated with HSV-1 genomes in a regular chromatin structure (Deshmane & Fraser, 1989). Histone variants such as macroH2A and chromatin proteins such as HP1, which typically associate with transcriptionally silenced heterochromatin, bind to latent HSV-1

genomes. The histones associated with lytic promoters are enriched in histone post translational modifications associated with heterochromatin, such as trimethylation of lysine 27 of histone H3 (H3K27me3) and di- and tri-methylation of lysine 9 of histone H3 (H3K9me2 and H3K9me3, respectively) (Wang et al., 2005; Cliffe, Garber, & Knipe, 2009; Bloom, Giordani, & Kwiatkowski, 2010). Moreover, the histones associated with lytic promoters are depleted in histone modifications associated with transcriptionally active euchromatin, such as dimethylation of lysine 4 of histone H3 (H3K4me2) (Wang et al., 2005; Cliffe et al., 2009; Bloom et al., 2010). The molecular switch that results in heterochromatinization of lytic genes and associated suppression of lytic gene expression is unknown.

The reduced expression of lytic genes may also result from a lack of cellular proteins required for expression. The HSV-1 IE gene co-activator host cell factor (HCF-1) is mostly cytoplasmic in neurons, rather than nuclear as in most other cells (Kolb & Kristie, 2008). Repression of HSV-1 lytic gene expression may also be mediated by LAT expression. LAT expression promotes enrichment of heterochromatin modifications on the histones associated with lytic genes (Wang et al., 2005; Cliffe et al., 2009). However, LAT has also been demonstrated to maintain HSV-1 genomes in a more transcriptionally active state, by limiting the deposition of heterochromatin histone modifications (Bloom et al., 2010). This later activity of LAT may be more relevant for HSV-1 reactivation than for establishment or maintenance of latency. The differences in LAT

mediated epigenetic regulation of HSV-1 genomes could reflect strain specific differences, or differences in the host model used.

1.4.1.2 Maintenance of latency.

During latency, the HSV-1 genome is regularly chromatinized and maintained in the nucleus as a dormant episome. The only HSV-1 transcripts expressed to appreciable levels are LATs. However, not all latently infected neurons express LAT. It is proposed that the repression of transcription of HSV-1 lytic genes is achieved through epigenetic modifications to the bound histones and association of silencing chromatin proteins. Consistent with such a model, latent HSV-1 genomes are enriched in histone tail modifications and histones that are typically associated with heterochromatin, including trimethylation of H3K9 and H3K27, dimethylation of H3K9, and macro H2A (Wang et al., 2005; Cliffe et al., 2009; Bloom et al., 2010). DNA methylation does not significantly contribute to repression during latency (Kubat, Tran, McAnany, & Bloom, 2004).

The HSV-1 genome contains 7 clusters of CCCTC binding protein (CTCF) binding motifs. Such motifs are insulator elements, they block transcription enhancers and act as boundary elements between hetero- and euchromatin regions. During latency, the CCCTC motifs are occupied by CTCF binding protein (Amelio, McAnany, & Bloom, 2006). Occupancy of CTCF contributes to lytic gene repression through the silencing of lytic gene enhancers (Amelio et al., 2006).

Latency can obviously only be maintained in live neurons. LAT may also contribute to neuron survival through inhibition of apoptosis.

Expression of LAT is sufficient to inhibit apoptosis induced by caspases 8 and 9, and also inhibits caspase 3 activation (Perng & Jones, 2010).

1.4.1.3 Reactivation from latency.

Stress, immunosuppression, menstruation, and exposure to UV-light are among the factors that promote reactivation from latency. However, the molecular mechanisms of reactivation from latency are unknown. Reactivation of lytic gene expression in neurons is induced by trichostatin A (TSA) (Arthur et al., 2001). TSA inhibits histone deacetylase (HDAC) activity and therefore promotes hyperacetylation of histones. Remodeling of the repressive chromatin associated with lytic loci is likely associated with reactivation from latency. Stress also stimulates the nuclear accumulation of HCF-1 (Kolb & Kristie, 2008; Whitlow & Kristie, 2009). Reactivation of HSV-1 lytic gene expression is likely facilitated by changes in the physical chromatin structure of lytic genes that increase DNA accessibility and thus allow recruitment of transcription proteins, such as HCF-1 and RNA polymerase II (RNAPII).

Following reactivation, HSV-1 proteins are expressed and DNA is replicated in the nucleus of the neuron. Progeny virions are assembled and carried by anterograde axonal transport to the axon termini. Released virions infect neighbouring cells and initiate lytic replication.

1.4.2 Lytic infection.

Lytic infection involves expression of all HSV-1 proteins, HSV-1 DNA replication, and the production of progeny virions. HSV-1 gene expression during lytic infection is temporally regulated. HSV-1 proteins

are classified as immediate early (IE), early (E), or late (L), based on requirements that limit their temporal expression. IE gene expression does not require de novo protein synthesis. The proteins required for IE gene transcription are pre-existing cellular proteins or components of infecting virions. The five IE genes encode proteins that regulate HSV-1 protein expression at the transcriptional and post-transcriptional levels, or modulate cellular antiviral responses. IE protein expression is required to activate E gene expression. E genes encode proteins that are required for HSV-1 DNA replication, among other functions. Expression of E proteins therefore results in HSV-1 DNA replication. L gene expression occurs after HSV-1 DNA replication begins. L genes tend to encode for proteins required for virion assembly, such as capsid, tegument, and membrane glycoproteins. Following L protein expression, progeny virions are assembled.

1.4.2.1 IE protein expression.

Genes are classified as IE if they do not require de novo protein synthesis for their transcription. A tegument protein, VP16 (U_L48, α-TIF), transactivates IE gene expression. VP16 comprises approximately 1 to 5% of the mature virions (Loret et al., 2008). It activates IE genes transcription in complex with two cellular co-activators, Oct-1 and HCF-1.

After virion-to-cell fusion, VP16 is released from the tegument into the cytoplasm. HCF-1 binds to VP16 in the cytoplasm and they shuttle to the nucleus. However, HCF-1 is not required for the nuclear

localization of VP16 (Narayanan, Nogueira, Ruyechan, & Kristie, 2005). IE promoters contain TAATGARAT sequence elements recognized by the cellular transcription factor Oct-1, as well as additional elements recognized by the cellular factors GA-binding protein (GABP) and Sp1. The VP16/HCF-1 complex cooperatively binds to Oct-1 at IE TAATGARAT elements, promoting the formation of the RNAPII pre-initiation complex. The transactivation activity of VP16 is not essential for activation of IE gene expression. In absence of VP16 transactivation, basal expression of IE genes is mediated by GABP and Sp1. However IE gene expression under these conditions is delayed in some cell types. HCF-1, on the other hand, is essential for IE gene expression. An 80% reduction in cellular HCF-1 levels resulted in more than a 90% reduction in the levels of ICP4 and ICP0 transcript accumulation (Narayanan et al., 2005). IE gene expression mediated by VP16/OCT-1, GABP, and SP1 was prevented in HCF-1 depleted cells (Narayanan et al., 2005). HCF-1 depletion did not inhibit transcription globally, the defect was specific for transcription mediated by IE promoters (Narayanan et al., 2005). Mutation of HCF-1 such that binding to VP16 is abrogated, or reduced, also decreases transcription of HSV-1 IE genes (Goto et al., 1997; Luciano & Wilson, 2002). HCF-1 is therefore specifically required for basal IE promoter transactivation, as well as for VP16 mediated transactivation.

HCF-1 binds to both the Sin3 HDAC complex and the Set1/Ash2 histone methyltransferase (HMT) complex (Wysocka, Myers, Laherty, Eisenman, & Herr, 2003). VP16 preferentially associates with HCF-1

bound to Set1 (Wysocka et al., 2003). Set1 mediated trimethylation of H3K4 is associated with active transcription and is important for HSV-1 IE gene transcription. Reductions in H3K4me3, either by methylation inhibitors or Set1 knockdowns, resulted in lower levels of HSV-1 transcription (Huang et al., 2006). Taken together, these results indicate that VP16 mediated recruitment of HCF-1 and its associated Set1 HMT to IE gene promoters is an important step in HSV-1 IE gene transactivation.

In addition to recruitment of the transcription machinery to IE promoters, VP16 has chromatin disrupting functions that may be important for activation of IE gene expression. The VP16 acidic activation domain targeted to heterochromatin induces unfolding of compact heterochromatin fibres and even propagates large-scale chromatin unfolding over hundreds of kbs (Tumbar, Sudlow, & Belmont, 1999). The chromatin decondensation induced by the VP16 acidic activation domain is independent of transcription (Tumbar et al., 1999). In the context of HSV-1 infection, VP16 recruits histone acetyltransferases (HATs) (GCN5, p300, and CBP) and ATP-dependent chromatin remodeling proteins (BRG and hBRM) to IE promoters (Herrera & Triezenberg, 2004). However, the activity of such proteins is not required for HSV-1 gene expression (Kutluay, DeVos, Klomp, & Triezenberg, 2009). Decreased expression of the p300, CBP, GCN5, or PCAF HATs or the BRM and Brg-1 chromatin remodeling complexes did not decrease HSV-1 IE expression (Kutluay et al., 2009). In fact, IE gene

transcription tended to be slightly increased in their absence (Kutluay et al., 2009).

Unlike histone acetylation, trimethylation of H3K4 is important for HSV-1 gene expression. Decreases in H3K4me3 modified histones associated with HSV-1 genes are associated with decreases in expression of these genes (Huang et al., 2006). VP16 preferentially associates with HCF that is complexed with Set1/Ash2 histone HMT (Wysocka et al., 2003). This association targets the HMT to HSV-1 IE promoters and promotes trimethylation of associated H3 K4 residues. Levels of H3K4me3 on HSV-1 genomes decrease in the absence of Set1, concomitant with a decrease in HSV-1 transcription (Huang et al., 2006).

VP16 is implicated in decreasing H3 occupancy at IE gene promoters and in maintaining IE genes relatively free of histones, probably by promoting IE gene transcription (Kutluay & Triezenberg, 2009).

HSV-1 encodes five IE proteins: ICP0, ICP4, ICP22, ICP27, and ICP47, four of which regulate HSV-1 gene expression at the transcriptional or posttranscriptional level. These proteins are discussed below.

1.4.2.1.1 ICP0.

ICP0 is not essential for HSV-1 replication. However, ICP0 mutant viruses replicate with delayed kinetics in several cell types. ICP0 is a transcription transactivator that activates expression from all temporal classes of HSV-1 promoters (IE, E, and L) as well as from some cellular promoters in the HSV-1 or cellular genome (Smiley, Smibert, & Everett,

1987; Cai & Schaffer, 1989; Cai & Schaffer, 1992; Jordan & Schaffer, 1997). The mechanism of such transactivation is yet unclear. However, ICP0 is known to induce gene expression without directly binding to DNA (Everett, Orr, & Elliott, 1991) [also discussed in section 1.3.2.2]. ICP0 does, however, interact with, and disrupt, several chromatin and chromatin modifying proteins. Therefore, the effects of ICP0 on transcription activation may be mediated through its modulation of chromatin structure.

ICP0 plays a role in the removal of H3 from viral genomes at later times after infection, and promotes the acetylation of H3 still associated with HSV-1 genomes (Cliffe & Knipe, 2008; Li et al., 2009). Interaction of ICP0 with the PCAF HAT complex stimulates acetylation of histones on viral gene promoters (Li et al., 2009). Furthermore, ICP0 localizes with and redistributes class I and II HDACs and displaces the HDAC component of the REST/coREST repressor complex (Lomonte et al., 2004; Gu, Liang, Mandel, & Roizman, 2005). ICP0 therefore contributes to maintaining the HSV-1 genome in a transcriptionally active state by manipulating chromatin modifying proteins to promote and maintain transcription-activating PTMs on the histones associated with HSV-1 genomes, and minimize such associations.

ICP0 also alters the host nuclear environment other than chromatin to favor HSV-1 replication. It functions as an E3 ubiquitin ligase and promotes the proteasome mediated degradation of several cellular proteins that may hinder or inhibit HSV-1 replication.

ICP0 mediates the degradation of ND10 components, such as PML and Sp100, which results in dissolution of ND10s (Everett, 2001). Furthermore, ICP0 promotes the proteasome dependent degradation of centromeric proteins (CENPs) A (an H3 variant), B, and C (Everett, Earnshaw, Findlay, & Lomonte, 1999; Lomonte, Sullivan, & Everett, 2001; Lomonte & Morency, 2007). ND10s and centromeres share several protein components, including hDaxx and Sp100. Localization of HSV-1 genomes adjacent to ND10s or centromeres is proposed to result from cellular attempts to silence the genomes. Thus, ICP0 mediated dissolution of centromeres and ND10s may be a mechanism to overcome such silencing attempts.

The cellular antiviral response mediated by IRF-3 is activated by HSV-1 infection. ICP0 counteracts this antiviral response by sequestering and degrading active IRF-3. Concomitantly, ICP0 sequesters the IRF-3 binding proteins CBP and p300 in foci juxtaposed to viral replication compartments (Melroe, Silva, Schaffer, & Knipe, 2007). In this context, ICP0 mediated de-regulation of chromatin modifying proteins is aimed at preventing expression of cellular genes (Melroe et al., 2007).

HSV-1 infection activates the cellular DNA damage response. In some cell types, ICP0 promotes the proteasome dependent degradation of the DNA dependent protein kinase catalytic subunit (DNA-PKcs) (Parkinson, Lees-Miller, & Everett, 1999). DNA-PK is a component of the DNA damage response. ICP0-mediated degradation of DNA-PKcs could

therefore counteract cellular responses aimed to prevent productive HSV-1 infection.

1.4.2.1.2 ICP4.

ICP4 is an immediate early protein that activates expression of E genes and represses expression of itself as well as other IE genes.

The mechanisms of ICP4 mediated IE gene repression are not fully understood. The IE gene repression function of ICP4 involves binding of ICP4 to consensus DNA sequences at the transcription start site of IE promoters. Repression of IE gene expression by ICP4 is mediated in part by the proximity and orientation of the ICP4 binding site relative to the TATA box (Kuddus, Gu, & DeLuca, 1995). The repressive function of ICP4 requires the ICP4 DNA binding domain. ICP4 binding to DNA is enhanced by its oligomerization (Kuddus & DeLuca, 2007). Thus, expression of high levels of ICP4 promotes the association of ICP4 with its binding sites in IE promoters, and thus contributes to repression of IE gene expression. ICP4, when bound to IE promoters, forms a complex with TATA-binding protein (TBP) and transcription factor IID (TFIID) (Smith, Bates, Rivera-Gonzalez, Gu, & DeLuca, 1993; Kuddus et al., 1995). This complex formation is suggested to mediate IE gene repression.

ICP4 binding to IE promoters is enhanced with high mobility group (HMG) A protein binding (Panagiotidis & Silverstein, 1999; Matta & Panagiotidis, 2008). HMG proteins are chromatin binding proteins that compete for H1 binding sites, structurally alter chromatin, and interact with chromatin regulatory proteins. HMG binds to several sequences in

IE promoters (Panagiotidis & Silverstein, 1999; Matta & Panagiotidis, 2008). This occupancy of IE promoters enhances ICP4 binding and therefore is proposed to enhance ICP4 mediated repression of IE genes (Panagiotidis & Silverstein, 1999; Matta & Panagiotidis, 2008). However, ICP4 does not directly bind to HMGA proteins (Panagiotidis & Silverstein, 1999). Therefore, Panagiotidis and Silverstein proposed that the enhanced binding of ICP4 to IE promoters results from HMG mediated bending of the promoter DNA (Panagiotidis & Silverstein, 1999). However, such a mechanism may not be relevant in the context of chromatinized HSV-1 genomes. HMGA occupancy on IE promoters is also reported to enhance ICP0 mediated transactivation of IE gene expression (Matta & Panagiotidis, 2008).

ICP4 mediated activation of E genes is proposed to result from the formation of complexes containing ICP4, TBP, and TAFs on E promoters (Sampath & Deluca, 2008). This complex formation subsequently recruits RNAPII and other transcription proteins and, consequently, E genes are transcribed.

1.4.2.1.3 ICP22.

ICP22 is required for efficient induction of the transcriptionally active RNAPII form in HSV-1 infected cells (Rice, Long, Lam, Schaffer, & Spencer, 1995; Spencer, Dahmus, & Rice, 1997). RNAPII normally exists in two forms. Hypophosphorylated RNAPII (IIa) forms the transcription pre-initiation complexes, whereas hyperphosphorylated RNAPII (IIo) engages in ongoing transcription. During HSV-1 infection, an intermediately phosphorylated RNAPII (IIi) form is induced and recruited

to replication compartments (Rice, Long, Lam, & Spencer, 1994). The IIi form is transcriptionally active in HSV-1 infected cells (Spencer et al., 1997). IPC22 mediated induction of IIi is likely important for supporting HSV-1 transcription in more restrictive cell types (such as human embryonic lung (HEL) cells).

As discussed in section 1.4.4, ICP22 is also required for the formation of virus-induced-chaperone-enriched (VICE) domains, which are thought to be important for degrading misfolded proteins later during infection (Bastian, Livingston, Weller, & Rice, 2010).

1.4.2.1.4 ICP27.

ICP27 is a multifunctional protein essential for transcription of HSV-1 E and L genes. ICP27 inhibits mRNA splicing and promotes the nuclear export and translation of HSV-1 mRNAs (Sandri-Goldin, 2008). Furthermore, ICP27 recruits RNAPII to viral replication sites (Dai-Ju, Li, Johnson, & Sandri-Goldin, 2006; Sandri-Goldin, 2008). Ubiquitination and degradation of RNAPIIo in RCs is proposed to promote L gene expression (Dai-Ju et al., 2006; Sandri-Goldin, 2008). This degradation is mediated by ICP27 (Dai-Ju et al., 2006; Sandri-Goldin, 2008).

As discussed in section 1.4.4, interaction of ICP27 with the chaperone Hsc70 is also important for the formation of VICE domains (Li, Johnson, Dai-Ju, & Sandri-Goldin, 2008; Sandri-Goldin, 2008).

1.4.2.2 E protein expression.

In contrast to the activation of IE gene expression, the mechanisms of activation of HSV-1 E gene expression are largely unknown. Exogenous

promoters recombined into HSV-1 genomes are expressed with E kinetics, indicating that the temporal regulation of HSV-1 E gene expression is not limited to viral promoters (Smiley et al., 1987). Moreover, the IE transactivators ICP0 and ICP4 activate expression from a limited set of endogenous, otherwise silenced, cellular genes, such as the α -globin genes (Cheung, Panning, & Smiley, 1997). ICP0 and ICP4 are each sufficient to activate α-globin expression, however the activation is not synergistic (Cheung et al., 1997). Thus, ICP0 and ICP4 transactivation of promoters is not specific to HSV-1 genomes. However, the α -globin promoter has the same transcription factor binding sites and arrangement as the HSV-1 thymidine kinase (TK) E promoter. Taken together, these data suggest that the mechanisms of activation of E gene expression by ICP0 and ICP4 may be largely independent of promoter sequence and are therefore more likely genome specific.

ICP0 transactivates expression from promoters of all HSV-1 kinetic classes (Cai & Schaffer, 1989; Cai & Schaffer, 1992). However, ICP0 mutants differ in the transactivation reporter gene expression from HSV-1 promoters of different kinetic classes. This suggests that the mechanisms of ICP0 mediated transactivation from IE, E, and L promoters may be different (Cai & Schaffer, 1989).

The transactivation activity of ICP0 is not essential for HSV-1 replication, whereas that of ICP4 is essential. In the absence of functional ICP4, E and L gene expression is not activated (DeLuca & Schaffer, 1988). ICP4 binds to TBP and TBP-associated factors (TAFs) on E promoters (Sampath & Deluca, 2008). Thus, ICP4 directly associates

with the RNAPII transcription machinery. In the absence of ICP4, TBP and RNAPII-containing complexes associate with IE, but not E or L, promoters (Sampath & Deluca, 2008). Mutation of the E promoter TATA box abrogates association of the TBP/RNAPII/ICP4 complex at E promoters (Sampath & Deluca, 2008). ICP4 may therefore be functionally required for recruitment of the RNAPII transcription machinery to E and L HSV-1 promoters. Alternatively, ICP4 association with RNAPII and associated factors may be a result of E gene expression. Consistent with the latter, ICP4 and RNAPII are found associated even on sequences downstream of HSV-1 E promoters. These results suggest that ICP4 and RNAPII remain associated during gene transcription (Sampath & Deluca, 2008).

In addition to regulation of E and L gene expression, ICP0 and ICP4 regulate each other. ICP0 and ICP4 physically interact (Yao & Schaffer, 1994; Liu et al., 2010). In the absence of ICP0 accumulation, ICP4 mediates silencing of ICP0 expression (Liu et al., 2010). However, the ICP4 mediated repression of ICP0 expression is alleviated when ICP0 accumulates (Liu et al., 2010). Thus ICP4 represses ICP0 expression, and ICP0 antagonizes this repression.

The de-silencing of cellular genes, and the largely HSV-1 promoter-indiscriminate transactivation mediated by ICP0 or ICP4 suggests that their mechanism of action may involve epigenetic modification of histones or disruption of chromatin. Consistent with such a model, ICP0 interacts with chromatin modifying proteins, such as HATs and HDACs, and disrupts centromeres, which are flanked by

domains of silenced heterochromatin (Everett et al., 1999; Lomonte et al., 2001; Lomonte et al., 2004; Gu et al., 2005; Lomonte & Morency, 2007; Cliffe & Knipe, 2008; Li et al., 2009).

1.4.2.3 HSV-1 DNA replication.

The HSV-1 E genes encode, among others, the proteins required for HSV-1 DNA replication. Specifically, HSV-1 encodes seven proteins required for genome replication, the single stranded DNA binding protein ICP8 (U_L29), an origin of replication binding protein (OBP, U_L9), a heterotrimeric helicase primase complex (U_L5, U_L8, and U_L52), a DNA polymerase (U_L30), and a processivity protein (U_L42). HSV-1 genomes contain three origins of replication, two copies of ori_S and one of ori_L. HSV-1 DNA replication initiates at any of these origins.

HSV-1 genome replication is thought to initially proceed through a theta mechanism. Subsequently, DNA replication is thought to switch to rolling-circle and homologous recombination (HR) mechanisms (Wilkinson & Weller, 2003). Consistent with the later model, large concatameric branched HSV-1 DNA structures are formed during HSV-1 DNA replication. HSV-1 does not encode for a DNA ligase. Therefore, at least a cellular ligase is required for HSV-1 DNA replication. It is unknown whether other cellular proteins are required for HSV-1 DNA replication or HR.

1.4.2.3.1 HSV-1 replication compartments.

Early during HSV-1 infection, foci containing ICP4 form adjacent to ND10 complexes (Everett, Sourvinos, & Orr, 2003; Everett, Sourvinos,

Leiper, Clements, & Orr, 2004). ICP27 also associates with these ICP4 foci, but is not required for their formation (Everett et al., 2004). In instances of unilateral nuclear genome entry, such as that which occurs in cells in the periphery of HSV-1 plaques, these primary ICP4 foci form unilaterally just inside of the nuclear envelope (Everett et al., 2004). It has been reported that ND10 proteins, such as PML, Sp100, and hDAXX, are recruited to sites adjacent to the ICP4 foci and form novel ND10-like structures (Everett et al., 2004). The formation of ICP4 foci adjacent to ND10, or of ND10-like structures adjacent to ICP4 foci, is correlated with HSV-1 replication. During low multiplicity infections with an ICP0 null virus, ICP4 foci do not localize adjacent to ND10s, nor do they contain detectable levels of ICP27 (Everett et al., 2004). Also under such conditions, HSV-1 replication is delayed. The replication delay of ICP0 null viruses is compensated by infection with higher multiplicities. Under such conditions, the ICP4 containing foci are again localized adjacent to ND10s (Everett et al., 2004). Whether localization of ICP4 foci adjacent to ND10s is required for replication of ICP0 null viruses, or such replication promotes the association of ICP4 foci adjacent to ND10s is unknown. As with the ICP4 containing foci, parental HSV-1 genomes localize adjacent to ND10 structures (Tang et al., 2003). The similar localization of HSV-1 parental genomes and ICP4 foci, adjacent to ND10, as well as the requirement of the ICP4 DNA binding domain for ICP4 foci formation, suggests that ICP4 foci also contain HSV-1 genomes (Everett et al., 2003; Livingston, DeLuca, Wilkinson, & Weller, 2008). With ICP8 expression, microfoci of ICP8 form adjacent to the ICP4 containing foci

(Livingston et al., 2008). ICP8 microfoci represent pre-replicative structures. In addition to ICP8, these structures contain the OBP (U_L9) and the helicase/primase complex (U_L5, U_L8, and U_L52) (Livingston et al., 2008). The formation of ICP8 containing microfoci is dependent on the formation of the ICP4 containing foci (Livingston et al., 2008). ICP8 is recruited into ICP4 containing foci, which eventually turn into viral replication compartments (Livingston et al., 2008). With HSV-1 DNA replication, the replication compartments increase in size. Eventually, replication compartments fill the nucleus. However, there is still some debate as to whether the initial replication compartments remain as discrete structures, or coalesce to form one large replicative structure (Sourvinos & Everett, 2002; Taylor, McNamee, Day, & Knipe, 2003; Everett et al., 2004).

1.4.2.3.2 Activation of cellular DNA damage response.

HSV-1 infection activates the host cell DNA damage response. A subset of the cellular proteins involved in the homologous recombination (HR) and non-homologous end joining (NHEJ) pathways of DNA repair are activated and even recruited to HSV-1 replication compartments. In contrast, other such proteins are degraded during infection. In some cell types, for example, ICP0 promotes the proteasome mediated degradation of DNA-PKcs (Lees-Miller et al., 1996; Parkinson et al., 1999).

NBS1, RPA, and RAD51 are recruited to pre-replicative sites containing the HSV-1 DNA polymerase, and maintained in mature RC (Wilkinson & Weller, 2004). Ataxia-telangiectasia-mutated (ATM), the MRN complex (Mre11, Rad50, and NBS1), and Ku86 are also recruited to

RC (Wilkinson & Weller, 2004; Shirata et al., 2005). ATM is active, and phosphorylates downstream targets, including NBS1 and Chk2 (Shirata et al., 2005). In contrast, RPA recruited to RC is not activated (Wilkinson & Weller, 2006). Cellular DNA repair proteins may be targeted to HSV-1 sites of replication to antagonize HSV-1 genome replication. Alternatively, they may play a positive role in HSV-1 genome replication and recombination.

While a subset of DNA repair proteins are activated or recruited to sites of HSV-1 DNA replication, others are sequestered away from such sites or inactivated. Phosphorylated H2A.X (γH2A.X) is associated with DNA double strand breaks and recruits DNA repair proteins. During HSV-1 infection, γH2A.X accumulates in the cellular chromatin peripheral to RC (Wilkinson & Weller, 2006). The activated, hyperphosphorylated, form of RPA is sequestered away from RC as well as from sites of γH2A.X in cellular chromatin (Wilkinson & Weller, 2006). A percentage of hyperphosphorylated RPA localizes with VICE domains adjacent to RC (Wilkinson & Weller, 2006). HSV-1 infection disrupts the ATM-Rad3-related (ATR) DNA damage signaling pathway. ATR is recruited to sites of DNA damage by ATRIP. During infection, ICP0 mediates the relocalization of ATRIP to VICE domains (Wilkinson & Weller, 2006). Thus, ATR and ATRIP occupy different nuclear domains during HSV-1 infection. Moreover, phosphorylation of the ATR downstream target, Chk1, is not detected suggesting that ATR is not activated or its activity is directed to other substrates (Shirata et al., 2005).

A subset of DNA repair proteins is activated during HSV-1 infection. However, the conventional signaling through both homologous repair (HR) and non-homologous end joining (NHEJ) DNA repair pathways is disrupted. Thus, HSV-1 infection both triggers and dysregulates DNA damage responses.

1.4.2.4 L protein expression and virion assembly.

HSV-1 late proteins are only expressed after HSV-1 DNA replication begins. Late genes mostly encode for proteins required to assemble progeny virions. HSV-1 capsids are assembled in the nucleus. They assemble through the interactions of the capsid proteins U_L19 and U_L6 with the scaffold proteins U_L26 and $U_L26.5$. Unit-length HSV-1 genomes are packaged through the portal and cleaved by the associated terminase complex (U_L15, U_L28, and U_L33). As the genome is encapsidated, the scaffold is cleaved and extruded from the capsid.

Final virion assembly is proposed to occur through an envelopment- de-envelopment mechanism. Capsids are transported to the inner nuclear membrane, where they bud into the internuclear membrane space. This process of primary envelopment requires disruption of the nuclear lamina mediated by U_L31 and U_L34 (Simpson-Holley, Baines, Roller, & Knipe, 2004; Simpson-Holley, Colgrove, Nalepa, Harper, & Knipe, 2005). Primary de-envelopment requires the HSV-1 kinase U_S3. Capsids released into the cytoplasm are associated with tegument proteins U_S3, U_L36, and U_L37. HSV-1 glycoproteins assemble in the Golgi membrane, where they associate with a subassembly of tegument proteins (Mettenleiter, 2006). The secondary envelopment of

HSV-1 capsids and tegument proteins occurs through interactions between tegument proteins and glycoproteins. Finally, the Golgi cisterna wrap around the capsid and tegument proteins to produce a mature virion in a vesicle-like structure. Fusion of the vesicle with the plasma membrane releases the virion into the extracellular environment.

1.5 HOST CELL NUCLEAR MORPHOLOGY DURING HSV-1 INFECTION.

Nuclear morphology is drastically altered during HSV-1 infection. HSV-1 replication compartments form and invade the nucleus. Some nuclear substructures, such as nucleoli and ND10, are disrupted, while others are formed (VICE). Furthermore, nuclear architecture is disrupted.

Viral replication compartments initially form in the interchromosomal space (Monier, Armas, Etteldorf, Ghazal, & Sullivan, 2000). As replication compartments expand, cellular chromatin is rearranged to occupy domains peripheral to RCs (Monier et al., 2000). For approximately the first 10 hours of infection, the nuclear volume expands to almost twice its original volume (Monier et al., 2000; Simpson-Holley et al., 2005). Rearrangement of the nuclear lamina is required to accommodate such expansion (Simpson-Holley et al., 2005). U_L 31 and U_L34 are sufficient for the redistribution of lamin A/C and lamina-associated polypeptide 2 (LAP2) during HSV-1 infection (Simpson-Holley et al., 2004; Simpson-Holley et al., 2005).

At later times after infection, cellular chromatin is compacted (Monier et al., 2000; Simpson-Holley et al., 2004). At such times, cellular chromatin is discontinuous and the lamina layer is perforated

(Simpson-Holley et al., 2005). This allows extension of RCs to the inner nuclear membrane.

1.5.1 Nucleoli.

Nucleoli are the nuclear sites of ribosomal RNA (rRNA) synthesis, and of 40s and 60s ribosome subunit assembly. Ribosomal genes are located in arrays of head-to-tail tandem repeats referred to as nucleolar organizing regions (NORs). The grouping of several NORs from different chromosomes forms the nucleolus. Nucleoli are dynamic structures: nucleolar proteins are free to diffuse through the nucleus and nuclear proteins are free to diffuse through the nucleoli. Nucleolar proteins are retained in the nucleolus through functional interactions, whereas non-nucleolar proteins are not (Raska, Shaw, & Cmarko, 2006). Two of the most abundant nucleolar proteins, nucleolin and nucleophosmin (B23) are redistributed during HSV-1 infection (Lymberopoulos & Pearson, 2007; Bertrand & Pearson, 2008; Calle et al., 2008; Bertrand, Leiva-Torres, Hyjazie, & Pearson, 2010). Nucleolin and nucleophosmin initially re-distribute from nucleoli to viral RC (Calle et al., 2008). Redistribution of nucleolin correlates with expression of the HSV-1 leaky L protein U_L24 (Bertrand & Pearson, 2008; Calle et al., 2008; Bertrand et al., 2010). U_L24 is required, and sufficient, to mediate this dispersal during HSV-1 infection (Lymberopoulos & Pearson, 2007; Bertrand & Pearson, 2008). At later times after infection, nucleophosmin accumulates in the nuclear periphery whereas nucleolin accumulates in granular structures adjacent to the nucleus (Calle et al., 2008). Why nucleolin is relocalized during HSV-1 infection remains to be elucidated. Nucleolin does,

however, contribute to HSV-1 replication efficiency. Down regulation of nucleolin inhibits HSV-1 replication (Calle et al., 2008).

1.5.2 ND10 (PML-NB).

ND10, or promyelocytic leukaemia (PML) nuclear bodies (PML-NBs) are proteinaceous bodies that occupy nuclear domains depleted of cellular chromatin. However, ND10s are surrounded by, and make point contacts with, chromatin fibres (Eskiw, Dellaire, & Bazett-Jones, 2004). Such contacts are proposed to mediate the positional stability and integrity of ND10s (Eskiw et al., 2004).

Many proteins localize to ND10s. However, only PML is required for their formation (Dellaire & Bazett-Jones, 2004; Lallemand-Breitenbach & de The, 2010). ND10s are implicated in many cellular processes, including apoptosis, DNA repair, gene regulation, and antiviral response (Dellaire & Bazett-Jones, 2004; Everett & Chelbi-Alix, 2007; Lallemand-Breitenbach & de The, 2010). Major protein components of ND10s, including PML and Sp100, are upregulated in response to interferon (IFN) (Regad & Chelbi-Alix, 2001). ND10s are therefore proposed to contribute to the cellular antiviral state (Everett, 2001; Regad & Chelbi-Alix, 2001).

ICP0 mediates dispersal of ND10s during HSV-1 infection (Everett, 2001). Proteasome-mediated degradation of some ND10 associated proteins is induced by ICP0 (Everett, 2001). Conversely, other components are dispersed from ND10 and may be recruited to HSV-1 sites of replication.

1.5.3 VICE (Virus-induced-chaperone-enriched) domains.

VICE domains are formed de novo at the periphery of HSV-1 replication compartments (Burch & Weller, 2004). They contain nuclear protein chaperones (Hcs70 and Hsp70) and co-chaperones (Hsp40), components of the 26S proteosome, and ubiquitin-conjugated proteins (Burch & Weller, 2004; Burch & Weller, 2005). VICE domain formation is independent of HSV-1 DNA replication, but requires HSV-1 protein expression. Their formation occurs early during infection and correlates with the disruption of ND10 (Livingston et al., 2008). ICP0, ICP27, and ICP22 localize to VICE domains (Burch & Weller, 2005; Li et al., 2008; Bastian et al., 2010). The formation of VICE domains is impaired in the absence of ICP0, ICP27, or ICP22 (Burch & Weller, 2005; Li et al., 2008; Bastian et al., 2010). However, foci still form at later times after infection with ICP0 or ICP27 mutant strains (Burch & Weller, 2004; Bastian et al., 2010). Therefore, although ICP0, ICP22, and ICP27 are important for VICE domain formation, only ICP22 is required (Burch & Weller, 2004; Li et al., 2008; Bastian et al., 2010).

VICE domains are sites of protein degradation. Ubiquitin-conjugated proteins of viral and cellular origin associate with these domains. VICE domain formation is associated with the ubiquitination and degradation of RNAPII, which is thought to promote L gene expression (Li et al., 2008). IRF-3 is activated as part of the cellular interferon stimulated antiviral response. ICP0 counteracts this response by sequestering activated IRF-3 and its associated histone acetyltransferase (CBP/p300) in VICE domains (Melroe et al., 2007).

Recruitment to VICE domains promotes the degradation of IRF-3 and attenuates its activation of downstream components (Melroe et al., 2007).

Viral proteins targeted for degradation in VICE domains include U_L6, the capsid portal protein (Burch & Weller, 2004).

1.6 CELLULAR CHROMATIN.

Cellular DNA is complexed with histones to form chromatin, the basic unit of which is the nucleosome. The nucleosome core particle is approximately 146bp of DNA wrapped 1.6 times around a histone octamer consisting of a histone H3-H4 heterotetramer and two H2A-H2B heterodimers. Nucleosomes form a regular repeating array separated by DNA. This chromatin organization is often referred to as "beads-on-a-string" and represents the first level of chromatin compaction. Linker histone H1 binds to DNA at nucleosome entry and exit points. Association of H1 promotes the formation of higher order chromatin structures. H1 binding to nucleosomes condenses chromatin into a fibre with a diameter of approximately 30nm. It is proposed that the 30nm fibres compact to form solenoid or zigzag structures (Woodcock & Ghosh, 2010). However, the structures formed by further compaction of cellular chromatin, and any associated proteins that assist in such compaction, are unknown.

1.6.1 Histones.

Histones are classified as canonical or variant based on their regulation of expression. Canonical histone expression is correlated with DNA replication, whereas variant histone expression is not. The majority of

chromatin is assembled during the S-phase of the cell cycle, when DNA is replicated. Therefore, canonical core histones are expressed to high levels during S-phase and are assembled in nucleosomes with nascent and replicated parental DNA. Conversely, variant histones are expressed throughout the cell cycle and their assembly in chromatin is not dependent on DNA replication. Variant core histones mostly exchange with those histones already assembled in chromatin.

1.6.1.1 Canonical histones.

The genes encoding canonical histones are located in 3 clusters on chromosomes 1, 6, and 12 (Tripputi et al., 1986; Albig, Kioschis, Poustka, Meergans, & Doenecke, 1997). The clusters of histone genes are not highly repeated, and the gene arrangement and orientation within the cluster is mostly irregular (Carozzi et al., 1984; Albig et al., 1997). Some genes encoding H2A and H2B, however, are arranged in divergent pairs with a relatively short nucleotide sequence separating them (Albig et al., 1997). The largest cluster of canonical histones is on chromosome 6. It consists of genes encoding all four core histones (H2A, H2B, H3, and H4) as well as many linker histone genes (H1.1, H1.2, H1.3, and H1.4) (Albig et al., 1997).

Synthesis of canonical histones is tightly regulated at transcriptional and post-transcriptional levels, to coincide with DNA synthesis. Canonical histone mRNA levels increase approximately 35-fold at the start of S-phase and rapidly decrease at the start of G_2 (Whitfield et al., 2000). The increase in mRNA levels is due to an increase in transcription and stabilization of histone mRNA.

Transcription of histone genes increases approximately 5-fold at the start of S-phase. Synthesis of histones is tightly coordinated with DNA replication. Inhibition of histone synthesis induces arrest of DNA synthesis (Nelson et al., 2002). Histone gene transcription is stimulated by phosphorylated NPAT (Marzluff & Duronio, 2002). Conversely, HIRA inhibits canonical histone transcription and thus induces arrest of DNA synthesis (Nelson et al., 2002). NPAT and HIRA are constitutively expressed, but are phosphorylated by CDK2/cyclin E during S-phase (Marzluff & Duronio, 2002). Phosphoylation activates NPAT, whereas it inhibits HIRA (Marzluff & Duronio, 2002).

Histone mRNA levels increase 35-fold at the start of S-phase (Whitfield et al., 2000). The 3` end of histone mRNAs forms a stem loop structure that is bound by stem loop binding protein (SLBP) during S-phase. During transcription, SLBP binds to the histone pre-mRNA stem loop and stabilizes binding of the U7 snRNA to the histone downstream element (HDE) (Marzluff & Duronio, 2002). Following processing, SLBP remains associated with the histone mRNA and enhances its stability and translation. Expression of SLBP is tightly coordinated with the cell cycle such that it is expressed during S-phase and rapidly degraded at the end of S-phase (Whitfield et al., 2000). SLBP degradation correlates with, but is not required for, histone mRNA degradation at the end of S-phase (Whitfield et al., 2000). Degradation of histone mRNAs is initiated by addition of uridines to the 3` end of the histone mRNA by terminal uridylyl transferases (TUTases) (Mullen & Marzluff, 2008). Histone mRNA is simultaneously degraded 5` to 3`, by mRNA decapping and

decay proteins, and 3` to 5`, by exosome proteins (Mullen & Marzluff, 2008).

1.6.1.2 Variant histones.

With the exception of H4, all histones types have variants. Transcription of variant core histone genes is not restricted to any particular phase of the cell cycle, neither are their transcripts particularly unstable in any phase. Typically, variant histone mRNAs are 5` capped, contain introns, and are polyadenylated.

1.6.1.2.1 H1 variants.

H1 has several variants, $H1^0$, H1.1, H1.2, H1.3, H1.4, H1.5, and H1t, of varying degrees of divergence. The majority of variance is within the C-terminal domains. $H1^0$ is a variant that is enriched in differentiated cells, H1.1 to H1.5 are expressed in somatic cells, and H1t is testis specific.

1.6.6.2.1.1 H1.2.

The gene encoding H1.2 is located within the main cluster of canonical histones on chromosome 6 (Albig et al., 1997). The H1.2 promoter is regulated by TATA, CCAAT, and H1-box (AAACACA) elements (Eilers, Bouterfa, Triebe, & Doenecke, 1994). The H1 box regulates S-phase dependent expression of H1.2 (Eilers et al., 1994). H1.2 mRNA transcripts have a 3` stem loop and are polyadenylated (Cheng, Nandi, Clerk, & Skoultchi, 1989; Doenecke, Albig, Bouterfa, & Drabent, 1994;

Alvelo-Ceron, Niu, & Collart, 2000). The polyadenylated H1.2 transcripts are expressed independent of the cell cycle.

H1 binds to core nucleosomes and stabilizes the formation of higher order chromatin structures. However, overexpression of H1.2 does not globally inhibit transcription, rather it increases expression of some genes (Brown, Alexander, & Sittman, 1996; Gunjan & Brown, 1999).

1.6.1.2.2 H2A variants.

H2A has several variants with differing divergence. H2A.Z has approximately 60% amino acid identity with H2A (Hatch & Bonner, 1990). H2A.Bbd, the most specialized H2A variant, is only 48% identical to H2A (Bao et al., 2004).

1.6.1.2.2.1 H2A.Z.

The H2A.Z genes are not clustered with other histone genes, and expression of H2A.Z is not dependent on DNA synthesis (Hatch & Bonner, 1990). Two genes encode H2A.Z isoforms, H2A.Za (H2A.Z2) and H2A.Zv (H2A.Z1) (Eirin-Lopez, Gonzalez-Romero, Dryhurst, Ishibashi, & Ausio, 2009). The DNA sequences encoding H2A.Za and H2A.Zv have divergent promoter sequences and the DNA sequences are as divergent from each other as they are from H2A, even though the encoded proteins are almost identical (Dryhurst et al., 2009). The H2A.Zv promoter has elements that are typical for variant histones: a TATA box, three CCAAT boxes, and several GC-boxes (Hatch & Bonner, 1990; Dryhurst et al., 2009). Conversely, the H2A.Za promoter does not contain a TATA box

(Dryhurst et al., 2009). Moreover, the positions of the CCAAT and GC-boxes in the H2A.Za promoter do not coincide with that of H2A.Zv (Dryhurst et al., 2009). The H2A.Z mRNA transcripts have introns and are polyadenylated (Hatch & Bonner, 1990). Despite the divergence in DNA sequence, H2A.Za and H2A.Zv share a high degree of amino acid sequence identity, differing at only three residues (Eirin-Lopez et al., 2009).

The assembly of H2A.Z into nucleosomes has been reported to stabilize as well as destabilize the histone octamer (Thambirajah et al., 2006; Ramaswamy & Ioshikhes, 2007; Jin & Felsenfeld, 2007). The stability of H2A.Z containing octamers may be dependent on the acetylation of other histones in the octamer or of H2A.Z itself (Thambirajah et al., 2006).

1.6.1.2.3 H2B.1.

Thus far one variant of H2B, H2B.1 (H2BFQ) has been identified (Collart et al., 1992). The gene encoding H2B.1 is located within the cluster of canonical histone genes on chromosome 1, where it is paired head-to-head with a gene encoding H2A. Transcripts of H2B.1 are alternatively processed to produce two mRNAs. One transcript (approximately 500bp) terminates immediately after the 3` stem loop and is cell cycle dependent (Collart et al., 1992). The other transcript is larger (approximately 2300bp), contains a 3` stem loop, and is polyadenylated (Collart et al., 1992). The longer transcript is constitutively expressed.

1.6.1.2.4 H3.3.

The histone variant H3.3 differs from canonical H3.1 and H3.2 at five and four amino acid residues, respectively (Table 1.1).

Expression of H3.3 is independent of DNA replication, as is typical for variant histones. However, H3.3 mRNA levels do increase during S-phase (Hake et al., 2006). Two genes encode H3.3, H3.3A and H3.3B (Brush, Dodgson, Choi, Stevens, & Engel, 1985). The H3.3 genes are not clustered with other histone genes, but are isolated and singular (Brush et al., 1985). The DNA sequences of H3.3A and H3.3B are as divergent from each other as they are from canonical H3.2, approximately 18% and 19%, respectively (Brush et al., 1985). However, H3.3A and H3.3B encode proteins with identical amino acid sequences (Brush et al., 1985). The conservation of H3.3 amino acid sequence despite the divergence of the DNA sequence suggests that H3.3 has a highly selective biological function. In addition to having divergent DNA sequences, H3.3A and H3.3B expression is also regulated by divergent promoters (Frank, Doenecke, & Albig, 2003). The H3.3A promoter contains an initiator element and Sp1 binding sites within a GC-rich region (Frank et al., 2003). Conversely, the H3.3B promoter contains CCAAT and TATA sequences. The H3.3 mRNAs have long 3` and 5` untranslated regions (UTR), contain introns, and are polyadenylated (polyA) (Brush et al., 1985). Typically, H3.3 mRNA is expressed to high levels in adult tissues and tissue culture cells, whereas it is expressed to low levels in fetal tissues (Frank et al., 2003).

H3.3 is assembled in chromatin via transcription associated chromatin assembly mechanisms. Therefore, H3.3 is typically enriched in the promoters and coding regions of transcriptionally active genes. The incorporation of H3.3 into nucleosomes has a destabilizing effect (Jin & Felsenfeld, 2007). Destabilization of histone interactions within the nucleosome core particle promotes an "open" chromatin structure that would permit access of proteins to DNA. In addition to inherent destabilization of the nucleosome, characteristically H3.3 has posttranslational modifications that are associated with transcriptionally active chromatin (Hake et al., 2006).

1.7 CHROMATIN ASSEMBLY AND NUCLEOSOME DISASSEMBLY.

Chromatin assembly and disassembly typically occurs in conjunction with DNA replication, gene transcription, or DNA repair. The majority of chromatin is assembled when DNA is replicated during the S-Phase of the cell cycle. This chromatin assembly is referred to as "DNA replication-dependent". Chromatin assembly associated with gene transcription and DNA repair, conversely, is "DNA replication-independent".

Histones that are not assembled in chromatin are bound by histone chaperones. Chromatin assembly and disassembly therefore involves the dynamic transfer of histones from chaperones to nucleosomes and vice versa.

1.7.1 DNA replication dependent chromatin assembly.

DNA replication is the semi-conservative copying of parental DNA into two daughter strands. Replication initiates at origins of replication scattered throughout the genome and proceeds bidirectionally. At the head of the replication fork the DNA helicase complex MCM (minichromosome maintenance) 2-7 separates the DNA strands. Topoisomerases are required to relieve the topological stress created during such separation. Replication protein A (RPA) binds to and stabilizes the single strand DNA.

DNA is synthesized 5` to 3` by DNA polymerases. DNA synthesis is therefore continuous on one strand, referred to as the leading strand, and discontinuous on the other, referred to as the lagging strand. Leading strand DNA synthesis is mainly catalyzed by DNA polymerase ε (Polε). The polymerase is tethered to the DNA by interactions with proliferating cell nuclear antigen (PCNA). Leading strand synthesis proceeds in the direction of replication fork movement. Lagging strand synthesis occurs as short fragments, called Okazaki fragments, synthesized in the direction opposite of replication fork movement. Synthesis of these fragments is initiated by RNA-DNA primers. Okazaki fragments are synthesized by Polα and extended by Polδ. As for Polε, Polα and Polδ are tethered to DNA by interactions with PCNA. The nicks between the fragments synthesized on the lagging strand are ligated by DNA ligase.

DNA synthesis requires access of DNA replication proteins to DNA. Therefore, existing chromatin structures must first be disassembled to

allow for such access. Following replication, nascent and parental DNA must again be assembled into chromatin. Canonical histone synthesis and DNA synthesis are tightly regulated to ensure an adequate supply of histones (Nelson et al., 2002). Inhibition of histone synthesis results in inhibition of DNA synthesis, and inhibition of DNA synthesis results in inhibition of histone synthesis.

Separation of the DNA strands first requires nucleosome disassembly. The H2A-H2B dimers are peripheral to the H3-H4 tetramer. Therefore, they are likely first removed from the nucleosome. FACT (facilitates chromatin transcription) is an H2A-H2B histone chaperone that associates with the MCM2-7 helicase and facilitates DNA unwinding (Tan, Chien, Hirose, & Lee, 2006; Das, Tyler, & Churchill, 2010). FACT may therefore be associated with removal of parental H2A-H2B dimers from nucleosomes during chromatin disassembly. Chromatin disassembly of parental H3-H4 tetramers is mediated by anti-silencing function 1 (ASF-1) (Adkins & Tyler, 2004; Groth et al., 2007). ASF-1 is an H3-H4 chaperone that binds dimers of H3-H4 at the interface required for H3-H4 tetramerization (Das et al., 2010). Therefore, ASF-1 association with H3-H4 during DNA replication-associated chromatin disassembly likely involves disruption of the parental H3-H4 tetramer into dimers. ASF-1 associates with the MCM2-7 complex via an H3-H4 bridge (Groth et al., 2007). The ASF-1 mediated chromatin disassembly of H3-H4 tetramers is important for DNA replication. Depletion of ASF-1 by RNAi impedes DNA unwinding, and therefore obstructs DNA synthesis (Groth et al., 2007). Likewise,

overexpression of H3-H4 compromises the ability of ASF-1 to accept parental H3-H4 dimers and also impedes DNA unwinding. During DNA replication, ASF-1 associates with both parental and newly synthesized H3-H4 dimers (Groth et al., 2007; Jasencakova et al., 2010). Newly synthesized and parental H3-H4 dimers are distinguished by their posttranslational modifications. Newly synthesized H3/H4 dimers are enriched in H4 K5 and K12 acetylation (Jasencakova et al., 2010). This acetylation is removed following assembly into chromatin.

The assembly of chromatin following DNA replication is semi-conservative. Parental and newly synthesized histones are assembled into chromatin following DNA replication. The H3-H4 tetramer is assembled first, followed by addition of two H2A-H2B dimers. Chromatin assembly factor 1 (CAF-1) is an H3.1-H4 histone chaperone that mediates chromatin assembly following DNA replication (Tagami, Ray-Gallet, Almouzni, & Nakatani, 2004; Takami, Ono, Fukagawa, Shibahara, & Nakayama, 2007). CAF-1 is targeted to sites of DNA synthesis by interaction with PCNA (Shibahara & Stillman, 1999). ASF-1 transfers newly synthesized and parental H3-H4 dimers to CAF-1 for chromatin assembly. CAF-1 binds to H3-H4 dimers on the face external to that required for tetramerization (Das et al., 2010). It is therefore unknown whether H3-H4 is assembled into chromatin as a dimer or a tetramer. Addition of H2A-H2B dimers to the H3-H4 tetramer may be mediated by the chaperones FACT, or NAP-1.

Nuclear autoantigenic sperm protein (NASP) is an H1 chaperone that mediates assembly of H1 into chromatin (Richardson et al., 2000;

Alekseev, Bencic, Richardson, Widgren, & O'Rand, 2003; Finn, Browne, Hodgson, & Ausio, 2008). During DNA replication, NASP may be recruited to sites of DNA synthesis through its interactions with ASF-1 and the MCM2-7 complex (Jasencakova et al., 2010). Taken together these results suggest that NASP mediates H1 assembly and disassembly into chromatin during DNA replication.

1.7.2 DNA-replication independent chromatin assembly.

DNA replication independent chromatin assembly occurs during gene transcription and DNA repair. DNA replication independent chromatin assembly and disassembly also involve histone exchange, where histones disassembled from the nucleosome are replaced with other histones. Histone exchange is mostly associated with active transcription, however, it also occurs independently of active transcription (Rufiange, Jacques, Bhat, Robert, & Nourani, 2007; Jamai, Imoberdorf, & Strubin, 2007).

1.7.2.1 Transcription.

Transcription proteins are recruited to transcriptionally active genes through chromatin interactions. However, transcription requires access of transcription proteins to the DNA. Therefore, the chromatin at transcriptionally active loci is modified, by posttranslational modifications or by incorporation of histone variants, so that it is less condensed and more accessible.

Concomitant with passage of the RNAPII along DNA, nucleosomes are disrupted and reassembled. RNAPII transcription is associated with loss of an H2A-H2B dimer from the nucleosome (Kireeva et al., 2002).

Under conditions of high levels of transcription, H3-H4 tetramers are also displaced. Following passage of RNAPII, nucleosomes may be reassembled with the histones that were originally displaced, or histones may be exchanged for variant histones.

The chromatin exchange of H2A-H2B dimers occurs throughout the entire gene (Jamai et al., 2007). Histone exchange is mediated by histone chaperones. FACT associates with RNAPII and mediates the disassembly and reassembly of H2A-H2B dimers in nucleosomes (Belotserkovskaya et al., 2003). FACT and NAP-1 mediate the nucleosome assembly and disassembly of dimers containing canonical H2A or H2A variants, including H2A.X and H2A.Bbd (Okuwaki, Kato, Shimahara, Tate, & Nagata, 2005). Nucleosome exchange of H2A.Z-H2B dimers is preferentially mediated by Chz1 (Luk et al., 2007).

The chromatin exchange of H3-H4 dimers (or tetramers) occurs predominantly within promoter regions and is mostly associated with transcription (Jamai et al., 2007; Kim, Seol, Han, Youn, & Cho, 2007). HIRA and ASF-1 mediate the exchange of dimers containing canonical H3 for the H3 variant H3.3 (Tagami et al., 2004). Recently, hDaxx was identified as an H3.3 chaperone. In combination with α-thalassemia/mental retardation syndrome protein (ATRX), hDaxx mediates the replication independent assembly of H3.3-H4 dimers into chromatin (Lewis, Elsaesser, Noh, Stadler, & Allis, 2010; Drane, Ouararhni, Depaux, Shuaib, & Hamiche, 2010). Such chromatin exchange has been shown to occur in regions of pericentric heterochromatin and telomeres (Lewis et al., 2010; Drane et al., 2010).

1.7.2.2 DNA repair.

The maintenance of cellular DNA integrity is important for cell viability. Damage that occurs to cellular DNA needs to be reliably repaired. Failure to accurately repair such damage predisposes the cell to apoptosis, transformation, or cancer. Accurate damage repair requires access of repair proteins to DNA.

Nucleosomes surrounding the site of DNA damage are disassembled to allow access of repair proteins to the DNA. Histone chaperones CAF-1 and ASF-1 are not required for this disassembly. However, they are required for nucleosome reassembly following DNA repair (Ransom, Dennehey, & Tyler, 2010).

Histone exchange at sites of DNA damage mediates DNA repair. In response to DSBs, histone H2A.X in the nucleosomes surrounding the break is phosphorylated (γH2A.X). Members of the phosphatidylinositol-3 kinase-like family of kinases (PIKK) mediate this phosphorylation. Phosphorylation of H2A.X occurs in large regions of chromatin on either side of the DSB. γH2A.X destabilizes the nucleosome and hinders H1 binding (Li et al., 2010). Depletion of H1 from nucleosomes surrounding DSBs and destabilization of γH2A.X-containing nucleosomes contributes to an "open" chromatin conformation accessible to DNA repair proteins and facilitates nucleosome disassembly. Following DNA repair, FACT mediates nucleosome exchange of γH2A.X-H2B dimers for H2A-H2B dimers (Ransom et al., 2010).

1.8 CHROMATIN REGULATION.

Modification of chromatin structure is a mechanism used by the cell to regulate access of proteins involved in gene expression, DNA replication, DNA repair and recombination, and therefore to regulate these processes. Chromatin structure can be altered by covalent posttranslational modifications to histones, or incorporation of variant histones.

DNA is wrapped around chromatin proteins. For transcription complexes to have access to the DNA, the association of DNA with histones has to be reversible. Moreover, regulating the compaction of chromatin can modulate the access of such complexes to DNA. This regulation is achieved physically, by post-translational modification of chromatin bound histones, and by incorporation of variant histones. Histones themselves can be posttranslationally modified to alter chromatin condensation and therefore DNA accessibility.

1.8.1 Physical Structures.

Higher order chromatin packaging acts as a physical barrier that prevents or limits access of proteins to DNA. The degree of chromatin compaction and association of histone or non-histone proteins that promote higher compaction can prevent or limit access of transcription or DNA replication proteins to DNA. H1 binding to chromatin promotes the formation of higher order structures (Kepert, Mazurkiewicz, Heuvelman, Toth, & Rippe, 2005).

Heterochromatin has a more condensed structure and is associated with transcriptionally silent genes. Euchromatin has a less

condensed structure and is therefore associated with transcriptionally active genes.

1.8.2 Posttranslational histone modifications.

Histones are covalently modified by addition of posttranslational modifications, including acetylation, methylation, ubiquitylation, phosphorylation, and ADP-ribosylation. These modifications alter histone-histone contacts or histone-DNA contacts and therefore alter chromatin compaction. Acetylation, methylation, and ubiquitylation are discussed below.

1.8.2.1 Acetylation.

Histone acetylation is a reversible process. Histone acetyltransferase complexes (HAT; or lysine acetyltransferase KAT) acetylate histones whereas histone deacetylase complexes (HDAC) deacetylate histones. Acetylation relaxes the basic chromatin structure. Relaxation is achieved through increased charge repulsion of the acetyl group with the DNA phosphate backbone. Acetylation also recruits chromatin-remodeling complexes that can alter or slide nucleosomes along the DNA, unwind nucleosomes, or promote nucleosome removal. Due to the relaxation of chromatin structure that is associated with acetylation, this covalent modification is typically associated with loci of active transcription, or euchromatin.

Acetylation promotes histone chromatin exchange. The relaxed chromatin structure is permissive for removal or replacement of core histones by histone chaperones and chromatin remodeling complexes

(Ito, Ikehara, Nakagawa, Kraus, & Muramatsu, 2000). Additionally, the affinity of H1 for chromatin binding is decreased when the core histones comprising the nucleosome are acetylated.

1.8.2.2 Methylation.

Methylation is a reversible posttranslational modification. Methylation is the addition of one, two, or three methyl groups to lysine residues of histones H3 or H4 by histone methyltransferases (HMTs). Some HMTs catalyze trimethylation, whereas others only catalyze mono- or mono- and dimethylation. Histones are demethylated by demethylases. As with HMTs, different HDMTs have varying ability to demethylate mono-, di-, and trimethylated residues.

Methylation of histone tails recruits regulatory proteins involved in gene activation, gene repression, and DNA repair (Shukla, Chaurasia, & Bhaumik, 2009).

1.8.2.3 Ubiquitylation.

Ubiquitylation is the addition of an ubiquitin protein. H2A and H2B are monoubiquitylated on K119 and K120, respectively. Ubiquitylation is catalyzed by ubiquitin ligases, and deubiquitylation is catalyzed by deubiquitylases (Higashi, Inoue, & Takashi, 2010). Ubiquitylation of H2A enhances binding of H1 (Higashi et al., 2010). uH2A and uH2B have been implicated in transcriptional activation and elongation, as well as in transcription inhibition (Osley, 2006; Higashi et al., 2010).

1.8.3 Histone variant-containing nucleosomes.

Variant histones have different properties that affect the stability of the core nucleosome and thus alter chromatin structure. Their assembly into nucleosomes alters intra- and inter- nucleosome contacts. Incorporation of histone variants that stabilize such contacts promotes the formation of more inaccessible chromatin. Whereas incorporation of variants that destabilize such contacts promotes a more accessible chromatin formation.

H3.3-containing nucleosomes are less stable than those that contain H3 (Jin & Felsenfeld, 2007). Therefore, nucleosomes with H3.3 are typically associated with loci of active transcription. The stability of H3.3 containing nucleosomes is even further decreased if they also contain H2A.Z (Jin & Felsenfeld, 2007). Such nucleosomes are highly unstable and are often associated with the "nucleosome-free" promoter region of actively transcribing genes.

H2A.Bbd-containing nucleosomes are bound to only 118bp of DNA (Bao et al., 2004). Such nucleosomes are unstable and less compact than those containing H2A (Bao et al., 2004; Okuwaki et al., 2005). The stability of H2A.Bbd containing nucleosomes is decreased even further if they also contain H3.3 (Okuwaki et al., 2005).

MacroH2A-containing nucleosomes are assembled in heterochromatic regions. Nucleosomes containing macroH2A are tightly associated with DNA (Abbott et al., 2004). This tight association is independent of the acetylation state of other core histones (Abbott et al., 2004). MacroH2A-H2B dimers assembled into nucleosomes are resistant

to NAP-1-mediated H2A-H2B chromatin exchange (Chakravarthy & Luger, 2006). Furthermore, such nucleosomes are resistant to chromatin remodeling (Angelov et al., 2003). The stabilization of the nucleosome and nucleosome-DNA contacts through incorporation of macroH2A is well suited for gene silencing.

1.9 HSV-1 GENOMES ASSOCIATE WITH CHROMATIN PROTEINS DURING LYTIC INFECTION.

Micrococcal nuclease (MCN) preferentially cleaves linker DNA between nucleosomes. Consequently, MCN digestion of chromatin produces a typical ladder pattern of DNA fragments sized in multiples of approximately 150bp. MCN digestions of parental and progeny HSV-1 genomes from lytically infected cells demonstrated, approximately 30 years ago, that the ladder pattern of DNA fragments typical of regular cellular chromatin was absent from HSV-1 DNA (Mouttet, Guetard, & Bechet, 1979; Leinbach & Summers, 1980; Muggeridge & Fraser, 1986). The HSV-1 DNA that was accessible to MCN was digested mostly to heterogeneously-sized fragments (Mouttet et al., 1979; Leinbach & Summers, 1980; Muggeridge & Fraser, 1986). The MCN digestion of accessible HSV-1 DNA occurred at a faster rate than that of cellular chromatin, indicating that HSV-1 DNA is more readily digested by MCN than cellular DNA (Leinbach & Summers, 1980). From these classic experiments, it was concluded that HSV-1 genomes are largely not associated in nucleosomes during lytic infection. Recent ChIP experiments, however, have demonstrated that histones do associate with HSV-1 genomes during lytic infection. Histones were found bound

to HSV-1 genes of all kinetic classes (Herrera & Triezenberg, 2004; Kent et al., 2004; Huang et al., 2006; Oh & Fraser, 2008; Cliffe & Knipe, 2008; Placek et al., 2009; Kutluay & Triezenberg, 2009). However, only one group has reported that the level of H3 associated with HSV-1 genomes is equivalent to that of cellular genes, and even in this report, the level decreased with time post infection, independent of HSV-1 gene transcription or DNA replication (Cliffe & Knipe, 2008). In contrast, other groups have reported an increase in histone occupancy on HSV-1 genomes in the absence of transcription (Kutluay & Triezenberg, 2009). Core histone association with HSV-1 genomes occurs as early as one hour after infection (Kent et al., 2004; Placek et al., 2009).

Deposition of histones usually occurs through transcription, DNA replication, or DNA repair associated mechanisms. How histones are deposited on HSV-1 genomes remains to be determined. Association of histones with HSV-1 genes occurs prior to, or in the absence of, their transcription and prior to HSV-1 DNA replication (Herrera & Triezenberg, 2004; Placek et al., 2009; Kutluay & Triezenberg, 2009). The histones associated with lytic HSV-1 genomes tend to be enriched in PTMs associated with active transcription, such as H3K9Ac, H3K14Ac, H3K4me3, and depleted of PTMs associated with gene repression, such as H3K9me2 (Kent et al., 2004; Huang et al., 2006).

Although several groups have demonstrated that histones bind to HSV-1 genomes, the types of interactions of histones with HSV-1 genomes were not addressed. Histones were shown to bind to HSV-1 genomes, but the typical nucleosomal ladder pattern of chromatinized

DNA was absent following MCN digestions of HSV-1 genomes. Recently, work from our lab (Lacasse & Schang, 2010) has addressed this issue. MCN digestions in combination with biochemical fractionation were used to demonstrate that the majority of HSV-1 DNA is in unstable nucleosome complexes that fractionate with cellular mono- and di-nucleosomes. Consistently, the HSV-1 DNA accessible to MCN was digested with faster kinetics than cellular chromatin (Lacasse & Schang, 2010). Consistent with previous MCN studies, however, a percentage of HSV-1 DNA was more resistant to MCN digestion (Lacasse & Schang, 2010). The HSV-1 DNA that fractionated as cellular mono- and di-nucleosomes was protected from MCN digestion to heterogeneously sized fragments ranging in size from approximately 150 to 300 base pairs (Lacasse & Schang, 2010). Modification of the HSV-1 MCN digestion protocol such that unstable nucleosome complexes released during digestion were protected from subsequent degradation demonstrated that the majority of HSV-1 DNA is indeed complexed in unstable nucleosomes during lytic infection (Lacasse & Schang, 2010, Lacasse, PhD Thesis 2010, University of Alberta).

1.9.1 HSV-1 proteins disrupt chromatin.

HSV-1 transcription transactivators, ICP0, ICP4, and VP16, and the tegument protein VP22 interact with chromatin modifying proteins and even disrupt chromatin. The presence of ICP0, ICP4, VP16 and VP22 in the tegument, and the IE expression of ICP4 and ICP0, suggests that the disruption of chromatin and mediation of chromatin modifying protein activity may be important early during HSV-1 infection.

1.10 RATIONALE AND HYPOTHESIS.

Naked parental HSV-1 genomes enter the nucleus where they become unstably chromatinized. Such chromatinization is proposed to regulate the access of proteins required for HSV-1 gene expression and DNA replication and recombination to HSV-1 DNA. Chromatin association with HSV-1 genomes may represent cellular attempts to silence HSV-1 gene expression through blocking or hindering access of transcription proteins to HSV-1 DNA. However, HSV-1 uses cellular transcription complexes that normally transcribe cellular chromatin. Therefore, transcription of HSV-1 genes may also be enhanced or promoted by chromatin marks that recruit cellular transcription factors. Infections with HSV-1 strains with mutations in genes encoding for proteins that disrupt or modify chromatin proteins suggest that such functions are important for initiation of productive infection. In the absence of such activities, HSV-1 genomes are silenced (quiescent). Later during infection, however, the histones must be removed or displaced from progeny genomes, as only histone-free genomes are packaged into capsids. Histones and HSV-1 genomes therefore have dynamic associations during lytic infection.

These models involving chromatin regulation of HSV-1 gene expression during lytic infection have yet to address the source of the histones that associate with HSV-1 genomes. HSV-1 genomes enter the nucleus, where the vast majority of histones are complexed in cellular chromatin. Early during infection, host cell mRNA and protein synthesis is inhibited. Moreover, the majority of histone synthesis is synchronized

with cellular DNA replication, and HSV-1 infects cells at any stage of the cell cycle. It is therefore unlikely that the histones that first associate with HSV-1 genomes are newly synthesized. Consistent with this conclusion, the absolute levels of histone H3 do not change during HSV-1 infection.

Incorporation of histones into cellular chromatin is dynamic. Histones normally disassociate from chromatin, diffuse, and reassociate in chromatin at a different site. I propose that histones initially move from domains of cellular chromatin to those domains containing HSV-1 genomes. Later during infection, histones are subsequently displaced away from domains containing HSV-1 genomes. My model is that cells mobilize histones in an attempt to silence HSV-1 gene expression, and that HSV-1 further mobilizes histones to counteract or prevent such silencing attempts. Therefore, my ***hypothesis*** is that

Histones are mobilized during infection with Herpes simplex virus type 1 (HSV-1).

Amino acid	H3 variant		
position	H3.1	H3.2	H3.3
31	Ala	Ala	Ser
87	Ser	Ser	Ala
89	Val	Val	Iso
90	Met	Met	Gly
96	Cys	Ser	Ser

TABLE 1.1: Differences in the amino acid sequence of H3 variants.

CHAPTER 2: MATERIALS AND METHODS

2.1 CENTRIFUGES.

The following centrifuges were used. A Beckman Counter Avanti J-E centrifuge with a fixed angle JA-14 rotor (referred to as JA-14). An Eppendorf centrifuge 5810R with an A-4-62 swinging bucket rotor (referred to as SBR), and an eppendorf GE035 fixed angle rotor (referred to as GE035). A Beckman XL-90 Ultracentrifuge with a swinging bucket SW-40 rotor (referred to as SW-40).

Benchtop eppendorf microfuges, Beckkman Coulter microfuge 18 (model cat# 367160) or Fisher Scientific micro-centrifuge models 235C or 235A (at 4°C), are referred to as such.

2.2 CELLS, DRUGS, AND REAGENTS.

African green monkey kidney (Vero; CCL-81, ATCC, distributed by Cedarlane Laboratories Ltd., ON, CA), n-33 (an ICP4 expressing Vero cell line (Smith & Schaffer, 1987); a generous gift from Dr. P. Schaffer, University of Pennsylvania, Philadelphia, PA, USA), and MCF-7 (a human breast adenocarcinoma cell line, ATCC, distributed by Cedarlane Laboratories Ltd., ON, CA) cells were propagated in Dulbecco's Modified Eagle's Medium (DMEM, cat# 11885, Invitrogen, Burlington, ON, CA), supplemented with 5% fetal bovine serum (FBS; cat# A15-70, PAA Laboratories Inc., Etobicoke, ON, CA), 50U/ml penicillin and 50µg/ml streptomycin (cat# 15140, Invitrogen, Burlington, ON, CA), at 37°C in 5% CO_2. U2OS osteosarcoma cells (a generous gift from Dr. J. Smiley,

University of Alberta) and HeLa cells stably expressing H2B-GFP fusion proteins (Kanda, Sullivan, & Wahl, 1998) (a generous gift from Dr. Z. Wang, University of Alberta) were propagated in DMEM, supplemented with 10% FBS, 50U/ml penicillin and 50μg/ml streptomycin, at 37°C in 5% CO_2.

Phosphonoacetic acid (PAA; cat# 284270, Sigma-Aldrich, Oakville, ON, CA) was prepared by E. Newman (University of Alberta). It was diluted in DMEM as a 100mg/ml stock and the pH was adjusted to neutrality with 10N NaOH. The stock was filter sterilized, aliquotted, and stored at -20°C. PAA was added to inoculum at a concentration of 400μg/ml and maintained in the medium throughout the course of infection.

n,n`-hexamethylene-bisacetamide (HMBA; cat# 224235-10G, Sigma-Aldrich, Oakville, ON, CA) was prepared in DMEM as a 500mM stock and filter sterilized. Aliquots were stored at -20°C. HMBA was used at a concentration of 5mM.

Ampicillin (sodium salt; Amp, cat# 11593-027, Invitrogen, Burlington, ON, CA) was diluted in autoclaved milliQ water as a 50mg/ml stock. Aliquots were stored at -20°C. Ampicillin was used at a concentration of 50μg/ml.

Kanamycin [Kan; cat# KO254, Sigma-Aldrich, Oakville, ON, CA] was stored at 4°C and used at a concentration of 50μg/ml.

Proteinase K (recombinant PCR grade, cat# 03 115 801 001, Roche Diagnostics, Indianapolis, IN, USA) was prepared by J. Lacasse as

a 100mg/ml stock in 1X STE (0.1M NaCl, 1mM EDTA [pH 8.0], 10mM Tris [pH 8.0]) with 0.1% [w/v] SDS. Aliquots were stored at -20°C.

2.3 VIRUSES AND VIRUS STOCK PREPARATION.

Wild-type HSV-1, strain KOS (passage 10; Dr. P. Schaffer, University of Pennsylvania, Philadelphia, PA, USA), and mutant strains n12, n212, (Dr. P. Schaffer, University of Pennsylvania, Philadelphia, PA, USA) and KM110 (Dr. J. Smiley, University of Alberta) are described (SMITH, 1964; DeLuca & Schaffer, 1988; Cai & Schaffer, 1989; Mossman & Smiley, 1999).

For preparation of KOS stocks, Vero cells were seeded at 50-60% confluency in T-150 flasks and infected with 0.05 to 0.1 plaque forming units (PFU) per cell of HSV-1 in 3-4ml of DMEM. After 1h of adsorption at 33°C in 5% CO_2, rocking and rotating every 10 min, inocula were removed and cells were washed twice with 10ml of phosphate buffered saline (PBS; 150mM NaCl, 1mM KH_2PO_4, 3mM Na_2HPO_4, pH 7.4) at 4°C. Thirteen to 15ml of 33°C DMEM supplemented with 10% FBS was added, and the cells were further incubated at 33°C in 5% CO_2. Cells were harvested at 95% or greater cytopathic effect (CPE) and pelleted at 3,200x*g* for 20min at 4°C (SBR). Extracellular virions were pelleted from the resulting supernatant by centrifugation at 10,000x*g* for 2h at 4°C (JA-14). Intracellular virions were isolated from the cell pellet through three cycles of freezing in a dry ice-ethanol bath and thawing in a 37°C water bath, followed by sonication at 88W (15% output on a 550W XL2020 ultrasonic processor, Mandel Scientific Company Ltd.) three times for 30s each at 10s intervals. Cellular debris was pelleted by

centrifugation at 3,200x*g* for 20min at 4°C (SBR). Intra- and extracellular virions were combined for the viral stock. The viral stock was stored in DMEM in 20 to 100μl aliquots at -80°C. Virus titres were determined by plaque assay on Vero cells [Section 2.5].

Preparation of n212 stocks was as for KOS, except that U2OS cells were used. The viral stock was stored in DMEM in 200μl aliquots at -80°C. n212 titres were determined by plaque assay on U2OS cells. Parallel titrations on Vero cells ensured a minimum 100-fold reduction in titres.

Preparation of n12 stocks was as for KOS, except that n-33 cells were used. The n12 stock was stored in DMEM in 200μl aliquots at -80°C. n12 titres were determined by plaque assay on n-33 cells. Parallel titrations on Vero cells ensured that n12 was unable to replicate to any detectable level in this cell line.

For preparation of KM110 stocks, U2OS cells were seeded to 50% confluency in T-150 flasks and infected with 0.05 PFU per cell in 3-4ml of DMEM supplemented with 5mM HMBA. After a 1h incubation at 33°C in 5% CO_2, rocking and rotating every 10min, 10ml of 33°C DMEM supplemented with 10% FBS and 5mM HMBA were added. Cells were harvested at 95% or greater CPE, and virions were isolated as for KOS stock preparation. The viral stock was stored in DMEM in 600μl aliquots at -80°C. KM110 titres were determined by plaque assay on U2OS cells in the presence of 5mM HMBA. Parallel titrations on Vero cells ensured a minimum 1,000-fold reduction in titres.

2.4 UV INACTIVATION OF HSV-1.

A KOS stock was centrifuged at 10,000x*g* for 1.5h at 4°C (JA-14) and the pellet was resuspended, typically in 1ml of PBS at 4°C. An aliquot (100-200μl) was reserved to determine the original titre by plaque assay on Vero cells. Additional aliquots (50-100μl) were UV inactivated in a Stratalinker 1800 (Stratagene) or under a UV lamp in a biosafety cabinet and titrated by plaque assay. The remaining stock was frozen in a dry ice- ethanol bath and stored at -80°C while the aliquots were titrated. The conditions which resulted in a 5-6 order of magnitude reduction in titre were used to inactivate the remaining stock. A reduction of this magnitude still fully transactivates a VP16-inducible promoter (M. St. Vincent, Ph.D. thesis 2010, University of Alberta). Inactivated stocks were stored in PBS in 200μl aliquots at -80°C.

2.5 PLAQUE ASSAY.

Vero cells ($2x10^5$) were seeded in 6-well plates and incubated at 37°C in 5% CO_2 for a minimum of 4h before titration. Purified HSV-1 stocks were serially diluted in 4°C DMEM in 15ml snap-cap tubes. For the first dilution, 5μl of purified HSV-1 stock were added to 495μl DMEM and gently vortexed (100-fold dilution, 10^{-2}), 100μl were then removed and added to 900μl DMEM (10-fold dilution, 10^{-3}). All subsequent dilutions were also 10-fold. Cell monolayers were overlayed with 150μl of the HSV-1 dilutions (typically 10^{-3} to 10^{-8} for wild-type KOS stocks) and incubated at 37°C in 5% CO_2 for 1h with rocking and rotating every 10min. Inocula were removed and cells were washed twice with 1.5ml of

PBS at 4°C. Washed cells were then overlaid with 2-3ml of 37°C 0.5% methylcellulose in DMEM supplemented with 10% FBS. The infected cells were incubated at 37°C in 5% CO_2 until well defined plaques were visible in the cell monolayers, typically 3 to 4 days. Two millilitres of 1X crystal violet (CV; 1g CV per 100ml of 17% [v/v] methanol in water) were added and the plates were incubated overnight at room temperature. The plates were then washed by gentle agitation in a bucket of water and air dried at room temperature before counting plaques.

Titrations on U2OS cells were as for Vero cells except that $1.6x10^5$ cells were seeded per well. U2OS cells do not form tight monolayers so plaques are not always well defined. Therefore, plaques were counted using a microscope prior to the addition of crystal violet.

2.6 TRANSFORMATIONS.

2.6.1 Transformation with RIKEN cDNA clones PX00928G15, ZX00125P01, and ZX01012E07.

Spots corresponding to cDNA clones containing sequences encoding H2A (PX00928G15), H2B (PX01012E07), and H4 (ZX00125P01) were punched out of the RIKEN cDNA book and dissolved in 25μl of 1X TE (10mM Tris [pH 7.6], 1mM EDTA [pH8.0]) by Dr. I. Ismail (Cross Cancer Institute, University of Alberta). I was given 10μl aliquots of each solution, which still contained the paper pulp. The aliquots were centrifuged briefly in a tabletop eppendorf microfuge to pack the paper pulp. Five microlitres of each were then diluted with 5μl of 1X TE and put in a 15ml snap-cap tube on ice for transformation. Library efficiency DH5α chemically

competent cells (cat# 18263-012, Invitrogen, Burlington, ON, CA) were thawed on ice. Aliquots of 100µl were added to each DNA containing tube. DH5α cells and plasmid DNA were incubated on ice for 30min with occasional gentle mixing, heat shocked in a 42°C water bath for 45s, and chilled on ice for 2min. The cells were diluted with 900µl of SOC media (20g/L tryptone, 5g/L yeast extract, 9mM NaCl, 2.5mM KCl, 10mM $MgCl_2$, 20mM glucose; pH 7.0) at room temperature and incubated at 37°C with shaking at 225rpm for 1h. Two hundred microlitres of each transformation were spread on SOB agar plates (20g/L tryptone, 5g/L yeast extract, 9mM NaCl, 2.5mM KCl, 10mM $MgCl_2$, 15g/L agar; pH 7.0) containing 50µg/ml Amp and incubated at 37°C for 17h. A single colony from each plate was used to inoculate 40ml of Luria-Bertani media (LB; 10g/L tryptone, 5g/L yeast extract, 170mM NaCl; pH7.0) containing 50µg/ml Amp. The cultures were incubated at 37°C for 17h with shaking, typically at 240 to 260rpm. An aliquot of each culture was reserved, mixed with glycerol (to a final concentration of 15%), frozen in a dry ice-ethanol bath, and stored at -80°C. Plasmids were isolated from the remaining bacterial cultures by alkaline lysis midiprep [Section 2.7].

2.6.2 Transformation with plasmid DNA following ligation.

Ligation reactions were diluted with 1volume of 1X TE. Ten microlitres of each ligation were transferred to a 15ml snap-cap tube on ice for transformation. Transformation was done as in Section 2.6.1 with two exceptions. First, subcloning efficiency DH5α chemically competent cells (cat# 18265-017, Invitrogen, Burlington, ON, CA) were used. Second, the

liquid cultures were incubated following transformation for 1.5-2h at 37°C with shaking, typically at 240-260rpm. Two hundred microlitres of the cultures were plated on SOB agar (pH 7.0) plates containing 50μg/ml of the appropriate antibiotic, either Amp or Kan, and incubated at 37°C for 17h. LB (pH 7.0), typically 3ml, containing 50μg/ml of Amp or Kan was inoculated with a single colony from a plate and incubated at 37°C for 17h with shaking (typically 240-260rpm). An aliquot of the culture was reserved, mixed with glycerol (to a final concentration of 15%), frozen in a dry ice-ethanol bath, and stored at -80°C. Plasmids were isolated from the remaining bacterial culture using a miniprep kit, either a GenEluteTM plasmid miniprep kit (cat# PLN-70, Sigma-Aldrich, Oakville, ON, CA) or a QIAprep spin miniprep kit (cat# 27104, QIAGEN, Mississauga, ON, CA).

For the GenElute TM plasmid miniprep kit, all centrifugations were done in a tabletop eppendorf microfuge. Bacteria from the overnight culture were pelleted and resuspended in 200μl of resuspension solution (cat# R1149) containing ribonuclease A solution (cat# R6148). Lysis solution (200μl; cat# L 1912) was added and mixed by inversion. The bacterial lysate was neutralized with 350μl of neutralization solution S3 (cat# N5158), and the cellular debris was pelleted by centrifugation at 18,000x*g* for 10min. Meanwhile, the GenElute Miniprep binding column (cat # G6415) was assembled and 500μl of column preparation solution (cat# C2112) was centrifuged through the column at 18,000x*g* for 1min. The flow-through was discarded and the cleared lysate was added to the column. The binding

column was then centrifuged at 18,000x*g* for 1min and the flow-through discarded. The column was washed with 750μl of wash solution (cat# W 3886) diluted with ethanol and centrifuged at 18,000x*g* for 1min. The flow-through was discarded and the column was again centrifuged at 18,000x*g* for 1min to remove excess wash solution. The dry column was transferred to a new collection tube and the bound DNA was eluted with 80-100μl of elution solution (10mM Tris, 1mM EDTA, pH approximately 8.0; cat# E5650) or with autoclaved milliQ water.

For the QIAPrep Spin miniprep kit, all centrifugations were done in a tabletop eppendorf microfuge at room temperature. Bacteria from the overnight culture were pelleted and resuspended in 250μl of buffer P1 containing ribonuclease A. Buffer P2 (250μl) was added and mixed by inversion. The bacterial lysate was mixed with 350μl of buffer P3, and the cellular debris was pelleted by centrifugation at 18,000x*g* for 10min. The cleared lysate was pipetted into the QIAprep spin column and centrifuged at 18,000x*g* for 1min. The flow-through was discarded. The spin column was then washed with 750μl of buffer PE diluted with ethanol and centrifuged at 18,000x*g* for 1min. The flow-through was discarded and the column was again centrifuged at 18,000x*g* for 1min to remove excess buffer PE. The column was transferred to a new collection tube and the bound DNA was eluted with 50-100μl of buffer EB or with autoclaved milliQ water.

2.7 PREPARATION OF PLASMID DNA BY ALKALINE LYSIS MIDIPREP.

The following procedure for isolation of plasmid DNA was adapted from Protocol 2: Preparation of Plasmid DNA by Alkaline Lysis with SDS: Midiprep from *Molecular Cloning 3rd edition* by Sambrook and Russel.

LB media (typically 40ml; pH 7.0) containing 50μg/ml of the appropriate antibiotic (Kan or Amp) was inoculated with transformed bacteria, either from a single colony on an agar plate or from a frozen bacterial culture, and incubated at 37°C for 16 or 17h with shaking at 240-260rpm. The culture was divided into 10ml aliquots in 15ml snap-cap tubes and bacteria was pelleted by centrifugation at 3,200x*g* for 10min at 4°C (SBR). The bacterial pellets were resuspended in 2.5ml of 1X STE (0.1M NaCl, 1mM EDTA [pH 8.0], 10mM Tris [pH 8.0]) and re-pelleted by centrifugation at 3,200x*g* for 10min at 4°C (SBR). The bacterial pellets were then resuspended in 200μl of alkaline lysis solution I (50mM glucose, 25mM Tris [pH8.0], 10mM EDTA [pH8.0]) containing 0.1mg/ml ribonuclease A (RNase A; cat# R-4642, Sigma-Aldrich, Oakville, ON, CA) at 4°C and transferred to 1.5ml eppendorf tubes. Four hundred microlitres of freshly prepared alkaline lysis solution II (0.2N NaOH, 1% [w/v] SDS) were added to each bacterial suspension and mixed by inversion before placing on ice. The bacterial lysate was mixed with 300μl of alkaline lysis solution III (3M potassium acetate, 11.5% [v/v] glacial acetic acid) at 4°C and the lysis suspension incubated on ice for 3 to 5min. Cellular debris was pelleted at 18,000x*g* in a tabletop microfuge for 5min at 4°C. Six hundred microlitres of the cleared lysate

were transferred to a new 1.5ml eppendorf tube and extracted with an equal volume of phenol:chloroform (1:1). Plasmid DNA was precipitated from the aqueous phase with an equal volume of isopropanol and pelleted in a tabletop microfuge at 18,000x*g* for 5min at room temperature. The pelleted DNA was rinsed with -20°C ethanol, dried, and resuspended in 1X TE or in autoclaved milliQ water.

2.8 PHENOL FREEZE-FRACTION PURIFICATION OF DNA FROM AGAROSE GEL.

The DNA to be purified was resolved on a 1% low melting point (LMP) agarose gel and excised. The gel slice was placed in a 1.5ml eppendorf tube and weighed. For every 100mg of gel, 100µl of UltraPure buffer saturated phenol (pH7.5 to 7.8; cat# 15513-047, Invitrogen, Burlington, ON, CA) was added and the gel slice was subjected to three cycles of freezing at -20°C and thawing at room temperature. An equal volume of 1X TE was added and then the sample was frozen at -20°C. The frozen sample was centrifuged at 16,000x*g* for 30min at 4°C (GE035). The aqueous layer was extracted with an equal volume of chloroform, typically 3 times, and the organic layers were back-extracted with an equal volume of 1X TE. The DNA was precipitated from the aqueous phase with 0.1 volume of 3M sodium acetate and 0.7 volume of isopropanol, or with 3 volumes of ethanol, at -20°C for at least 1h and up to overnight. The DNA was pelleted by centrifugation at 16,000x*g* for 20 to 30min at 4°C (GE035).

2.9 PLASMIDS.

2.9.1 Green fluorescent protein (GFP)- H1 expression plasmids.

The GFP-H1 plasmids (GFP-H1^0, GFP-H1.1, GFP-H1.2, GFP-H1.3, GFP-H1.4, and GFP-H1.5) were described previously (Th'ng, Sung, Ye, & Hendzel, 2005). Briefly, DNA sequences encoding the H1 variants were amplified by polymerase chain reaction (PCR) from human neuroblastoma cell (SK-N-SH) genomic DNA. The 5` primer contained a flanking BglII restriction site and the 3` primer contained a flanking BamH1 site. These restriction sites were used for directional in-frame sub-cloning into pEGFP-C1 (Clontech, Mountain View, CA, USA).

2.9.2 GFP-H3.3 expression plasmid.

pEGFP-H3.3 plasmid was a generous gift from Dr. John Th'ng (Northern Ontario School of Medicine, Thunder Bay Regional Health Sciences Centre, Thunder Bay, ON, Ca). The DNA sequence encoding H3.3, with flanking 5` BglII and 3` EcoR1 restriction sites was sub-cloned into pEGFP-C1 (Clontech, Mountain View, CA, USA).

2.9.3 GFP-H2A.Za and GFP-H2A.Zv expression plasmids.

pGFP-H2A.Za and pGFP-H2a.Zv were a generous gift from Dr. J. Ausio, University of Victoria. DNA sequences encoding the H2A.Z variants were PCR amplified from cloned cDNA. The 5` primer contained a flanking Kpn1 restriction site and the 3` primer contained a flanking BamH1 restriction site. These restriction sites were used for directional in-frame sub-cloning into pEGFP-N1 (Clontech, Mountain View, CA, USA).

2.9.4 GFP-H2A expression plasmid.

The DNA sequence encoding H2A was PCR amplified from cDNA clone PX00928G15 obtained from the Riken Mouse cDNA library. The H2A primers contained flanking BglII (5`) and SalI (3`) restriction sites for directional in-frame sub-cloning into pEGFP-C1 (Clontech, Mountain View, CA, USA). The primer sequences and PCR conditions are listed in Tables 2.1 and 2.2, respectively. The H2A sequence was PCR amplified (eppendorf mastercycler gradient, model# 5531 13690) using Platinum *Pfx* DNA polymerase (cat# 11708, Invitrogen, Burlington, ON, CA) and the supplied *Pfx* amplification buffer (at 1X) in a final reaction volume of 20µl. The H2A PCR product was resolved on a 1% LMP agarose gel and purified by phenol freeze fractionation [Section 2.8].

pEGFP-C1 (2µg) and the agarose gel purified H2A PCR product were digested with 10 and 20U, respectively, of BglII (cat# 15213, Invitrogen, Burlington, ON, CA) in 1X React3 (R3; 50mM Tris [pH8.0], 10mM $MgCl_2$, 100mM NaCl) for 1.5h at 37°C. The digested DNA was extracted once with an equal volume of chloroform. Extracted DNA was precipitated with 3.5 volumes of ethanol at -20°C for 1h, and pelleted at 16,000*x*g for 20min at 4°C (GE035). DNA pellets were resuspended in 1X React10 (R10; 100mM Tris [pH7.6], 10mM $MgCl_2$, 150mM NaCl) in autoclaved milliQ water and digested with 10U (pEGFP-C1) or 20U (H2A PCR product) of SalI (cat# 15217, Invitrogen, Burlington, ON, CA) at 37°C for 1.5h. Digested DNA was extracted with an equal volume of chloroform, precipitated with 3.5 volumes of ethanol at -20°C, and pelleted by centrifugation at 16,000x*g* for 20min at 4°C (GE035). The

DNA pellets were resuspended in autoclaved MilliQ water. An aliquot of each was resolved on a 0.7% agarose gel to calculate DNA concentrations. The H2A PCR product was ligated to pEGFP-C1 with 0.1U T4 DNA ligase (cat# 15224-017, Invitrogen, Burlington, ON, CA) per ligation reaction in 1X DNA ligase reaction buffer (50mM Tris [pH 7.6], 10mM $MgCl_2$, 5% [w/v] polyethylene glycol-8000, 1mM dithiothreitol [DTT]) in autoclaved milliQ water. Ligation reactions had insert:vector molar ratios of 100:1, 200:1, and 500:1. The ligation reactions were incubated in a covered room temperature water bath for 27h. The clone of interest was obtained from colonies transformed with ligation reactions that had insert:vector molar ratios of 100:1 or 200:1.

The DNA sequence encoding the GFP-H2A fusion protein was confirmed by sequencing [Section 2.10]. A six amino acid linker (ser ala leu arg ser thr) joins GFP and H2A.

2.9.5 GFP-H2B expressing plasmid.

The DNA sequence encoding H2B was obtained from cDNA clone PX01012E07 from the Riken Mouse cDNA library. Clone PX01012E07 (27μg) and pEGFP-C1 (6μg; Clontech, Mountain View, CA, USA, Mountain View, CA, USA) were digested with 30 or 10U, respectively, of PstI (cat# 15215, Invitrogen, Burlington, ON, CA) in 1X React2 (R2; 50mM Tris [pH8.0], 10mM $MgCl_2$, 50mM NaCl) at 37°C for 2.75 or 2.5h, respectively. The digested DNA was extracted once with an equal volume of chloroform, precipitated with 3.5 volumes of ethanol at -20°C, and pelleted by centrifugation at 16,000x*g* for 15min at 4°C (GE035).

PX01012E07 and pEGFP-C1 pellets were resuspended in 1X R3 in autoclaved milliQ water and digested with 30 or 10U, respectively, of BglII at 37°C for 2 or 1.5h, respectively. Digested pEGFP-C1 was extracted once with an equal volume of chloroform, precipitated with 3.5 volumes of ethanol at -20°C, and pelleted by centrifugation at 16,000x*g* for 15min at 4°C (GE035). Digested PX01012E07 was resolved on a 1% LMP agarose gel and the 590 base pair band containing the sequence encoding H2B was excised. DNA was purified from the agarose by phenol freeze fractionation [Section 2.8]. The PX01012E07 and pEGFP-C1 DNA pellets were resuspended in autoclaved milliQ water. An aliquot of each was resolved on a 0.7% agarose gel to calculate DNA concentrations. The DNA fragment encoding H2B was ligated to pEGFP-C1 with 0.1U T4 DNA ligase per reaction in 1X DNA ligase reaction buffer in autoclaved milliQ water. The ligation reactions had insert:vector molar ratios of 50:1, 100:1, 200:1, and 500:1. Ligations were incubated in a covered room temperature water bath overnight. The clone of interest was obtained from colonies transformed with ligation reactions that had insert:vector molar ratios of 200:1 and 500:1.

In the resulting construct, pEGFP-H2B*, the sequence encoding H2B was not in frame with that encoding EGFP. A DNA linker (5`-AAGTCCGGAGAGCTCAAAGATCTCAAA -3`) was synthesized (Integrated DNA technologies [IDT], Biochemistry DNA Core Facility, University of Alberta) for insertion between the EGFP and H2B coding sequences. pEGFP-H2B* (3µg) and the DNA linker (2µg) were digested with 10U of BspEI (cat# R05405, New England Biolabs, Pickering, ON, CA) in 1X

NEBuffer 3 (100mM NaCl, 50mM Tris [pH7.9], 10mM $MgCl_2$, 1mM DTT) at 37°C for 2h. The digested DNA was chloroform extracted, precipitated with 3.5 volumes of ethanol at -20°C for 1h, and pelleted by centrifugation at 16,000x*g* for 20min at 4°C (GE035). The DNA pellets were resuspended in 1X R3 in milliQ water and digested with 10U of BglII at 37°C for 1.5h. The digested DNA was chloroform extracted, precipitated with 3.5 volumes of ethanol at -20°C, and pelleted by centrifugation at 16,000x*g* for 20min at 4°C (GE035). DNA pellets were resuspended in autoclaved milliQ water. An aliquot of each was resolved on a 0.7% agarose gel to calculate DNA concentration. The DNA linker was ligated with pEGFP-H2B* with 0.1U T4 DNA ligase per ligation reaction in 1X DNA ligase reaction buffer in milliQ water. Ligation reactions had insert:vector molar ratios of 100:1, 200:1, 500:1, and 1000:1. The reactions were incubated in a covered room temperature water bath for 27.5h. The clone of interest was obtained from colonies transformed with ligation reactions that had insert:vector molar ratios of 500:1 and 1000:1.

The DNA sequence encoding the GFP-H2B fusion protein was confirmed by sequencing [Section 2.10]. An eight amino acid (ser gly glu leu lys asp leu lys) linker joins GFP to H2B.

2.9.6 GFP-H4 expressing plasmid.

The DNA sequence encoding H4 was PCR amplified from cDNA clone ZX00125P01 obtained from the Riken Mouse cDNA library. The H4 primers contained flanking BglII (5`) and PstI (3`) restriction sites for

directional in-frame sub-cloning into pEGFP-C1 (Clontech, Mountain View, CA, USA, Mountain View, CA, USA). The primer sequences and PCR conditions are listed in Tables 2.1 and 2.2, respectively. The H4 sequence was PCR amplified (eppendorf mastercycler gradient, model# 5531 13690) using Platinum *Pfx* DNA polymerase (cat# 11708, Invitrogen, Burlington, ON, CA) with the supplied *Pfx* amplification buffer (at 1X) in a final reaction volume of 20μl. The H4 PCR product was resolved on a 1% LMP agarose gel and purified by phenol freeze fractionation [Section 2.8].

pEGFP-C1 (2μg) and the agarose gel purified H4 PCR product were digested with 10 or 20U, respectively, of BglII in 1X R3 at 37°C for 2h. The digested DNA was extracted once with an equal volume of chloroform, precipitated with 3.5 volumes of ethanol at -20°C, and pelleted by centrifugation at 16,000x*g* for 20min at 4°C (GE035). DNA pellets were resuspended in autoclaved milliQ water with 1X R2 and digested with 10U (pEGFP-C1) or 20U (H4 PCR product) of PstI at 37°C for 1.5h. Digested DNA was extracted with an equal volume of chloroform and precipitated with 3.5 volumes of ethanol at -20°C. Precipitated DNA was pelleted by centrifugation at 16,000x*g* for 20min at 4°C (GE035). The DNA pellets were resuspended in autoclaved milliQ water. An aliquot of each was resolved on a 0.7% agarose gel to calculate DNA concentrations. The H4 PCR product was ligated to pEGFP-C1 with 0.1U T4 DNA ligase per reaction in 1X DNA ligase reaction buffer in autoclaved milliQ water. Ligation reactions had insert:vector molar ratios of 100:1, 200:1, and 500:1. The ligations were incubated in a

covered room temperature water bath for 40h. The clone of interest was obtained from colonies transformed with ligation reactions that had an insert:vector molar ratio of 200:1.

The DNA sequence encoding the GFP-H4 fusion protein was confirmed by sequencing [Seciton 2.10]. A five amino acid linker (ser gly leu arg ser) joins GFP to H4.

2.10 PLASMID PURIFICATION FOR SEQUENCING.

The GFP-histone constructs, pEGFP-H2A, pEGFP-H2B, and pEGFP-H4, were confirmed by sequencing. Approximately 9μg of each plasmid was diluted in 100μl of 1X TE (pH 7.6) and purified using a QIAQuick PCR purification kit (cat# 28104,QIAGEN, Mississauga, ON, CA) as follows. All centrifugations were done in a tabletop microfuge at room temperature. The DNA in 1X TE was diluted with 5 volumes (500μl) of buffer PB. A QIAquick spin column was assembled in a collection tube, and the DNA was centrifuged through the column at 18,000x*g* for 1min. The flow-through was discarded. The bound DNA was washed with 750μl of buffer PE and the column was centrifuged at 18,000x*g* for 1min. The flow-through was discarded, and the column was centrifuged at 18,000x*g* for 1 min to remove any residual buffer PE. The QIAquick column was placed in a 1.5ml eppendorf tube. Forty microlitres of autoclaved milliQ water was put in the centre of the column and incubated at room temperature for 1min. DNA bound to the column was eluted by centrifugation at 18,000x*g* for 1min. The eluted DNA was resolved on a 0.7% agarose gel to calculate DNA concentration. The

purified plasmids were diluted to 125ng per µl in autoclaved milliQ water. Five microlitres of each were submitted to the Biochemistry DNA Core facility (University of Alberta) for sequencing using the standard CMV promoter (fwd) primer (5`-CGCAAATGGGCGGGTAGGCGTG) and the EGFP C Terminal primer (5`-CATGGTCCTGCTGGAGTTCGTG). Both primers were provided by the sequencing facility.

2.11 TRANSFECTIONS.

Vero (2-3 x10^5) or U2OS (1.4-2 x10^5) cells were seeded in 6-well plates and incubated at 37°C in 5% CO_2 overnight. Plasmid DNA was transfected using Lipofectamine 2000 (cat# P/N 52887, Invitrogen, Burlington, ON, CA). For each well to be transfected, 4µl or 2µl of Lipofectamine 2000 (for Vero or U2OS cells, respectively) was added to one 1.5ml eppendorf tube containing 100µl of DMEM. Plasmid DNA (typically 3 or 1.5µg for Vero or U2OS cells, respectively) was added to another 1.5ml eppendorf tube, also containing 100µl of DMEM. After a 10min incubation at room temperature, the lipofectamine in DMEM was added to the plasmid DNA in DMEM and gently mixed. Following additional 30 (U2OS) or 60 (Vero) min incubation at room temperature, the volume in each eppendorf was brought up to 1ml with room temperature DMEM. Media was then vacuumed from the cells and cells were overlaid with the transfection mix. The overlayed cells were incubated at 37°C in 5% CO_2 for 4h (U2OS) or 6h (Vero) before adding 1ml of 37°C DMEM supplemented with 10% FBS to each well. Cells were

further incubated at 37°C in 5% CO_2 for at least 12h, or 24h for GFP-H4, before any other procedure.

2.12 STERILIZATION OF COVERSLIPS.

Coverslips, 18 x 18mm (thickness 1; cat# 12-542A, Fisher Scientific, Ottawa, ON, CA) or 12mm diameter circle (thickness 1D; cat# 12-545-82, Fisher Scientific, Ottawa, ON, CA), were washed in 70% ethanol for at least 5min. They were then placed in a beaker of milliQ water and autoclaved. Prior to seeding cells, coverslips were placed in the wells of tissue culture plates and allowed to air dry overnight.

2.13 FLUORESCENCE RECOVERY AFTER PHOTOBLEACHING (FRAP).

Transfected cells were seeded onto sterile 18 x 18mm coverslips (thickness 1; cat# 12-542A, Fisher Scientific, Ottawa, ON, CA) in 6-well plates (typically, 3.4 to 4.0x10^5 Vero and 1.6 to 2.0x10^5 U2OS cells). Seeded cells were incubated at 37°C in 5% CO_2 for at least 4h before infection. Inoculum was prepared by diluting purified HSV-1 stocks in 4°C DMEM. For mock infections, 4°C DMEM (1ml) containing no virus was used. Cells were overlaid with 400µl of innocula and incubated at 37°C in 5% CO_2 for 1h, rocking and rotating every 10min. Inocula were removed and cells were washed twice with 1.5ml of PBS at 4°C. Cells were then overlaid with 2ml of 37°C DMEM supplemented with 5 or 10% FBS for Vero or U2OS cells, respectively, and incubated at 37°C in 5% CO_2.

Histone mobilization was evaluated from 4 to 5 or 7 to 8 hours post infection (hpi). Each slide was used for less than 1h of data collection to ensure cell viability. Slides were prepared as follows. A 1/2" round adhesive template was placed in the center of the slide. A thin layer of vacuum grease was applied around the template, which was then removed and replaced with media from the well containing the coverslip. The coverslip was mounted cell side down to form a sealed chamber. Isopropanol was applied to the end of the slide and run over the coverslip. The slide was then promptly placed on a heated (37°C) stage on a Zeiss NLO 510 multiphoton microscope. Cells were viewed on a 37°C 40x F-Fluor oil immersion objective lens (NA 1.3, WD 0.12mm). FRAP was performed using a 25mW Argon laser (488nm) with a band pass filter of 505-530nm and a pinhole of 1,000 (approximately 15 Airy units). A 1.5µm wide region passing across the cell nucleus was photobleached, typically with 30 iterations at 90 to 100% intensity. Fixed cells expressing GFP-histones were used as controls to ensure complete photobleaching. Whole cell imaging was performed at 0.5 to 1% intensity. Sixty fluorescent and DIC images (512 x 512, 12 bit) were collected for each experiment at timed intervals before and after bleaching. Images were analyzed with Zeiss LSM software. Contrast and brightness were adjusted for figure preparation with Adobe Photoshop.

2.14 IMMUNOFLUORESCENCE.

Transfected cells were seeded onto sterile 12mm diameter circle coverslips (thickness 1D; cat# 12-545-82, Fisher Scientific, Ottawa, ON, CA) in 24-well plates (typically, $1x10^5$ Vero and $0.8x10^5$ U2OS cells).

Seeded cells were incubated at 37°C in 5% CO_2 for at least 4h before infection. Inoculum was prepared by diluting purified HSV-1 stocks in 4°C DMEM. For mock infections, 4°C DMEM without virus was used. Cells were overlayed with 150µl of inocula and incubated at 37°C in 5% CO_2 for 1h, rocking and rotating every 10min. Inocula were removed and cells were washed twice with 1ml of PBS at 4°C. Washed cells were then overlaid with 1ml of 37°C DMEM supplemented with 5 or 10% FBS for Vero or U2OS cells, respectively, and incubated at 37°C in 5% CO_2.

At 4.5 or 7.5hpi, infected cells were washed with 4°C PBS and fixed with 5% formaldehyde at room temperature for 10 or 15 min. Fixed cells were washed four times with PBS at 4°C. All subsequent washes and incubations were performed at room temperature unless otherwise indicated. Cells were permeabilized with CSK buffer (0.5% [v/v] Triton X-100, 10mM PIPES [pH 6.8], 50mM NaCl, 300mM Sucrose, 3mM $MgCl_2$) for 6min or with -20°C 100% MeOH for 1min. After permeabilizing, the cells were washed three times with PBS for 5min. Cells were then incubated in 600µl of blocking buffer (4% [v/v] normal goat serum [cat# G9023-5ml, Sigma-Aldrich, Oakville, ON, CA], 2% [w/v] bovine serum albumin [Albumin fraction V from bovine blood, cat# 70195, United States Biochemical corp., Cleveland, OH, USA] in PBS) for 1h with slow rocking. The blocking buffer was removed and 500-600µl of mouse monoclonal α-ICP4 (cat# 1101-897, Goodwin Institute for Cancer Research Inc, Plantation, FL, USA) diluted 1:10,000 in blocking buffer was added. The cells were then further incubated for 2h with slow rocking. The primary antibody was removed and cells were washed twice

with 0.05% (v/v) Tween in PBS, or thrice with PBS, for 10min each. Following washing, cells were incubated with 500-600μl of AlexaFluor 594 conjugated goat anti-mouse IgG (H+L) (cat# A11005, Molecular probes, Invitrogen, Burlington, ON, CA) diluted 1:1,000 in blocking buffer for 1h with slow rocking. Cells were then washed twice with 0.05% (v/v) Tween in PBS, or thrice with PBS, for 10min each. To counterstain nuclei, cells were incubated with 500-600μl of Hoechst 33258 (cat# 861405, Sigma-Aldrich, Oakville, ON, CA) diluted to 0.2μg/ml in PBS for 5min. Cells were then washed twice with PBS for 5min. Coverslips were rinsed in milliQ water and mounted onto slides with Vectashield mounting medium (cat# H-1000, Vector Laboratories Inc., Burlingame, CA, USA). The coverslips were then sealed with clear nail enamel.

The cells were viewed on a Leica DM IRB microscope. In infections with wild-type HSV-1 strain KOS, a minimum of 90 transfected and 300 non-transfected cells from at least 2 experiments were counted for each GFP-H1 variant at 4 and 7hpi, except for GFP-H1^0, H1.4, and H1.5 7hpi in which a minimum of 50 transfected and 90 non-transfected cells were counted from one experiment. For infections with HSV-1 mutant strains, a minimum of 170 or 214 transfected and 488 or 414 non-transfected Vero or U2OS cells, respectively, were counted from at least 2 experiments, except for strain n212 at 4hpi in Vero cells transfected with GFP-H3.3, in which 60 transfected and 245 non-transfected cells were counted from one experiment, and at 7hpi in U2OS cells transfected with GFP-H3.3, in which 128 transfected and 168 non-transfected cells were

counted from one experiment. For Vero cells transfected with GFP-H3.3 and infected with UV-inactivated KOS, 25 and 40 transfected cells were counted at 4 and 7hpi, respectively, and 150 non-transfected cells were counted at 4 and 7hpi from one experiment. For U2OS cells infected with UV-inactivated KOS, a minimum of 80 transfected and non-transfected cells were counted at 4 and 7hpi from one experiment.

Confocal images were collected with Zeiss laser scanning confocal (LSM 510) or multiphoton (NLO 510) microscopes, on a 40x F-Fluor oil immersion objective lens (NA 1.3, WD 0.12mm) using 25mW Argon (488nm) and 1mW HeNe (543nm) lasers with band pass filters of 500-550 and 548-623 or a long pass filter of 560nm, respectively. Imaging was performed at 5 or 100% of the Argon or HeNe laser intensities, respectively, with pinholes set at approximately 1.5 Airy units for each. Fluorescent images (512 x 512, 12 bit) were analyzed with Zeiss LSM software. Image contrast and brightness were adjusted for figure preparation using Adobe Photoshop.

2.15 PROTEOMIC ANALYSIS OF NUCLEAR PROTEINS DURING HSV-1 INFECTION.

2.15.1 HSV-1 Infection.

MCF-7 cells were seeded in 100mM dishes and incubated overnight at 37°C in 5% CO_2. When the dishes were approximately 85% confluent ($4.9x10^6$ cells), the cells were mock infected or infected with 5PFU per cell of HSV-1 strain KOS. Inoculum was prepared by diluting purified HSV-1 stock in 4°C DMEM. For mock infections, 4°C DMEM containing no

virus was used. Cells were overlayed with 1.5ml of inocula and incubated at 37°C in 5% for 1h, rocking and rotating every 10min. Inocula was removed and cells were washed twice with 5ml of 4°C DMEM. Cells were overlayed with 10ml of 37°C DMEM with 5% FBS and incubated at 37°C in 5% CO_2.

2.15.2 Nuclear extract preparation.

At 6hpi, the cells were rinsed with 5ml of 4°C DMEM and trypsinized with 1X Trypsin in PBS (from 10X stock of 0.5% Trypsin EDTA; cat# 15400, Invitrogen, Burlington, ON, CA). Trypsinized cells were collected with 5-10ml of DMEM with 5% FBS, transferred to 50ml conical tubes, and pelleted by centrifugation at 245x*g* for 10min at 4°C (SBR). Cells were washed with 10ml of PBS at 4°C and re-pelleted by centrifugation at 245x*g* for 10min at 4°C (SBR). The pelleted MCF-7 cells were then resuspended in 1ml of PBS at 4°C and transferred to 1.5ml eppendorf tubes. The cells were then pelleted at 515x*g* for 10min at 4°C (GE035). The cell pellet was resuspended in five times the packed cell volume (PCV) of 1X lysis buffer (10mM HEPES [pH 7.9], 1.5mM MgCl2, 10mM KCl, 1mM DTT) at 4°C. Cells were then incubated on ice for 15min. For every 100µl of lysis buffer added to the cell pellet, 2µl of 10% (v/v) NP-40 were added. The cells were pulse vortexed at the maximum setting for 1s and pelleted by centrifugation at 1700x*g* for 5min at 4°C (GE035). The cytoplasmic fraction (supernatant) was transferred to a 1.5ml eppendorf tube, frozen in liquid nitrogen, and stored in a liquid nitrogen storage dewer. The nuclear pellet was washed once with 1ml of 1X lysis buffer at

4°C and re-pelleted by centrifugation at 1700x*g* for 5min at 4°C (GE035). The nuclear pellet was resuspended in two times the PCV of 1X nuclear extraction buffer (NEB; 20mM HEPES [pH 7.9], 1.5mM MgCl2, 420mM NaCl, 0.2mM EDTA [pH 8.0], 25% [v/v] glycerol, 1mM DTT) at 4°C and the nuclei rotated for 30min at 4°C. Extracted nuclei were pelleted at 16,000x*g* for 10min at 4°C (GE035). The nuclear extract (supernatant) was removed to a 1.5ml eppendorf and reserved.

2.15.3 Reductive alkylation and trichloroacetic acid (TCA) precipitation of the nuclear extract.

The protein concentration of nuclear extracts prepared from mock and HSV-1 infected MCF-7 cells [Section 2.15.2] was determined by Bradford's assay. Five hundred micrograms of each nuclear extract were aliquotted for reductive alkylation and TCA precipitation. DTT (one hundredth volume of 1M) was added to the extracts, and the extracts were incubated at 30°C for 30min. Freshly prepared 500mM iodoacetic acid (IAA; cat# I8136, Sigma-Aldrich, Oakville, ON, CA) was diluted in the extracts to a final concentration of 5mM. The extracts were then incubated at 30°C for an additional 30min. The IAA reaction was quenched with 0.1 volume of 1M DTT for 30min at 30°C. Proteins were precipitated from the nuclear extracts with 1 volume of 40% (w/v) TCA (cat# TX1045-1, EMD Chemicals, Gibbstown, NJ, USA) for 15min at 4°C. Precipitated proteins were pelleted at 16,000x*g* for 15min at 4°C (GE035) and the supernatant aspirated.

2.15.4 Proteomic analysis.

The protein pellets obtained in Section 2.15.3 were shipped to Dr. A. Emilie at the CH Best Institute in Toronto, ON, Canada for mass spectrometry analysis.

2.16 ICP4 WESTERN BLOT.

2.16.1 HSV-1 Infection.

n-33 (1.9 x10^5) cells were seeded in 12-well plates and incubated at 37°C in 5% CO_2 for at least 4h. Cells were mock infected or infected with 5 PFU per cell of HSV-1, strains KOS or UV-inactivated KOS. Inoculum was prepared by diluting purified HSV-1 stocks in 4°C DMEM. For mock infections, 100µl of 4°C DMEM containing no virus was used. Cells were overlayed with 100µl of inocula and incubated at 37°C in 5% CO_2 for 1h, rocking and rotating every 10min. Inocula were removed, cells were washed twice with 1ml of PBS at 4°C, and overlaid with 1ml of 37°C DMEM supplemented with 5% FBS. Infected cells incubated at 37°C in 5% CO_2.

2.16.2 Preparation of whole cell lysate.

At 2 or 4hpi, infected cells were washed twice with 0.5-1ml of PBS at 4°C. Cells were lysed with 60µl of Nonidet P-40 (NP-40; cat# N-3516, Sigma-Aldrich, Oakville, ON, CA) lysis buffer (150mM NaCl, 1% [v/v] NP-40, 50mM Tris [pH 7.6]) at 4°C by incubating on ice for 20min with occasional rocking. Lysates were collected and transferred to 1.5ml eppendorf tubes before sonication at 88W (15% output on a 550W XL2020 ultrasonic processor) 6 times for 20s each at 10s intervals.

Cellular debris was pelleted at 16,000x*g* for 15min at 4°C (GE035). The resulting cleared supernatant was reserved for western blot.

2.16.3 Semi-dry protein transfer.

Volumes of lysates [Section 2.16.2] from an equivalent number of cells were used for the following procedures. SDS-polyacrylamide gels (8% resolving, 5% stacking) were prepared and resolved using a BioRad Miniprotean 3 system. Cell lysates were loaded and resolved at 50V (8V/cm) for 30min then at 100V (15V/cm) for 1h at room temperature. After resolution, the gel was equilibrated in cathode buffer (0.1% [w/v] SDS, 1X Tris-CAPS [pH 9.6]) for 30min. A pre-cut PVDF membrane (0.2μM; BioRad, Mississauga, ON, CA) was equilibrated in anode buffer (15% MeOH, 1X Tris-CAPS [pH 9.6]) for 30min. During the last 10min, 2 pieces of thick chromatography paper (cat# 05-714-4; Fisher Scientific, Ottawa, ON, CA) were added to the cathode buffer, and two to the anode buffer. The transfer stack was assembled in a semi-dry transfer apparatus (trans-blot SD semi-dry transfercell; BioRad, Mississauga, ON, CA) as follows. The two chromatography papers soaked in anode buffer were layered onto the anode of the transfer apparatus and the gel was placed on top of the papers. The membrane was placed on top of the gel and then the two chromatography papers soaked in cathode buffer were added to the stack. Proteins were transferred onto the PVDF membrane at a constant current of $2mA/cm^2$ (~100mA) for 1h at room temperature.

2.16.4 Detection of ICP4.

Following transfer, the membrane was incubated in 10ml of blocking buffer (1:1 Odyssey Blocking buffer [cat# 927-4000, LI-COR Biosciences, Lincoln, NE, USA]:PBS) for 1h at room temperature with slow rocking. The blocking buffer was removed and the PVDF membrane was further incubated for 20h at 4°C with slow rocking in 10ml of mouse monoclonal α-ICP4 (cat# ab6514, Abcam, Cambridge, MA, USA) diluted 1:5,000 in blocking buffer. The membranes were then washed three times for 5min each in 0.1% (v/v) Tween in PBS and once with PBS at room temperature. After washing, the membranes were incubated for 1h with slow rocking at room temperature with 10ml of goat anti-mouse IgG (H+L) conjugated with AlexaFluor 680 (cat# A21058; Molecular Probes, Invitrogen, Burlington, ON, CA) or IRDye 800 (cat# 610-132-121; Rockland Immunochemicals Inc., Mississauga, ON, CA), and diluted 1:10,000 in blocking buffer. Membranes were then washed three times with 0.1% (v/v) Tween in PBS at room temperature for 5min each and once with PBS. The membrane was scanned using a LI-COR Biosciences Odyssey Infrared Imaging system. Protein standards and AlexaFluor 680 were detected in the 700nm channel and IRDye 800 in the 800nm channel.

Product		Restriction site	Sequence (5` to 3`)	Tm (°C)
H2A	forward	BglII	ATAAGATCTACTATGTCTGGACGTGGTAAGCA	58.8
	reverse	SalI	ATTGTCGACTCTGTTGCTTATTTCCCCTTGG	63.7
H4	forward	BglII	TAAAGATCTATGTCTGGTCGTGGCAAGGG	62.3
	reverse	PstI	TAACTGCAGTTAACCGCCGAATCCGTAGAG	65.3

TABLE 2.1: PCR Primers.
Primers used to amplify sequences encoding H2A and H4 from cDNA plasmids PX00928G15 and ZX00125P01, respectively. Primers were designed using Vector NTI Advance 10 software (Invitrogen). The restriction site sequence is underlined.

	PCR Amplification Product	
	H2A	H4
Forward primer	6pmol	6pmol
Reverse primer	6pmol	6pmol
Template	10ng	10ng
dNTP	0.3µM	0.3µM
Platinum *Pfx* polymerase	1.25U	1.25U
$MgSO_4$	0.5mM	0.5mM
Annealing Tm:		
First 6 cycles	41.5-50.7°C	43.1-53.5°C
Subsequent 14 cycles	51.5-60.7°C	53.1-63.5°C

TABLE 2.2: Conditions for PCR amplification of H2A and H4. Conditions used to amplify sequences encoding H2A and H4 from cDNA plasmids PX00928G15 and ZX00125P01, respectively.

CHAPTER 3: LINKER HISTONES ARE MOBILIZED DURING INFECTION WITH HERPES SIMPLEX VIRUS TYPE 1 (HSV-1)

A version of this Chapter was published in the Journal of Virology:

Linker Histones are Mobilized during Infection with Herpes Simplex Virus Type 1. Conn, K.L., Hendzel, M.J., and Schang, L.M.

(Sept. 2008) Vol. 82 (No. 17) p.8629-8646.

ABSTRACT

Histones interact with herpes simplex virus type 1 (HSV-1) genomes and localize to replication compartments early during infections. However, HSV-1 genomes do not interact with histones in virions and are deposited in nuclear domains devoid of histones. Moreover, late viral replications compartments are also devoid of histones. The processes whereby histones come to interact with HSV-1 genomes, to be later displaced, remain unknown. However, they would involve the early movement of histones to the domains containing HSV-1 genomes and the later movement away from them. Histones unbind from chromatin, diffuse through the nucleoplasm, and rebind at different sites. Such mobility is upregulated by, for example, phosphorylation or acetylation. We evaluated whether HSV-1 infection modulates histone mobility, using fluorescence recovery after photobleaching. All somatic H1 variants were mobilized to different degrees. H1.2, the most mobilized, was mobilized at 4h and further so at 7h after infection, resulting in increases in its

"free" pools. H1.2 was mobilized to a "basal" degree under conditions of little to no HSV-1 protein expression. This basal mobilization required nuclear native HSV-1 genomes but was independent of HSV-1 proteins and most likely due to cellular responses. Mobilization above this basal degree, and increases in H1.2 free pools, however, depended on immediate-early or early HSV-1 proteins, but not on HSV-1 genome replication or late proteins. Linker histone mobilization is a novel consequence of cell-virus interactions, which is consistent with the dynamic interactions between histones and HSV-1 genomes during lytic infection; it may also participate in the regulation of viral gene expression.

3.1 INTRODUCTION.

HSV-1 is a nuclear replicating DNA virus that undergoes latent or lytic infections in neurons or epithelial cells, respectively. The infecting viral genomes are delivered to nuclear domains adjacent to ND10s, domains that are devoid of cellular chromatin (Ascoli & Maul, 1991; Ishov & Maul, 1996; Maul, Ishov, & Everett, 1996). Lytic HSV-1 genomes then replicate in these domains forming small replication compartments. The compartments grow and coalesce into large replication compartments, which later occupy large nuclear domains (Lukonis, Burkham, & Weller, 1997; Sourvinos & Everett, 2002; Taylor et al., 2003). Infected nuclei grow, and cellular chromatin becomes marginalized, to accommodate the growth of the replication compartments (Monier et al., 2000; Simpson-Holley et al., 2005).

Nuclear DNA is typically complexed in chromatin. The basic unit of chromatin is the nucleosome core particle, 146 base pairs (bp) of DNA

wrapped around a core histone octamer of two molecules each of H2A, H2B, H3, and H4. Linker histone H1 binds to DNA at the sites where it enters and exits the core nucleosome, promoting the formation of higher order chromatin structures. Latent HSV-1 genomes are regularly chromatinized and, with exception of LAT, transcriptionally silent (Stevens, Wagner, Devi-Rao, Cook, & Feldman, 1987; Deshmane & Fraser, 1989; Arthur et al., 2001). Digestion of latent HSV-1 genomes with micrococcal nuclease (MCN) consequently produces a "ladder" of DNA fragments sized in multiples of 146bp (Deshmane & Fraser, 1989). Transcriptionally active lytic HSV-1 genomes, in contrast, are not regularly chromatinized and their digestion with MCN mainly produces heterogeneously sized DNA fragments (Mouttet et al., 1979; Leinbach & Summers, 1980; Muggeridge & Fraser, 1986). They were therefore classically considered not to interact with histones. However, chromatin immunoprecipitation (ChIP) analyses have demonstrated that core histones bind to HSV-1 genomes (Herrera & Triezenberg, 2004; Kent et al., 2004; Huang et al., 2006; Oh & Fraser, 2008), as well as a relative depletion of H3, or enrichment of H3 bearing modifications of transcribed chromatin, at active HSV-1 promoters (Herrera & Triezenberg, 2004; Kent et al., 2004; Huang et al., 2006). Recently, it was demonstrated that HSV-1 genomes associate with proteins in unstable complexes that co-purify with cellular mono- and dinucleosomes (Lacasse & Schang, 2010). It is now commonly accepted that HSV-1 genomes interact with histones during lytic infection too.

The expression of HSV-1 genes is temporally regulated. The immediate early (IE) genes are expressed first, followed by the early (E) and then the late (L) ones. The virion protein VP16, in complex with two cellular proteins (OCT-1 and host cell factor; HCF-1) binds to TAATGARAT sequences in IE promoters and recruits cellular general transcription factors and RNA polymerase II (RNAPII). The immediate early proteins ICP0 and ICP4 then activate E gene transcription (Everett, 1984). However, the specific mechanisms of E gene transactivation by ICP0 or 4 are not yet fully characterized. They do not activate transcription by binding to specific DNA sequences and, consequently, they even activate transcription driven by non-HSV-1 promoters recombined into HSV-1 genomes (Smiley et al., 1987; Smibert & Smiley, 1990).

Consistent with histones binding to lytic HSV-1 genomes, all HSV-1 transcription transactivators disrupt chromatin. VP16 promotes the depletion of H3 from HSV-1 genomes, and recruits histone modifying, and other chromatin remodeling, complexes characteristic of transcription activation (Tumbar et al., 1999; Wysocka et al., 2003; Memedula & Belmont, 2003; Herrera & Triezenberg, 2004). High mobility group proteins (HMG) enhance the transactivation activity of ICP4 (Panagiotidis & Silverstein, 1999), and they also compete with H1 for chromatin binding sites (Catez, Brown, Misteli, & Bustin, 2002; Catez et al., 2004). ICP0 induces the degradation of centromere proteins such as CENP A, an H3 variant (Everett et al., 1999; Lomonte et al., 2001; Lomonte & Morency, 2007). ICP0 also disrupts histone modifying

complexes associated with chromatin condensation or inactivation of transcription (Lomonte et al., 2004; Gu et al., 2005; Gu & Roizman, 2007).

In the absence of functional VP16, ICP0, and ICP4, HSV-1 genomes are transcriptionally inactive or "quiescent" (Harris & Preston, 1991; Preston & Nicholl, 1997). Quiescent HSV-1 genomes associate with histones, too, and the chromatin associated with these genomes contains modifications and proteins characteristic of silenced heterochromatin (Samaniego, Neiderhiser, & DeLuca, 1998; Everett, Murray, Orr, & Preston, 2007; Coleman et al., 2008). In the absence of only two transcriptional activators, VP16 and ICP0 (as in the mutant strain KM110), HSV-1 also establishes quiescent infections in some cells, such as Vero, but replicates (with delayed kinetics) in others, such as U2OS (Mossman & Smiley, 1999). Even in the absence of only one transactivator, such as in the ICP0 mutant strain n212, HSV-1 replicates with delayed kinetics in some cell types (Vero) (Cai & Schaffer, 1992).

The associations of histones with HSV-1 genomes during lytic infection are not yet fully characterized. Nonetheless, HSV-1 genomes are associated in unstable complexes that co-purify with cellular mono- and dinucleosomes, and histones H1 and H2B localize to early replication compartments (Monier et al., 2000; Simpson-Holley et al., 2004; Simpson-Holley et al., 2005). HSV-1 genomes are not associated with histones within virions, however, and are deposited in nuclear domains adjacent to ND10s, which are devoid of cellular chromatin (Ascoli & Maul, 1991; Ishov & Maul, 1996; Maul et al., 1996; Oh & Fraser, 2008).

The viral replication compartments are again depleted of histones (H1, H2B, H4, and serine 10-phosphorylated H3) later during infection (Spencer, Kruhlak, Jenkins, Sun, & Bazett-Jones, 2000; Monier et al., 2000; Simpson-Holley et al., 2004; Simpson-Holley et al., 2005). Presently, the processes whereby histones come to interact with HSV-1 genomes early after infection, to be displaced later on remain unknown. However, histones normally disassociate or are displaced from chromatin, diffuse, and re-bind at different sites. Such mobilization is regulated by, for example, competition for the chromatin binding sites or post-translational modifications. I therefore evaluated whether HSV-1 infection deregulates histone mobilization.

Here I show that linker histones are mobilized during HSV-1 infection, resulting in increases in the pools of "free" H1. Nuclear native HSV-1 genomes, but not HSV-1 proteins, were required for basal H1.2 mobilization, whereas IE or E HSV-1 proteins were required to further enhance H1.2 mobilization and increase its free pool. Such H1.2 mobilizations are consistent with IE or E HSV-1 protein expression inducing or requiring them. In either case, mobilization of linker histones during HSV-1 infection is a novel consequence of cell-virus interactions that is consistent with the dynamic interactions between histones and HSV-1 genomes. Histone mobilization could also play a role in the regulation of viral gene expression.

3.2 RESULTS.

3.2.1 Somatic linker histone variants are differentially mobilized in HSV-1 infected cells.

My first objective was to test whether histones are mobilized in HSV-1 infected cells. To this end, we used fluorescence recovery after photobleaching (FRAP) in cells expressing green fluorescent protein (GFP)-histone H1 fusion proteins. GFP-H1 fusion proteins behave as endogenous H1, and moderate levels of expression do not adversely affect the expressing cells (Lever, Th'ng, Sun, & Hendzel, 2000; Misteli, Gunjan, Hock, Bustin, & Brown, 2000). However, the effects of GFP-H1 fusion protein expression on HSV-1 replication were unknown. I therefore first analyzed ICP4 expression in cells expressing different GFP-H1 fusion variants (see Table 3.1 for H1 variant nomenclatures). Progression of HSV-1 infection, as evaluated by immunofluorescence against ICP4, was not adversely affected by the expression of moderate levels of any GFP-H1 variant (Figure 3.1). Cells expressing any of the GFP-H1 variants had similar expression of ICP4, and also similar ICP4 accumulation, into replication compartments at 4 or 7 hpi as cells not expressing any GFP-H1 (Figure 3.1, examples of ICP4 as nuclear diffuse or in replication compartments in cells expressing GFP-H1; Figure 3.2, quantitation). The nuclear localization of GFP-H1 was maintained even at late times post infection (Figure 3.1, Figure 3.3). Furthermore, these experiments confirmed previously published results that have shown histones co-localizing with early replication compartments but partly displaced from them at late times (Figure 3.1, rightmost panels).

As a first test for histone mobilization, I analyzed the FRAP recovery kinetics of different GFP-H1 variants in Vero cells infected for 7h with HSV-1 KOS. Mobilization was evaluated by the time to recover 50% of the original fluorescence (T_{50}) in the photobleached area (Figure 3.4). Mobilization and T_{50} are inversely related, such that a higher degree of mobilization results in a shorter T_{50} (Figure 3.4). All H1 variants except for H1.4 were significantly mobilized in cells infected with 30 PFU/cell of KOS ($P<0.05$) (Table 3.2, Figure 3.5), although the individual variants were differentially mobilized. H1.2 was mobilized the most; its T_{50} was reduced to less than half (42.3%) of that in mock-infected cells (T_{50}, 6.9 ± 0.5 and 14.8 ± 0.4s, respectively) (Table 3.2, Figure 3.5). The HSV-1 and mock-infected cells shown in Figure 3.5 C, for example, were equally photobleached with the same laser intensity and duration. However, H1.2 was mobilized to such extent that the fluorescence in the photobleached region of the infected cell had already recovered at 4s to a greater degree than in the mock infected one. H1.1, H1.5, $H1^0$, and H1.3 were also mobilized, but to lesser degrees (T_{50} reduced to 57%, 59%, 63%, and 64% of those in mock-infected cells) (Table 3.2). H1.4 was apparently mobilized as well (T_{50} 66% of that in mock-infected cells), but the mobilization was not statistically significant ($P = 0.08$) (Table 3.2, Figure 3.5). Consistently, the fluorescence in the photobleached region in the HSV-1 infected cell expressing GFP-H1.4 had recovered to a similar degree as in the mock infected one at 4s (Figure 3.5 D).

The differential average mobilization of the H1 variants could have resulted from differential mobilization of each variant in all infected cells,

or to similar mobilization of each variant in different sized sub-populations of infected cells. Therefore, I evaluated the percentage of cells with the highest H1 mobilization, defined as those in which the T_{50} was lower than one standard deviation below the average T_{50} in mock-infected cells. A similar percentage of infected cells had mobilized H1.1 or H1.5 to this extent (75% and 71%, respectively), and H1.1 and H1.5 were also mobilized on average to a similar degree (57% and 59% of mock, respectively) (Table 3.2). However, more cells had mobilized H1.5 than $H1^0$ to this extent (71% and 52% respectively), although these variants were also mobilized on average to a similar degree (59% and 63% of mock, respectively) (Table 3.2). The differential mobilization of each H1 variant is therefore a combination of the degree of mobilization in each cell together with the size of the population of cells that mobilize H1 to a certain degree.

H1 may be mobilized by cellular or viral factors. To identify such putative factors, I focused on H1.2, a variant that is biologically relevant for HSV-1. H1.2 is expressed in all cells that HSV-1 infects and its expression is cell-cycle independent. Moreover, H1.2 was mobilized the most and the vast majority of infected cells (92%) had mobilized H1.2 to more than one standard deviation below the average T_{50} in mock infected cells.

3.2.2 H1.2 is already mobilized at early times post infection but it is further mobilized at later times.

I had initially evaluated mobilization at 7hpi, when all HSV-1 proteins are expressed and HSV-1 genomes are replicated. HSV-1 transcription,

protein expression, DNA replication, or cellular responses to them, may therefore contribute to the mobilization of linker histones. The number of different HSV-1 proteins expressed, their levels, and the number of viral genomes increases as infection proceeds. I therefore also evaluated H1.2 mobility at early times post infection. H1.2 was already significantly mobilized at 4hpi ($P<0.01$) when IE and E proteins are expressed to high levels. Its T_{50} was decreased to 72% or 62% in cells infected with 10 or 30 PFU/cell, respectively (T_{50}, 9.3 ± 0.7 or 7.3 ± 0.6s, respectively) (Table 3.3, Figure 3.6 A). H1.2 was further mobilized at 7hpi, when IE, E, and L proteins are expressed and genomes are replicated. Its T_{50} was decreased to 61% or 42% in cells infected with 10 or 30 PFU/cell, respectively (T_{50}, 9.4 ± 1.0 or 6.9 ± 0.5s, respectively) ($P<0.01$) (Table 3.3, Figure 3.6 A). These results suggest that expression of specific HSV-1 proteins or HSV-1 DNA replication enhances H1.2 mobilization.

Concomitantly with the increase in H1.2 mobilization, the population of cells with the highest H1.2 mobilization had also increased from 4 to 7hpi (from 36% to 63%, or 61% to 92% for cells infected with 10 or 30 PFU/cell, respectively) (Table 3.3, Figure 3.6 B). The size of this population was also dependent on multiplicity of infection. At both early and late times, a larger population of cells infected with 30 than with 10 PFU/cell had such high H1.2 mobilization.

The mobilization of H1.2 may result from changes in its low- or high- affinity binding to chromatin, or in the residence time (the time that it is bound to chromatin). I next evaluated the time required to

recover 90% of the original fluorescence in the photobleached region (T_{90}) (Figure 3.4). Whereas T_{50} is influenced the most by low affinity binding, T_{90} is influenced the most by high affinity binding. As with T_{50}, H1.2 T_{90} was decreased in HSV-1 infected cells at early and late times post infection (30 PFU/cell 4 and 7hpi and 10 PFU/cell 7hpi, $P<0.01$; 10 PFU/cell 4hpi, n.s.) (Table 3.3, Figure 3.6 A). Moreover, the relative decreases in H1.2 T_{50} and T_{90} were not significantly different from each other ($P>0.05$). Thus, the mobilization of H1.2 resulted from changes in both low- and high- affinity chromatin binding.

To address whether the mobilization of H1.2 affected the residence time, I evaluated the level of H1.2 in the so-called free pool (i.e., not bound to chromatin). The surrogate measure for the free pool is the level of recovery of fluorescence at the first time point after photobleaching (Figure 3.4). Fixed cells show no recovery (i.e. complete bleaching) at this (or any other) time point. The recovery of fluorescence in live cells at the first time point therefore reflects only the very rapidly diffusing histone molecules, which are considered unbound to chromatin (i.e., "free"). The pool of free H1.2 was significantly increased to 119 ± 5% in Vero cells infected with 10 or 30 PFU/cell of KOS at 4hpi, and remained increased at 7hpi (to 141 ± 7% or 174 ± 6%, respectively) ($P<0.01$) (Table 3.4, Figure 3.7). The relative binding to, and dissociation or displacement from, chromatin is therefore differentially altered in infected cells, such that a larger population of H1.2 is not bound to chromatin at any given time.

To evaluate the percentage of infected cells with an increased pool of free H1.2, I considered the cells with the largest pools of free H1.2,

defined as those in which such pool was greater than one standard deviation above the average level of free H1.2 in mock-infected cells. More than 50% of cells had pools of free H1.2 increased to this extent at any time (Table 3.4). Therefore, the level of free H1.2 is increased throughout the population of infected cells.

Early and late H1.2 mobilizations therefore occur through changes to both low- and high- affinity binding to chromatin. Furthermore, the chromatin residence time of H1.2 is altered such that there is a net increase in the pool of H1.2 not bound to chromatin at any given time.

3.2.3 H1.2 mobilization does not require VP16 or ICP0, whereas free H1.2 increases in their absence only if HSV-1 proteins are expressed.

To test whether specific HSV-1 proteins contributed to H1.2 mobilization, I used the HSV-1 strain KM110, which is mutated in ICP0 (stop codon at codon 212) and VP16 (stop codon at codon 422) (Mossman & Smiley, 1999). KM110 fails to activate IE gene expression and, as a result, cannot replicate in Vero cells.

ICP4 was undetectable in more than 90% or 85% of cells infected with 30 PFU/cell of KM110 at 4 or 7hpi, respectively (Table 3.5, Figure 3.8, KM110 Vero), regardless of whether they expressed GFP-H1.2 or not. In the cells in which it was detected, ICP4 was mainly nuclear diffuse. Less than 2% of cells had ICP4 accumulation into (mostly small) replication compartments (Table 3.5, Figure 3.8, KM110 Vero). H1.2 was nonetheless mobilized at early and late times, independently of multiplicity of infection (10, 30, or 60 PFU/cell; $P>0.05$, pairwise

comparisons, Tukey's honestly significantly different-HSD). I therefore analyzed all multiplicities together. H1.2 T_{50} was decreased to 80% of mock-infected cells at 4 or 7hpi in cells infected with 10, 30, or 60 PFU/cell (T_{50} = 11.6 ± 0.3s) ($P<0.01$) (Table 3.3, Figure 3.9, KM110 Vero). Like in KOS infected cells, H1.2 mobilization in KM110 infected cells was a result of changes in both low- and high- affinity binding. H1.2 T_{50} and T_{90} were decreased to similar extents ($P>0.05$) (Table 3.3). In contrast to cells infected with KOS, however, neither the average H1.2 mobilization nor the size of the population with the highest mobilization of H1.2 were further increased at later times.

Although H1.2 was mobilized, the average levels of free H1.2 were not increased at either early or late times post infection (at 10, 30, or 60 PFU/cell) ($P>0.05$) (Table 3.4, Figure 3.7, KM110). The relative rates of H1.2 binding and dissociation or displacement were therefore equally altered such that there was no net increase in the pools of free H1.2.

Taken together, these results show that the "basal" mobilization of H1.2 was independent of VP16 and ICP0, and occurred under conditions in which there was little to no HSV-1 transcription or protein expression. In contrast, VP16, ICP0, HSV-1 transcription, specific HSV-1 proteins, or genome replication are required to enhance the basal mobilization of H1.2, and to increase its free pool. Alternatively, the increase in the pool of free H1.2 may be required for HSV-1 gene expression.

Both VP16 and ICP0 disrupt chromatin. To test whether their biochemical activities were directly involved in H1.2 mobilization, I analyzed KM110 infections of U2OS cells. U2OS cells complement the

replication defects of HSV-1 mutants in ICP0 or VP16 (Yao & Schaffer, 1995). Consequently, all HSV-1 proteins are expressed and HSV-1 DNA is replicated during KM110 infection of U2OS cells (Mossman & Smiley, 1999). U2OS cells, however, do not complement any of the known biochemical activities of ICP0 or VP16.

At 4hpi, 47% of U2OS cells infected with 30 PFU/cell of KM110 had nuclear diffuse ICP4, whereas 27% had accumulated it into replication compartments (Table 3.5, Figure 3.8, KM110 U2OS). At 7hpi, 26% of cells had nuclear diffuse ICP4, whereas 63% had it accumulated into replication compartments (Table 3.5, Figure 3.8, KM110 U2OS). Cells expressing GFP-H1.2 or not had similar expression of ICP4, and similar ICP4 accumulation into replication compartments (Figure 3.8, KM110 U2OS).

H1.2 was mobilized in U2OS cells in the absence of VP16 and ICP0. At early times post infection, however, the degree of mobilization was dependent on multiplicity of infection. H1.2 was significantly mobilized in U2OS cells infected with 30 PFU/cell (83% of mock-infected cells; $P<0.01$) but not in those infected with 10 PFU/cell (96% of mock infected cells; $P>0.05$) (Table 3.6, Figure 3.9, KM110 U2OS). At later times, H1.2 was further mobilized and the degree of mobilization was no longer dependent on multiplicity ($P>0.05$, Tukey's HSD). H1.2 T_{50} was decreased to 54% of that in mock infected cells in cells infected with 10 or 30 PFU/cell of KM110 (T_{50} = 5.9 ± 0.4s) (Table 3.6, Figure 3.9, KM110 U2OS). H1.2 was thus further mobilized at later times, alongside the increase in the number and levels of HSV-1 proteins expressed.

As in Vero cells, the mobilization of H1.2 at early and late times was a result of changes to both low- and high- affinity chromatin binding. H1.2 T_{90} was decreased to a similar extent as T_{50} for both multiplicities evaluated (T_{90} vs. T_{50} $P>0.1$) (Table 3.6). Further like KOS infected Vero cells, free H1.2 was increased in KM110 infected U2OS cells in a multiplicity independent manner ($P>0.05$, Tukey's HSD). Free H1.2 was increased to 113 ± 3% ($P<0.05$) at 4hpi and to 149 ± 4% ($P<0.01$) at 7hpi (Table 3.4, Figure 3.10, KM110).

H1.2 was equally mobilized at late times in U2OS cells infected with KM110 or KOS, although the cells had to be infected with lower multiplicities of KOS because of the major distortion of nuclear morphology at high multiplicities. Nonetheless, H1.2 T_{50} was reduced to 66% or 40% in U2OS cells infected with 6 PFU/cell of KOS at 4 or 7hpi, respectively (T_{50}, 8.0 ± 0.6 or 5.8 ± 0.4s, respectively) ($P<0.01$) (Table 3.6, Figure 3.9, KOS U2OS). Concomitantly, H1.2 T_{90} was also decreased at early and late times (Table 3.6). As expected, free H1.2 was increased to 116 ± 6% at 4, and to 178 ± 6% at 7hpi ($P<0.01$) (Table 3.4, Figure 3.10, KOS). The biochemical activities of VP16 or ICP0 were therefore not required in U2OS cells to increase the pool of free H1.2, or to enhance its mobilization.

3.2.4 The degree of H1.2 mobilization and increase in free H1.2 are associated with HSV-1 protein expression or DNA replication.

I next infected Vero cells with the ICP0 mutant strain n212 to test whether progression of infection was required to mobilize H1.2 above the basal level. n212 carries the same ICP0 mutation as KM110, but has

wild-type VP16 (Cai & Schaffer, 1989). Unlike KM110, n212 genes are expressed and its DNA is replicated in Vero cells, although both are delayed at low multiplicities of infection (Cai & Schaffer, 1989).

As expected (Cai & Schaffer, 1989), 78% of cells infected with 30 PFU/cell of n212 had nuclear diffuse ICP4 at 4hpi and only 11% had accumulated it into replication compartments, in comparison to 40% and 52%, of cells infected with wild-type KOS, respectively (Table 3.5, Figure 3.8). The population with ICP4 accumulated into replication compartments increased to 56% at 7hpi, whereas that with nuclear diffuse ICP4 decreased to 37%, in comparison to 78% and 9% in cells infected with wild-type KOS, respectively (Table 3.5, Figure 3.8). ICP4 accumulation into replication compartments was thus delayed relative to that in KOS infected cells, but it was still independent of H1.2 (Figure 3.8, n212 Vero).

H1.2 was also significantly mobilized in n212 infected Vero cells ($P<0.01$). In contrast to KOS infected ones, however, the mobilization was multiplicity dependent. At 4hpi, H1.2 T_{50} was decreased to 74%, 72%, and 54% in cells infected with 10, 30, or 60 PFU/cell of n212, respectively (T_{50}, 9.9 ± 0.6, 8.7 ± 0.6, and 7.0 ± 0.8s, respectively) ($P<0.05$ 10-60, 30-60 PFU/cell, Tukey's HSD) (Table 3.3, Figure 3.9, n212 Vero). H1.2 T_{50} was also decreased in a multiplicity dependent manner at 7hpi, to 64%, 54%, or 41% in cells infected with 10, 30, or 60 PFU/cell, respectively (T_{50} = 9.3 ± 0.9, 7.1 ± 0.6, or 5.0 ± 0.7s, respectively) ($P<0.01$ 10-60 PFU/cell, Tukey's HSD) (Table 3.3, Figure 3.9, n212 Vero).

As in infections with KOS, H1.2 mobilization in n212 infected Vero cells was the result of changes to low- and high- affinity chromatin binding. Moreover, there was also a net increase in the pools of free H1.2. In contrast to KOS infected cells, however, the increase in free H1.2 in n212-infected cells was also dependent on multiplicity ($P<0.05$ 10-60, 30-60 PFU/cell, Tukey's HSD). At 4hpi, free H1.2 was significantly increased ($P<0.01$) to 115 ± 4% and 136 ± 8% in cells infected with 30 or 60 but not in cells infected with 10 PFU/cell (Table 3.4, Figure 3.7, n212). At 7hpi, the increases in the pools of free H1.2 were no longer dependent on multiplicity ($P>0.05$, Tukey's HSD). Free H1.2 was increased to 152 ± 9%, 145 ± 5%, or 161 ± 9% in cells infected with 10, 30, or 60 PFU/cell (Table 3.4, Figure 3.7, n212).

U2OS cells complement ICP0 mutations, such that n212 replicates with the same kinetics as wild-type HSV-1. As expected, H1.2 was mobilized in U2OS cells infected with n212 ($P<0.01$) in a multiplicity independent manner ($P>0.05$ at 4 and 7hpi, Tukey's HSD). At either multiplicity evaluated (10 or 30 PFU/cell), H1.2 T_{50} was reduced to 55% and further to 44% at 4 or 7hpi, respectively (T_{50} = 5.2 ± 0.3 and 4.8 ± 0.4s, respectively) (Table 3.6, Figure 3.9, n212 U2OS). Low- and high-affinity chromatin binding were equally affected (T_{90} vs. T_{50}; $P>0.05$ for 10 and 30 PFU/cell at 4hpi and 10 PFU/cell at 7hpi, $P<0.05$ for 30 PFU/cell at 7hpi) (Table 3.6). As expected, the pools of free H1.2 were also significantly increased in a multiplicity independent manner ($P>0.05$ at 4 and 7hpi, Tukey's HSD). Free H1.2 was increased to 152 ± 3% and 184 ± 4% at 4 and 7hpi, respectively ($P< 0.01$) (Table 3.4, Figure 3.10, n212).

The degree of H1.2 mobilization and the increase in free H1.2 were dependent on multiplicity of infection under conditions in which expression of HSV-1 proteins and genome replication are also dependent on multiplicity. Therefore, HSV-1 transcription, specific HSV-1 proteins, or genome replication are involved in enhancing H1.2 mobilization and increasing the levels of free H1.2. Alternatively, enhanced H1.2 mobilization or increase in free H1.2 may be required for HSV-1 transcription or DNA replication.

3.2.5 Neither the enhanced mobilization of H1.2 nor the increase in the levels of free H1.2 require HSV-1 DNA replication.

I next evaluated H1.2 mobility under conditions in which HSV-1 DNA replication was inhibited. To this end, infected cells were treated with 400μg/ml phosphonoacetic acid (PAA) to inhibit the HSV-1 DNA polymerase (Schang, Rosenberg, & Schaffer, 2000).

H1.2 was still significantly mobilized in Vero cells infected with KOS in the presence of PAA ($P>0.01$). H1.2 T_{50} was decreased to 34% of control at 7hpi in Vero cells infected with 30 PFU/cell of KOS and treated with PAA (T_{50} = 7.4 ± 1.0s) (Table 3.7, Figure 3.11 A, B, and D, the same degree as in the absence of PAA ($P>0.05$) (Table 9, Figure 11 A and B). Also as in the absence of PAA, H1.2 mobilization was the result of changes to low- and high- affinity chromatin binding (T_{90} vs. T_{50}; $P>0.05$ for 30 PFU/cell of KOS treated with PAA at 7hpi) (Table 3.7). Moreover, there was still a net increase in the pool of free H1.2 ($P<0.01$). Free H1.2 was increased to 161 ± 7% at 7hpi in PAA-treated cells infected with 30 PFU/cell of KOS (Figure 3.11 C, Table 3.7), as in the cells not treated

with PAA (P>0.05). HSV-1 genome replication or strictly late HSV-1 proteins are therefore not required for the enhanced late mobilization of H1.2 or to increase its free pool.

3.2.6 Infecting virions with cross-linked genomes are not sufficient to mobilize H1.2.

H1.2 was still mobilized to a basal level in Vero cells infected with KM110, although the vast majority of cells had little to no detectable ICP4 expression. Virion fusion with the host cell membrane or virion proteins (other than VP16 and ICP0) may therefore be sufficient to induce the basal mobilization of H1.2. I thus evaluated the mobilization of H1.2 in cells infected with UV inactivated KOS, which fuses with the host cell and releases capsid and tegument proteins but expresses no HSV-1 genes. As expected, ICP4 expression was not detected in Vero or U2OS cells infected with 30 PFU/cell of UV inactivated KOS (Table 3.5, Figure 3.8, UV).

H1.2 was not mobilized at any time in either Vero or U2OS cells infected with UV inactivated KOS, even at multiplicities of 60 PFU/cell (P>0.05) (Table 3.3, Table 3.6, Figure 3.9, UV). Furthermore, the pools of free H1.2 were not increased at any time in either Vero or U2OS cells infected with any multiplicity (10, 30, or 60 PFU/cell) (Table 3.4, Figure 3.7 and Figure 3.10, UV). Viral fusion, capsid and tegument proteins (other than VP16 or ICP0), or cross-linked HSV-1 genomes were therefore not sufficient to induce H1.2 mobilization or to increase its free pool.

3.3 DISCUSSION.

Here I show that linker histones are mobilized during HSV-1 infection. Mobilization of H1.2 resulted from changes to low- and high- affinity chromatin binding and led to a net increase in its free pool. H1.2 was mobilized to a basal degree under conditions of little to no HSV-1 gene expression (KM110 infection of Vero cells). However, mobilization was further increased above the basal degree, and the pool of free H1.2 increased, only if IE and E HSV-1 proteins were expressed. Such increases were independent of HSV-1 genome replication or L proteins.

Each of the somatic H1 variants except H1.4 were significantly mobilized during HSV-1 infection, although each was mobilized to a different degree and in differently sized sub-populations of cells. H1.2 was the most readily mobilized, whereas $H1^0$ was the least. H1.2 is also ubiquitously expressed, including in epithelial cells and fibroblasts (Pehrson & Cole, 1982; Lennox & Cohen, 1983), and is therefore biologically relevant for lytic HSV-1 infections. $H1^0$, in contrast, is enriched in differentiated cells, such as neurons (Pehrson & Cole, 1982; Lennox & Cohen, 1983). Its restricted mobilization may therefore be more relevant to latent infections.

Approximately 40% of total nuclear H1.2 was in the free pool at 7h after infection (Table 3.4 Vero 7hpi KOS 30), when histone synthesis is inhibited (Yager & Bachenheimer, 1988; Sorenson et al., 1991; Spencer et al., 1997). The increase in free H1.2 was therefore most likely from pre-existing pools, such as those in cellular chromatin. H1 mobilization occurs through modulation of its binding to, and dissociation or

displacement from, chromatin. Mobilization during infection may have resulted from promoting dissociation of H1.2 from chromatin, decreasing its affinity for chromatin binding, or competition for its binding sites.

The basal mobilization of H1.2 under conditions of little to no HSV-1 protein expression (Figure 3.9, Table 3.3) was not due to virion fusion with the cell membrane or to proteins in the infecting virions (other than VP16 or ICP0). Infection with UV-inactivated HSV-1 did not induce it. Therefore, structural virion proteins or lipids are not sufficient to induce basal H1.2 mobilization, but non-structural viral proteins are not required either. These results suggest that the basal mobilization of H1.2 is triggered by the presence of nuclear native (i.e., non-cross linked) viral DNA.

KM110 did not induce the late enhancement of H1.2 mobilization in Vero cells, although it did so in complementing U2OS cells, in which its replication was restored (Figure 3.9). The lack of enhanced mobilization of H1.2 in KM110 infections of Vero cells may have resulted from the inhibition of HSV-1 transcription or of expression of specific IE or E proteins. Conversely, the failure to further mobilize H1.2 may have resulted in the inhibition of HSV-1 transcription and protein expression.

In contrast to the mobilization during productive infection, basal mobilization of H1.2 during non-productive infection did not result in an increase in its free pool (compare KM110 in Figure 3.7 and Figure 3.10). Under these latter conditions, H1.2 binding to chromatin was therefore altered such that there was an increased rate of exchange, but the rates of chromatin binding and dissociation or displacement were not altered

relative to each other. HSV-1 proteins therefore alter the H1.2 chromatin exchange rates such that there is an increase in its free pool.

Linker histones were therefore mobilized during HSV-1 infection. Mobilization of H1.2 to a basal degree only required nuclear, transcription competent, HSV-1 genomes. Such requirements suggest that this mobilization does not result from viral proteins, but rather from cellular mechanisms. Foreign nuclear DNA is potentially detrimental to the cell. Expression of foreign genes could have adverse affects on cell growth or survival. Cellular mechanisms may have evolved to detect and subsequently silence gene expression from such DNA. Mobilization of histones would increase the population of histones that would initially be available to bind to foreign DNA, and silence it. Basal mobilization of H1.2 in response to nuclear HSV-1 genomes is consistent with such mechanisms.

H1.2 was further mobilized, increasing its free pool, when HSV-1 immediate-early or early proteins were expressed. Expression of specific IE or E proteins may therefore be directly or indirectly required for the enhanced mobilization of H1.2. Alternatively, the enhanced mobilization of H1.2 may be required for transcription of HSV-1 IE or E genes. In either scenario, further mobilization of H1.2 suggests an HSV-1 mechanism to counteract cellular silencing of HSV-1 genomes.

FIGURE 3.1 Expression of ICP4 as nuclear dispersed or accumulated into replication compartments in Vero cells expressing GFP-H1.2. Digital fluorescent micrographs of Vero cells expressing GFP-H1.2 and stained with α-ICP4 antibodies. Cells were transfected with plasmids expressing green fluorescent protein (GFP) fused to H1.2 and infected with 30 PFU/cell of HSV-1 strain KOS. Cells were fixed at 4.5 (**4**) or 7.5 (**7**) hpi as indicated and stained for ICP4. Single (**α-ICP4**, **GFP-H1.2**, **DIC**) and merged (**Merge**) images are shown. Cells with ICP4 expressed as nuclear diffuse (**ND**) or replication compartments (**RC**) are indicated. Rightmost panels, 16x digital enlargement of the regions indicated by the boxes on the leftmost "merge" images, highlighting the colocalization of H1.2 and ICP4 signals (pixels in different shades of yellow and orange)

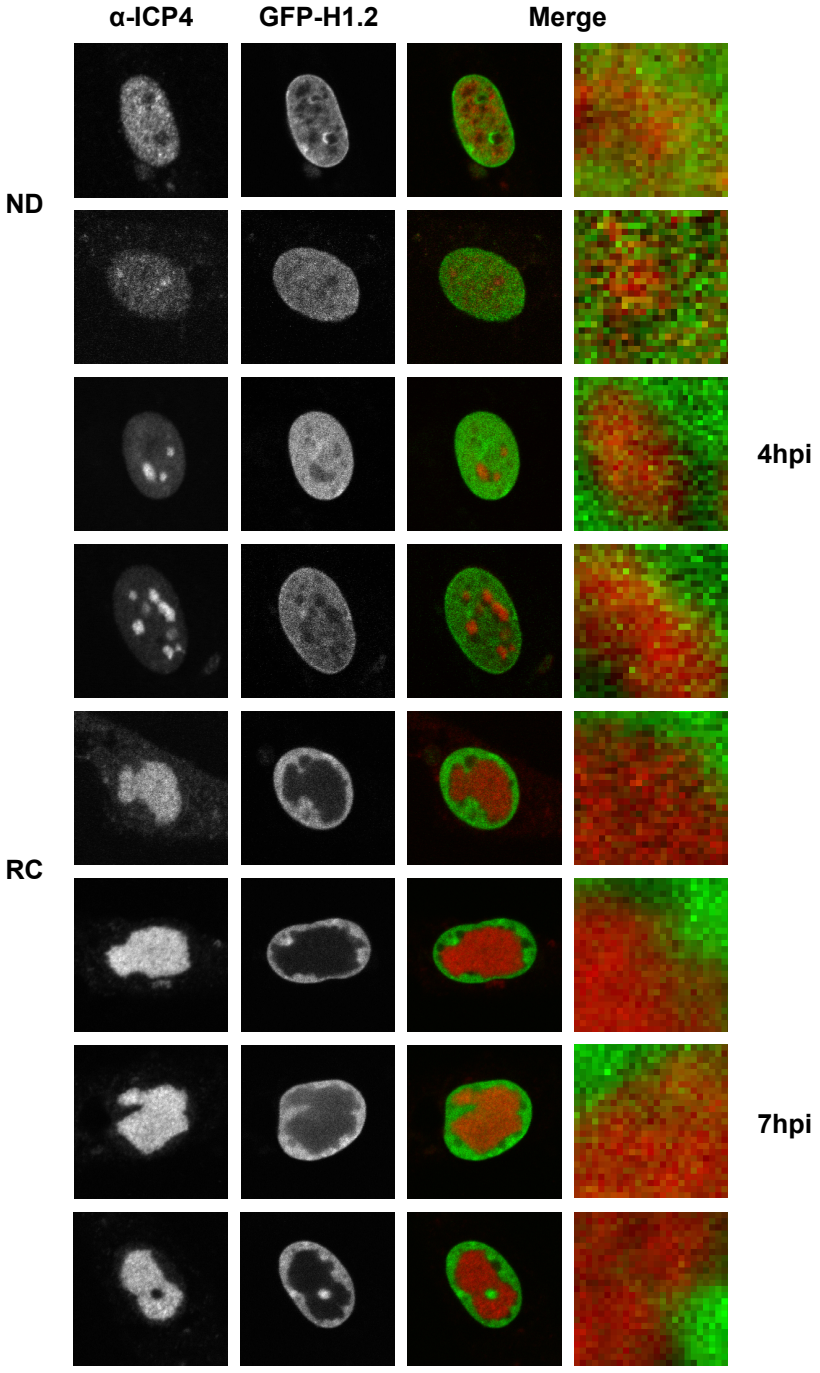
α-ICP4
GFP-H1.2
Merge
ND
RC
4hpi
7hpi

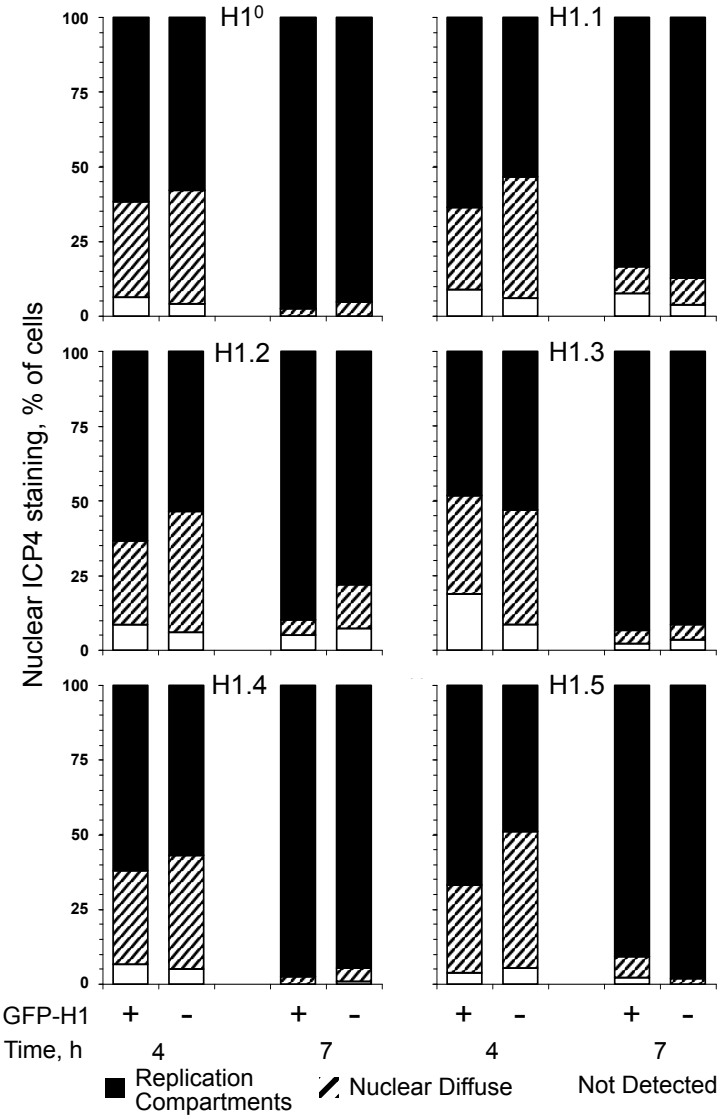

FIGURE 3.2: ICP4 expression and accumulation into replication compartments in Vero cells expressing or not GFP-H1 somatic variants. Bar graph representing the percentage of HSV-1 infected cells transfected with each GFP-H1 somatic variant and expressing ICP4 as nuclear diffuse or accumulated into replication compartments. Vero cells were transfected with plasmids expressing GFP fused to each H1 somatic variant (**H1^0**, **H1.1**, **H1.2**, **H1.3**, **H1.4**, or **H1.5**), infected with 30 PFU/cell of HSV-1 strain KOS, fixed at 4.5 (**4**) or 7.5 (**7**) hpi and stained for ICP4. Nuclear expression of ICP4 and accumulation into replication compartments (see Figure 3.1) in cells in which GFP-H1 was expressed (**+**) or not (**-**) was evaluated by fluorescence microscopy.

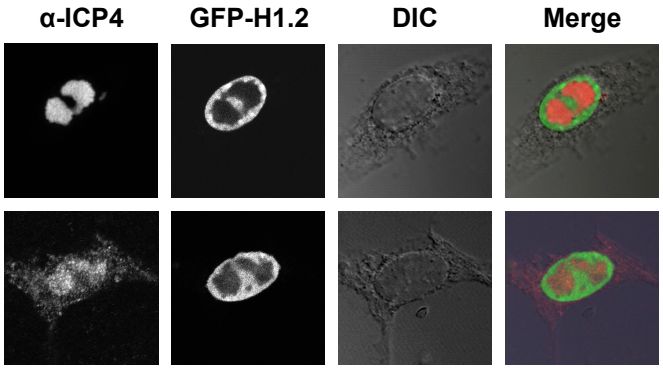

FIGURE 3.3: Expression of GFP-H1.2 in HSV-1 infected Vero cells is strictly nuclear. Digital fluorescent micrographs of Vero cells expressing GFP-H1.2 and stained with α-ICP4 antibodies. Cells were transfected with plasmids expressing GFP fused to H1.2 and infected with 30 PFU/cell of HSV-1 strain KOS. Cells were fixed at 7.5 (**7**) hpi and stained for ICP4. Single (**α-ICP4**, **GFP-H1.2**, **DIC**) and merged (**Merge**) images are shown. Cells show strictly nuclear localization of GFP-H1.2 regardless of whether the ICP4 signal is nuclear (top) or nuclear and cytoplasmic (bottom). The GFP-H1.2 images are over-exposed to highlight the lack of cytoplasmic signal.

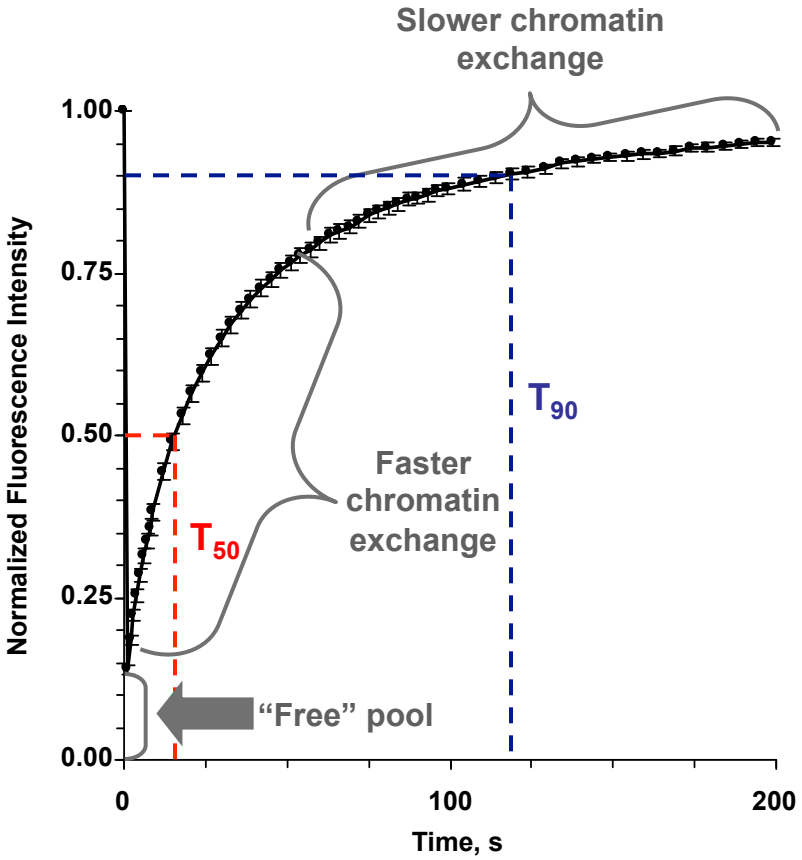

FIGURE 3.4: Linker histone fluorescence recovery after photobleaching. Line graph representing the relative fluorescence intensity of the photobleached nuclear region in a cell expressing GFP-H1 fusion proteins plotted against time. Time is plotted on a linear scale. The first measure after photobleaching is indicative of the population of core histones not bound to chromatin and therefore freely diffusing. Fluorescence recovery is biphasic. The early fast recovery phase represents the population of core histones with faster chromatin exchange, whereas the slow recovery phase represents the population with slower chromatin exchange. T_{50}, the time required for 50% of the initial fluorescence intensity to be recovered, is used as a surrogate measure to evaluate fast chromatin exchange. T_{90}, the time required for 90% of the initial fluorescence intensity to be recovered, is used as a surrogate measure to evaluate slow chromatin exchange.

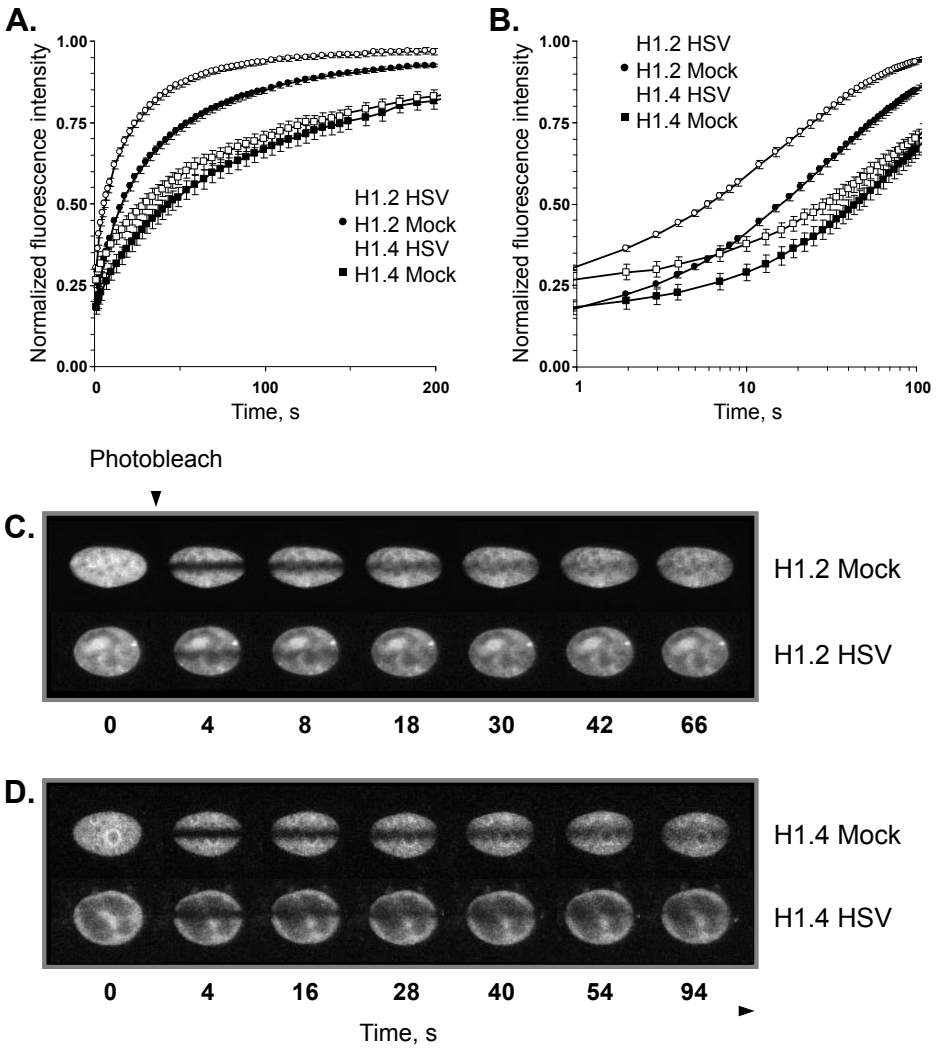

FIGURE 3.5: Somatic linker histone variants are differentially mobilized in HSV-1 infected cells. A) Line graphs representing the normalized fluorescence intensity of the photobleached nuclear region against time. Vero cells were transfected with plasmids expressing GFP fused to H1.2 (**circle**) or H1.4 (**square**). Transfected cells were mock-infected (**filled**) or infected with 30 PFU/cell of HSV-1 strain KOS (**open**). Nuclear mobility of each GFP-H1 variant was examined from 7 to 8hpi by fluorescence recovery after photobleaching (FRAP). Error bars, SEM; n≥15; time plotted on a linear scale. **B)** Same data presented on a semi-logarithmic scale. Lines indicate the times when 50% of the original relative fluorescence is recovered (T_{50}). **C-D)** Composite images of Vero cells expressing GFP-H1.2 (**C**) or GFP-H1.4 (**D**) infected as described in **A**. Images were collected prior to (**0**), or at the indicated times after, photobleaching.

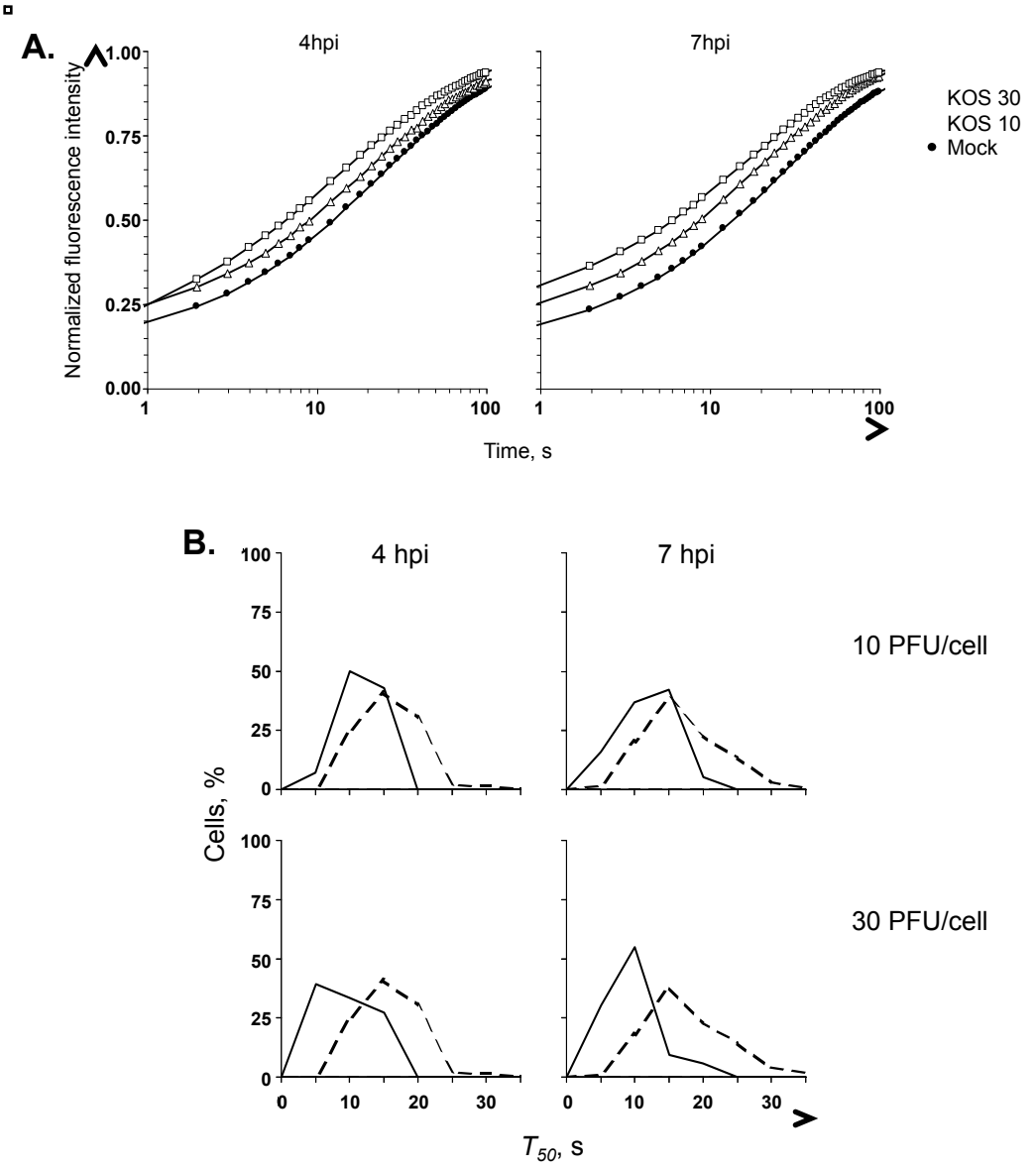

FIGURE 3.6: H1.2 mobilization increases with multiplicity of, and time after, infection. A) Line graphs representing the normalized fluorescence intensity of the photobleached nuclear region over time. Vero cells were transfected with plasmids expressing GFP-H1.2, and mock infected (**filled circles**) or infected with 10 (**open triangles**) or 30 (**open squares**) PFU/cell of HSV-1 strain KOS. Nuclear mobility of GFP-H1.2 was examined from 4 to 5 hpi (**4hpi**) or 7 to 8 hpi (**7hpi**) by FRAP. Solid or dashed lines, times when 50 or 90% of the original relative fluorescence was recovered (T_{50} *or* T_{90}), respectively. Mock infected cells had not recovered 90% of the original relative fluorescence when the measurements were stopped at 100s. **B)** Frequency distribution plots of the T_{50} per individual cell as evaluated by FRAP. Dashed or solid lines, mock or HSV-1 strain KOS infected cells, respectively; (n≥14).

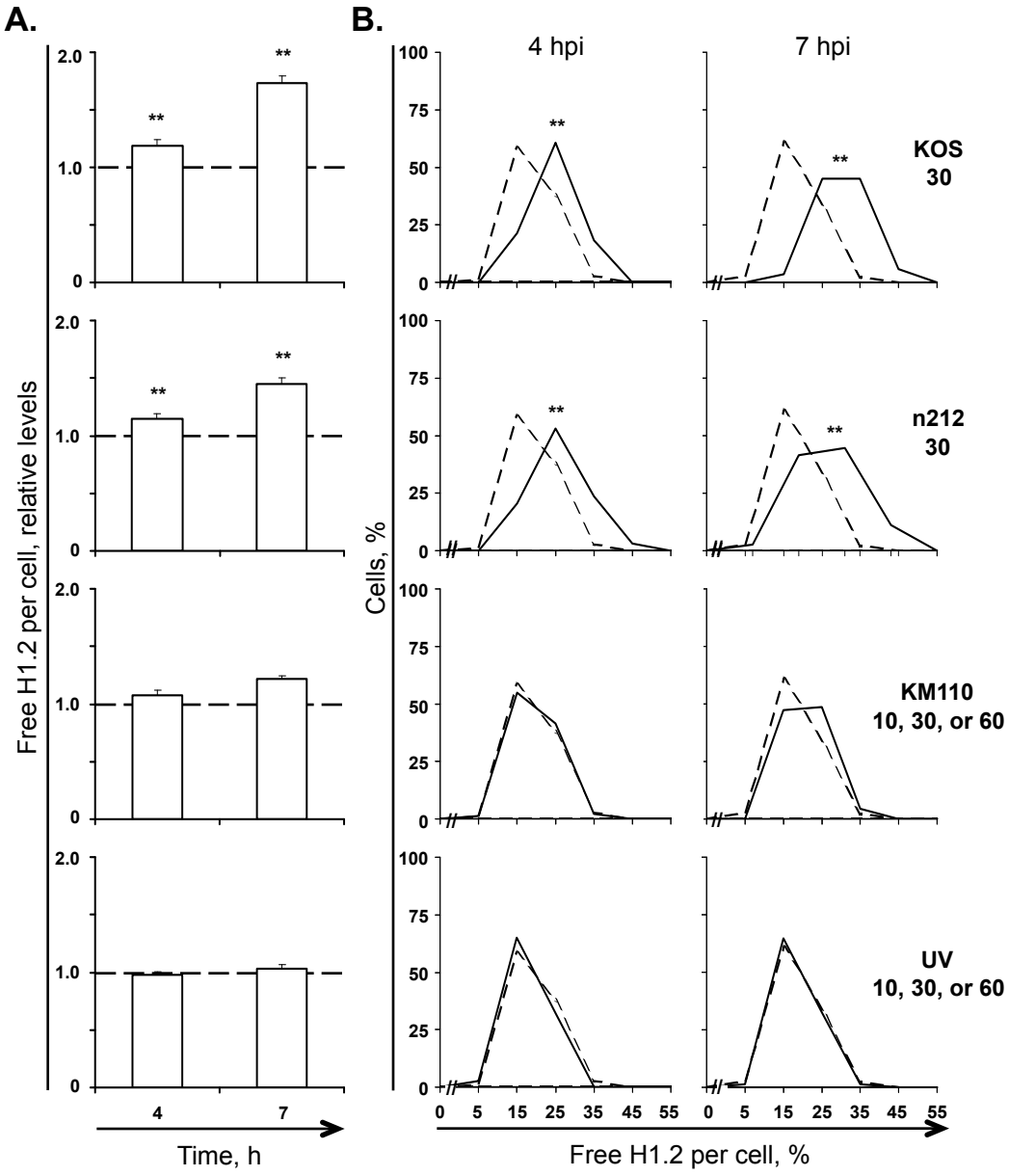

FIGURE 3.7: The increase in free H1.2 requires HSV-1 protein expression. A) Bar graphs representing the average level of free H1.2 in HSV-1 infected cells normalized to mock-infected cells and plotted against time postinfection. Vero cells were transfected with plasmids expressing GFP-H1.2. Transfected cells were mock infected or infected with the indicated multiplicity of HSV-1 strain **KOS**, **n212**, **KM110**, or **UV**-inactivated KOS. Free GFP-H1.2 was evaluated from 4 to 5 hpi (**4 hpi**) or 7 to 8 hpi (**7 hpi**) by FRAP. Error bars, SEM; n ≥ 17. **B)** Frequency distribution plots of the level of free H1.2 per individual cell as evaluated by FRAP. Dashed or solid lines, mock-infected or HSV-1 infected cells, respectively. **, P < 0.01.

FIGURE 3.8: ICP4 expression and accumulation into replication compartments in Vero and U2OS cells expressing or not GFP-H1.2 and infected with wild-type or mutant HSV-1 strains. Bar graphs representing the percentage of HSV-1-infected cells transfected with GFP-H1.2 and expressing ICP4 as nuclear diffuse or accumulated into replication compartments. Vero or U2OS cells were transfected with plasmids expressing GFP-H1.2. Cells were infected with 30 PFU per cell of HSV-1 strain **KOS**, **n212**, **KM110**, or **UV**-inactivated KOS or with 6 PFU per cell of HSV-1 strain KOS (U2OS cells only). Cells were fixed at 4.5 (**4**) or 7.5 (**7**) hpi and stained for ICP4. Nuclear expression of ICP4 and accumulation into replication compartments in cells in which GFP-H1.2 was expressed (**+**) or not **(-**) were evaluated by fluorescence microscopy.

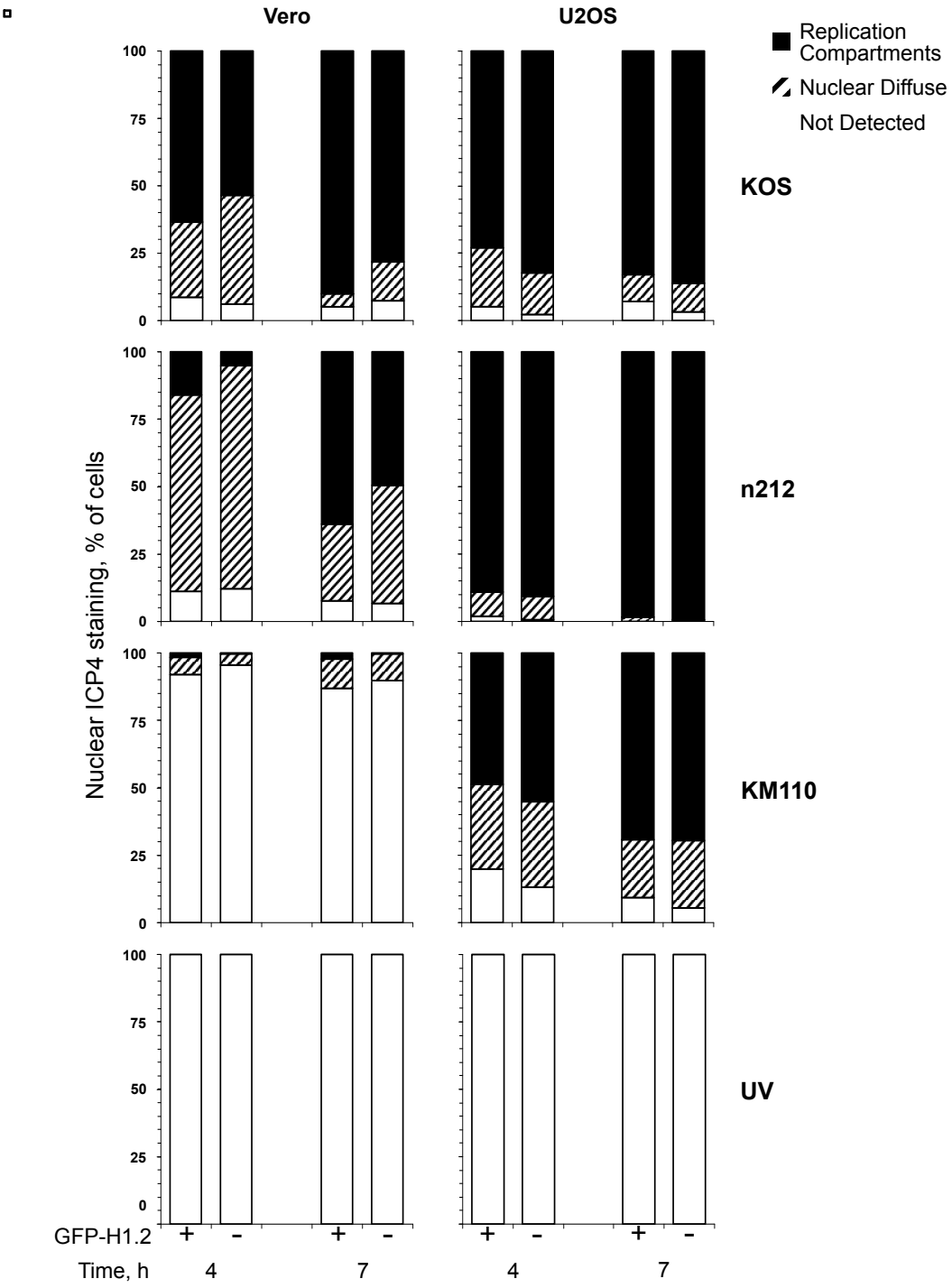
Vero
U2OS
Replication Compartments
Nuclear Diffuse
Not Detected
KOS
n212
KM110
UV
Nuclear ICP4 staining, % of cells
100
75
50
25
0
GFP-H1.2
+
-
Time, h
4
7

FIGURE 3.9: Mobilization of H1.2 requires nuclear HSV-1 genomes but not ICP0 or VP16. Line graphs representing the average H1.2 T_{50} in HSV-1-infected cells normalized to mock-infected cells and plotted against time postinfection. Vero or U2OS cells were transfected with plasmids expressing GFP-H1.2. Transfected cells were mock infected or infected with 6, 10, 30, 60, 10 to 30, 30 to 60, or 10 to 60 PFU per cell of HSV-1 strain **KOS**, **n212**, **KM110**, or **UV**-inactivated KOS. Nuclear mobility of GFP-H1.2 was examined from 4 to 5 hpi (**4**) or 7 to 8 hpi (**7**) by FRAP. Error bars, SEM; n ≥ 25, except for Vero KOS 10 at 4 and 7 hpi, Vero n212 60 at 4 and 7 hpi, U2OS KOS 6 at 4hpi, U2OS KM110 10 at 4 and 7 hpi, and U2OS KM110 30 at 7 hpi, n ≥ 14. Vero KOS data are a summary of the data presented in Figure 3.6.

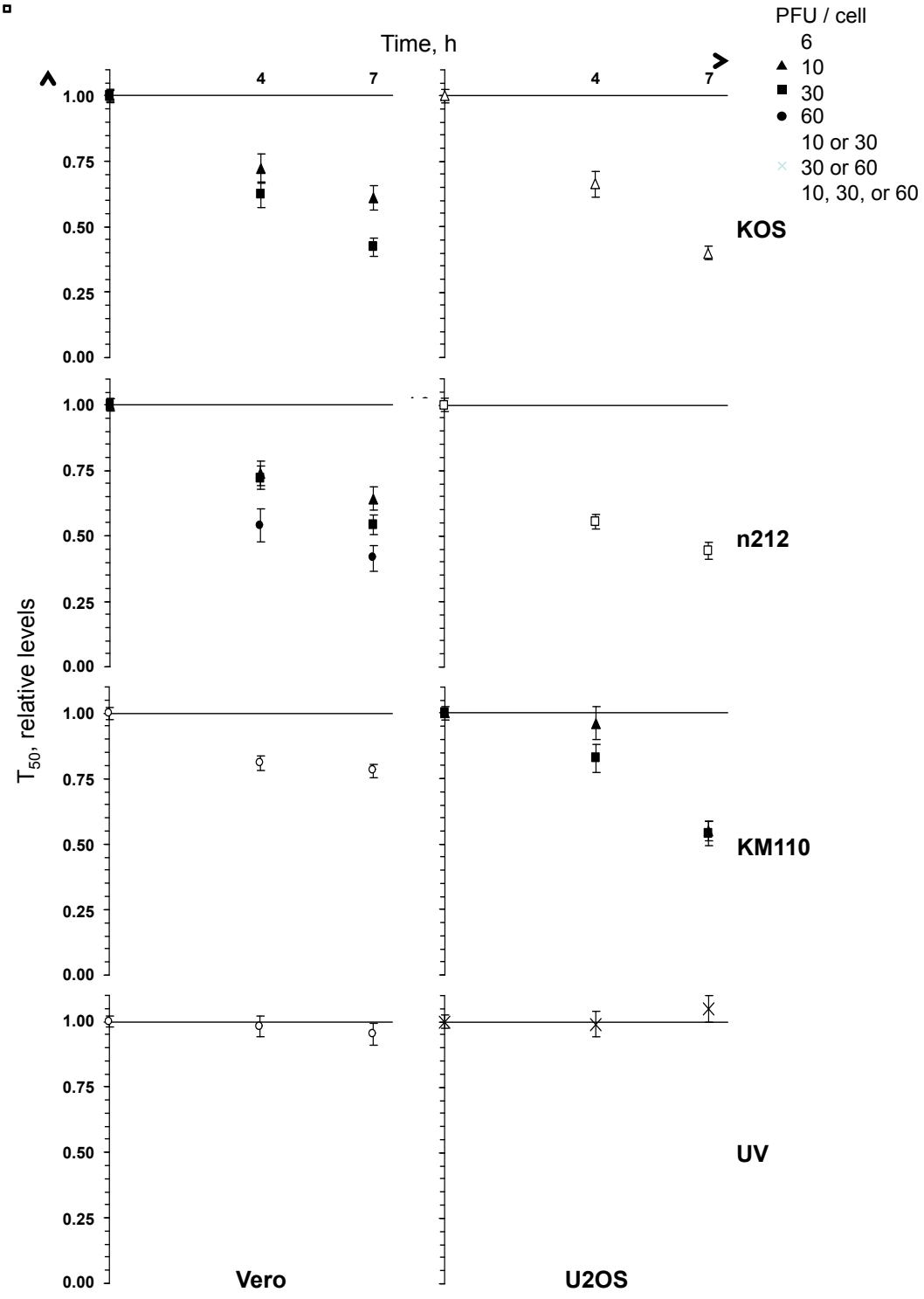
Time, h
4
7
4
7
PFU / cell
6
10
30
60
10 or 30
30 or 60
10, 30, or 60
KOS
n212
KM110
UV
T50, relative levels
1.00
0.75
0.50
0.25
0.00
Vero
U2OS

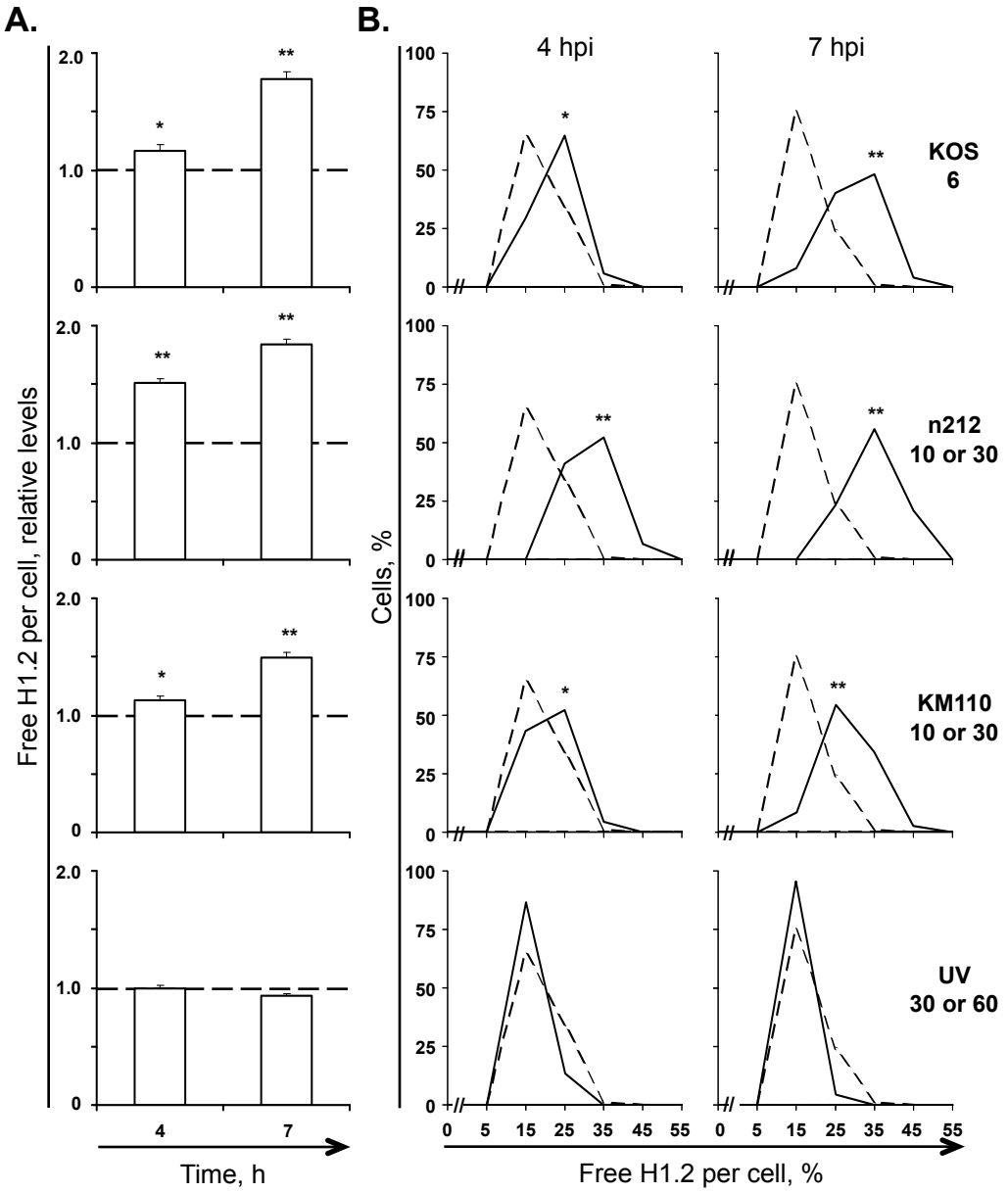

FIGURE 3.10: VP16 and ICP0 are not directly required to increase the pool of free H1.2. A) Bar graphs representing the average level of free H1.2 in HSV-1 infected cells normalized to mock-infected cells and plotted against time postinfection. U2OS cells were transfected with plasmids expressing GFP-H1.2. Transfected cells were mock infected or infected with the indicated multiplicity of HSV-1 strain **KOS**, **n212**, **KM110**, or **UV**-inactivated KOS. Free GFP-H1.2 was evaluated from 4 to 5 hpi (**4 hpi**) or 7 to 8 hpi (**7 hpi**) by FRAP. Error bars, SEM; n ≥ 17. **B)** Frequency distribution plots of the level of free H1.2 per individual cell as evaluated by FRAP. Dashed or solid lines, mock-infected or HSV-1 infected cells, respectively. **, $P < 0.01$; *, $P < 0.05$.

FIGURE 3.11: Enhanced H1.2 mobilization or increased free H1.2 do not require HSV-1 genome replication. A) Line graphs representing the normalized fluorescence intensity of the photobleached nuclear region over time. Vero cells were transfected with plasmids expressing GFP-H1.2, and mock infected or infected with 30 PFU per cell of HSV-1 strain KOS in the presence of 400μg/ml of PAA or no drug (data from Figure E Panel A replotted for comparison). Nuclear mobility of GFP-H1.2 was examined from 7 to 8 hpi by FRAP. Error bars, SEM; n ≥ 18. Time plotted on a linear scale. **B)** Same data as in Panel A, plotted on a semi-logarithmic scale. Solid or dashed lines, times when 50 or 90% of the original relative fluorescence was recovered (T_{50} or T_{90}), respectively. Mock-infected cells had not recovered 90% of the original relative fluorescence when the measurements were stopped at 100 s. **C)** Frequency distribution plot of the percentage of free H1.2 per individual cell evaluated by FRAP as described for Panel A. Dashed or solid lines, mock-infected or HSV-1-infected cells treated with 400μg/ml of PAA or no drug (data from Figure 3.7 replotted for comparison). **D)** Frequency distribution plot of the T_{50} per individual cell evaluated by FRAP as described for Panel A. Dashed or solid lines, mock-infected or HSV-1-infected cells treated with 400μg/ml of PAA or no drug (data from Figure 3.6 Panel B replotted for comparison. ** $P < 0.01$.

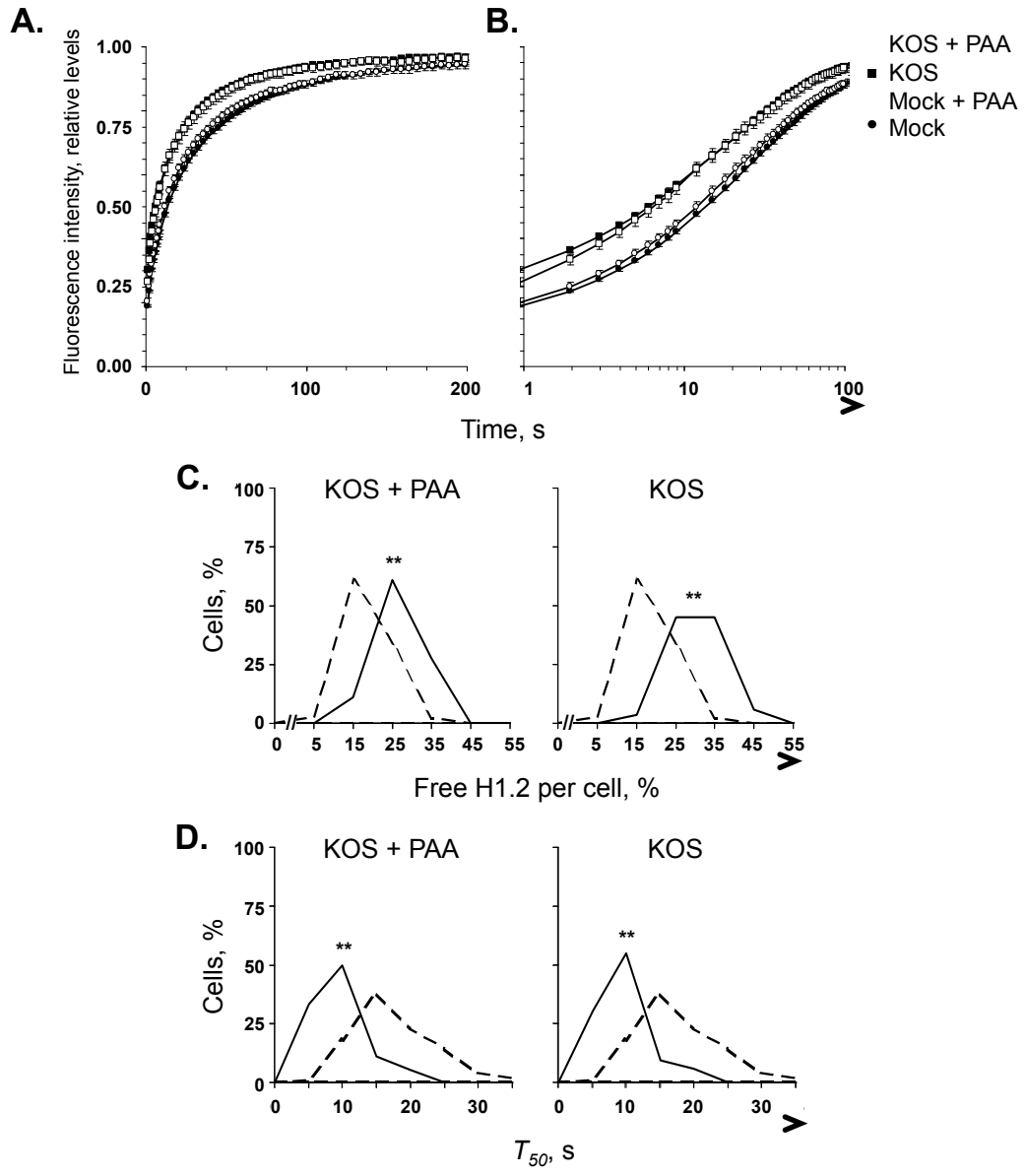
A.
B.
Fluorescence intensity, relative levels
1.00
0.75
0.50
0.25
0.00
0
100
200
1
10
100
Time, s
KOS + PAA
KOS
Mock + PAA
Mock
C.
KOS + PAA
KOS
Cells, %
100
75
50
25
0
**
0 5 15 25 35 45 55
Free H1.2 per cell, %
D.
KOS + PAA
KOS
Cells, %
0 10 20 30
T_{50}, s

H1 Variant			Accession
Doenecke[a]	Parseghian[b]	Seyedin[c]	Number
H1^0	-	-	NP_005309
H1.1	H1a	H1a	NP_005316
H1.2	H1^s-1	H1c	NP_005310
H1.3	H1^s-2	H1d	NP_005311
H1.4	H1^s-4	H1e	NP_005312
H1.5	H1^s-3	H1b	NP_005313

TABLE 3.1: Nomenclatures of the H1 variants used in this work.
[a] From Doenecke et al., 1994 ; the nomenclature used in our work.
[b] From Parseghian et al., 1994
[c] From Seyedin et al., 1979

H1 Variant	T_{50} (s) (avg ± SEM)		HSV/Mock ratio (%) (avg ± SEM)	% Cells with high H1 mobilization[a]
	Mock	HSV		
$H1^0$	23.6 ± 2.0	15.2 ± 1.8	63.3 ± 6.7	52
H1.1	27.3 ± 1.8	13.4 ± 1.3	57.0 ± 7.2	75
H1.2	17.6 ± 1.0	6.6 ± 0.5	42.3 ± 3.4	92
H1.3	23.1 ± 2.8	13.7 ± 1.8	63.8 ± 10.1	69
H1.4	49.5 ± 8.1	32.5 ± 5.3	66.4 ± 7.0	60
H1.5	43.1 ± 5.4	26.4 ± 5.2	59.3 ± 10.8	71

TABLE 3.2: Mobility of somatic H1 variants in mock- and HSV-1-infected cells.

[a] Percentage of cells in which the T_{50} was >1 SD lower than the average T_{50} in mock-infected cells.

Hour Post Infection	Virus Strain	PFU/ cell	T_{50} (avg ± SEM)		% Cells with high H1 mobilization, T_{50}[a]	T_{90} (avg ± SEM)		% Cells with high H1 mobilization, T_{90}[b]
			Absolute (s)	Relative (%)		Absolute (s)	Relative (%)	
4	-	-	13.2 ± 0.4	100	13	110.1 ± 2.8	100	11
	KOS	10	9.3 ± 0.7	72 ± 6	36	87.8 ± 7.0	80 ± 8	31
		30	7.3 ± 0.6	62 ± 5	61	69.1 ± 6.0	63 ± 6	42
	n212	10	9.9 ± 0.6	74 ± 5	52	79.0 ± 5.5	72 ± 6	38
		30	8.7 ± 0.6	72 ± 5	44	83.7 ± 5.6	76 ± 6	31
		60	7.0 ± 0.8	54 ± 6	78	60.9 ± 6.8	55 ± 7	78
	KM110	10, 30, or 60	11.5 ± 0.4	81 ± 3	32	93.8 ± 3.3	85 ± 3	29
	UV	10, 30, or 60	12.9 ± 0.5	98 ± 4	19	94.6 ± 3.9	86 ± 4	21
7	-	-	14.8 ± 0.4	100	17	112.3 ± 2.9	100	16
	KOS	10	9.4 ± 1.0	61 ± 4	63	76.8 ± 5.9	68 ± 4	63
		30	6.9 ± 0.5	42 ± 3	92	65.0 ± 4.5	58 ± 5	74
	n212	10	9.3 ± 0.9	64 ± 5	58	89.3 ± 8.7	80 ± 8	43
		30	7.1 ± 0.6	54 ± 4	83	76.6 ± 3.4	68 ± 3	71
		60	5.0 ± 0.7	41 ± 5	82	66.1 ± 9.6	59 ± 10	71
	KM110	10, 30, or 60	11.7 ± 0.4	78 ± 3	40	97.7 ± 3.7	87 ± 3	29
	UV	10, 30, or 60	13.2 ± 0.5	95 ± 4	27	102.7 ± 5.0	91 ± 5	33

TABLE 3.3: Mobilization of H1.2 in Vero cells infected with wild-type or mutant HSV-1 strains.

[a] Percentage of cells in which the T_{50} was >1 SD lower than the average T_{50} in mock-infected cells.

[b] Percentage of cells in which the T_{90} was >1 SD lower than the average T_{90} in mock-infected cells.

			4hpi		7hpi	
Cell Type	Virus Strain	PFU/ cell	Relative Free H1.2 (avg ± SEM)	% Cells with large increase in free H1.2[a]	Relative Free H1.2 (avg ± SEM)	% Cells with large increase in free H1.2[a]
Vero	-	-	1.00 ± 0.01	15	1.00 ± 0.02	15
	KOS	10	1.19 ± 0.05	64	1.41 ± 0.07	63
		30	1.19 ± 0.05	52	1.74 ± 0.06	92
	n212	10	1.15 ± 0.05	48	1.52 ± 0.09	71
		30	1.15 ± 0.04	35	1.45 ± 0.05	75
		60	1.36 ± 0.08	72	1.61 ± 0.09	88
	KM110	10, 30, or 60	1.08 ± 0.04	30	1.22 ± 0.03	49
	UV	10, 30, or 60	0.97 ± 0.03	13	1.03 ± 0.03	14
U2OS	-	-	1.00 ± 0.02	20	1.00 ± 0.02	19
	KOS	6	1.16 ± 0.06	53	1.78 ± 0.06	100
	n212	10 or 30	1.52 ± 0.03	95	1.84 ± 0.04	100
	KM110	10 or 30	1.13 ± 0.03	39	1.49 ± 0.04	89
	UV	30 or 60	1.00 ± 0.02	13	0.93 ± 0.02	5

TABLE 3.4: Levels of free H1.2 in cells infected with wild-type or mutant HSV-1 strains.

[a] Percentage of cells in which the level of free H1.2 was >1 SD above the average level in mock-infected cells.

			Localization (avg ± SEM) at:					
			4hpi			7hpi		
Cell Type	Virus Strain	PFU/ cell	% Not detected	% Nuclear dispersed	% Replication compartment	% Not detected	% Nuclear dispersed	% Replication compartment
Vero	KOS	30	9 ± 2	40 ± 7	52 ± 8	13 ± 6	9 ± 4	78 ± 5
	n212	30	12 ± 1	78 ± 5	11 ± 5	7 ± 2	37 ± 10	56 ± 11
	KM110	30	94 ± 2	5 ± 2	1 ± 0	90 ± 2	10 ± 1	1 ± 1
	UV	30	100	0	0	100	0	0
U2OS	KOS	6	4 ± 1	19 ± 3	78 ± 4	6 ± 2	16 ± 5	79 ± 5
	n212	30	1 ± 1	10 ± 6	88 ± 6	0	1 ± 0	99 ± 0
	KM110	30	26 ± 10	47 ± 2	27 ± 12	11 ± 4	26 ± 6	63 ± 3
	UV	30	100	0	0	100	0	0

TABLE 3.5: Nuclear ICP4 localization in cells infected with wild-type or mutant HSV-1 strains.

Hour Post Infection	Virus Strain	PFU/ cell	T_{50} (avg ± SEM)		% Cells with high H1 mobilization, T_{50}[a]	T_{90} (avg ± SEM)		% Cells with high H1 mobilization, T_{90}[b]
			Absolute (s)	Relative (%)		Absolute (s)	Relative (%)	
4	-	-	10.7 ± 0.4	100	16	88.6 ± 3.3	100	14
	KOS	6	8.0 ± 0.6	66 ± 5	76	64.7 ± 5.0	73 ± 7	53
	n212	10 or 30	5.2 ± 0.3	55 ± 3	84	55.1 ± 3.0	62 ± 4	52
	KM110	10	11.2 ± 0.9	96 ± 6	22	97.5 ± 8.6	110 ± 8	22
		30	7.7 ± 0.5	83 ± 5	38	66.4 ± 6.4	75 ± 8	42
	UV	30 or 60	11.8 ± 0.6	99 ± 5	22	93.9 ± 5.6	106 ± 6	24
7	-	-	12.4 ± 0.4	100	15	102.9 ± 3.7	100	16
	KOS	6	5.8 ± 0.4	40 ± 3	100	59.7 ± 5.1	58 ± 4	88
	n212	10 or 30	4.8 ± 0.4	44 ± 3	93	52.1 ± 4.9	51 ± 6	67
	KM110	10	6.8 ± 0.5	55 ± 4	88	58.6 ± 4.9	57 ± 5	75
		30	5.0 ± 0.4	54 ± 5	94	44.3 ± 6.5	43 ± 9	78
	UV	30 or 60	14.0 ± 0.6	105 ± 5	19	114.7 ± 5.9	111 ± 6	23

TABLE 3.6: Mobilization of H1.2 in U2OS cells infected with wild-type or mutant HSV-1 strains.

[a] Percentage of cells in which the T_{50} was >1 SD lower than the average T_{50} in mock-infected cells.

[b] Percentage of cells in which the T_{90} was >1 SD lower than the average T_{90} in mock-infected cells.

Parameter	PAA	Mobilization (avg ± SEM)		% Cells with high H1 mobilization[a]
		Absolute (s)	Relative to mock-infected cells	
T_{50}	+	7.4 ± 1.0	0.34 ± 0.05	94*
	-	6.9 ± 0.5	0.42 ± 0.03	92*
T_{90}	+	67.4 ± 6.0	0.60 ± 0.04	94**
	-	65.0 ± 4.5	0.58 ± 0.05	74**
Free H1.2	+	-	1.61 ± 0.07	94***
	-	-	1.74 ± 0.06	92***

TABLE 3.7: Mobilization of H1.2 in Vero cells infected with 30 PFU/cell of HSV-1 KOS and treated with PAA.

[a]*, percentage of cells in which the T_{50} was >1 SD lower than the average T_{50} in mock-infected cells; **, percentage of cells in which the T_{90} was > 1 SD lower than the average T_{90} in mock-infected cells; ***, percentage of cells in which the level of free H1.2 was > 1 SD above the average level of free H1.2 in mock-infected cells.

CHAPTER 4: CORE HISTONES H2A, H2B, H3.3, AND H4 ARE MOBILIZED DURING HSV-1 INFECTION.

This Chapter contains unpublished data.

ABSTRACT

HSV-1 genomes are associated with histones in unstable nucleosomes during lytic infection. However, the association of histones with HSV-1 genomes changes during the replication cycle. The genomes are not associated with histones in capsids and input genomes are deposited in nuclear domains devoid of histones. Late during infection, HSV-1 genomes again occupy nuclear domains depleted of histones. The source of the histones that interact with HSV-1 genomes has yet to be addressed. During infection, histone synthesis is inhibited, and the total level of nuclear H3 remains relatively constant. It is therefore unlikely that the histones that first interact with HSV-1 genomes are synthesized de novo, or that histones associated with HSV-1 genomes are degraded later during infection. Histone association with chromatin is dynamic in that histones normally disassociate from chromatin, diffuse through the nucleoplasm, and reassociate at a different site. Therefore, I propose that the histones that associate with HSV-1 genomes early during infection are mobilized from cellular chromatin. I further propose that histones are mobilized away from domains containing HSV-1 genomes later during infection such that histone-free genomes can be

encapsidated. Consistent with this hypothesis, I have shown that linker histones are mobilized during HSV-1 infection (Chapter 3). However, chromatinization also requires core histones. Here, I evaluate whether core histone mobility was altered during HSV-1 infection using fluorescence recovery after photobleaching. All core histones evaluated, H2A, H2B, H3.3, and H4, were mobilized. The mobilization resulted in increases to the levels of H2A, H2B, H3.3, and H4 available in the free pool at 4 and 7h after infection. Such mobilization may result from expression of HSV-1 IE, E, or L proteins, HSV-1 transcription, HSV-1 DNA replication, or cellular responses to infection. However, different histones were likely mobilized through different mechanisms. HSV-1 infection differentially altered the rates of core histone fast chromatin exchange. The rates of H2A and H3.3 fast chromatin exchange were increased early during infection, whereas that of H2B was decreased later on. This differential mobilization of the core histones during HSV-1 infection suggests the existence of different mobilization mechanisms.

4.1 INTRODUCTION.

During lytic infection, HSV-1 genomes are associated with core histones in unstable nucleosomes (Herrera & Triezenberg, 2004; Kent et al., 2004; Huang et al., 2006; Lacasse & Schang, 2010). However, HSV-1 genomes are not associated with histones in virions and input virions are deposited in nuclear domains depleted of cellular histones (Ascoli & Maul, 1991; Ishov & Maul, 1996; Maul et al., 1996; Oh & Fraser, 2008). Consequently, HSV-1 genomes are initially not associated with histones; they come to be associated with them after entering the nucleus.

It is unlikely that the histones first associated with HSV-1 genomes during infection are synthesized de novo. HSV-1 infects cells at any stage of the cell cycle, whereas canonical core histones are synthesized only during S-phase (Yager & Bachenheimer, 1988; Marzluff & Duronio, 2002; Gunjan, Paik, & Verreault, 2005). Moreover, synthesis of core histones is tightly regulated at transcriptional and post-transcriptional levels. Transcript stability further restricts canonical core histone synthesis to S-phase. In contrast to canonical core histones, variant core histones are synthesized throughout the cell cycle (Kamakaka & Biggins, 2005). Transcription of variant core histone genes is not restricted to any phase of the cell cycle and their transcripts are not particularly unstable at any phase either. During HSV-1 infection, however, host cell transcription and processing of host cell polyadenylated mRNA transcripts are inhibited, and mRNA is degraded (Yager & Bachenheimer, 1988; Sorenson et al., 1991; Spencer et al., 1997). It is therefore unlikely that either the canonical or variant core histones that associate with HSV-1 genomes are synthesized de novo in the infected cell. Later in infection, HSV-1 genomes again occupy nuclear domains partially depleted of histones (Monier et al., 2000; Simpson-Holley et al., 2004; Simpson-Holley et al., 2005). It is unlikely that histones removed from HSV-1 genomes later during infection are degraded, in that the levels of nuclear H3 remain constant during HSV-1 infection (Kent et al., 2004; Huang et al., 2006). HSV-1 genomes therefore most likely dynamically associate with pre-existing histones.

Core histone incorporation in nucleosomes is dynamic. Histones normally unbind from chromatin, diffuse through the nucleoplasm, and re-bind at a different site. The chromatin exchange of H2A/H2B dimers is faster than that of H3/H4 dimers, indicating that the H3/H4 tetramer is more stably incorporated in chromatin (Hendzel & Davie, 1990; Kent et al., 2004; Higashi et al., 2007). The overall chromatin exchange of core histones is slow, occurring in hours. However, there is a fast component to core histone chromatin exchange. The rate of chromatin exchange is increased by cellular processes such as transcription, or by core histone modifications such as acetylation

The chromatin exchange of core histones is evaluated in live cells by fluorescence recovery after photobleaching (FRAP). Such studies have corroborated the dynamic incorporation of core histones in chromatin. Plotting the FRAP of core histones against time distinguishes three histones populations; an unbound population, a fast exchanging population, and a slow exchanging population bound (Figure 4.1). The fluorescence immediately after photobleaching represents the histone population that is rapidly diffusing. This population is considered not bound in chromatin and is available in the so-called “free” pool (Figure 4.1). The subsequent fluorescence recovery is biphasic (Figure 4.1). The initial fast recovery phase represents the histone population that is weakly bound in chromatin and therefore undergoing fast, or low-affinity, chromatin exchange. The later slower recovery phase represents the histone population that is tightly bound in chromatin and therefore undergoing slow, or high-affinity, chromatin exchange. The fast

chromatin exchange of core histones is mostly associated with transcription.

The majority of core histones (up to 80%) are tightly bound in chromatin and therefore undergo slow chromatin exchange (Kimura & Cook, 2001). Only the unbound histones and those that are weakly bound in chromatin would be promptly available to bind to HSV-1 genomes during infection. These histones diffuse through the nucleoplasm and therefore are able to reach domains containing HSV-1 genomes. Such histones may have a higher propensity to re-bind to DNA loci with no- or low- histone occupancy, such as infecting HSV-1 genomes. However, the histones that associate with HSV-1 genomes can also disassociate and diffuse through the nucleoplasm to domains containing cellular chromatin, or to those containing HSV-1 genomes.

Later in infection, histones are depleted from HSV-1 replication compartments (Monier et al., 2000; Simpson-Holley et al., 2004; Simpson-Holley et al., 2005). Histones may therefore be prevented from re-binding to HSV-1 genomes and thus have a higher propensity to re-bind to cellular chromatin.

Consistent with the requirement for histone mobilization for histone association with HSV-1 genomes, I have demonstrated that linker histones are mobilized during HSV-1 infection (Conn, Hendzel, & Schang, 2008). I therefore next evaluated the mobility of core histones during HSV-1 infection.

4.2 RESULTS.

4.2.1 GFP-H2A, GFP-H2B, GFP-H3.3, and GFP-H4 are incorporated in cellular chromatin.

GFP tagged core histones are incorporated in chromatin and have the properties of endogenous histones (Kanda et al., 1998; Kimura & Cook, 2001; Higashi et al., 2007). Previous reports have shown that placement of the GFP tag on the amino (N)- or carboxyl (C)- terminus of H2A did not affect its nucleosome incorporation (Higashi et al., 2007). To evaluate core histone mobility during HSV-1 infection, I constructed plasmids expressing GFP fused to the N-terminus of the canonical core histones H2A, H2B, and H4, and was provided with a plasmid expressing GFP fused to the N-terminus of the variant histone H3.3. Placement of the GFP tag on the C-terminus of H2B and H4 resulted in expression of fusion proteins that had dispersed nuclear staining and did not have strictly nuclear localization. Histones N-terminally tagged with GFP, in contrast, had structured nuclear staining and were strictly nuclear. Moreover, the fluorescence of GFP-tagged histones in mitotic cells was consistent with their incorporation into mitotic chromosomes. Together, these results indicate that the N-terminally tagged GFP histones are incorporated into nucleosomes.

Canonical core histones are synthesized along with new DNA during the S-phase of the cell cycle. However, a constitutive promoter drives expression of the GFP-core histone fusion proteins. The transfected canonical histone fusion proteins were therefore expressed throughout the cell cycle. I first evaluated whether such expression of

the GFP-core histones had adverse effects. Transfected cells showed strict nuclear localization of the GFP-core histones, regardless of cell type (for example see Figure 4.2 GFP-H3.3 Panel). Incorporation of the GFP-core histones into chromosomes was obvious through mitosis (Figure 4.3), whereas no obvious cytoplasmic or extra-chromosomal fluorescence was observed. Moreover, expression of no GFP-core histone appeared to vastly affect chromosome morphology, alignment, or separation during cell division. The GFP-core histones also appear not to be substantially overexpressed. No extra-chromosomal fluorescence was observed during mitosis nor was diffuse nuclear staining observed during interphase (Figure 4.2, Figure 4.3).

Although a large population of extra-nucleosomal GFP-core histones was not observed, higher expressing cells could conceivably have a higher level of free nuclear GFP-core histones. Therefore, I analyzed whether the degree of GFP-core histone expression affected the level of GFP-core histone available in the free pool. There was no correlation between the degree of expression of GFP-H2A, GFP-H2B, GFP-H3.3, and GFP-H4 and their levels in the free pools, as measured by the relative nuclear fluorescence intensity (Figure 4.4). In my studies, the population of core histones available in the free pool (i.e. not bound in chromatin) was, on average, approximately 15 to 20% at any given time (Table 4.1, Figure 4.4, Figure 4.6 mock infected cells). These values are comparable to what other studies have reported for H2A-GFP, H3-GFP, and H4-GFP, but higher than previously reported for H2B-GFP (approximately 5%) (Kimura & Cook, 2001). The discrepancy in the level

of H2B in the free pool may reflect cell-type specific or construct specific differences. My transiently expressed fusion protein had GFP fused to the N-terminus of H2B with an 8 amino acid linker. The stably expressed H2B used by Kimura and Cook (Kimura & Cook, 2001) had GFP fused to the C-terminus of H2B with a 6 amino acid linker (Kanda et al., 1998). The N-terminus of H2B is external to the nucleosome, whereas the C-terminus is central. It is therefore possible that the placement of the GFP-tag on H2B could affect nucleosome incorporation and as a result alter the levels available in the free pool.

4.2.2 GFP-H2B and GFP-H3.3 expression do not substantially affect HSV-1 replication.

The expression of GFP-core histones does not obviously affect the expressing cells. The potential effects of GFP-core histone expression on HSV-1 replication, however, were still unknown. To evaluate such effects, I analyzed ICP4 expression in cells expressing GFP-H2B or GFP-H3.3. Progression of HSV-1 infection, as evaluated by expression of ICP4 and its accumulation into replication compartments, was not adversely affected by expression of either (Figure 4.5). Cells expressing or not GFP-H2B or GFP-H3.3 had similar ICP4 expression and accumulation into replication compartments at 4 or 7 hours after infection with 30 PFU per cell of HSV-1 strain KOS (Figure 4.5).

Figure 4.2 shows examples of U2OS cells expressing GFP-H3.3 with nuclear dispersed (ND) ICP4 or ICP4 accumulated into replication compartments (RC). These experiments also demonstrate that GFP-H3.3 colocalizes with replication compartments. Such colocalization does not

correlate in any obvious manner with the level of ICP4 expression, the degree of ICP4 accumulation into the replication compartment, the size of the replication compartment, or the time after infection.

4.2.3 H2A, H2B, H3.3, and H4 are mobilized during HSV-1 infection.

As a measure for core histone mobilization, I evaluated the FRAP recovery kinetics of the GFP-core histones. The overall slow recovery of core histones indicates that the majority of core histones are stably incorporated into chromatin. Consequently, the majority of core histones are not available for initial deposition on HSV-1 genomes in any timescale relevant to infection. I therefore evaluated the core histone populations that would be available to initially interact with, or bind to, HSV-1 genomes. Namely, the population that is not stably incorporated in chromatin, which includes those core histones available in the free pool and those undergoing faster chromatin exchange (Figure 4.1). As a surrogate measure for the population undergoing faster chromatin exchange, I used the rate of initial fluorescence recovery after photobleaching, which is the slope between the first and second time points after photobleaching (Figure 4.1).

The canonical core histones H2A, H2B, and H4 and the variant core histone H3.3 were all mobilized at early and later times after infection with HSV-1 strain KOS (Figure 4.6), as demonstrated by their faster fluorescence recovery after photobleaching. The mobilization of core histones at early and late times after infection suggests that HSV-1

transcription, expression of HSV-1 proteins, HSV-1 DNA replication, or cellular responses to them alter the exchange rate of core histones.

Consistent with the core histone mobilization observed by FRAP, core histones H4 and H2A were identified as enriched in proteomic analysis of 0.4M NaCl extracts from HSV-1 infected nuclei over extracts from mock-infected nuclei. Extraction of core histones normally requires higher (0.8M to 2M) NaCl concentrations. The extraction of H4 and H2A at a lower NaCl concentration is consistent with lower affinity chromatin associations or increased chromatin exchange.

4.2.4 The pools of free H2A, H2B, H3.3, and H4 are increased during HSV-1 infection.

The chromatin exchange of H2A, H2B, H3.3, and H4 is altered during HSV-1 infection. This altered chromatin exchange results in increases in the levels of free H2A, H2B, H3.3, and H4 (Table 4.1). To test whether HSV-1 infection or the degree of GFP-core histone expression results in the increases to the free pools, I evaluated the level of each GFP-core histone available in the free pool against the relative nuclear fluorescence intensity for each cell. In HSV-1 infected cells expressing GFP-H2A, GFP-H2B, GFP-H3.3, or GFP-H4, the levels of GFP-core histones available in the free pools did not correlate with their levels of expression, measured as relative nuclear fluorescence (Figure 4.7). Notably, the populations of HSV-1 infected cells had more uniform levels of expression of each GFP-core histone than mock-infected cells did (compare the x-axis distribution of Figure 4.7 and Figure 4.4), yet wider ranges of free histone levels per cell (compare the y-axis distribution of

Figure 4.7 and Figure 4.4). The increases in the free pools of core histones during HSV-1 infection consequently reflect changes in core histone chromatin exchange, rather than differences in core histone expression levels.

The pool of free H2A was increased to 117 ± 5% already at 4h after infection with 30 PFU per cell of HSV-1 strain KOS, that of H2B to 133 ± 5%, of H3.3 to 171 ± 7%, and of H4 to 140 ± 7% (Figure 4.8, Table 4.1) ($P<0.01$, Student's T-test; 1-tail). The pools of free H2A, H2B, H3.3, and H4 remained increased at 7hpi, to 174 ± 7, 169 ± 7, 155 ± 7, and 157 ± 9%, respectively (Figure 4.8, Table 4.1) ($P<0.01$, Student's T-test; 1-tail). The rates of core histone chromatin binding and unbinding (or displacement) are therefore altered relative to each other so that a greater percentage of core histones are not bound to chromatin at any given time. These data suggest that HSV-1 transcription, expression of HSV-1 proteins, HSV-1 DNA replication, or cellular responses to them increase the pools of free core histones.

The increase in the levels of core histones available in the free pools could reflect an extreme increase to the free pools in a sub-population of infected cells or a general increase to the free pools in the whole population of infected cells. I therefore evaluated the percentage of free histone on a cell-to-cell basis. This analysis demonstrated that the increase in the levels of H2A, H2B, H3.3, and H4 in the free pool was spread through the population of infected cells (Figure 4.8 Panel B). I next analyzed the cells with the largest pools of free H2A, H2B, H3.3, or H4, defined as those in which such pools were greater than 1 standard

deviation (SD) above the average level of free core histone in mock-infected cells. At least 40% or 70% of infected cells had their free pools of core histones increased to this large extent (Table 4.1) at 4 or 7hpi, respectively. In a normal population distribution, only approximately 16% of cells would have their free pools increased by this degree. Thus, the pools of free H2A, H2B, H3.3, and H4 are not only increased during HSV-1 infection, but they are increased in the majority of infected cells at later times after infection.

4.2.5 The fast chromatin exchange rates of H2A, H2B, H3.3, and H4 are differentially altered during HSV-1 infection.

HSV-1 infection altered core histone chromatin exchange such that the pools of free H2A, H2B, H3.3, and H4 were increased. I next evaluated whether HSV-1 infection influenced the fast chromatin exchange rates of these core histones. The initial rate of fluorescence recovery after photobleaching was used as a proxy for fast chromatin exchange (or low-affinity chromatin binding events) of H2A, H2B, H3.3, and H4 (Figure 4.1).

Infection with HSV-1 differentially altered the fast chromatin exchange of H2A, H2B, H3.3, and H4. The fast chromatin exchange rate of H2A was increased to 1.49 ± 0.25 fold ($P<0.05$, Student's T-test; 1-tail) at 4h after infection with 30 PFU per cell of HSV-1 strain KOS (Figure 4.9, Table 4.2). Frequency distribution analyses of the rate of initial fluorescence recovery per cell suggest that the fast chromatin exchange rate of H2A is increased mostly in a sub-population of infected cells

(Figure 4.9 Panel B 4hpi). Consistently, only 33% of cells had a large increase in the fast chromatin exchange rate of H2A, defined as those in which the rate of fast chromatin exchange was greater than one SD above the average rate of fast chromatin exchange in mock-infected cells (Table 4.2). The fast chromatin exchange rate of H2A was not significantly different from that of mock-infected cells at 7hpi, although it still showed a tendency to be increased (Figure 4.9, Table 4.2).

As for H2A, the fast chromatin exchange rate of H3.3 was increased at 4hpi (by 2.50 ± 0.22 fold) ($P<0.01$, Student's T-test; 1-tail) (Figure 4.9, Table 4.2). The fast chromatin exchange rate of H3.3, however, was increased throughout the population of infected cells (Figure 4.9 Panel B 4hpi). Seventy percent of cells had a large increase in the fast chromatin exchange rate of H3.3 (Table 4.2). The fast chromatin exchange rate of H3.3 in HSV-1 infected cells at 7hpi was similar to that in mock-infected cells, although it still showed a tendency to be increased (Figure 4.9, Table 4.2). These data demonstrate that the fast chromatin exchange rates of H2A and H3.3 are increased at early times after infection. Consequently, HSV-1 transcription, protein expression, HSV-1 DNA replication, or cellular responses to them increase the relative rates of H2A and H3.3 low-affinity chromatin association and disassociation.

In contrast to H2A and H3.3, the fast chromatin exchange rate of H2B was similar to that of mock-infected cells at 4hpi and decreased, to 0.77 ± 0.07, at 7hpi ($P>0.05$ and $P<0.01$, respectively, Student's T-test; 1-tail) (Figure 4.9, Table 4.2). The decrease in the fast chromatin

exchange rate of H2B occurred throughout the population of infected cells (Figure 4.9 Panel B 7hpi). However, only 34% of cells had a decrease in the fast chromatin exchange rate of H2B, greater than one SD below the average rate of fast chromatin exchange in mock-infected cells (Table 4.2). This percentage is approximately 2-fold larger than expected for a normal population distribution. The decrease in fast H2B chromatin exchange suggests that HSV-1 gene transcription, HSV-1 proteins, HSV-1 DNA replication, or cellular responses to them decreases the rates of H2B low-affinity chromatin association and disassociation.

Unlike the other core histones evaluated, the fast chromatin exchange rate of H4 was not increased or decreased relative to mock-infected cells at either 4 or 7hpi (Figure 4.9, Table 4.2).

4.2.6 Stably expressed GFP-H2B is mobilized in HeLa cells during HSV-1 infection.

H2A, H2B, H3.3, and H4 are mobilized during HSV-1 infection. The core histone GFP fusion proteins I evaluated were expressed from transiently transfected expression vectors. I next evaluated the mobilization of H2B-GFP in HeLa cells that stably express this fusion protein from integrated copies of an H2B-GFP expression vector (Kanda et al., 1998). The pool of free H2B-GFP was larger in the stably transfected HeLa cells than in the transiently transfected Vero cells (24% in comparison to approximately 16%, respectively) (Table 4.3, mock-infected cells). As for the transiently transfected cells, however, the level of free H2B-GFP in HeLa cells did not correlate with the degree of H2B-GFP expression (Figure 4.10). As expected, the stably transfected cells had more homogenous levels of

H2B-GFP expression than the transiently transfected cells did (compare the x-axis distribution of Figure 4.4 and Figure 4.10, mock-infected cells)

HSV-1 infection increased the mobility of H2B (Figure 4.11). Even though the HeLa cells had an inherently larger pool of free H2B-GFP, the free pool was still increased during HSV-1 infection (Figure 4.11 Panels B and C, Table 4.3). The pool of free H2B-GFP was increased to 115 ± 4% at 4h after infection with 30 PFU per cell of HSV-1 strain KOS. At 7hpi, it was increased to 145 ± 5% ($P<0.01$, Student's T-test; 1-tail) (Figure 4.11 Panels B and C, Table 4.3). The increase in free H2B reflects changes in H2B chromatin binding. As with transiently expressed H2B, there was no correlation between the degree of H2B expression and its level in the free pool, as measured by the relative nuclear fluorescence intensity (Figure 4.10 KOS 30).

The pool of free H2B was increased throughout the population of infected cells. Greater than 50% of cells had a large increase in their pool of free H2B at 4 or 7hpi (Figure 4.11 Panel B, Table 4.3). These data demonstrate that HSV-1 gene transcription, HSV-1 protein expression, HSV-1 DNA replication, or cellular responses to them alter the rates of chromatin association and disassociation relative to each other such that the level of free H2B is increased.

As in transiently transfected cells, the fast chromatin exchange of stably expressed H2B was decreased in HSV-1-infected HeLa cells relative to mock-infected cells (Figure 4.11 Panels D and E). The rate of initial fluorescence recovery was decreased to 0.83 ± 0.03 and 0.65 ± 0.04 fold at 4 and 7hpi, respectively ($P<0.05$ and $P<0.01$, respectively,

Student's T-test; 1-tail) (Table 4.4). The fast chromatin exchange rate of H2B was decreased throughout the population of infected cells. At 7hpi, greater than 80% of cells had a decrease in H2B fast chromatin exchange, larger than one SD below the average rate of fast chromatin exchange (Figure 4.11 Panel E, Table 4.4). HSV-1 transcription, HSV-1 proteins, HSV-1 DNA replication, or cellular responses to them therefore decrease the rates of H2B low-affinity chromatin association and disassociation.

Taken together, these data demonstrate that the mobilization of H2B during HSV-1 infection is similar in two unrelated cell lines, regardless of whether the GFP-H2B fusion proteins are transiently or stably expressed. Furthermore, the GFP-H2B fusion proteins were mobilized during infection regardless of whether the GFP tag was attached to the N- or C- terminus.

4.3 DISCUSSION.

The core histones H2A, H2B, H3.3, and H4 were all mobilized at early and late times during infection with HSV-1. These mobilizations affected both analyzed parameters of core histone chromatin exchange. The pools of free H2A, H2B, H3.3, and H4 were increased, and the rates of fast chromatin exchange of H2A, H2B, and H3.3 were altered. Consequently, HSV-1 transcription, expression of HSV-1 proteins, HSV-1 DNA replication, or cellular responses to them, alter the relative rates of core histone chromatin association and disassociation such that the free pools are increased and affect the low-affinity chromatin exchange of H2A, H2B, and H3.3.

To increase the steady-state level of H2A, H2B, H3.3, and H4 not bound in chromatin, the rates of chromatin association and disassociation must be altered relative to each other. Thus, the relative rate of chromatin dissociation is increased relative to the rate of chromatin association. It is not possible to distinguish between increases in dissociation or decreases in association rates analyzing only the levels of core histone available in the free pool, which represent the transient equilibrium between chromatin association and disassociation.

The rates of initial fluorescence recovery of H2A and H3.3 were increased during HSV-1 infection. Thus, HSV-1 transcription, HSV-1 proteins, HSV-1 DNA replication, or cellular responses to them increase the rate of fast chromatin exchange of H2A and H3.3. In order to increase the overall rate of fast chromatin exchange, the relative rates of low-affinity chromatin association and disassociation could both be increased. Thus, the low-affinity chromatin binding of H2A and H3.3 is likely destabilized relative to mock-infected cells. In addition to faster rates of low-affinity chromatin exchange, the pools of free H2A and H3.3 were increased. The rates of chromatin association and disassociation are increased relative to mock-infected cells, but also altered relative to each other to increase the level available in the free pool. That is, the rate of chromatin disassociation (or displacement) is greater than the relative rate of chromatin association.

Unlike H2A and H3.3, the rate of initial fluorescence recovery of H2B was decreased during HSV-1 infection. HSV-1 proteins, HSV-1 DNA replication, or cellular responses to them therefore decrease the rate of

fast chromatin exchange of H2B. To decrease the overall rate of fast chromatin exchange, the rates of H2B low-affinity chromatin association and disassociation should both be decreased. However, the pool of free H2B is still increased during HSV-1 infection. Although both the rates of H2B chromatin association and disassociation are decreased relative to mock-infected cells, they are also offset relative to each other to achieve an increase the pool of free H2B. The rate of low-affinity chromatin association of H2B must be further decreased than the rate of chromatin disassociation (or displacement). At the extreme, H2B low-affinity chromatin association may be blocked. Then, H2B could only re-bind chromatin through the slower high-affinity chromatin association, and the pool of free H2B would be increased. Overall, these data suggest that the chromatin affinity of bound H2B in HSV-1 infected cells is higher than that in mock-infected cells. Furthermore, unbound H2B is less likely to re-bind chromatin or more likely to re-bind chromatin through a slower mechanism of chromatin association (such as the high-affinity chromatin associations).

Nucleosome core particles are hetero-octamers of 4 core histones, H2A, H2B, H3, and H4. The association of HSV-1 genomes with histones in unstable nucleosomes therefore requires all four core histones. The mobilization of all core histones during infection provides a source for all the histones required for assembly of nucleosome core particles with HSV-1 genomes.

The differences in the mobilization of H2A, H2B, H3.3, and H4 during HSV-1 infection most likely indicate different mechanisms of core

histone mobilization. If a single mechanism resulted in mobilization of all histones, then mobilization of all should have had the same requirements. Most surprisingly, histones H2A and H2B, which form one of the nucleosome dimers, were mobilized differently. H2A has variants, H2A.Z, H2A.X, H2A.Bbd, and macroH2A. The different mobilization of H2A and H2B suggests that the mobilized population of H2B likely forms dimers with some of the H2A variants.

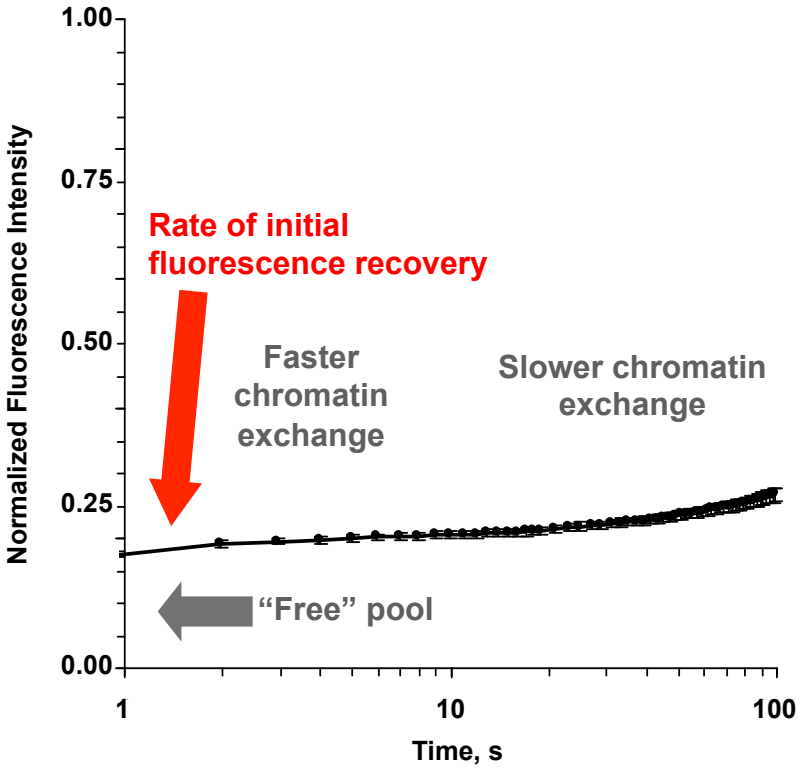

FIGURE 4.1: Core histone fluorescence recovery after photobleaching. Line graph representing the relative fluorescence intensity of the photobleached nuclear region in a cell expressing GFP-core histone fusion proteins plotted against time. Time is plotted on a semi-logarithmic scale. The first measure after photobleaching is indicative of the population of core histones not bound to chromatin and therefore freely diffusing. The fluorescence recovery is biphasic. The early fast recovery phase represents the population of core histones with faster chromatin exchange, whereas the slow recovery phase represents the population with slower chromatin exchange. The rate of initial fluorescence recovery is used as a surrogate measure to evaluate fast chromatin exchange.

FIGURE 4.2: Expression of ICP4 as nuclear dispersed or accumulated into replication compartments in U2OS cells expressing GFP-H3.3. Digital fluorescent micrographs of U2OS cells expressing GFP-H3.3 and stained with α-ICP4 antibodies. Cells were transfected with plasmids expressing GFP-H3.3 and infected with 5 PFU/cell of HSV-1 strain KOS. Cells were fixed at 2.5 (**2 hpi**), 4.5 (**4 hpi**) or 7.5 hpi (**7 hpi**) as indicated and stained for ICP4. Single (**α-ICP4**, **GFP-H3.3**, differential interference contrast, **DIC**) and merged (**Merge**) images are shown. Cells with ICP4 expressed as nuclear dispersed (**ND**) or replication compartments (**RC**) are indicated. Rightmost panels, 16x digital enlargement of the regions indicated by the boxes on the leftmost "merge" images, highlighting the colocalization of H3.3 and ICP4 signals (pixels in different shades of yellow and orange)

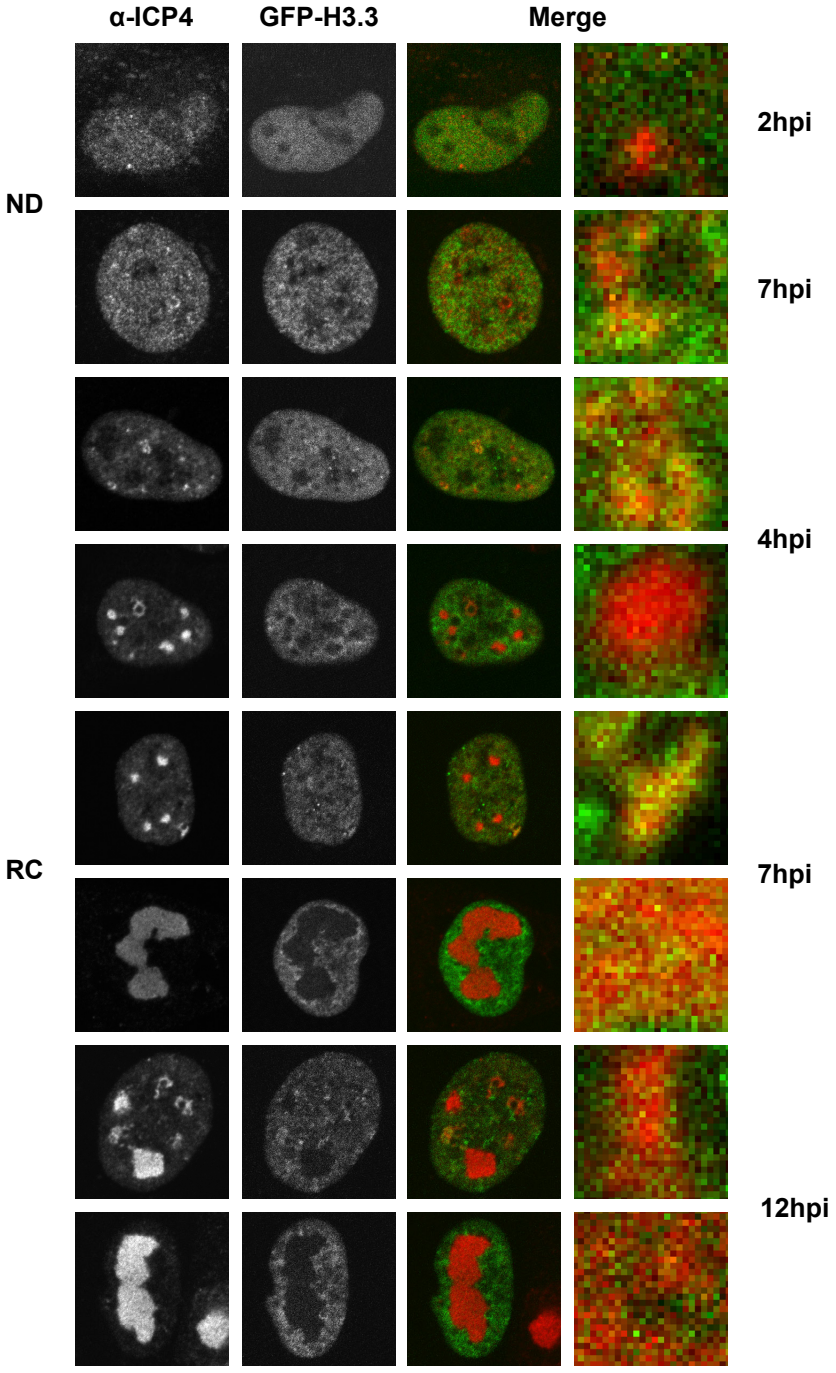
α-ICP4
GFP-H3.3
Merge
ND
RC
2hpi
7hpi
4hpi
7hpi
12hpi

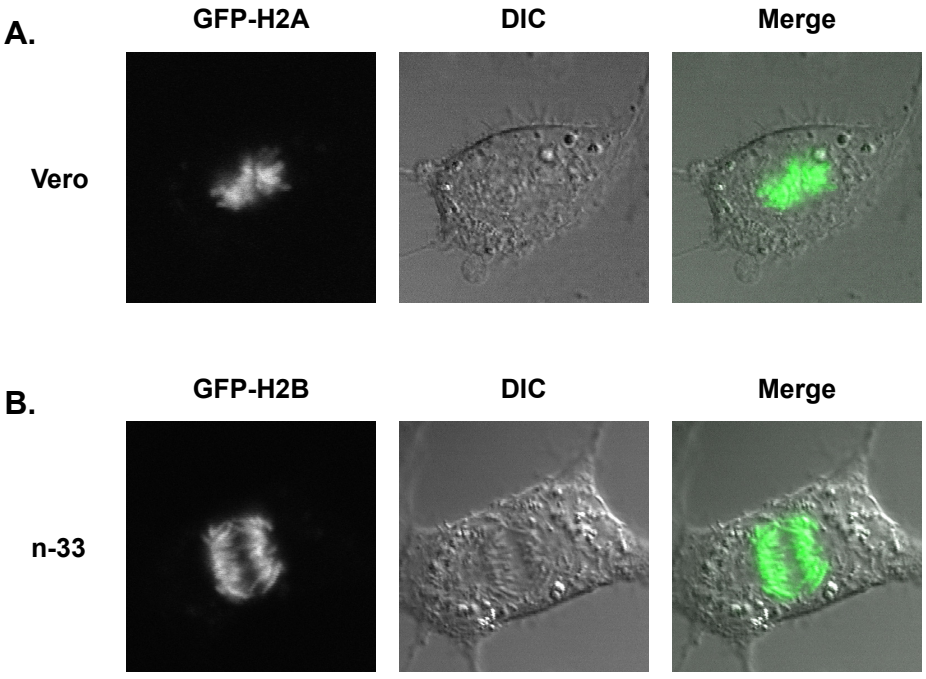

FIGURE 4.3: GFP-H2A and GFP-H2B are incorporated in mitotic chromosomes. Digital fluorescent micrographs of Vero (**A**) and n-33 (**B**) cells expressing GFP-H2A and GFP-H2B, respectively. Vero cells were transfected with plasmids expressing GFP-H2A (**GFP-H2A**) and n-33 cells were transfected with plasmids expressing GFP-H2B (**GFP-H2B**). Transfected cells were mock-infected. Live cells were observed on a 2-photon confocal microscope from 7 to 8 hpi. Single (**GFP-Histone** and differential image contrast, **DIC**) and merged (**Merge**) images are shown. Cells show strictly chromosomal localization of GFP-Histones.

FIGURE 4.4: The percent of free GFP-core histone per cell does not correlate with the level GFP-core histone expression. Dot plots representing the level of GFP-core histone in the free pool of each individual cell against its normalized fluorescence intensity. Vero cells were transfected with plasmids expressing GFP-H2A (**H2A**), GFP-H2B (**H2B**), GFP-H3.3 (**H3.3**), or GFP-H4 (**H4**). Transfected cells were mock-infected and nuclear mobility of each GFP-core histone was evaluated from 4 to 5 hpi (**4 hpi**) or 7 to 8 hpi (**7 hpi**) by FRAP.

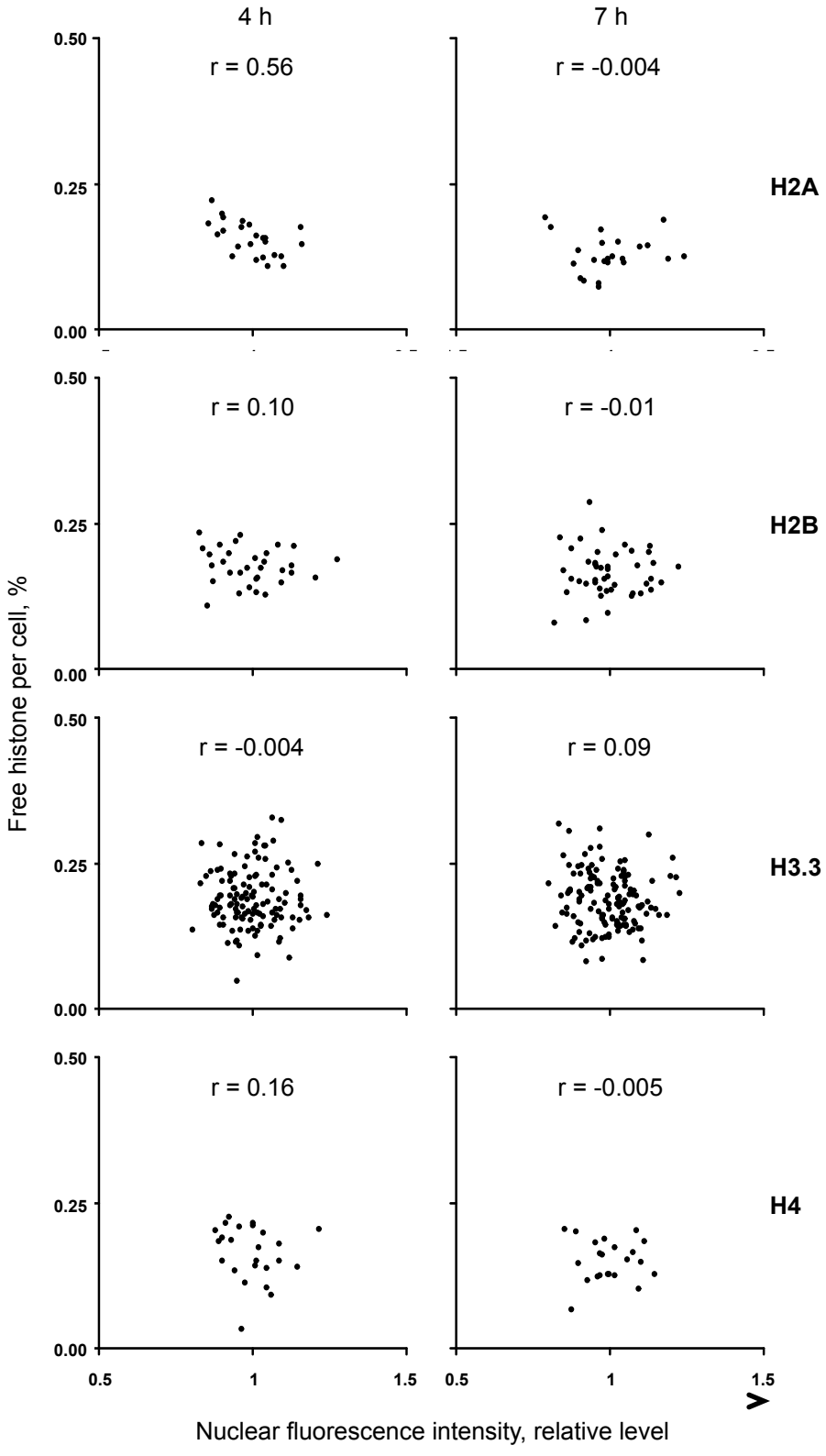
4 h
7 h
r = 0.56
r = -0.004
H2A
r = 0.10
r = -0.01
H2B
r = -0.004
r = 0.09
H3.3
r = 0.16
r = -0.005
H4
0.50
0.25
0.00
0.5
1
1.5
Free histone per cell, %
Nuclear fluorescence intensity, relative level

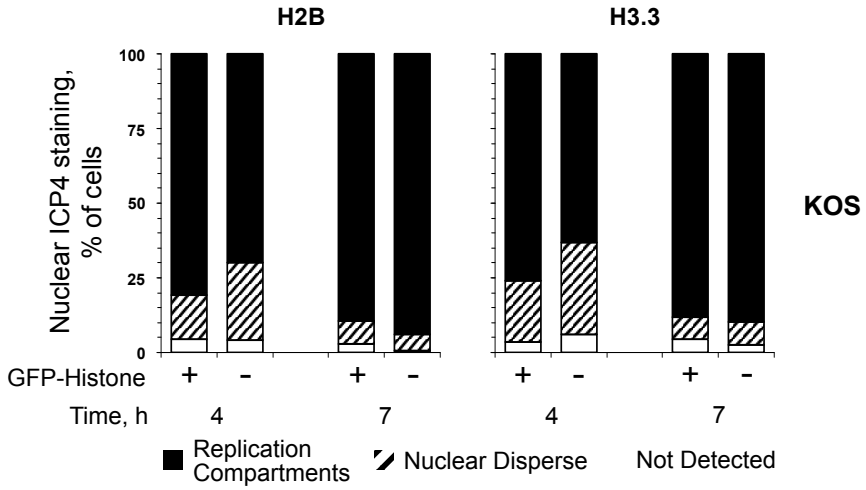

FIGURE 4.5: ICP4 expression and accumulation into replication compartments in Vero cells expressing GFP-H2B or GFP-H3.3 and infected with wild-type HSV-1 strain KOS. Bar graphs representing the percentage of HSV-1-infected cells transfected with GFP-H2B or GFP-H3.3 and expressing ICP4 as nuclear dispersed or accumulated into replication compartments. Vero cells were transfected with plasmids expressing GFP-H2B or GFP-H3.3. Cells were infected with 30 PFU per cell of HSV-1 strain KOS. Cells were fixed at 4.5 (**4**) or 7.5 (**7**) hpi and stained for ICP4. Nuclear expression of ICP4 and its accumulation into replication compartments in cells in which GFP-H2B or GFP-H3.3 were expressed (**+**) or not (**-**) were evaluated by fluorescence microscopy.

FIGURE 4.6: Core histones H2A, H2B, H3.3, and H4 are mobilized in Vero cells at early and late times after infection with HSV-1. Line graphs representing the normalized fluorescence intensity of the photobleached nuclear region against time. Vero cells were transfected with plasmids expressing GFP-H2A (**H2A**), GFP-H2B (**H2B**), GFP-H3.3 (**H3.3**), or GFP-H4 (**H4**). Transfected cells were mock-infected (**filled circle**) or infected with 10 (**open triangle**) or 30 (**open circle**) PFU per cell of HSV-1 strain KOS. Nuclear mobility of each GFP-core histone was evaluated from 4 to 5 hpi (**4 hpi**) or 7 to 8 hpi (**7 hpi**) by FRAP. Error bars, SEM; n ≥ 20. Time plotted on a semi-logarithmic scale.

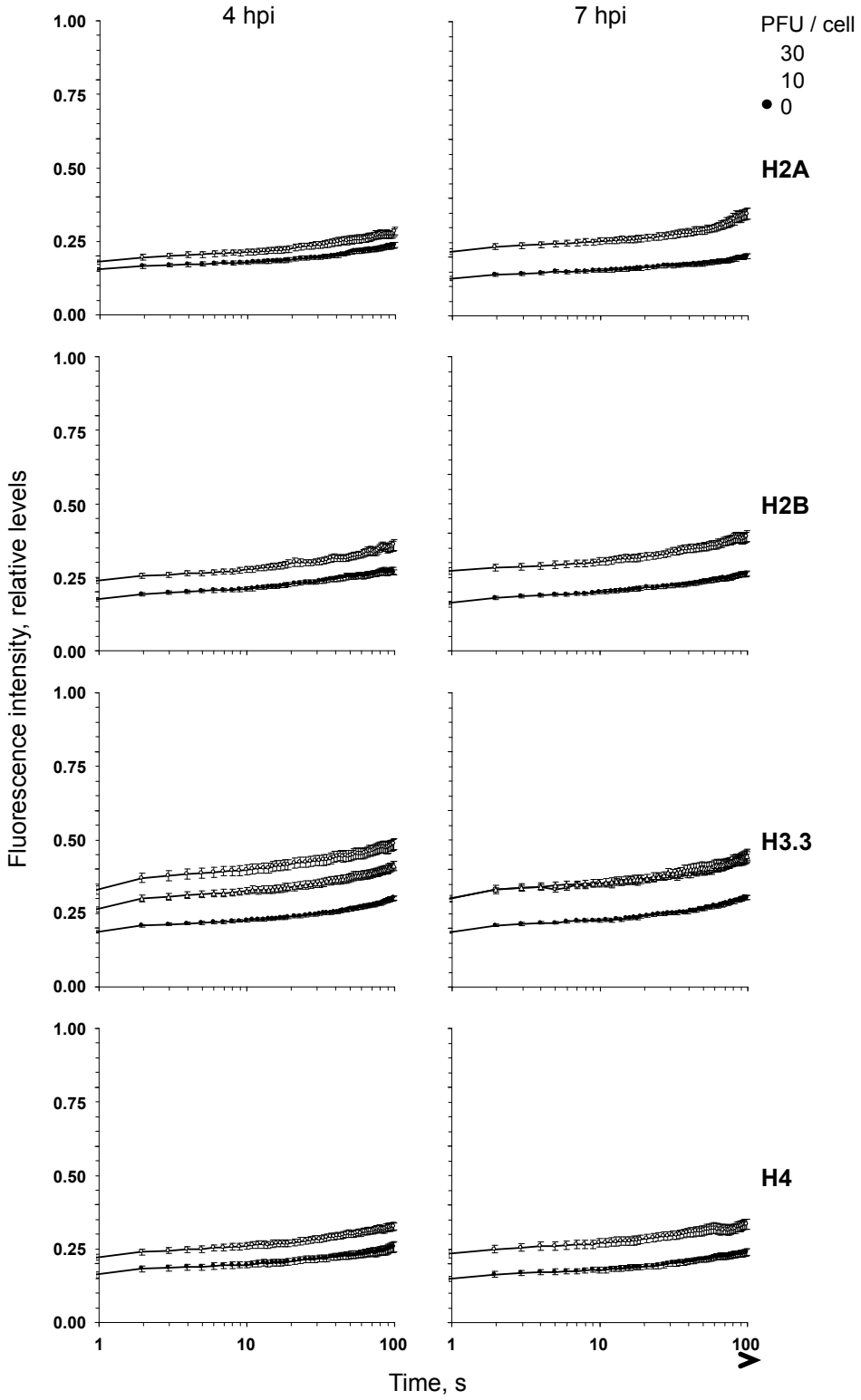
4 hpi
7 hpi
PFU / cell
30
10
0
H2A
H2B
H3.3
H4
Fluorescence intensity, relative levels
1.00
0.75
0.50
0.25
0.00
1
10
100
Time, s

FIGURE 4.7: The percent of free GFP-core histone per cell does not correlate with the level GFP-core histone expression. Dot plots representing the level of GFP-core histone in the free pool of each individual cell against its normalized fluorescence intensity. Vero cells were transfected with plasmids expressing GFP-H2A (**H2A**), GFP-H2B (**H2B**), GFP-H3.3 (**H3.3**), or GFP-H4 (**H4**). Transfected cells were infected with 30 PFU per cell of HSV-1 strain KOS. Nuclear mobility of each GFP-core histone was evaluated from 4 to 5 hpi (**4 hpi**) or 7 to 8 hpi (**7 hpi**) by FRAP.

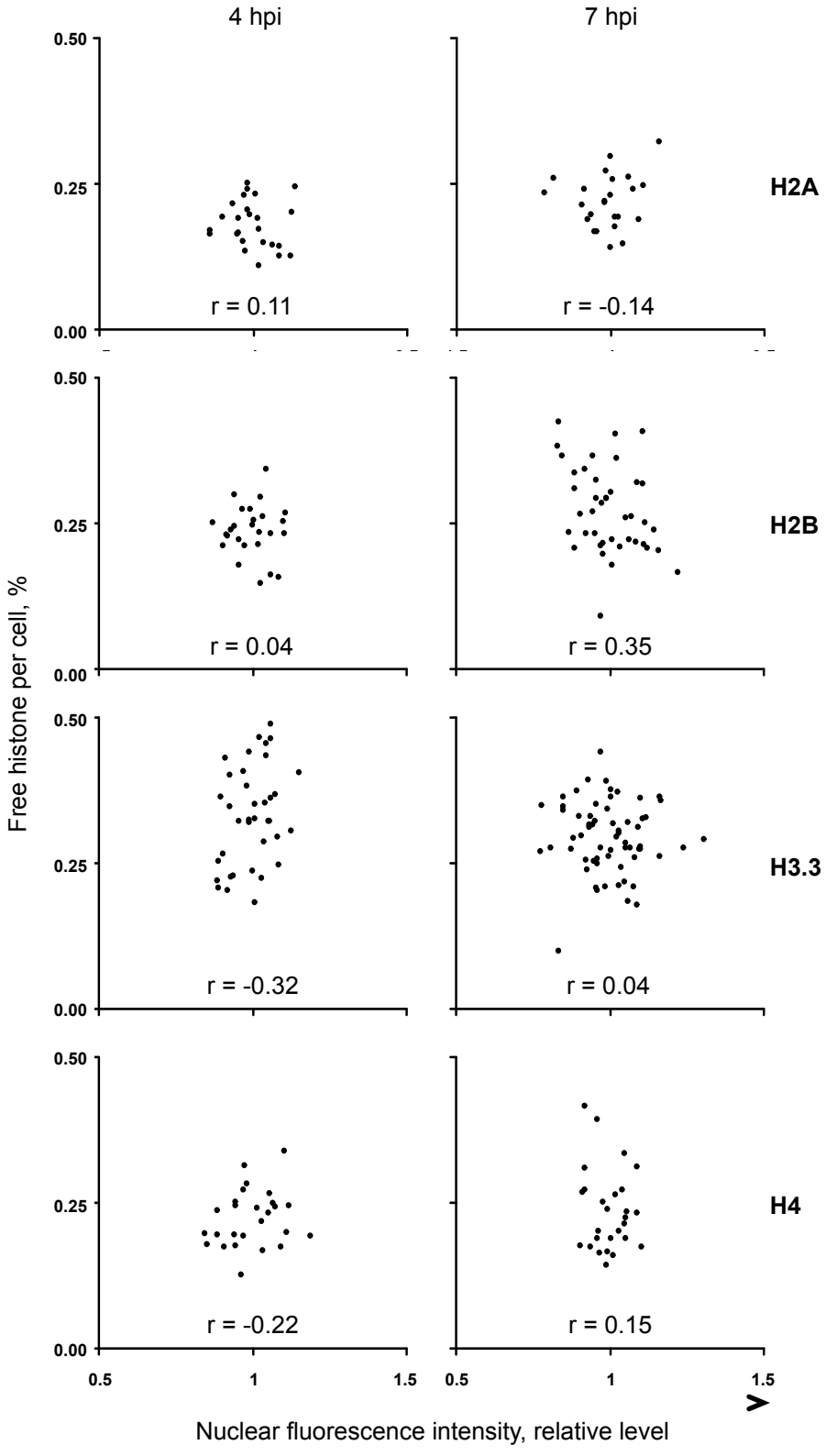
4 hpi
7 hpi
H2A
H2B
H3.3
H4
r = 0.11
r = -0.14
r = 0.04
r = 0.35
r = -0.32
r = 0.04
r = -0.22
r = 0.15
0.50
0.25
0.00
0.5
1
1.5
Free histone per cell, %
Nuclear fluorescence intensity, relative level

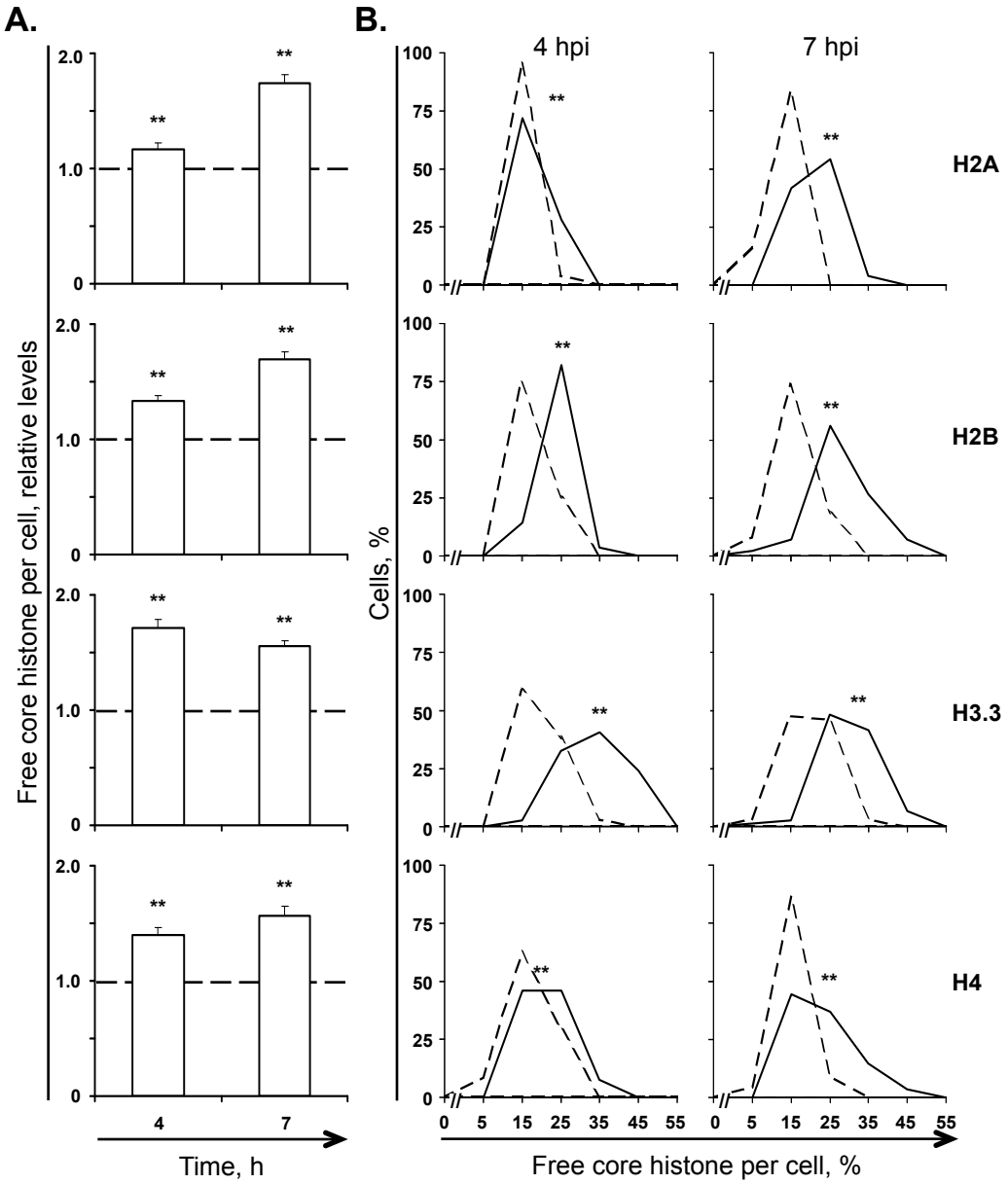

FIGURE 4.8: The pools of free H2A, H2B, H3.3, and H4 are increased during HSV-1 infection. A) Bar graphs representing the average percentage of free H2A, H2B, H3.3, and H4 in HSV-1 infected cells normalized to mock infected cells. Vero cells were transfected with plasmids encoding GFP-H2A (**H2A**), GFP-H2B (**H2B**), GFP-H3.3 (**H3.3**), or GFP-H4 (**H4**). Transfected cells were mock-infected or infected with 30 PFU per cell of HSV-1 strain KOS. Nuclear mobility of the GFP-histones was evaluated from 4 to 5 hpi (**4**) or 7 to 8 hpi (**7**) by FRAP. Error bars, SEM; n ≥ 20. **B)** Frequency distribution plots of the percentage of free H2A, H2B, H3.3, and H4 per individual cell evaluated by FRAP as described for Panel A. Dashed or solid lines, mock or HSV-1 strain KOS infected cells, respectively. *, $P < 0.05$, **, $P < 0.01$.

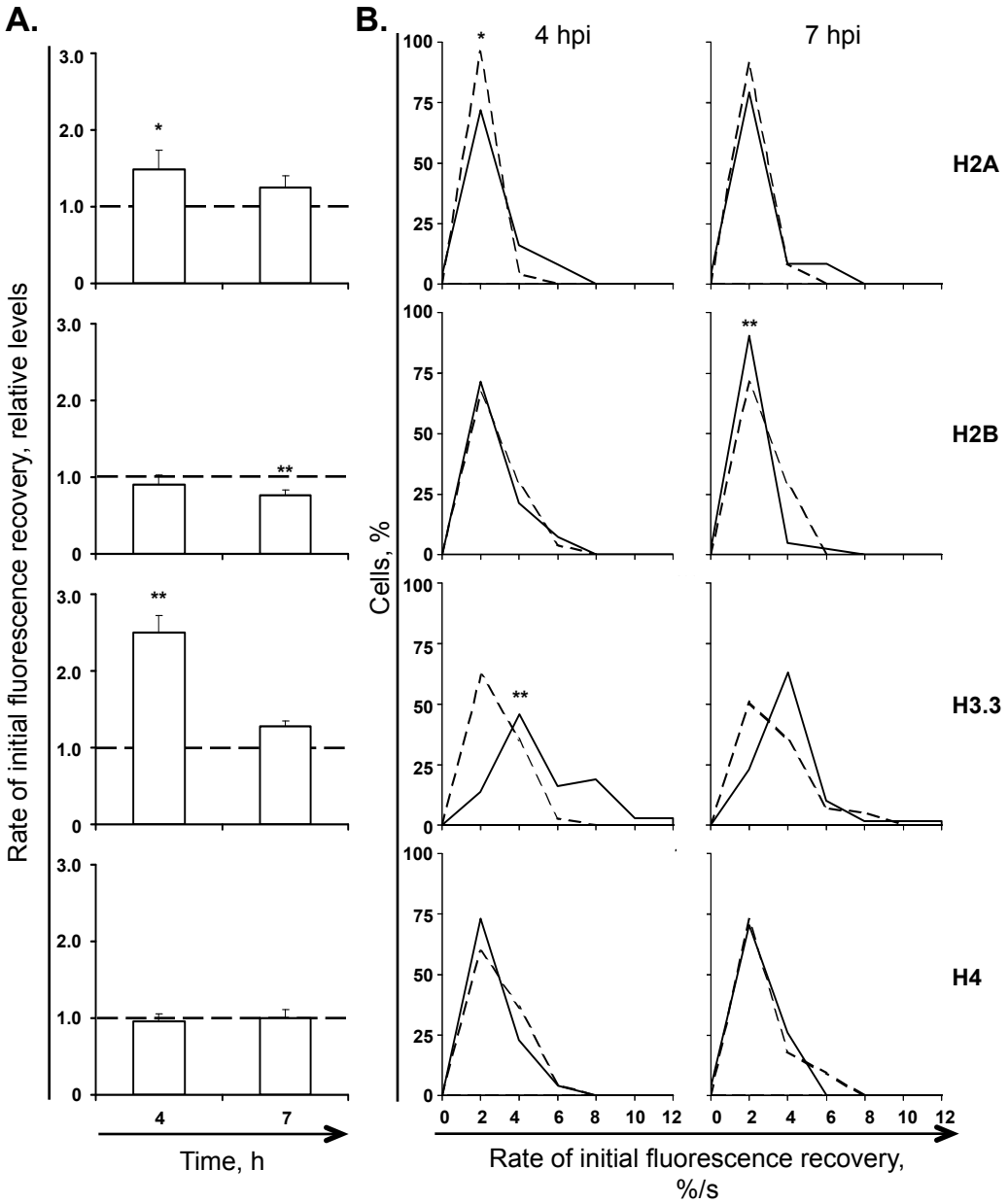

FIGURE 4.9: The rate of initial fluorescence recovery of H2A and H3.3 tends to increase, whereas that of H2B tends to decrease, during HSV-1 infection. A) Bar graphs representing the average rate of initial fluorescence recovery after photobleaching in HSV-1 infected cells normalized to mock infected cells. Vero cells were transfected with plasmids encoding GFP-H2A (**H2A**), GFP-H2B (**H2B**), GFP-H3.3 (**H3.3**), or GFP-H4 (**H4**). Transfected cells were mock-infected or infected with 30 PFU per cell of HSV-1 strain KOS. Nuclear mobility of the GFP-histones was evaluated from 4 to 5 hpi (**4**) or 7 to 8 hpi (**7**) by FRAP. Error bars, SEM; n ≥ 20. **B)** Frequency distribution plots of the rate of initial fluorescence recovery after photobleaching per individual cell evaluated by FRAP as described for Panel A. Dashed or solid lines, mock or HSV-1 strain KOS infected cells, respectively. *, $P < 0.05$, **, $P < 0.01$.

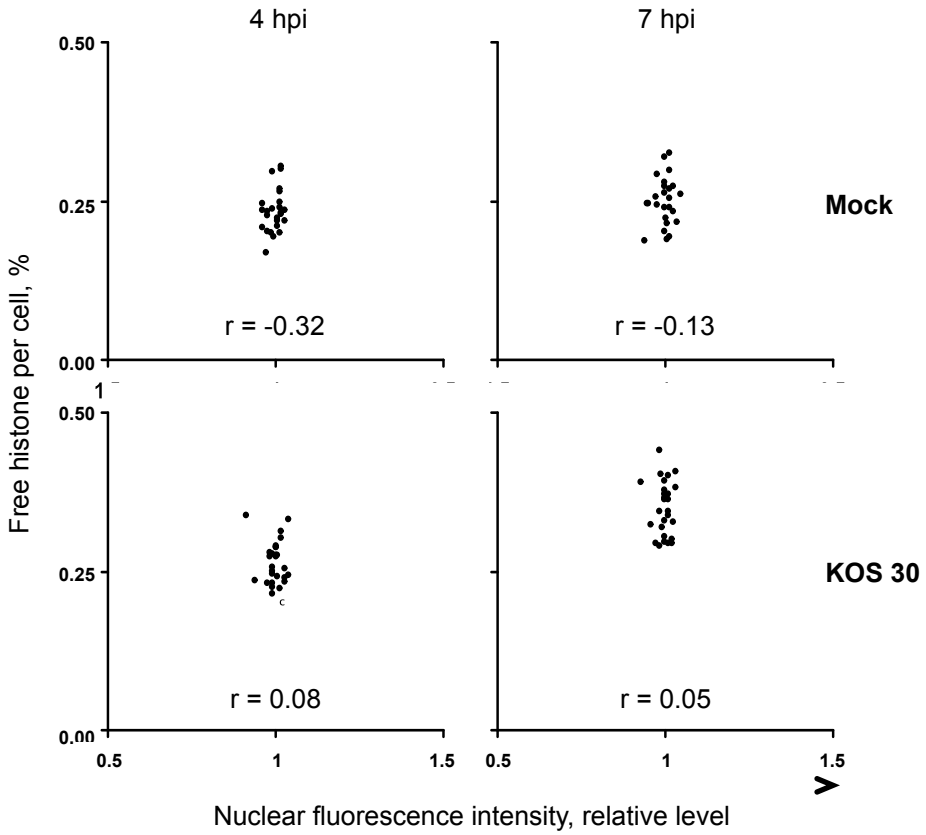

FIGURE 4.10: The percent of free GFP-H2B per cell does not correlate with the level of GFP-H2B expression in stably transfected HeLa cells. Dot plots representing the level of GFP-H2B in the free pool of each individual cell against its normalized fluorescence intensity. HeLa cells were infected with 30 PFU per cell of HSV-1 strain KOS. Nuclear mobility of GFP-H2B was evaluated from 4 to 5 hpi (**4 hpi**) or 7 to 8 hpi (**7 hpi**) by FRAP.

FIGURE 4.11: HeLa cells stably expressing GFP-H2B mobilize core histone H2B during infection with HSV-1. A) Line graphs representing the normalized fluorescence intensity of the photobleached nuclear region against time. HeLa cells stably transfected with plasmids encoding GFP-H2B were mock-infected (**filled**) or infected with 30 PFU per cell of HSV-1 strain KOS (**open**). Nuclear mobility of GFP-H2B was examined from 4 to 5 hpi (4hpi) or 7 to 8 hpi (7hpi) by FRAP. Error bars, SEM; n ≥ 25. Time plotted on a semi-logarithmic scale. **B)** Bar graph representing the average level of free H2B in HSV-1 infected cells, evaluated by FRAP as described for Panel A, normalized to mock infected cells and plotted against time postinfection. Error bars, SEM; n ≥ 25. **C)** Frequency distribution plots of the percentage of free H2B per individual cell evaluated by FRAP as described for Panel A. Dashed or solid lines, mock or HSV-1 strain KOS infected cells, respectively. **D)** Bar graph representing the average rate of initial fluorescence recovery after photobleaching in HSV-1 strain KOS infected cells normalized to mock infected cells evaluated by FRAP as described for Panel A. Error bars, SEM; n ≥ 25. **E)** Frequency distribution plots of the rate of initial fluorescence recovery after photobleaching per individual cell evaluated by FRAP as described for Panel A. Dashed or solid lines, mock or HSV-1 strain KOS infected cells, respectively. *, $P < 0.05$; **, $P < 0.01$.

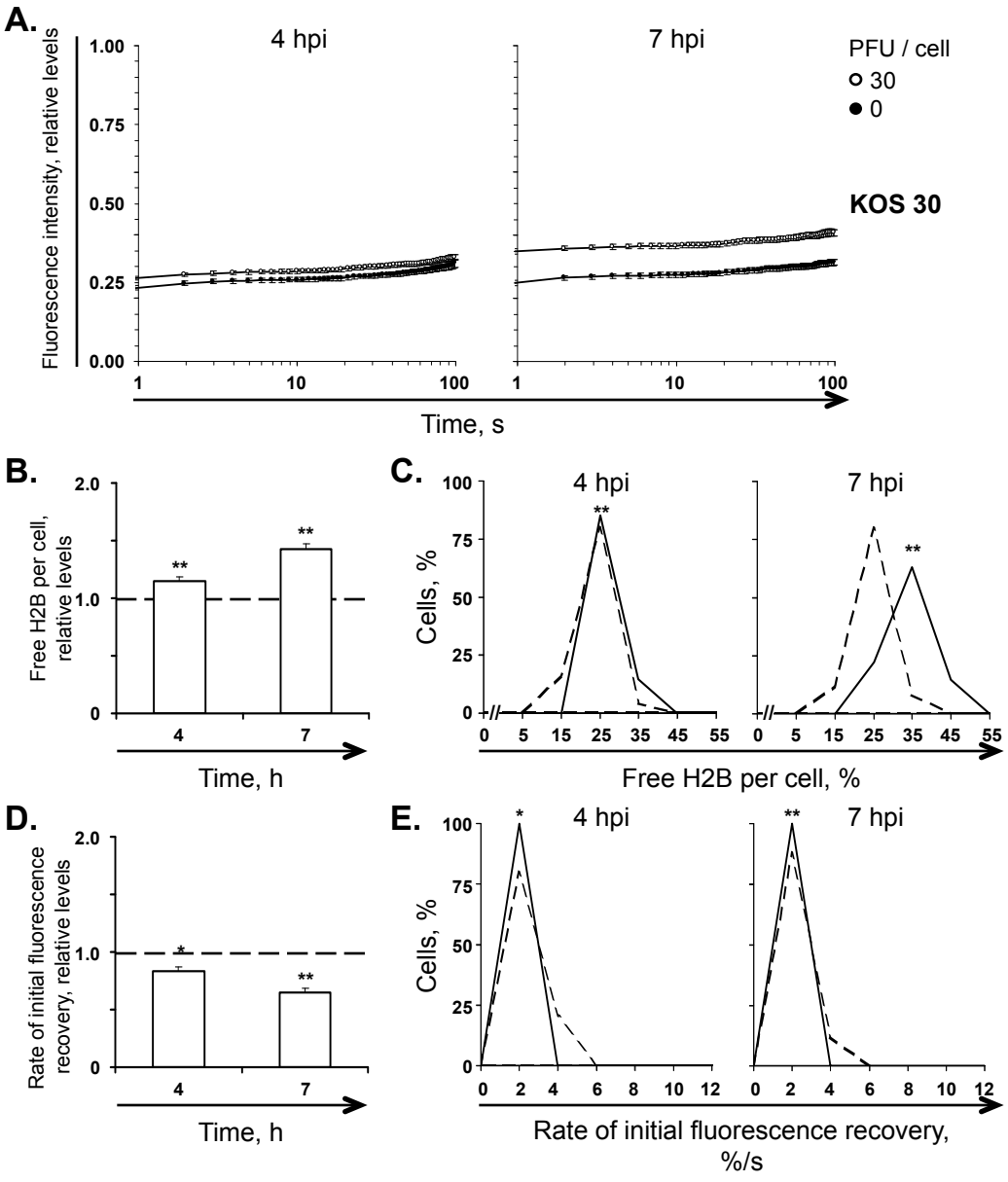
A.
4 hpi
7 hpi
PFU / cell
30
0
KOS 30
Fluorescence intensity, relative levels
1.00
0.75
0.50
0.25
0.00
1
10
100
Time, s
B.
Free H2B per cell, relative levels
2.0
1.0
0
**
4
7
Time, h
C.
4 hpi
7 hpi
Cells, %
100
75
50
25
0
0 5 15 25 35 45 55
Free H2B per cell, %
D.
Rate of initial fluorescence recovery, relative levels
*
E.
Rate of initial fluorescence recovery, %/s
0 2 4 6 8 10 12

Histone Variant	Virus Strain	PFU/ cell	4hpi Free core histone (avg ± SEM) Absolute	4hpi Free core histone (avg ± SEM) Relative	4hpi % Cells with large increase in free[a]	7hpi Free core histone (avg ± SEM) Absolute	7hpi Free core histone (avg ± SEM) Relative	7hpi % Cells with large increase in free[a]
H2A	-	-	0.15 ± 0.01	1.00 ± 0.04	17	0.13 ± 0.01	1.00 ± 0.05	17
	KOS	30	0.18 ± 0.01	1.17 ± 0.05	40	0.22 ± 0.01	1.74 ± 0.07	96
H2B	-	-	0.17 ± 0.01	1.00 ± 0.03	16	0.16 ± 0.01	1.00 ± 0.03	11
	KOS	30	0.24 ± 0.01	1.33 ± 0.05	79	0.27 ± 0.01	1.69 ± 0.07	88
H3.3	-	-	0.19 ± 0.01	1.00 ± 0.02	15	0.18 ± 0.01	1.00 ± 0.02	11
	KOS	30	0.33 ± 0.01	1.71 ± 0.07	89	0.30 ± 0.01	1.55 ± 0.05	84
H4	-	-	0.16 ± 0.01	1.00 ± 0.06	17	0.15 ± 0.01	1.00 ± 0.05	18
	KOS	30	0.22 ± 0.01	1.40 ± 0.07	58	0.23 ± 0.01	1.57 ± 0.09	70

TABLE 4.1: Levels of free H2A, H2B, H3.3, and H4 in Vero cells infected with HSV-1 strain KOS.
[a] Percentage of cells in which the level of free H1.2 was >1 SD above the average level in mock-infected cells.

			4hpi				7hpi			
Histone Variant	Virus Strain	PFU/ cell	Rate of initial fluorescence recovery, %/s (avg ± SEM) Absolute	Rate of initial fluorescence recovery, %/s (avg ± SEM) Relative	Fast chromatin exchange, % of cells Increased [a]	Fast chromatin exchange, % of cells Decreased [b]	Rate of initial fluorescence recovery, %/s (avg ± SEM) Absolute	Rate of initial fluorescence recovery, %/s (avg ± SEM) Relative	Fast chromatin exchange, % of cells Increased [a]	Fast chromatin exchange, % of cells Decreased [b]
H2A	-	-	1.12 ± 0.09	1.00 ± 0.08	17	8	1.34 ± 0.12	1.00 ± 0.08	8	13
	KOS	30	1.65 ± 0.27	1.49 ± 0.25	28	12	1.09 ± 0.22	1.25 ± 0.16	33	8
H2B	-	-	1.87 ± 0.15	1.00 ± 0.07	19	16	1.62 ± 0.10	1.00 ± 0.06	20	15
	KOS	30	1.63 ± 0.22	0.90 ± 0.12	18	32	1.22 ± 0.11	0.77 ± 0.07	2	34
H3.3	-	-	2.05 ± 0.13	1.00 ± 0.06	14	13	2.31 ± 0.13	1.00 ± 0.05	14	11
	KOS	30	4.12 ± 0.37	2.50 ± 0.22	70	0	2.99 ± 0.19	1.27 ± 0.07	20	1
H4	-	-	1.98 ± 0.21	1.00 ± 0.09	14	32	1.54 ± 0.26	1.00 ± 0.17	9	5
	KOS	30	1.81 ± 0.20	0.95 ± 0.10	19	19	1.57 ± 0.19	0.99 ± 0.11	11	4

TABLE 4.2: Rate of initial fluorescence recovery of H2A, H2B, H3.3, and H4 in Vero cells infected with HSV-1 strain KOS.

[a] Percentage of cells in which the rate of initial fluorescence recovery was >1 SD above the average rate of initial fluorescence recovery in mock-infected cells.

[b] Percentage of cells in which the rate of initial fluorescence recovery was >1 SD lower than the average rate of initial fluorescence recovery in mock-infected cells.

Hour Post Infection	Virus Strain	PFU/ cell	Free H2B (avg ± SEM)		% Cells with large increase in free H2B[a]
			Absolute	Relative	
4	-	-	0.23 ± 0.01	1.00 ± 0.02	16
	KOS	30	0.26 ± 0.01	1.15 ± 0.04	52
7	-	-	0.25 ± 0.01	1.00 ± 0.02	20
	KOS	30	0.35 ± 0.01	1.43 ± 0.05	100

TABLE 4.3: Levels of free H2B in HeLa cells infected with HSV-1 strain KOS.

[a] Percentage of cells in which the level of free H2B was >1 SD above the average level in mock-infected cells.

Hour Post Infection	Virus Strain	PFU/ cell	Rate of initial fluorescence recovery, %/s (avg ± SEM)		% Cells with large increase in the initial rate of recovery [a]	% Cells with large decrease in the initial rate of recovery [b]
			Absolute	Relative		
4	-	-	1.53 ± 0.10	1.00 ± 0.06	20	12
	KOS	30	1.27 ± 0.05	0.83 ± 0.03	0	19
7	-	-	1.59 ± 0.06	1.00 ± 0.04	20	12
	KOS	30	1.03 ± 0.06	0.65 ± 0.04	4	81

TABLE 4.4: Rate of initial fluorescence recovery of H2B in HeLa cells infected with HSV-1 strain KOS.

[a] Percentage of cells in which the rate of initial fluorescence recovery was >1 SD above the average rate of initial fluorescence recovery in mock-infected cells.

[b] Percentage of cells in which the rate of initial fluorescence recovery was >1 SD lower than the average rate of initial fluorescence recovery in mock-infected cells.

CHAPTER 5: REQUIREMENTS FOR THE MOBILIZATION OF CORE HISTONES H2B AND H3.3 DURING HSV-1 INFECTION.

This Chapter contains unpublished data.

ABSTRACT

Core histones H2A, H2B, H3.3, and H4 are all mobilized during HSV-1 infection increasing the level of core histones available in the free pools. However, their rates of fast chromatin exchange are differentially altered. The rates of H2A and H3.3 were increased early during infection, whereas that of H2B was decreased later on and that of H4 was unchanged. Therefore, HSV-1 transcription, DNA replication, expression of specific HSV proteins, or cellular responses to infection may increase the pools of free core histones or alter the rates of H2A, H2B, or H3.3 fast chromatin exchange. The differences in the mechanisms of mobilization of core histones suggest responses to different factors. To investigate the requirements for core histone mobilization, I focused on H2B and H3.3, which represent the different mechanisms of mobilization. H2B and H3.3 had common and unique requirements for mobilization. The increases to the free pools of H2B and H3.3, and the changes to their rates of fast chromatin exchange, were independent of HSV-1 DNA replication or L proteins. The early increase in free H2B, its decrease in fast chromatin exchange, and the basal increase in free H3.3 were also independent of HSV-1 gene transcription and IE or E proteins. Such mobilization therefore likely reflects cellular responses to infection. The

larger H3.3 mobilization, however, required VP16 or ICP0 at early times and, like the larger mobilization of H2B, expression of HSV-1 IE or E proteins at later times.

5.1 INTRODUCTION.

Core histones are mobilized during HSV-1 infection. Such mobilization could be due to HSV-1 gene transcription, expression of HSV-1 proteins, HSV-1 DNA replication, cellular responses to them, or a combination of these mechanisms. The mobilization of all the core histones altered their chromatin exchange such that the levels of H2A, H2B, H3.3, and H4 in the free pools were increased. Although all the pools of free core histones were increased, their rates of fast chromatin exchange were differentially altered during HSV-1 infection. The fast chromatin exchange rates of H2A and H3.3 were increased, that of H2B decreased, and that of H4 was unchanged, relative to mock-infected cells. The differential changes in the parameters of histone mobilization that I analyzed suggest that there are likely different mechanisms of core histone mobilization. Such different mechanisms would likely also require different viral factors.

While the pools of free H2B and H3.3 were both increased during HSV-1 infection, the rate of H2B fast chromatin exchange was decreased whereas that of H3.3 was increased. If there were indeed different mechanisms of core histone mobilization, their differential mobilizations indicate that these histones may be representative of such different mechanisms. I therefore focused on the mobilization of H2B and H3.3 in my evaluation of the requirements for core histone mobilization during HSV-1 infection.

In addition to potentially representing different models for core histone mobilization during HSV-1 infection, H2B and H3.3 represent structurally different components of the nucleosome. H3.3 is a component of the core nucleosome tetramer (consisting of two H3/H4 dimers), whereas H2B is a component of the dimers with H2A that bind to the H3/H4 tetramer. Moreover, the H2A/H2B dimers attach to the H3/H4 tetramer through contacts between H2A and H4 (Luger, Mader, Richmond, Sargent, & Richmond, 1997). Therefore, H3.3 and H2B make no contacts within the core nucleosome. As yet another difference, the H3/H4 tetramer is more stably incorporated in chromatin than the H2A/H2B dimers, as demonstrated by the slower chromatin exchange of H3 (likely H3.1) and H4 relative to that of H2A and H2B (Kimura & Cook, 2001).

The chromatin exchange of H2B and H3.3 occurs through common and unique mechanisms. H2B is a canonical core histone, and is consequently only synthesized during the S-phase of the cell cycle. As such, H2B is initially incorporated in chromatin by DNA replication dependent mechanisms. However, a population of H2B is highly mobile and undergoes transcription associated chromatin exchange (Kimura & Cook, 2001). Thus, H2B incorporation in chromatin occurs by both DNA replication dependent and independent mechanisms. H3.3, in contrast, is a variant core histone that is expressed throughout the cell cycle. Its incorporation in chromatin occurs by DNA replication independent mechanisms, such as transcription-associated chromatin exchange.

H2B and H3.3 represent structurally different aspects of the nucleosome and have common and unique mechanisms of chromatin exchange. They may also be mobilized by different mechanisms during HSV-1 infection. I used mutant viruses and drug treatments to evaluate the requirements for core histone H2B and H3.3 mobilization. I also tested whether the different parameters of such mobilization indeed reflect different requirements.

5.2 RESULTS.

5.2.1 HSV-1 DNA replication is not required for H2B or H3.3 mobilization.

H2B is incorporated in chromatin by DNA replication dependent and independent mechanisms, whereas H3.3 is typically incorporated in chromatin by DNA replication independent mechanisms. The mobilization of H2B and H3.3 at early and late times after HSV-1 infection suggests that HSV-1 DNA replication, or cellular responses to it, may mobilize core histones. I therefore first analyzed whether HSV-1 DNA replication was required to mobilize H2B and H3.3. To this end, infected cells were treated with 400μg/ml of phosphonoacetic acid (PAA) to inhibit the HSV-1 DNA polymerase (Schang et al., 2000).

PAA treatment alone appeared to increase the chromatin exchange of H2B and H3.3 in mock-infected cells (Figures 5.1 A and 5.2 A, compare open and closed circles). Despite this slight effect in mock-infected cells, H2B and H3.3 were mobilized to a similar degree in Vero cells infected with 30 PFU per cell of KOS in the presence or absence of

PAA (Figures 5.1 and 5.2, Table 5.1). In cells treated with PAA, mobilization of H2B and H3.3 altered their relative rates of chromatin binding and unbinding such that their free pools were increased ($P<0.01$, Student's T-test; 1-tail) (Figure 5.1 Panels B and C, Figure 5.2 Panels B and C, Table 5.1). In the presence or absence of PAA, the pool of free H2B was increased to a similar level (to 158 ± 7% and 169 ± 7%, respectively) ($P>0.05$, Tukey's HSD) (Figure 5.1 Panels B and C, Table 5.1). As in the absence of PAA, free H2B was increased throughout the population of infected cells. At 7hpi, 93% of infected cells treated with PAA had a large increase in free H2B, in comparison to the expected 16% of cells from a normal frequency distribution (Figure 5.1 Panel C, Table 5.1). The pool of free H3.3 was increased to 137 ± 6% in Vero cells infected with 30 PFU per cell and treated with PAA, the same degree as in the absence of PAA, 155 ± 5% ($P>0.05$, Tukey's HSD) (Figure 5.2 Panels B and C, Table 5.1). Free H3.3 was also increased throughout the population of infected cells treated with PAA. At 7hpi, 64% of cells had a large increase to their pool of free H3.3 (Figure 5.2 Panel C, Table 5.1). HSV-1 DNA replication or strictly L proteins are therefore not required to increase the pools of free H2B or H3.3. Alternatively, the DNA damage response induced by PAA would have to mobilize H2B and H3.3 to exactly the same extent as DNA replication would have done if PAA were not present. Therefore, these results suggest that HSV-1 transcription, HSV-1 IE or E proteins, or cellular responses to them, are required to increase the levels of H2B and H3.3 available in the free pool.

The relative rates of H2B and H3.3 fast chromatin exchange were similar in Vero cells infected with 30 PFU per cell of KOS and treated or not with PAA ($P>0.05$, Tukey's HSD) (Figure 5.1 Panels D and E, Figure 5.2 Panels D and E, Table 5.1). The fast chromatin exchange rate of H2B in cells infected in the presence of PAA had a tendency to be decreased, to 0.88 ± 0.07 fold, whereas that of H3.3 had a tendency to increase, to 1.40 ± 0.18 fold (Figure 5.1 Panels D and E, Figure 5.2 Panels D and E, Table 5.1). However, neither the decrease in the rate of H2B chromatin exchange nor the increase in the rate of H3.3 chromatin exchange reached statistical significance ($P>0.05$, Student's T-test; 1-tail). These data suggest that HSV-1 DNA replication or strictly L proteins are not required to alter the rates of fast chromatin exchange of H2B or H3.3. Alternatively, but highly unlikely, HSV-1 DNA replication may be required to mobilize H2B and H3.3. However, the requirement for such mobilization is masked by H2B and H3.3 mobilization induced by the DNA damage response activated by PAA treatment.

5.2.2 H3.3 mobilization, and the large increase in its free pool, requires HSV-1 IE or E proteins but not VP16 or ICP0.

HSV-1 DNA replication and strictly L proteins were not required to mobilize histone H3.3. I therefore tested whether HSV-1 transcription or expression of specific HSV-1 IE or E proteins contributed to H3.3 mobilization. To this end, I used the HSV-1 strain KM110, which has a mutation in ICP0 (stop codon at codon 212) and VP16 (stop codon at

codon 422) (Mossman & Smiley, 1999). KM110 fails to activate expression of IE genes and is therefore unable to replicate in Vero cells.

In Vero cells infected with KM110, ICP4 was undetectable in 95 ± 1% or 80 ± 4% of cells infected with 30 PFU per cell of KM110 at 4 or 7hpi, respectively, regardless of whether the cells expressed GFP-H3.3 or not (Figure 5.3, Table 5.2). In the cells in which ICP4 was detected, it was mainly nuclear dispersed. Less than 5% of cells had ICP4 accumulated into replication compartments, even at 7hpi (Figure 5.3, Table 5.2).

Under such conditions of little to no HSV-1 transcription and protein expression, H3.3 was only slightly mobilized at early or late times after infection (Figure 5.4 KM110). The rates of H3.3 chromatin association and disassociation were altered relative to each other such that there was a marginal increase in the pool of free H3.3 (Figure 5.5 KM110, Table 5.3). It was increased to 111 ± 3% and 121 ± 5% at 4 and 7h, respectively, after infection with 30 PFU per cell of strain KM110 ($P<0.05$ and $P<0.01$, respectively, Student's T-test; 1-tail) (Figure 5.5 KM110, Table 5.3). The increase in free H3.3 during infections with KM110 was to a lesser degree ($P<0.01$, Tukey's HSD) than during infections with wild-type KOS (171 ± 7% and 155 ± 5% at 4 and 7hpi with 30 PFU per cell of KOS, respectively) (Figure 5.5 compare KOS 30 to KM110 30, Table 5.3). Although VP16, ICP0, HSV-1 transcription, and HSV-1 IE or E proteins are not required to increase the pool of free H3.3 by a marginal degree, they are required to increase it to a larger degree.

The pool of free H3.3 was still marginally increased under conditions of little to no HSV-1 transcription or protein expression. However, the fast chromatin exchange rate of H3.3 was not altered. The average rate of fast chromatin exchange of H3.3 was not increased at early or late times after infection with 30 PFU per cell of KM110 (1.08 ± 0.09 and 1.10 ± 0.12 at 4 and 7hpi, respectively) ($P>0.05$, Student's T-test; 1-tail) (Figure 5.6 KM110 30, Table 5.4). These data suggest that HSV-1 transcription, expression of specific HSV-1 IE or E proteins, the direct biochemical activities of VP16 or ICP0, or cellular responses to them are required to increase the rate of H3.3 low-affinity chromatin exchange.

VP16 and ICP0 disrupt chromatin. Their biochemical activities may therefore be directly required to increase the pool of free H3.3 to a larger degree or to increase its rate of fast chromatin exchange. To test these possibilities, I analyzed KM110 infections of U2OS cells. U2OS cells complement the replication defects of HSV-1 mutants in ICP0 or VP16, but do not complement any of the known biochemical activities of ICP0 or VP16 (Yao & Schaffer, 1995). HSV-1 proteins are expressed and HSV-1 DNA is therefore replicated during KM110 infections of U2OS cells (Mossman & Smiley, 1999).

At 4h after infection with 30 PFU per cell of KM110, 49 ± 4% of cells had ICP4 expressed as nuclear dispersed, whereas 32 ± 7% had accumulated it into replication compartments (Figure 5.3 KM110 U2OS; Table 5.2). Cells had similar ICP4 expression and accumulation into replication compartments whether GFP-H3.3 was expressed or not

(Figure 5.3 KM110 U2OS). As for KOS infections, GFP-H3.3 colocalized with ICP4 during KM110 infections of U2OS cells (Figure 5.7). Also as for KOS infections, such colocalization did not correlate in any obvious manner with the level of ICP4 expression, the degree of ICP4 accumulation into replication compartments, or the time after infection (Figure 5.7). VP16 and ICP0 are therefore not required for the co- or distinct localization of ICP4 and GFP-H3.3 during HSV-1 infection.

H3.3 was mobilized during KM110 infections of U2OS cells in the absence of VP16 and ICP0 (Figure 5.8 KM110). Such mobilization resulted in large increases in the pool of free H3.3 ($P<0.01$, Student's T-test; 1-tail). The pool of free H3.3 was increased to 126 ± 6% at 4 hours after infection of U2OS cells with 30 PFU per cell of KM110 and to 156 ± 7% at 7hpi (Figure 5.9 KM110 30, Table 5.3). The pool of free H3.3 was increased throughout the population of KM110 infected U2OS cells. Fifty percent or 85% of cells had their pools of free H3.3 increased to a large degree at 4 or 7hpi, respectively (Figure 5.9 Panel B KM110 30, Table 5.3). The free pool of H3.3 was equally increased at later times in U2OS cells infected with KM110 or KOS ($P>0.05$, Tukey's HSD), although the cells had to be infected with lower multiplicities of KOS due to nuclear morphological changes at higher multiplicities. Nonetheless, the pool of free H3.3 was increased to 194 ± 7% or 164 ± 5% at 4 or 7 hours after infection, respectively, with 6 PFU per cell of KOS ($P<0.01$, Student's T-test; 1-tail) (Figure 5.8 KOS, Figure 5.9 KOS 6, Table 5.3). HSV-1 transcription or expression of IE or E proteins is therefore required to

increase the pool of free H3.3 to a large degree, whereas the direct biochemical activities of VP16 or ICP0 are not.

Infection of U2OS cells with KM110 did not significantly alter the rate of H3.3 fast chromatin exchange. However, the fast chromatin exchange rate of H3.3 still had a tendency to be increased at early and late times (1.29 ± 0.25 and 1.16 ± 0.12 fold, respectively) after infection with 30 PFU per cell of KM110 (Figure 5.10 KM110 30, Table 5.4), in contrast to infections of U2OS cells with KOS. The rate of H3.3 fast chromatin exchange was increased to 1.55 ± 0.16 fold at 4 hours after infection of U2OS cells with 6 PFU per cell of KOS ($P<0.01$, Student's T-test; 1-tail) (Figure 5.10 KOS 6, Table 5.4). The rate of fast chromatin exchange still showed a tendency to be increased at later times after infection (to 1.37 ± 0.18 fold) (Figure 5.10 KOS 6, Table 5.4). However, statistical significance was not achieved. These data suggest that HSV-1 transcription or expression of HSV-1 IE or E proteins is not sufficient to increase the rate of H3.3 low-affinity chromatin exchange in U2OS cells. However, the absolute average values for the rate of H3.3 fast chromatin exchange in KM110 and mock-infected U2OS cells are high (Table 5.4). The already high rate of H3.3 fast chromatin exchange in mock-infected cells may therefore conceal any affect during KM110 infection. Further experiments are required to determine whether transcription or expression of HSV-1 IE or E proteins is sufficient or not to increase the rate of H3.3 fast chromatin exchange in KM110 infected U2OS cells. If transcription or expression of HSV-1 IE or E proteins is indeed not

sufficient to increase the rate of H3.3 fast chromatin exchange, then the direct biochemical activities of VP16 or ICP0 may be required.

5.2.3 The degree of HSV-1 IE or E protein expression correlates with the degree of increase in free H3.3, but not with the rate of H3.3 fast chromatin exchange.

To test whether progression of infection was required to increase the pool of free H3.3 by a large degree, or to increase the rate of H3.3 fast chromatin exchange, I evaluated H3.3 mobility during n212 infections of Vero cells. n212 carries the same ICP0 mutation as KM110, but has wild-type VP16 (Cai & Schaffer, 1989). Therefore, this strain replicates in Vero cells. At low multiplicities of infection, however, HSV-1 protein expression and DNA replication are delayed relative to wild-type infection (Cai & Schaffer, 1989).

The accumulation of ICP4 into replication compartments was delayed relative to KOS-infected cells, as expected (Cai & Schaffer, 1989). At 4 hpi, 57 ± 5% of cells infected with 30 PFU per cell of n212 had nuclear dispersed ICP4 and only 36 ± 5% had it accumulated into replication compartments, in comparison to 24 ± 4% and 71 ± 5% of cells infected with wild-type KOS, respectively (Figure 5.3, Table 5.2). At 7hpi, the population of cells with ICP4 accumulated into replication compartments had increased to 68 ± 5%, whereas that with nuclear dispersed ICP4 had decreased to 27 ± 5%, in comparison to 90 ± 3% and 7 ± 1% in cells infected with wild-type KOS, respectively (Figure 5.3,

Table 5.2). Cells expressing or not GFP-H3.3 had similar ICP4 expression and accumulation into replication compartments (Figure 5.3).

H3.3 was mobilized during n212 infections of Vero cells (Figure 5.4 n212). Such mobilization altered the relative rates of H3.3 chromatin association and disassociation such that the pool of free H3.3 was increased ($P<0.01$, Student's T-test; 1-tail) (Figure 5.5 n212 30, Table 5.3). The pool of free H3.3 was increased to 131 ± 6% ($P<0.01$, Student's T-test; 1-tail) at early times after infection of Vero cells with 30 PFU per cell of n212 (Figure 5.5 n212 30, Table 5.3). Although still increased, the pool of free H3.3 was increased to a lesser degree than during infections with wild-type KOS ($P<0.01$, Tukey's HSD) (Figure 5.5 compare KOS 30 to n212 30 4hpi, Table 5.3). At later times after infection with n212, however, the pool of free H3.3 was increased to a similar degree as in cells infected with wild-type KOS ($P>0.05$, Tukey's HSD) (Figure 5.5, Table 5.3). As with wild-type infections of Vero cells, the pool of free H3.3 was increased throughout the population of n212-infected cells. At early and late times, 61% and 89% of n212-infected cells, respectively, had a large increase in their pool of free H3.3, in comparison to the 16% expected for a normal distribution (Figure 5.5 Panel B n212 30, Table 5.3). The rate of H3.3 fast chromatin exchange had a tendency to be increased during n212 infection, to 1.29 ± 0.16 or 1.31 ± 0.13 fold at 4 or 7hpi, respectively (Figure 5.6 n212 30, Table 5.4). However, statistical significance was not achieved. The rate of H3.3 fast chromatin exchange at early times after infection was increased to a lesser extent than during wild-type KOS infections ($P<0.01$, Tukey's HSD) (Figure 5.6, Table 5.4).

Together, these data demonstrate that the degree of increase in the level of free H3.3 correlates with the progression of infection, whereas the increase in the rate of H3.3 fast chromatin exchange does not.

U2OS cells complement the replication defects of n212 such that this strain replicates with the same kinetics as wild-type KOS (Yao & Schaffer, 1995). Consistently, greater than 80% of cells had ICP4 accumulated into replication compartments at 4 or 7 h after infection with 30 or 6 PFU per cell of HSV-1 strain n212 or KOS, respectively (Figure 5.3, Table 5.2). As expected, H3.3 was mobilized during n212 infection of U2OS cells (Figure 5.8 n212). Such mobilization resulted in an increase in the pool of free H3.3. The pool of free H3.3 was increased to 163 ± 7% ($P<0.01$, Student's T-test; 1-tail) at 4h after infection of U2OS cells with 30 PFU per cell of n212 (Figure 5.9 n212 30, Table 5.3). Free H3.3 was increased to a lesser degree than in cells infected with wild-type KOS (194 ± 7%) ($P<0.01$, Tukey's HSD) (Figure 5.9 KOS 6, Table 5.3). This difference in the degree of increase in the pools of free H3.3 during KOS or n212 infections may reflect the population of cells with increased free pools. Indeed, 100% of cells infected with KOS had increased their pools of free H3.3 to a large degree at 4hpi, whereas only 88% of cells infected with n212 had (Table 5.3). At 7hpi, the pool of free H3.3 was increased to a similar degree ($P>0.05$, Tukey's HSD) in n212 or KOS infected cells (183 ± 6% or 164 ± 5%, respectively) (Figure 5.9, Table 5.3), and the same percentage of cells, 100% or 96%, respectively, had increased their free pools to a large degree (Table 5.3).

n212 infection of U2OS cells altered the relative rates of H3.3 chromatin association and disassociation to increase the pool of free H3.3, but did not increase the rate of H3.3 low-affinity chromatin exchange. Neither at early nor at late times after infection of U2OS cells with 30 PFU per cell of n212 was the rate of H3.3 fast chromatin exchange altered from that of mock-infected cells (Figure 5.10 n212 30, Table 5.4). Transcription of HSV-1 genomes and expression of HSV-1 proteins (other than ICP0) are therefore not sufficient to increase the rate of H3.3 low-affinity chromatin exchange in U2OS cells. ICP0 may therefore be required to increase the rate of H3.3 fast chromatin exchange.

Taken together, these data demonstrate that the magnitude of increase in the level of free H3.3, but not the rate of H3.3 fast chromatin exchange, correlates with the progression of HSV-1 infection. Moreover, ICP0 may be required to increase the rate of fast chromatin exchange of H3.3 during HSV-1 infection.

5.2.4 Infecting virions with cross-linked genomes are not sufficient to mobilize H3.3.

The pool of free H3.3 was still marginally increased in Vero cells infected with KM110, even though the majority of cells had little to no detectable ICP4 expression (Figures 5.3 and 5.5, Table 5.2). Virion fusion with the host cell membrane or virion proteins, other than VP16 or ICP0, may therefore be sufficient to increase the pool of free H3.3. I analyzed H3.3 mobility during infection with UV-inactivated KOS. During such infections, the virion still fuses with the host cell membrane and releases

the capsid and tegument proteins. However, the HSV-1 genome is cross-linked so no HSV-1 proteins are expressed. H3.3 was not mobilized, and its free pool was not increased, in Vero cells at early times, or U2OS cells at early or late times, after infection with 30 PFU per cell of UV-inactivated KOS (Figures 5.4, 5.5, 5.6, 5.8, 5.9, and 5.10 UV, Tables 5.3 and 5.4). Thus, virion fusion with the host cell membrane and release of capsid and tegument proteins is not sufficient to increase the pool of free H3.3, or to substantially alter the rate of fast H3.3 chromatin exchange.

Interestingly, the pool of free H3.3 was increased, to 121 ± 5% ($P<0.01$, Student's T-test; 1 tail), at late times after infection of Vero cells with 30 PFU per cell of UV-inactivated KOS (Figure 5.5 UV 30, Table 5.3). Had the UV-inactivated stock not been sufficiently inactivated, then infecting virions with non-cross-linked genomes would have been transcribed and HSV-1 proteins would have been expressed. However, Vero and U2OS cells were infected with the same stock of UV-inactivated KOS and the pool of free H3.3 was not increased in U2OS cells (Figure 5.5). Therefore, the increase in free H3.3 at later times after infection of Vero cells with UV-inactivated KOS likely reflects a cell-type specific response. Infection of Vero cells with UV-inactivated KOS may marginally alter the relative rates of H3.3 chromatin binding and unbinding such that a slight increase in the pool of free H3.3 is just detectable at later times after infection.

5.2.5 Mobilization of H2B, and the large increase in its free pool, does not require VP16, ICP0, or HSV-1 protein expression.

HSV-1 DNA replication, strictly L proteins, VP16, or ICP0 were not required to mobilize H3.3. HSV-1 transcription or expression of HSV-1 IE or E proteins, however, was required to increase the pool of free H3.3 by a large degree. As with H3.3, mobilization of H2B did not require HSV-1 DNA replication or strictly L proteins. I next analyzed whether H2B mobilization, and the large increase in its free pool, required the same HSV-1 factors as H3.3 did.

I first tested whether HSV-1 gene transcription or expression of HSV-1 IE or E proteins contributed to H2B mobilization using the HSV-1 mutant strain KM110 (Mossman & Smiley, 1999). ICP4 was undetectable in more than 80% of Vero cells infected with 30 PFU per cell of KM110 at 4hpi but in only 40% of cells at 7hpi (Figure 5.11, Table 5.5). When ICP4 staining was detected, it was mainly nuclear dispersed. Less than 20% of cells had ICP4 accumulated into replication compartments, even at 7hpi (Figure 5.11, Table 5.5). Expression of ICP4 and accumulation of ICP4 into replication compartments was similar in cells expressing GFP-H2B or not (Figure 5.11).

H2B was mobilized at early and late times after KM110 infection of Vero cells (Figure 5.12 Panel A). Such mobilization altered the relative rates of H2B chromatin association and disassociation such that there was an increase in the pool of free H2B ($P<0.01$, Student's T-test; 1-tail) (Figure 5.13 Panel A Vero, Table 5.6). The pool of free H2B was increased to 120 ± 4% or 125 ± 5% at 4 or 7hpi, respectively, in Vero

cells infected with 30 PFU per cell of KM110 (Figure 5.13 Panel A Vero, Table 5.6). The increase in free H2B occurred throughout the population of infected cells. Approximately 50% of cells had increased their pools of free H2B by a large degree at either time after infection, in comparison to the 16% expected from a normal distribution (Figure 5.13 Panel B Vero, Table 5.6). The pool of free H2B was increased to the same degree at 4h after infection with 30 PFU per cell of KM110 or wild-type KOS ($P>0.05$, Tukey's HSD) (Figure 5.13 Panel A Vero, Table 5.6). In contrast, ICP4 was detected in only approximately 15% of KM110 infected cells but in more than 95% of KOS infected cells (Figure 5.11 Vero, Table 5.5). Thus, the increase in free H2B at early times after infection did not correlate with the degree of HSV-1 IE (ICP4) protein expression, and therefore with the degree of HSV-1 gene transcription. At 7hpi, the pool of free H2B was increased to a larger degree in KOS infected cells than in KM110 infected cells, to 169 ± 7% or 125 ± 5%, respectively ($P<0.01$, Tukey's HSD) (Figure 5.13 Vero, Table 5.6). These differences reflect the different populations of infected cells with large increases in free H2B (88% of KOS infected cells versus 48% of KM110 infected cells) (Figure 5.13 Panel B Vero, Table 5.6). Alternatively, HSV-1 transcription or protein expression may contribute to the degree of increase in the level of free H2B at later times after infection. Taken together, these data demonstrate that the increase in free H2B does not require VP16 or ICP0. Moreover, the early increase in free H2B does not require or correlate with HSV-1 transcription or IE protein expression.

As for wild-type KOS, the rate of H2B fast chromatin exchange was decreased during infections with KM110 (Figure 5.14 Vero, Table 5.7). The rate of fast H2B chromatin exchange was decreased 0.76 ± 6 fold ($P<0.01$, Student's T-test; 1-tail) at 4h after infection of Vero cells with 30 PFU per cell of KM110 (Figure 5.13 Vero, Table 5.7). In contrast, the rate of fast chromatin exchange was similar in KM110 or mock-infected cells at 7hpi (Figure 5.14 Vero, Table 5.7).

The decrease in H2B fast chromatin exchange occurred at earlier times after KM110 than KOS infection (Figure 37, Table 20). The rate of fast H2B chromatin exchange during KOS infection was similar to that in mock-infected cells at 4 and decreased to 0.77 ± 0.07 fold at 7hpi ($P<0.01$ at 7hpi, Student's T-Test; 1-tail) (Figure 5.14 Vero, Table 5.7). VP16, ICP0, HSV-1 gene transcription, or IE or E protein expression are therefore not required to decrease the rate of H2B low-affinity chromatin exchange at early times after infection.

The increase in free H2B did not appear to correlate with HSV-1 gene transcription or protein expression. To further test this preliminary conclusion, I analyzed H2B mobilization during KOS and KM110 infections of U2OS cells. U2OS cells complement the replication defects of KM110 but do not complement any of the known biochemical activities of ICP0 or VP16 (Yao & Schaffer, 1995).

HSV-1 protein expression and DNA replication are delayed during KM110 infections of U2OS cells relative to infections with wild-type KOS. At 4hpi, 60 ± 4% or 80 ± 6% of cells infected with 30 PFU per cell of KM110 or 6 PFU per cell of KOS, respectively, had ICP4 accumulated

into replication compartments (Figure 5.11, Table 5.5). At 7hpi, 76 ± 2% of KM110 infected cells or 89 ± 4% of KOS infected cells had ICP4 accumulated into replication compartments (Table 5.5). For both strains, however, cells had similar ICP4 expression and accumulation into replication compartments regardless of whether GFP-H2B was expressed or not (Figure 5.11 U2OS).

The free pool of H2B was increased to a similar degree in U2OS cells infected with KM110 or KOS, although cells were infected with a lower multiplicity of KOS due to the nuclear morphological changes at higher multiplicities. Free H2B was increased to 111 ± 3% or 114 ± 4%, ($P<0.01$, Student's T-test; 1-tail) at 4h after infection of U2OS cells with 30 PFU per cell of KM110 or 6 PFU per cell of KOS, respectively (Figure 5.13 U2OS, Table 5.6). The free pool of H2B was increased to 124 ± 5% in KOS or KM110 infected cells ($P<0.01$, Student's T-test; 1-tail) at 7hpi, (Figure 5.13 U2OS, Table 5.6). Greater than 50% of infected cells had a large increase in free H2B at later times after infection (Table 5.6), indicating that the increase in free H2B is spread throughout the population of infected cells.

Although the pools of free H2B were increased to a similar degree during infections of U2OS cells with KM110 or KOS, the rate of H2B fast chromatin exchange was not. As in Vero cells infected with KOS, the fast chromatin exchange rate of H2B was reduced in U2OS cells at later times after infection with 6 PFU per cell of KOS (by 0.55 ± 0.05 fold) ($P<0.01$, Student's T-test; 1-tail) (Figure 5.14 U2OS, Table 5.7). In U2OS cells infected with 30 PFU per cell of KM110, however, the fast chromatin

exchange of H2B was not reduced at early or late times after infection (Figure 5.14 U2OS, Table 5.7). HSV-1 gene transcription or IE or E protein expression are therefore not sufficient to decrease the rate of fast H2B chromatin exchange in U2OS cells. VP16 or ICP0 are therefore required.

The relatively small increase in free H2B (to approximately 125%) at later times after infection of U2OS cells was surprising. The increase in free H2B in KOS infected Vero cells is much larger (to approximately 170%) (Table 5.6). Furthermore, the absolute level of free H2B in U2OS cells is lower than in Vero cells at later times after infection (0.23 ± 0.01 compared to 0.27 ± 0.01, respectively) (Table 5.6). The pools of free H3.3 were increased to a similar magnitude at later times during KOS infections of Vero and U2OS cells (~155% and 165%, respectively). Moreover, the absolute levels of free H3.3 were similar (0.30 ± 0.01 or 0.31 ± 0.01, respectively) (Table 5.3). These data suggest that H2B may not be as mobile in U2OS cells. Alternatively, the degree of protein expression in U2OS cells may influence the magnitude of increase in free H2B. I therefore analyzed H2B mobilization during infection of U2OS cells with a higher multiplicity of KOS.

At 4 or 7h after infection of U2OS cells with 15 PFU per cell of KOS, the pool of free H2B was increased to 123 ± 4% or 157 ± 5%, respectively ($P<0.01$, Student's T-test; 1-tail) (Figure 5.15, Table 5.6). The pool of free H2B was increased to a slightly greater degree in cells infected with a higher multiplicity at early times after infection (to 114 ± 4% or 123 ± 4% for 6 or 15 PFU per cell, respectively) (Figures 5 and 15,

Table 5.6). This difference was enhanced at later times (124 ± 5% or 157 ± 5% for 6 or 15 PFU per cell, respectively) ($P<0.01$, Student's T-test; 1-tail) (Figure 5.15, Table 5.6). The magnitude of increase in the level of free H2B is therefore larger in U2OS cells infected with higher multiplicities. Unfortunately, the nuclear morphology of the cells was highly distorted at later times after infection with this higher multiplicity. Therefore, the analyses of the larger increase in free H2B at higher multiplicities of infection are limited by the intrinsic limitations of the system. Although the multiplicity of infection influenced the degree of increase in free H2B, it did not influence its fast chromatin exchange rate. The fast chromatin exchange rate of H2B was similar at either multiplicity (Table 5.7).

5.3 DISCUSSION.

The mobilization of H3.3 and H2B during infections with wild-type and mutant HSV-1 strains demonstrated that they have common and unique requirements for mobilization during infection.

The chromatin exchange of H3.3 and H2B both occur through DNA replication independent mechanisms, whereas that of H2B also occurs through DNA replication dependent mechanisms. H2B and H3.3 were still mobilized when HSV-1 DNA replication was inhibited, demonstrating that HSV-1 DNA-replication and strictly L proteins are not required for the mobilization of either. Alternatively, HSV-1 DNA replication may be required, however H2B and H3.3 are mobilized as a result of induction of DNA damage responses during PAA treatment.

This scenario is highly unlikely, however, because the mobilization of H2B and H3.3 resulting from HSV-1 DNA replication or DNA damage responses would have to be to the same degree. Therefore, the most likely explanation is that HSV-1 DNA replication and L proteins are not required for such mobilization. The changes in H2B and H3.3 chromatin exchange that contribute to the increase in the free pools of H2B and H3.3 and alter the rates of H2B and H3.3 fast chromatin exchange therefore likely occur through DNA replication independent mechanisms. Such mechanisms include, for example, transcription associated chromatin exchange.

HSV-1 gene transcription and expression of HSV-1 IE and E proteins differentially affected the mobilization of H2B and H3.3. The mobilization of H3.3 was more closely linked to HSV-1 transcription and the expression of HSV-1 proteins than that of H2B. The degree of increase in the pool of free H2B was independent of HSV-1 transcription, or IE and E proteins, at least at early times after infection, whereas the degree of increase in the free pool of H3.3 correlated with the levels of HSV-1 gene transcription or HSV-1 IE and E protein expression. HSV-1 transcription, HSV-1 IE or E proteins, or cellular responses to them, therefore alter the rates of H3.3 chromatin association and disassociation relative to each other to increase the pool of free H3.3. Alternatively, the pool of free H3.3 may be increased if transcription of HSV-1 genomes displaces H3.3 that is bound to the genomes.

When HSV-1 genomes were transcribed and IE or E proteins expressed, the fast chromatin exchange rate of H3.3 was increased.

Thus, HSV-1 transcription or expression of HSV-1 IE and E proteins alters the low-affinity chromatin association and disassociation of H3.3 such that both are increased. Alternatively, but not exclusively, high levels of HSV-1 transcription could also contribute to increase the rate of H3.3 fast chromatin exchange.

Although the level of HSV-1 transcription or protein expression correlated with the increase in free H3.3, HSV-1 transcription and protein expression were actually not required to mobilize it. During KM110 infections of Vero cells, ICP4 was detected in only approximately 5 or 20% of cells at 4 or 7h, respectively. Nonetheless, the pool of free H3.3 was still increased by a large degree in 25 or 37% more cells at 4 or 7h, respectively. Even cells that had no detectable ICP4 expression therefore had altered rates of H3.3 chromatin exchange such that their pool of free H3.3 was increased. HSV-1 virion binding and fusing with the host cell, release of capsid and tegument proteins into the cell, capsid docking at the nuclear pore, or genome delivery to the nucleus could induce changes in H3.3 chromatin association and dissociation to increase the pool of free H3.3. However, infection of Vero cells with UV-inactivated KOS failed to increase the pool of free H3.3 at early times after infection. Although not significantly different, the pool of free H3.3 in Vero cells at early times after infection with KM110 tended to be greater than after infection with UV-inactivated KOS (111 ± 3% and 93 ± 3%, respectively) (Table 5.3). Moreover, a larger population of KM110 infected cells had increased their pools of free H3.3 by a large degree than UV-inactivated KOS infected cells (25% or 0%, respectively) (Table

5.3). These results suggest that virion binding and fusion, or entry of the tegument and capsid proteins into the cell, does not alter the rates of H3.3 chromatin exchange to a detectable degree. Transcription competent nuclear HSV-1 genomes are therefore required to increase the pool of free H3.3 by a basal level at early times after infection. At later times after infection with KM110 or UV-inactivated KOS, however, the pools of free H3.3 were increased relative to those in mock-infected cells, and they were increased to the same degree (121 ± 5%, Table 5.3). Whether similar mechanisms contribute to both increases in free H3.3 is presently unknown. The increase in the pool of free H3.3 at later times after infection with UV-inactivated KOS may be the result of an indirect effect of infection. For example, nuclear entry of non-chromatinized DNA could activate a cellular foreign DNA response that affects histone chromatin exchange. Nuclear entry of cross-linked HSV-1 genomes may also induce changes in core histone chromatin exchange through activation of DNA damage responses. Alternatively, as UV-inactivated stocks are not 100% inactivated, viable virions may be present and infections with these virions may increase the pool of free H3.3. However, if this were the case, then the pool of free H3.3 should have also been increased during infection of U2OS cells with UV-inactivated KOS as the same stock was used (compare Figure 5.5 UV 30 7hpi to Figure 5.9 UV 30 7hpi)

The magnitude of the increase in the free pool of H3.3 increases when HSV-1 genomes are transcribed and proteins are expressed. These results suggest that different events may contribute to the overall H3.3

mobilization during infection. An early basal mobilization, which requires only nuclear, transcription competent, HSV-1 genomes results in a marginal increase in the free pool of H3.3. An enhanced later mobilization, which requires HSV-1 transcription or expression of HSV-1 IE or E proteins, results in a larger increase in the free pool of H3.3. Such enhanced mobilization involves a tendency towards faster rates of low-affinity H3.3 chromatin exchange. The enhanced mobilization may be the result of HSV-1 transcription, expression of specific IE or E proteins, or cellular responses to infection. Conversely, the enhanced mobilization of H3.3 may be required for HSV-1 gene expression. Mobilization or displacement of H3.3 away from HSV-1 genomes would decrease H3.3 occupancy on HSV-1 genomes, potentially allowing for HSV-1 gene transcription.

Different HSV-1 factors are required to increase the pool of free H3.3 or the rate of H3.3 fast chromatin exchange, suggesting that different mechanisms contribute to each parameter. Under conditions of little to no HSV-1 transcription and protein expression, as during KM110 infections of Vero cells, the pool of free H3.3 was still marginally increased. However, the fast chromatin exchange rate of H3.3 was not. The rate of H3.3 chromatin association may therefore be decreased relative to that of chromatin dissociation. Alternatively the rate of chromatin dissociation may be increased relative to that of chromatin association. Any such changes would result in an increase in the free pool of H3.3 without substantially affecting the overall rate of low-affinity H3.3 chromatin exchange. The relative differences in H3.3 chromatin

association and disassociation that contribute to the increase in the level of free H3.3 may therefore be due to changes in slow, high-affinity, H3.3 chromatin exchange.

During n212 infection of Vero cells, HSV-1 genes are transcribed and proteins are expressed. However, protein expression is delayed relative to wild-type infections. The pool of free H3.3 was increased to a similar degree at later times after infection of Vero cells with n212 as it was at early times after infection with wild-type KOS (180 ± 10% or 171 ± 7%, respectively) (Figure 5.5, Table 5.3). The fast chromatin exchange rate of H3.3 at early or late times during infection with n212, however, did not approach the magnitude of increase that occurred at early times during KOS infection ($P<0.01$, Tukey's HSD) (Figure 5.6, Table 5.4). Taken together, these data demonstrate that the changes in H3.3 chromatin exchange during n212 infection have a greater impact on the level of H3.3 in the free pool than on the overall rate of H3.3 fast chromatin exchange. Thus, ICP0 may contribute to the increase in the fast chromatin exchange rate of H3.3, but not to the increase in the pool of free H3.3. Taken together, these data demonstrate that the HSV-1 factors that increase the rate of H3.3 fast chromatin exchange at early times and increase the pool of free H3.3 at early and late times are different. These differences suggest that the different parameters of H3.3 mobilization may be altered by different mechanisms.

Analysis of H3.3 mobilization during infection with HSV-1 mutant strains has demonstrated that there are at least two mobilization events. A "basal" mobilization alters the chromatin exchange of H3.3 such that

the free pool of H3.3 is marginally increased without substantially altering the fast chromatin exchange rate of H3.3. This basal mobilization requires only nuclear transcription competent HSV-1 genomes, and likely reflects a cellular response to infection. An "enhanced" mobilization, on the other hand, alters the chromatin exchange of H3.3 such that the free pool of H3.3 is increased to a greater degree and the fast chromatin exchange rate of H3.3 is increased. Such mobilization requires, and correlates with, HSV-1 transcription and expression of HSV-1 IE and E proteins. It may therefore represent viral effects, cellular responses, or a combination of viral effects and cellular responses during infection. Alternatively, enhanced H3.3 mobilization may be required for, or a consequence of, HSV-1 gene transcription.

Unlike H3.3, the increase in free H2B did not correlate with the degree of HSV-1 transcription or IE or E protein expression. Under conditions of little to no HSV-1 transcription and protein expression, as during KM110 infections of Vero cells, the pool of free H2B was increased at early and late times (Figure 5.13, Table 5.6). The increase was to the same degree as in KOS infected cells at early times after infection, even though HSV-1 gene transcription and protein expression are both at higher levels in KOS infected cells. During KOS infections, greater than 95% of cells had detectable ICP4 expression and approximately 75% already had ICP4 accumulated into replication compartments (Table 5.5). During KM110 infections, however, ICP4 was not detectable in more than 80% of cells, and only 1% of cells had ICP4 accumulated into replication compartments (Table 5.5). Moreover, the population of KM110 infected

cells that had large increases in their level of free H2B was much greater than the population of cells that had detectable ICP4 expression (50% compared to approximately 13%) (Tables 5.5 and 5.6). The pool of free H2B was increased to a similar degree at early and late times after infection with KM110 (120 ± 4% or 125 ± 5%, respectively), even though more cells had detectable ICP4 expression at later times (approximately 13% or 61% at 4 or 7h, respectively) (Tables 5.5 and 5.6). Thus, ICP4 expression, or its accumulation into replication compartments, does not correlate with the magnitude of increase in the level of H2B available in the free pool at early times after HSV-1 infection. The increase in free H2B at early times after infection could result from changes in H2B chromatin exchange due to HSV-1 virion binding and fusion with the host cell, release of capsid and tegument proteins, capsid docking at the nuclear pore, or HSV-1 genomes entering the nucleus. Analysis of the free pool of H2B during infections with UV-inactivated KOS would clarify whether such processes were sufficient to increase the pool of free H2B. Alternatively, the early increase in free H2B may be due to cellular responses to infection.

HSV-1 gene transcription or protein expression did not correlate with the degree of increase in free H2B at early times after infection. Yet the free pool of H2B was increased to a greater degree at later times after infection when HSV-1 genes were transcribed and IE or E proteins were expressed. HSV-1 gene transcription or expression of HSV-1 IE or E proteins therefore contribute to, or enhance, the changes in H2B chromatin exchange that result in an increase in the pool of free H2B.

Conversely, the changes in H2B chromatin exchange that increase the pool of free H2B may enhance HSV-1 gene transcription.

The mobilization of H2B that results in a decrease in the fast chromatin exchange rate of H2B did not correlate with HSV-1 transcription or protein expression either. The rates of fast chromatin exchange of H2B were similar at early and late times after infection of Vero cells with KOS or KM110, even though KOS-infected cells had more detectable ICP4 expression at either time (Figure 5.14, Tables 5.5 and 5.7).

Taken together, these data demonstrate that H2B mobilization during HSV-1 infection is likely the result of more than one mobilization event. The decrease in the fast chromatin exchange rate of H2B and the increase in the pool of free H2B did not require, or correlate with, HSV-1 transcription or protein expression. In cellular chromatin, the fast chromatin exchange of H2B is associated with transription. The decrease in H2B fast chromatin exchange could therefore reflect inhibition of cellular transcription. Such a scenario would indicate that a larger percentage of H2B is bound to cellular DNA than to HSV-1 genomes. Therefore the detectable changes in H2B chromatin exchange would mostly reflect changes in cellular transcription associated H2B exchange. This mobilization could also reflect a cellular response to infection. Alternatively, HSV-1 input tegument or capsid proteins may alter the chromatin association of H2B to decrease the rate of fast H2B chromatin exchange and increase the free pool of H2B. HSV-1 transcription or expression of IE or E proteins enhances the alteration of

H2B chromatin exchange to further increase the pool of free H2B. The further increase in the level of free H2B may be a consequence of HSV-1 genome transcription, a specific HSV-1 IE or E protein, or a cellular response.

During infections of U2OS cells with KM110 the pool of free H2B was increased. However, the fast chromatin exchange rate of H2B was not substantially altered (Figure 5.13, Figure 5.14). Thus, VP16 or ICP0 may be required to decrease the rate of fast chromatin exchange in U2OS cells. To distinguish whether VP16 or ICP0 are required to decrease the rate of fast H2B chromatin exchange, H2B mobility could be evaluated during infections with HSV-1 strains n212 or V422, which have the same ICP0 and VP16 mutations, respectively, found in strain KM110.

In summary, the mobilizations of H2B and H3.3 during HSV-1 infection are consistent with two mechanisms of core histone mobilization. The early mobilization of H2B is independent of HSV-1 gene transcription and expression of specific IE or E proteins and therefore likely to result from cellular responses to infection. The early mobilization of H3.3, on the other hand, requires VP16 or ICP0 and its magnitude correlates with the levels of HSV-1 gene transcription or expression of specific HSV-1 IE or E proteins, suggesting a response to viral factors. However, the pool of free H3.3 is still increased, albeit to a lesser degree, in the absence of VP16, ICP0, and HSV-1 gene transcription, indicating that cellular responses also mobilize H3.3. Expression of specific HSV-1 IE or E proteins, or HSV-1 gene

transcription, induces further core histone mobilization at later times after infection.

FIGURE 5.1: The increase in free H2B does not require HSV-1 DNA replication. A) Line graphs representing the normalized fluorescence intensity of the photobleached nuclear region against time. Vero cells were transfected with plasmids encoding GFP-H2B. Transfected cells were mock-infected (**circle**) or infected with 30 PFU per cell of HSV-1 strain KOS (**square**) in the presence of 400μg/ml of PAA (**open**) or no drug (**filled**) (data from Figure 5.12 replotted for comparison). Nuclear mobility was examined from 7 to 8 hpi by FRAP. Error bars, SEM; n ≥ 23. Time plotted on a semi-logarithmic scale. **B)** Bar graph representing the average percentage of free H2B evaluated by FRAP as described in for Panel A in HSV-1 infected cells normalized to mock infected cells treated with 400μg/ml of PAA or no drug (data from Figure 5.13 replotted for comparison). Error bars, SEM; n ≥ 23. **C)** Frequency distribution plots of the free H2B per individual cell evaluated by FRAP as described for panel A. Dashed or solid lines, mock-infected or HSV-1 infected cells, respectively, treated with 400μg/ml of PAA or no drug (data from Figure 5.13 were replotted for comparison). **D)** Bar graph representing the average rate of initial fluorescence recovery after photobleaching evaluated by FRAP as described for Panel A in HSV-1 infected cells normalized to mock infected cells treated with 400μg/ml of PAA or no drug (data from Figure 5.14 replotted for comparison). Error bars, SEM; n ≥ 23. **E)** Frequency distribution plots of the rate of initial fluorescence recovery after photobleaching per individual cell evaluated by FRAP as described for Panel A. Dashed or solid lines, mock or HSV-1 infected cells, respectively, treated with 400μg/ml of PAA or no drug (data from Figure 5.14 replotted for comparison). *, $P < 0.05$; **, $P < 0.01$.

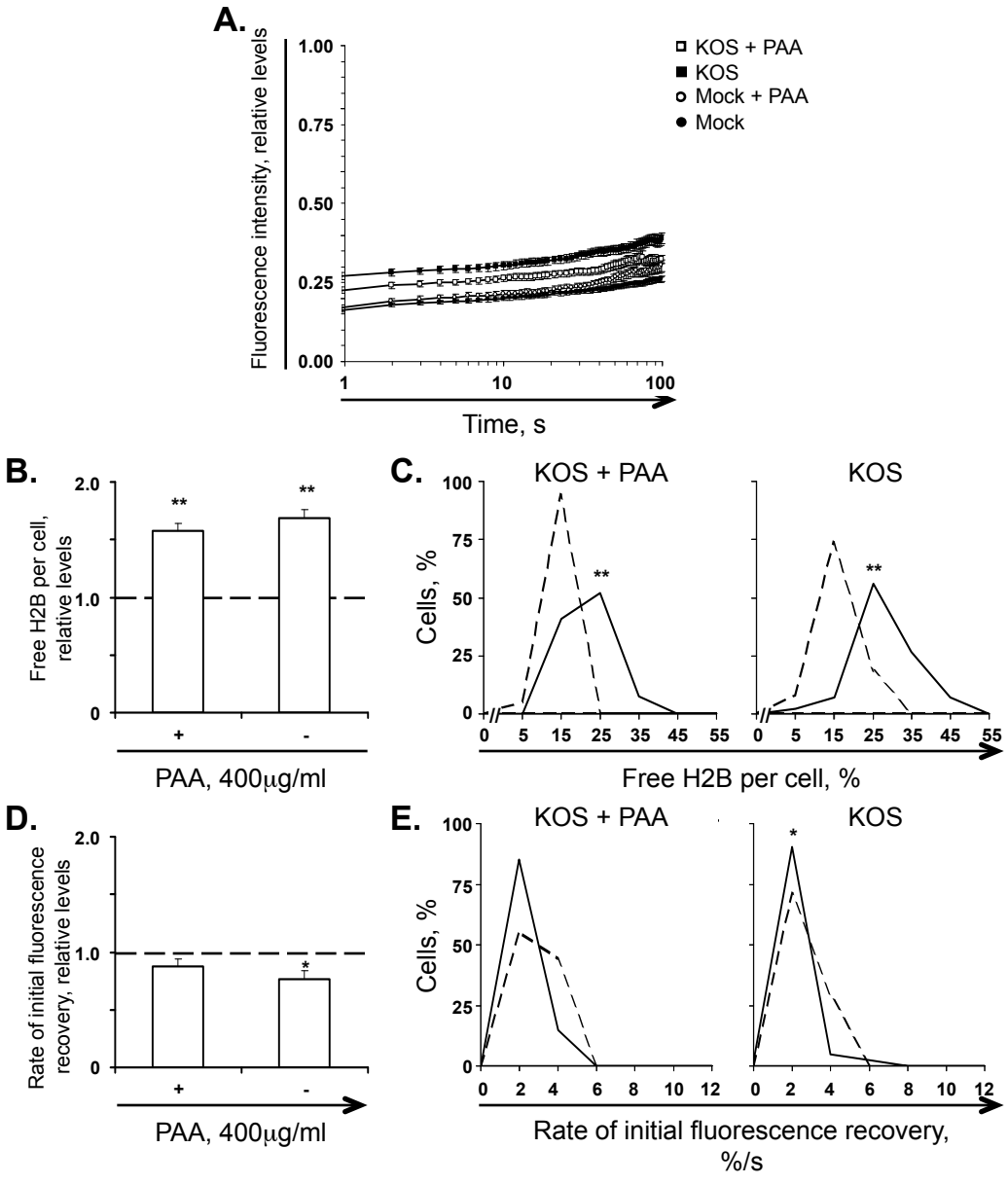
A.
Fluorescence intensity, relative levels
1.00
0.75
0.50
0.25
0.00
1
10
100
Time, s
KOS + PAA
KOS
Mock + PAA
Mock
B.
Free H2B per cell, relative levels
2.0
1.0
0
**
**
+
-
PAA, 400μg/ml
C.
KOS + PAA
KOS
Cells, %
100
75
50
25
0
**
**
0 5 15 25 35 45 55
Free H2B per cell, %
D.
Rate of initial fluorescence recovery, relative levels
2.0
1.0
0
*
+
-
PAA, 400μg/ml
E.
KOS + PAA
KOS
Cells, %
100
75
50
25
0
*
0 2 4 6 8 10 12
Rate of initial fluorescence recovery, %/s

FIGURE 5.2: The increase in free H3.3 does not require HSV-1 DNA replication. A) Line graphs representing the normalized fluorescence intensity of the photobleached nuclear region against time. Vero cells were transfected with plasmids encoding GFP-H3.3. Transfected cells were mock-infected (**circle**) or infected with 30 PFU per cell of HSV-1 strain KOS (**square**) in the presence of 400μg/ml of PAA (**open**) or no drug (**filled**; data from Figure 5.4 replotted for comparison). Nuclear mobility was examined from 7 to 8 hpi by FRAP. Error bars, SEM; n ≥ 28, except for mock-infected cells treated with PAA n = 20. Time plotted on a semi-logarithmic scale. **B)** Bar graph representing the average percentage of free H3.3 evaluated by FRAP as described for Panel A in HSV-1 infected cells normalized to mock infected cells treated with 400μg/ml of PAA or no drug (data from Figure 5.5 replotted for comparison). Error bars, SEM; n ≥ 28, except for mock-infected cells treated with PAA n = 20. **C)** Frequency distribution plots of the percentage of free H3.3 per individual cell evaluated by FRAP as described for Panel A. Dashed or solid lines, mock-infected or HSV-1 infected cells, respectively, treated with 400μg/ml of PAA or no drug (data from Figure 5.5 replotted for comparison). **D)** Bar graph representing the average rate of initial fluorescence recovery after photobleaching evaluated by FRAP as described for Panel A in HSV-1 infected cells normalized to mock infected cells treated with 400μg/ml of PAA or no drug (data from Figure 5.6 replotted for comparison). Error bars, SEM; n ≥ 28, except for mock-infected cells treated with PAA n = 20. **E)** Frequency distribution plots of the rate of initial fluorescence recovery after photobleaching per individual cell evaluated by FRAP as described for Panel A. Dashed or solid lines, mock or HSV-1 infected cells, respectively, treated with 400μg/ml of PAA or no drug (data from Figure 5.6 replotted for comparison). **, $P < 0.01$.

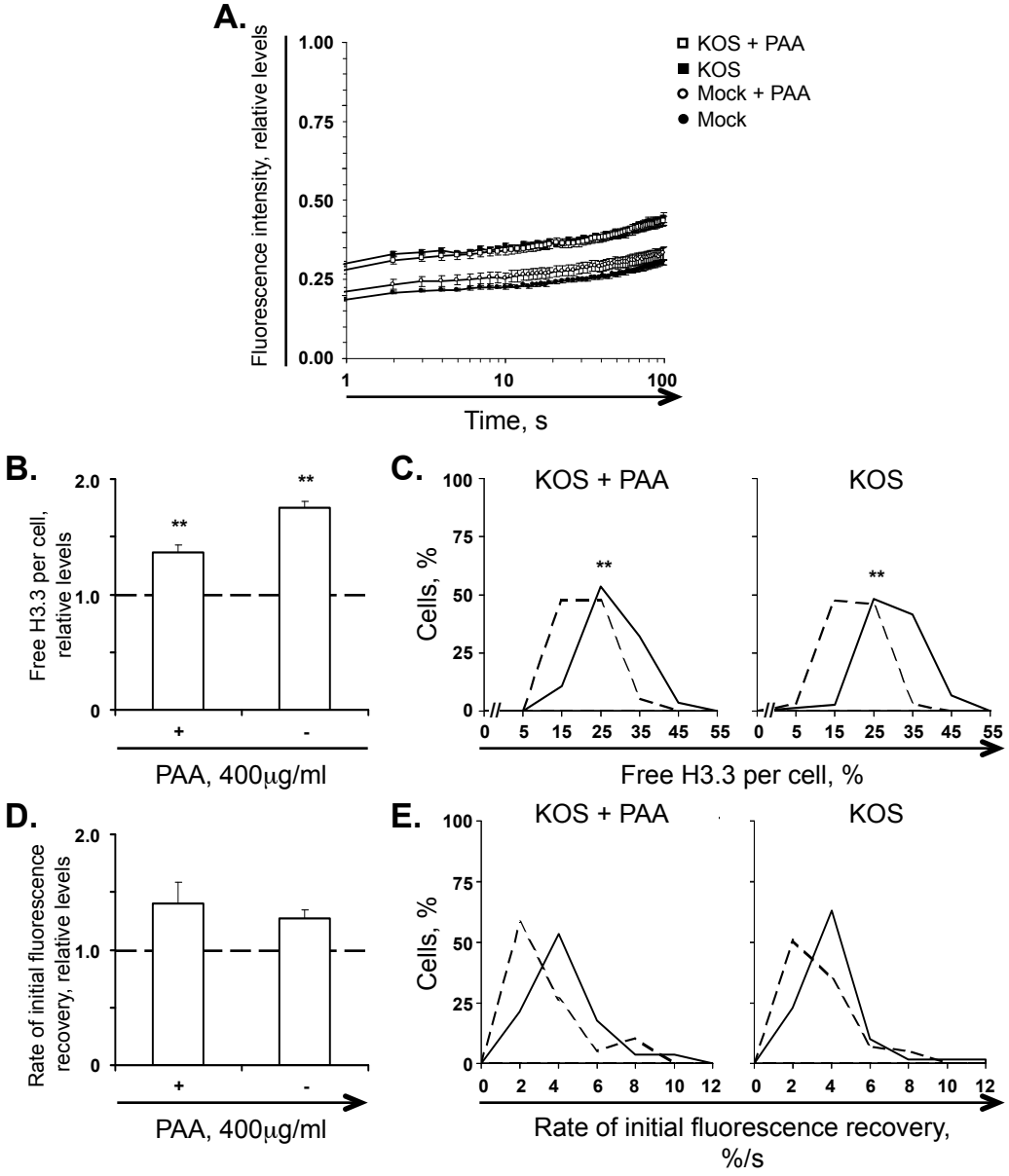
A.
Fluorescence intensity, relative levels
1.00
0.75
0.50
0.25
0.00
1
10
100
Time, s
KOS + PAA
KOS
Mock + PAA
Mock
B.
Free H3.3 per cell, relative levels
2.0
1.0
0
**
**
+
-
PAA, 400μg/ml
C.
KOS + PAA
KOS
Cells, %
100
75
50
25
0
**
**
0 5 15 25 35 45 55
Free H3.3 per cell, %
D.
Rate of initial fluorescence recovery, relative levels
2.0
1.0
0
+
-
PAA, 400μg/ml
E.
KOS + PAA
KOS
Cells, %
100
75
50
25
0
0 2 4 6 8 10 12
Rate of initial fluorescence recovery, %/s

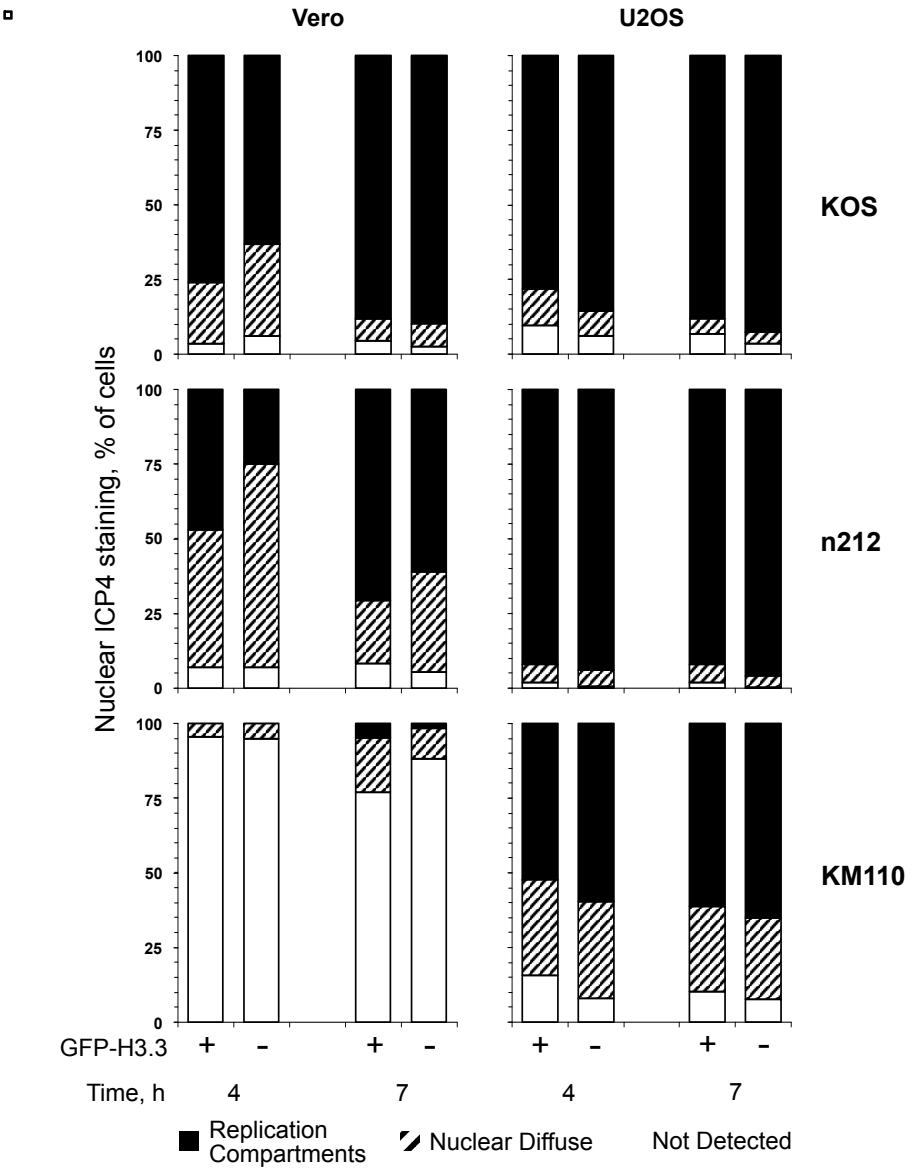

FIGURE 5.3: ICP4 expression and accumulation into replication compartments in Vero and U2OS cells expressing or not GFP-H3.3 and infected with wild-type or mutant HSV-1 strains. Bar graphs representing the percentage of HSV-1-infected cells transfected with GFP-H3.3 and expressing ICP4 as nuclear diffuse or accumulated into replication compartments. Vero or U2OS cells were transfected with plasmids expressing GFP-H3.3. Cells were infected with 30 PFU per cell of HSV-1 strain **KOS**, **n212**, or **KM110** or with 6 PFU per cell of HSV-1 strain KOS (U2OS cells only). Cells were fixed at 4.5 (**4**) or 7.5 (**7**) hpi and stained for ICP4. Nuclear expression of ICP4 and its accumulation into replication compartments in cells in which GFP-H3.3 was expressed (**+**) or not (**-**) were evaluated by fluorescence microscopy. Vero KOS data replotted from Figure 4.5 for comparison.

FIGURE 5.4: Mobilization of H3.3 requires HSV-1 protein expression. Line graphs representing the normalized fluorescence intensity of the photobleached nuclear region against time. Vero cells were transfected with plasmids expressing GFP-H3.3. Transfected cells were mock-infected (**filled circle**) or infected with 10 (**open triangle**) or 30 (**open circle**) PFU per cell of HSV-1 strains KOS, n212, KM110, or UV-inactivated KOS as indicated. Nuclear mobility of GFP-H3.3 was evaluated from 4 to 5 hpi (**4 hpi**) or 7 to 8 hpi (**7 hpi**) by FRAP. Error bars, SEM; n ≥ 32, except for n212 at 4 and 7 hpi, n ≥ 27. Time plotted on a semi-logarithmic scale.

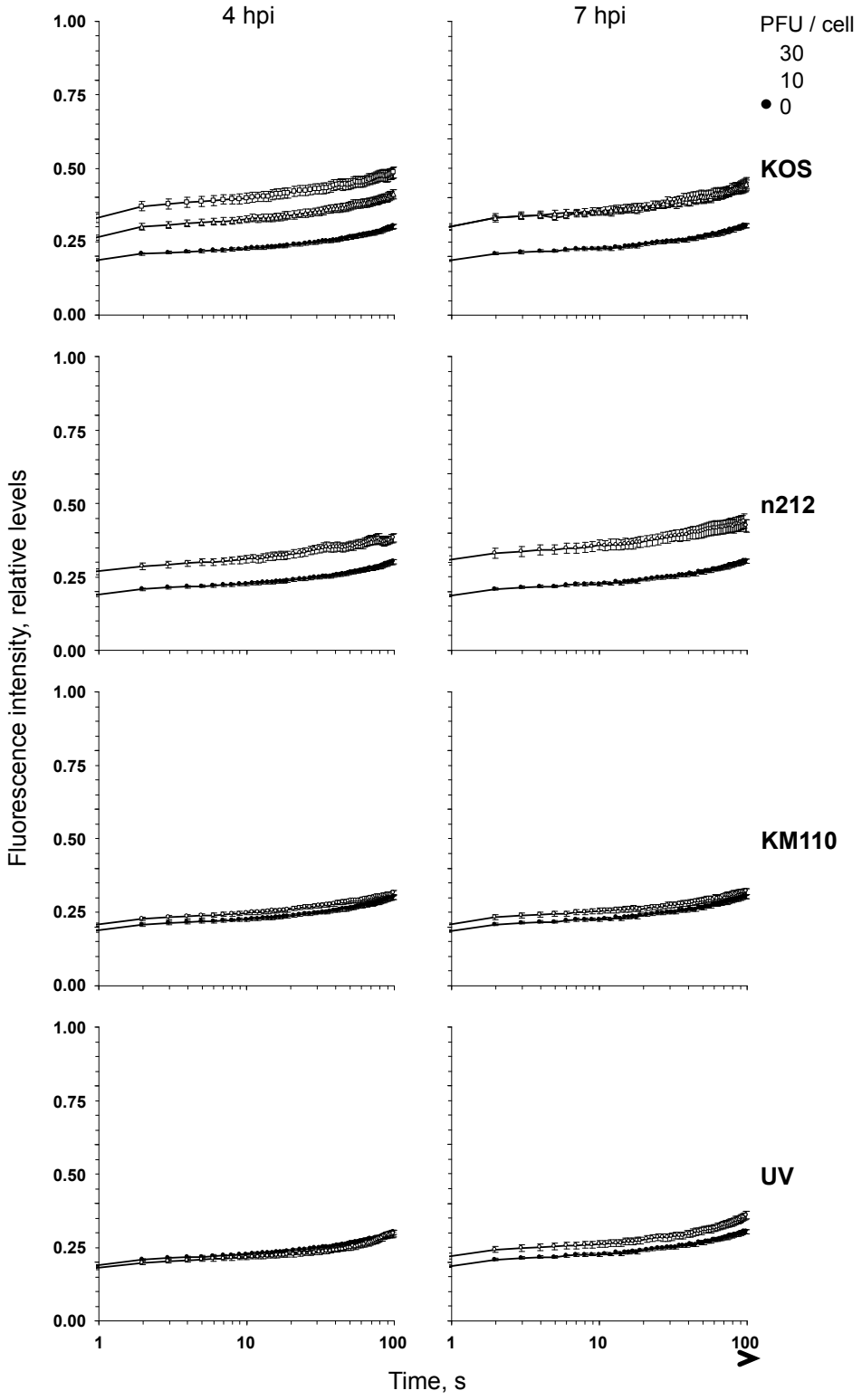
4 hpi
7 hpi
PFU / cell
30
10
0
KOS
n212
KM110
UV
Fluorescence intensity, relative levels
1.00
0.75
0.50
0.25
0.00
1
10
100
Time, s

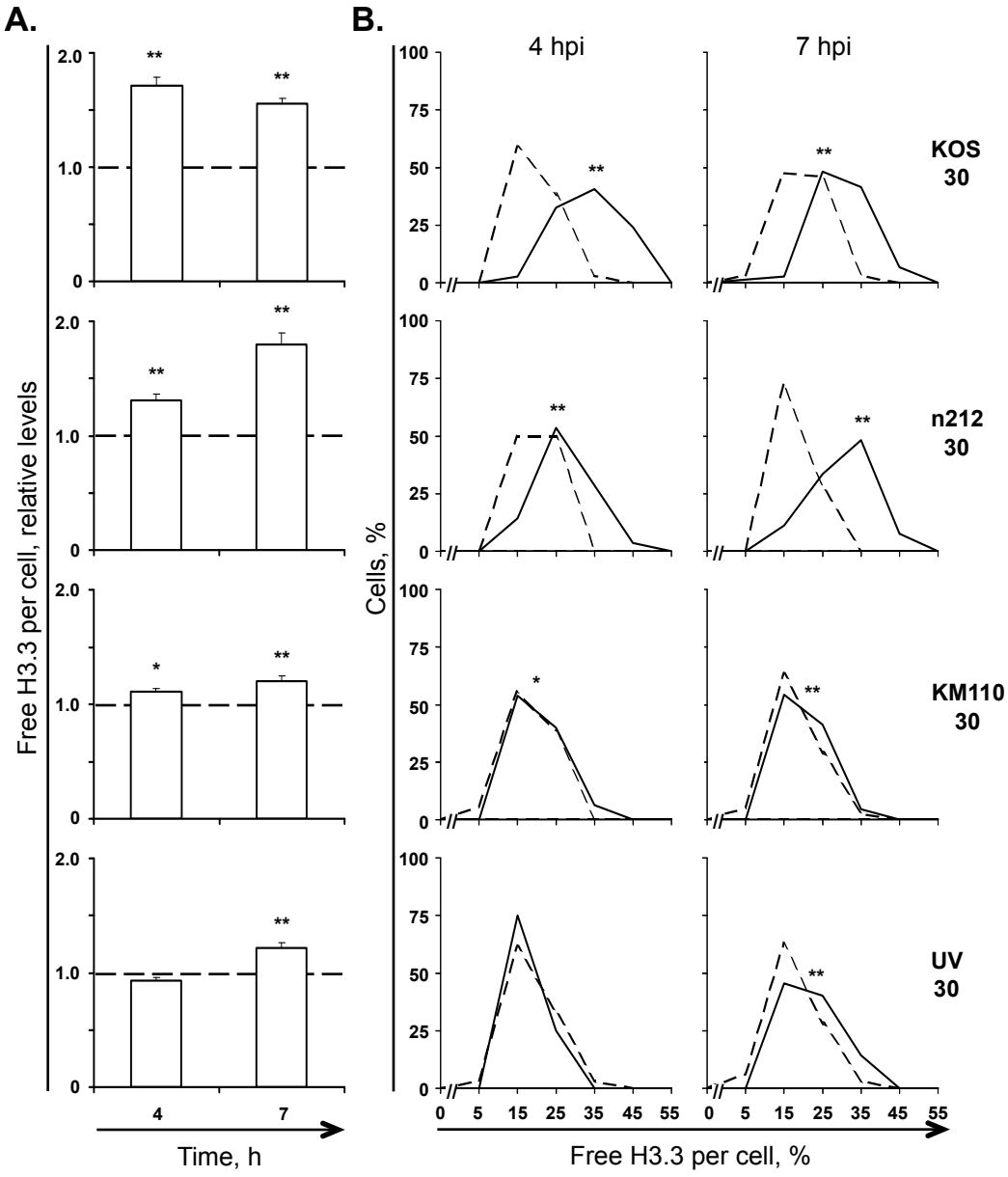

FIGURE 5.5: The large increase in free H3.3 requires HSV-1 protein expression. A) Bar graphs representing the average percentage of free H3.3 in HSV-1 infected cells normalized to mock infected cells. Vero cells were transfected with plasmids encoding GFP-H3.3. Transfected cells were mock-infected or infected with 30 PFU per cell of HSV-1 strain KOS (**KOS 30**), n212 (**n212 30**), KM110 (**KM110 30**), or UV-inactivated KOS (**UV 30**). Nuclear mobility of GFP-H3.3 was evaluated from 4 to 5 hpi (**4**) or 7 to 8 hpi (**7**) by FRAP. Error bars, SEM; n ≥ 32, except for n212 30 at 4 and 7 hpi, n ≥ 27. **B)** Frequency distribution plots of the percentage of free H3.3 per individual cell evaluated by FRAP as described for Panel A. Dashed or solid lines, mock or HSV-1 infected cells, respectively. *, $P < 0.05$, **, $P < 0.01$.

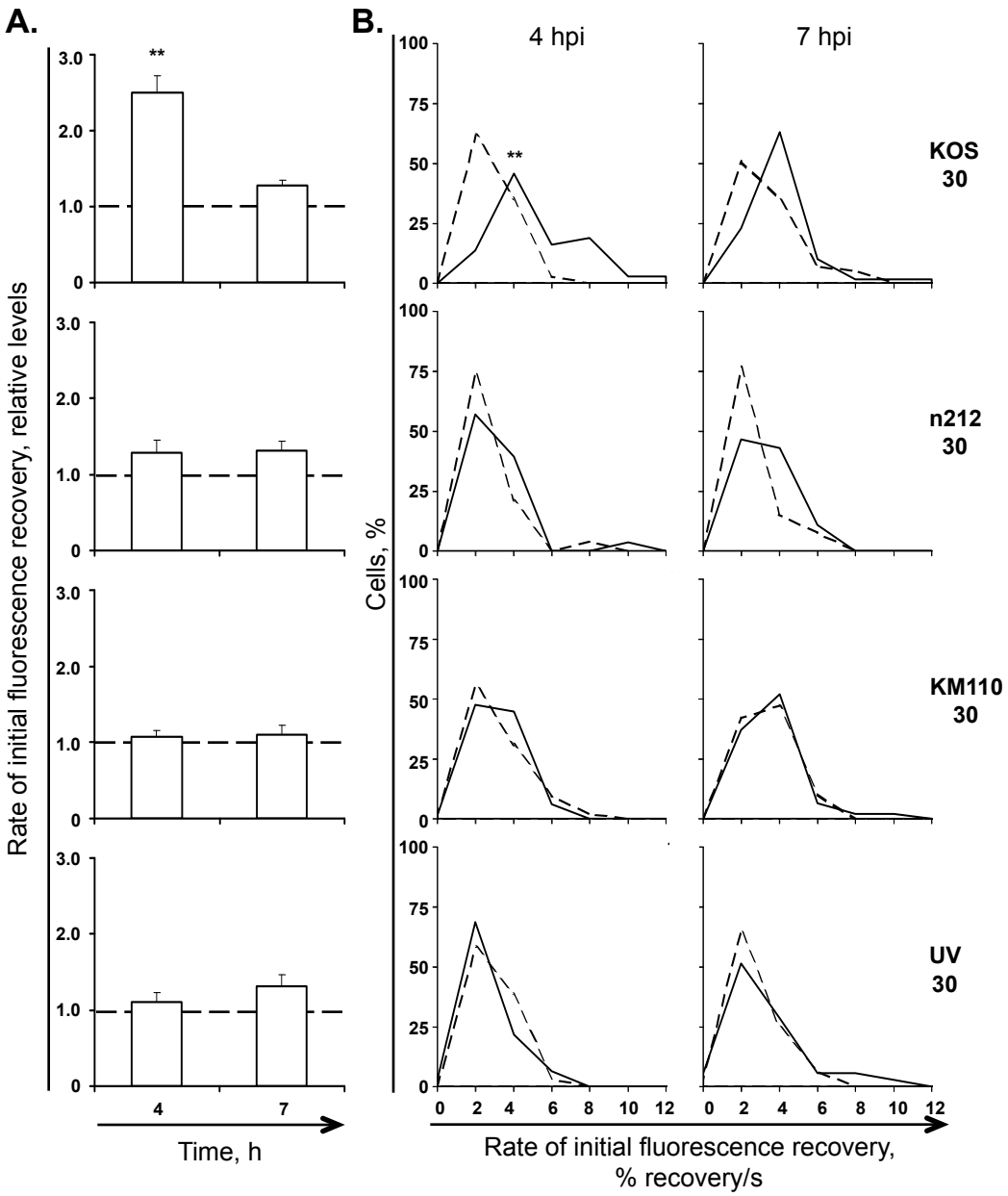

FIGURE 5.6: The rate of initial fluorescence recovery of H3.3 had a tendency to increase when HSV-1 proteins are expressed. A) Bar graphs representing the average rate of initial fluorescence recovery after photobleaching in HSV-1 infected cells normalized to mock infected cells. Vero cells were transfected with plasmids encoding GFP-H3.3. Transfected cells were mock-infected or infected with 30 PFU per cell of HSV-1 strain KOS (**KOS 30**), n212 (**n212 30**), KM110 (**KM110 30**), or UV-inactivated KOS (**UV 30**). Nuclear mobility of GFP-H3.3 was evaluated from 4 to 5 hpi (**4**) or 7 to 8 hpi (**7**) by FRAP. Error bars, SEM; n ≥ 32, except for n212 30 at 4 and 7 hpi, n ≥ 27. **B)** Frequency distribution plots of the rate of initial fluorescence recovery after photobleaching per individual cell evaluated by FRAP as described for Panel A. Dashed or solid lines, mock or HSV-1 infected cells, respectively. **, $P < 0.01$.

FIGURE 5.7: Expression of ICP4 as nuclear dispersed or accumulated into KM110 replication compartments in U2OS cells expressing GFP-H3.3. Digital fluorescent micrographs of U2OS cells expressing GFP-H3.3 and stained with α-ICP4 antibodies. Cells were transfected with plasmids expressing GFP-H3.3 and infected with 5 PFU/cell of HSV-1 strain KM110. Cells were fixed at 2.5 (**2 hpi**), 4.5 (**4 hpi**) or 7.5 hpi (**7 hpi**) as indicated and stained for ICP4. Single (**α-ICP4**, **GFP-H3.3**, **DIC**) and merged (**Merge**) images are shown. Cells with ICP4 expressed as nuclear dispersed (**ND**) or replication compartments (**RC**) are indicated. Rightmost panels, 16x digital enlargement of the regions indicated by the boxes on the leftmost "merge" images, highlighting the colocalization of H3.3 and ICP4 signals (pixels in different shades of yellow and orange)

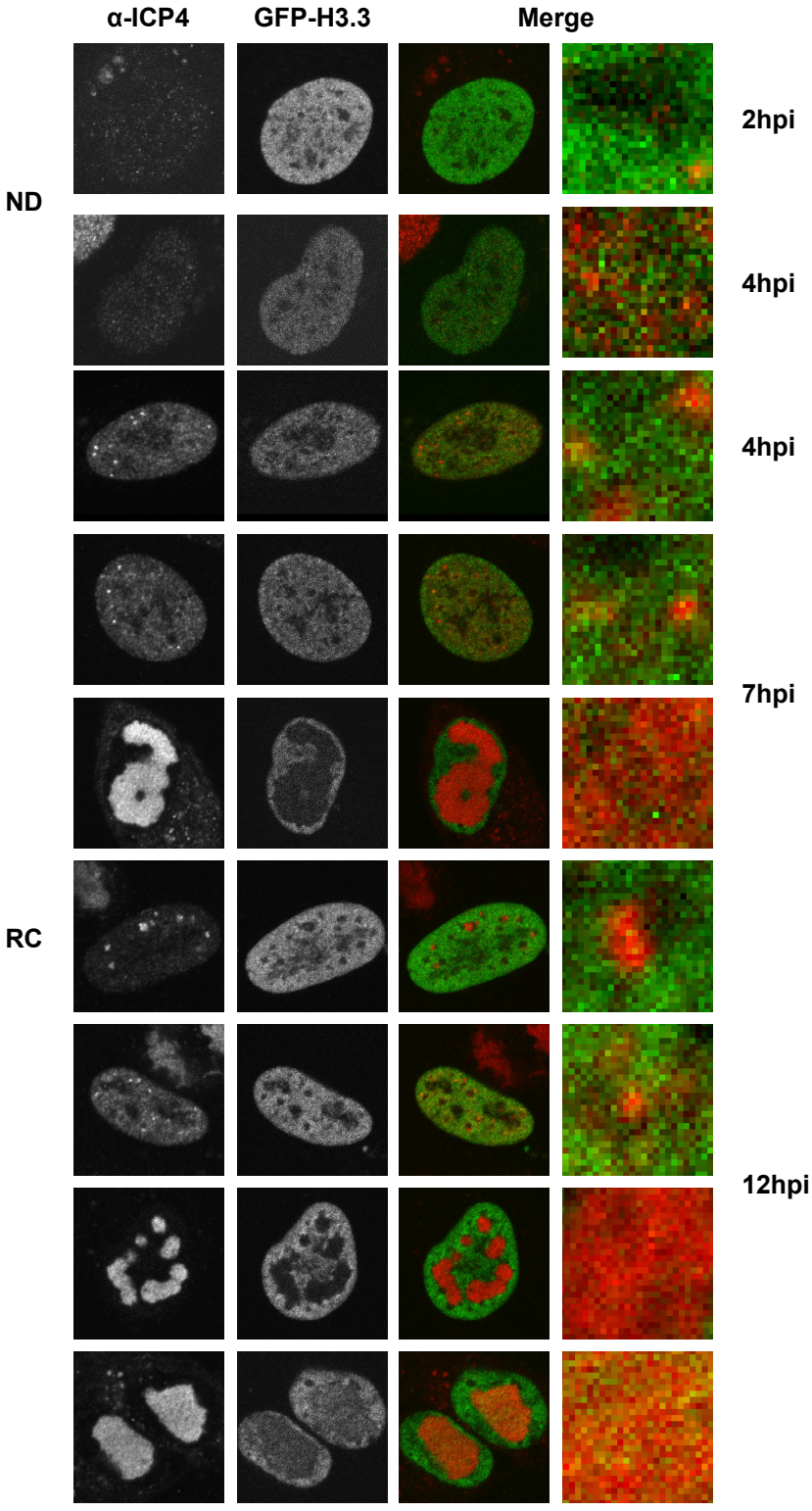
α-ICP4
GFP-H3.3
Merge
ND
RC
2hpi
4hpi
4hpi
7hpi
12hpi

FIGURE 5.8: Mobilization of H3.3 does not requireVP16 or ICP0. Line graphs representing the normalized fluorescence intensity of the photobleached nuclear region against time. U2OS cells were transfected with plasmids expressing GFP-H3.3. Transfected cells were mock-infected (**filled circle**) or infected with 6 (**open square**) or 30 (**open circle**) PFU per cell of HSV-1 strains KOS, n212, KM110, or UV-inactivated KOS as indicated. Nuclear mobility of GFP-H3.3 was evaluated from 4 to 5 hpi (**4 hpi**) or 7 to 8 hpi (**7 hpi**) by FRAP. Error bars, SEM; n ≥ 24. Time plotted on a semi-logarithmic scale.

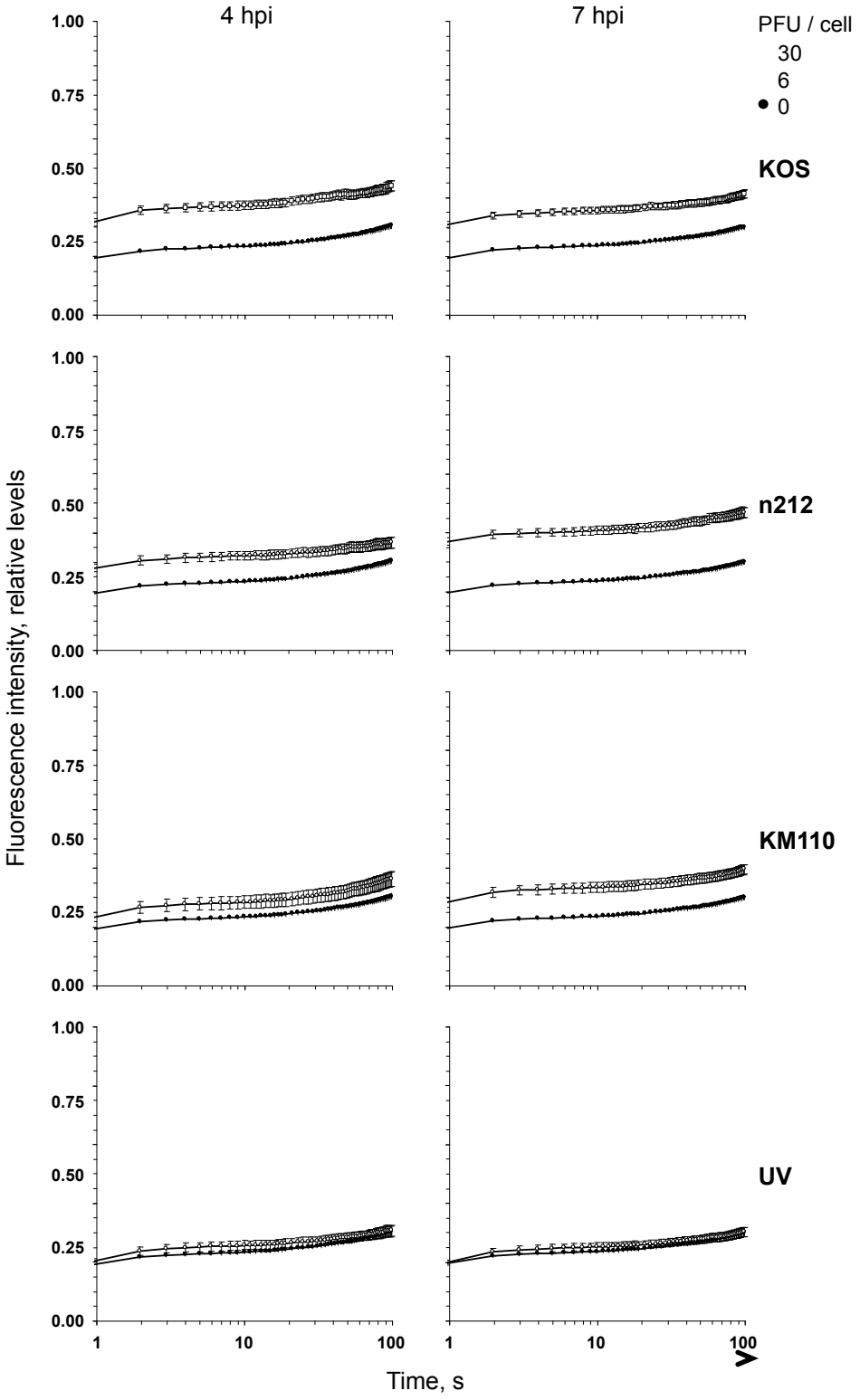
4 hpi
7 hpi
PFU / cell
30
6
0
KOS
n212
KM110
UV
Fluorescence intensity, relative levels
1.00
0.75
0.50
0.25
0.00
1
10
100
Time, s

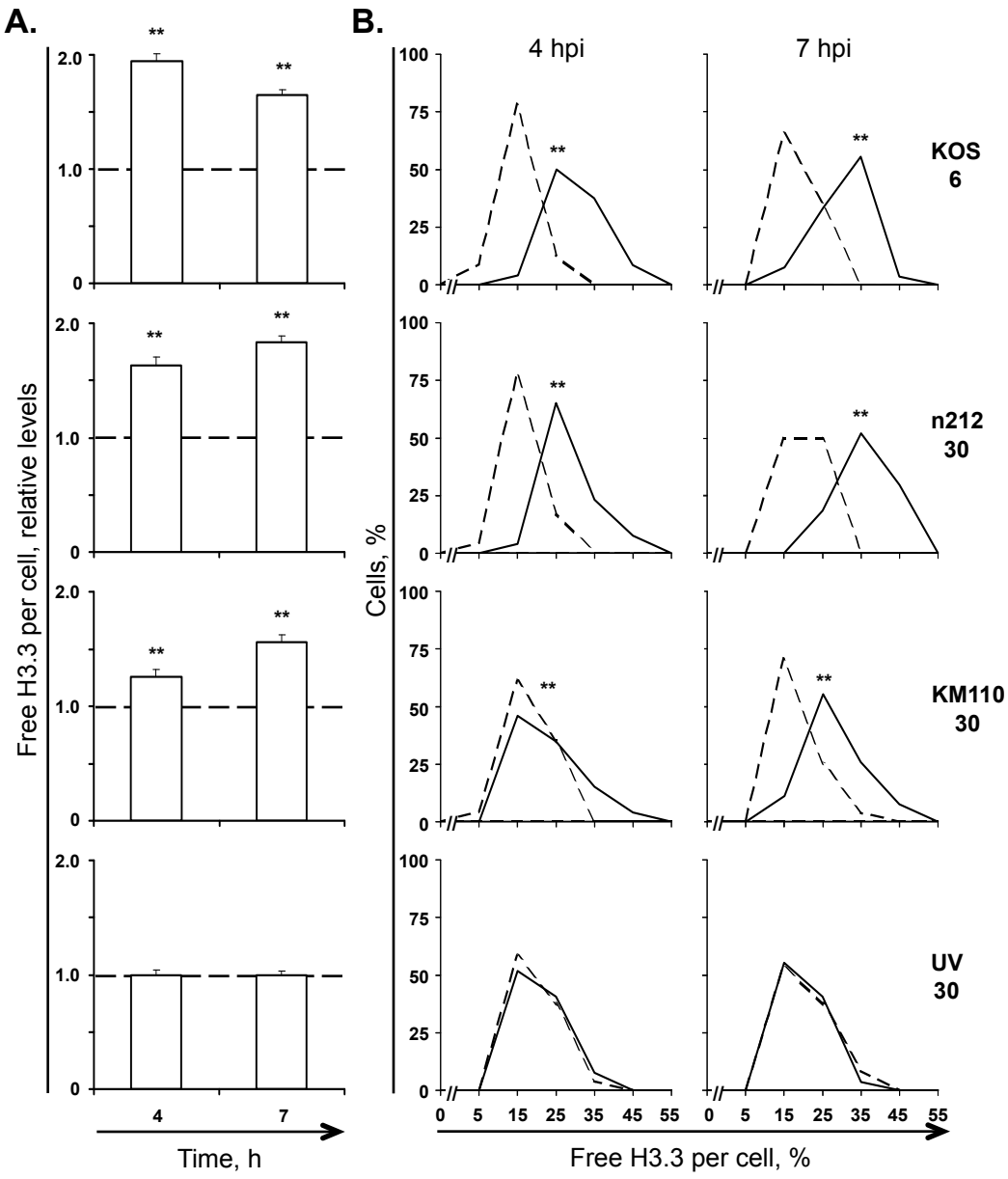

FIGURE 5.9: The large increase in free H3.3 does not require VP16 or ICP0. **A)** Bar graphs representing the average percentage of free H3.3 in HSV-1 infected cells normalized to mock infected cells. U2OS cells were transfected with plasmids encoding GFP-H3.3. Transfected cells were mock-infected or infected with 6 PFU per cell of HSV-1 strain KOS (**KOS 6**) or 30 PFU per cell of HSV-1 strain n212 (**n212 30**), KM110 (**KM110 30**), or UV-inactivated KOS (**UV 30**). Nuclear mobility of GFP-H3.3 was evaluated from 4 to 5 hpi (**4**) or 7 to 8 hpi (**7**) by FRAP. Error bars, SEM; n ≥ 24. **B)** Frequency distribution plots of the percentage of free H3.3 per individual cell evaluated by FRAP as described for Panel A. Dashed or solid lines, mock or HSV-1 infected cells, respectively. **, P <0.01.

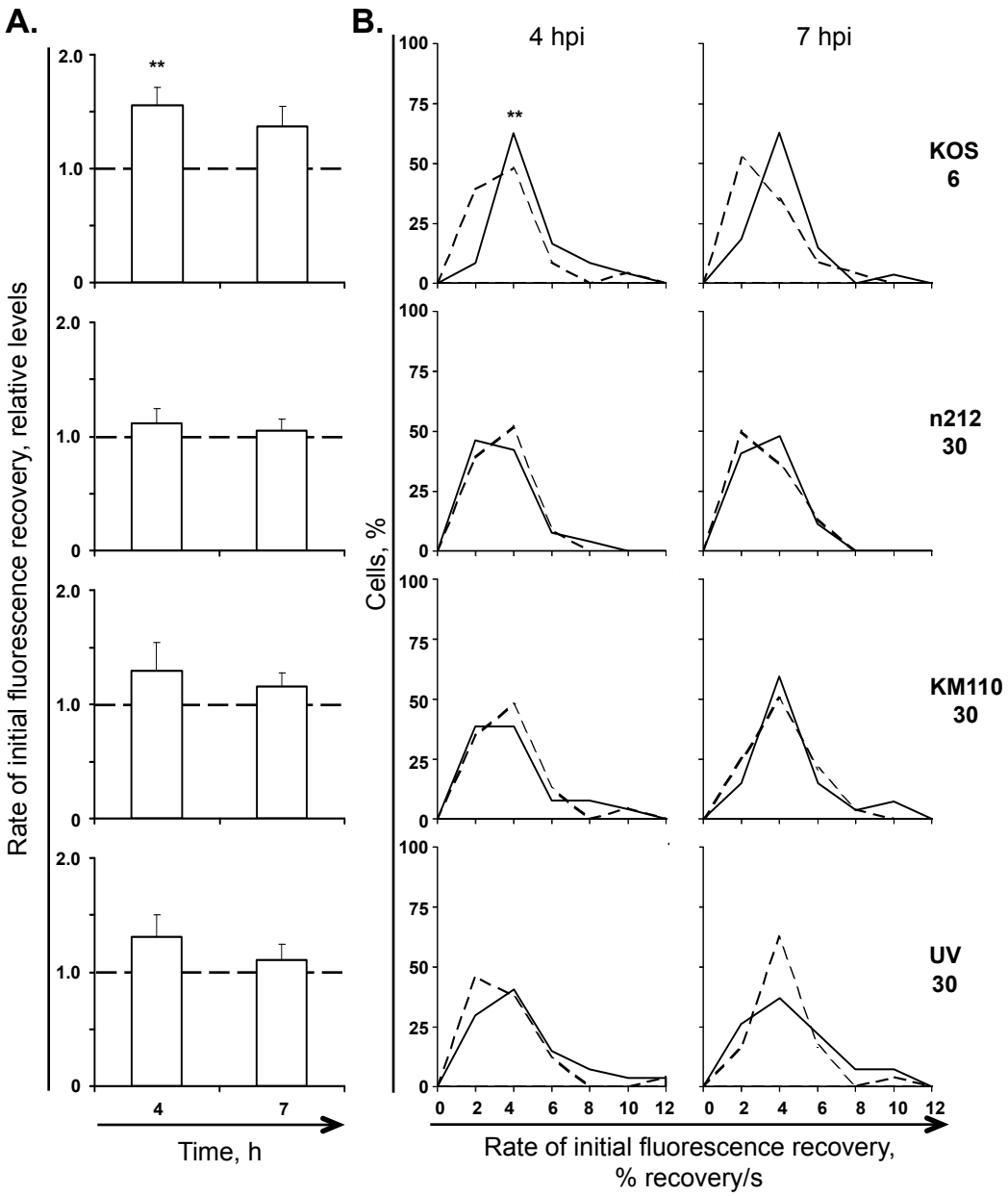

FIGURE 5.10: The rate of initial fluorescence recovery of H3.3 has a tendency to increase during infection of U2OS cells with HSV-1. A) Bar graphs representing the average rate of initial fluorescence recovery after photobleaching in HSV-1 infected cells normalized to mock infected cells. U2OS cells were transfected with plasmids encoding GFP-H3.3. Transfected cells were mock-infected or infected with 6 PFU per cell of HSV-1 strain KOS (**KOS 6**) or 30 PFU per cell of HSV-1 strain n212 (**n212 30**), KM110 (**KM110 30**), or UV-inactivated KOS (**UV 30**). Nuclear mobility of GFP-H3.3 was evaluated from 4 to 5 hpi (**4**) or 7 to 8 hpi (**7**) by FRAP. Error bars, SEM; n ≥ 24. **B)** Frequency distribution plots of the rate of initial fluorescence recovery after photobleaching per individual cell evaluated by FRAP as described for Panel A. Dashed or solid lines, mock or HSV-1 infected cells, respectively. **, $P < 0.01$.

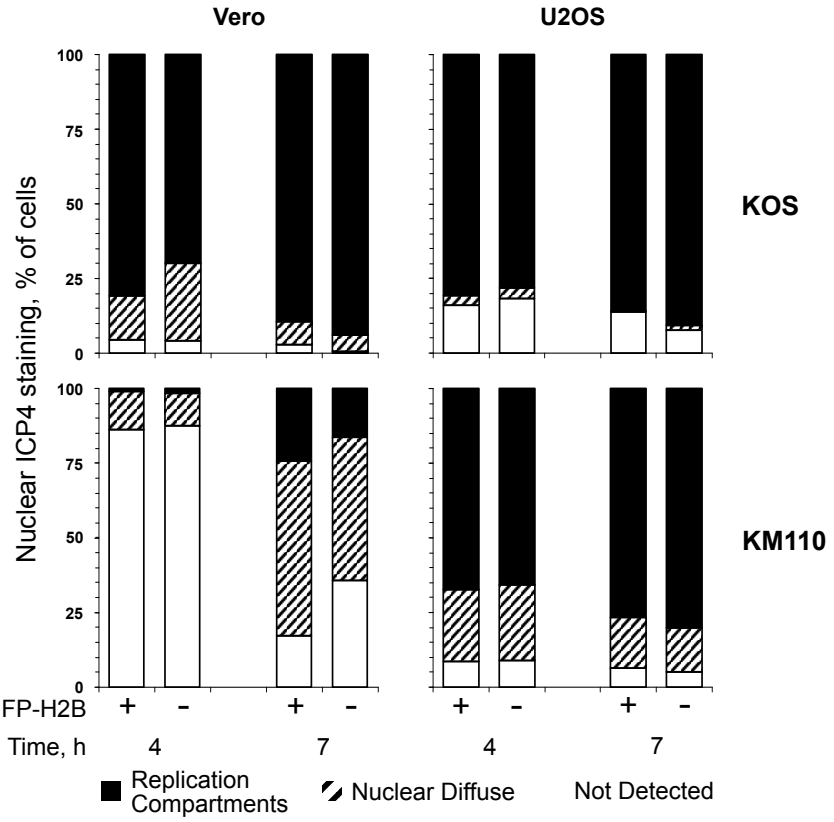

FIGURE 5.11: ICP4 expression and accumulation into replication compartments in Vero or U2OS cells expressing or not GFP-H2B and infected with wild-type or mutant HSV-1 strains. Bar graphs representing the percentage of HSV-1-infected cells transfected with GFP-H2B and expressing ICP4 as nuclear diffuse or accumulated into replication compartments. Vero or U2OS cells were transfected with plasmids expressing GFP-H2B. Cells were infected with 30 PFU per cell of HSV-1 strain **KOS** or **KM110**, or with 6 PFU per cell of HSV-1 strain KOS (U2OS cells). Cells were fixed at 4.5 (**4**) or 7.5 (**7**) hpi and stained for ICP4. Nuclear expression of ICP4 and its accumulation into replication compartments in cells in which GFP-H2B was expressed (**+**) or not (**-**) were evaluated by fluorescence microscopy. Vero KOS data replotted from Figure 4.5 for comparison.

FIGURE 5.12: Mobilization of core histone H2B does not require VP16 or ICP0. Line graphs representing the normalized fluorescence intensity of the photobleached nuclear region against time. Vero (**A**) and U2OS (**B**) cells were transfected with plasmids expressing GFP-H2B. Transfected cells were mock-infected (**filled circle**) or infected with 6 (**open triangle**), 15 (**open square**), or 30 (**open circle**) PFU per cell of HSV-1 strain KOS or KM110 as indicated. Nuclear mobility of GFP-H2B was evaluated from 4 to 5 hpi (**4 hpi**) or 7 to 8 hpi (**7 hpi**) by FRAP. Error bars, SEM; n ≥ 28. Time plotted on a semi-logarithmic scale.

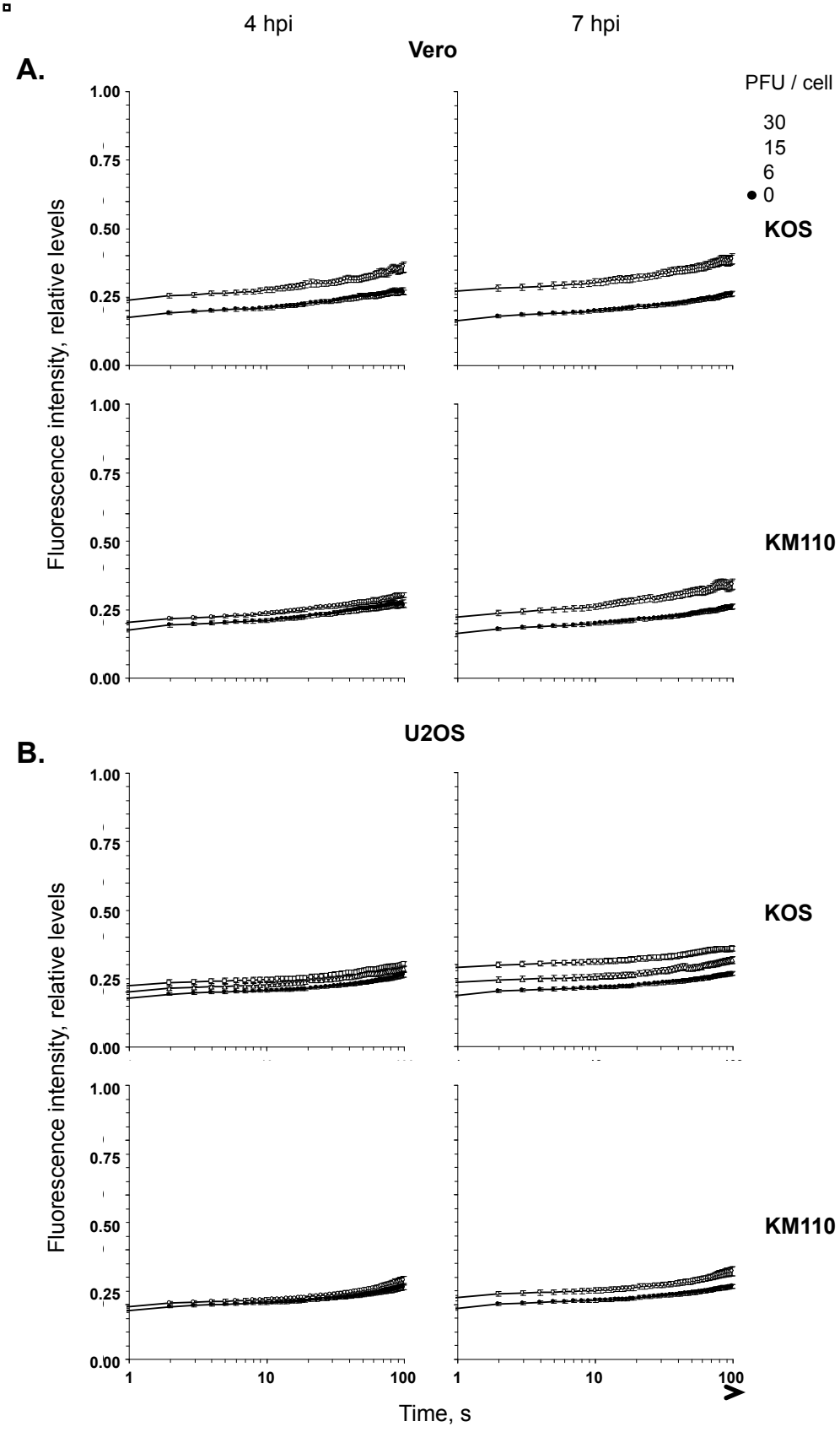
4 hpi
7 hpi
Vero
A.
PFU / cell
30
15
6
0
KOS
KM110
Fluorescence intensity, relative levels
1.00
0.75
0.50
0.25
0.00
U2OS
B.
KOS
KM110
1
10
100
Time, s

FIGURE 5.13: The increase in free H2B does not require VP16 or ICP0. **A)** Bar graphs representing the average level of free H2B in HSV-1 infected cells normalized to mock infected cells. Vero (**Vero**) and U2OS (**U2OS**) cells were transfected with plasmids encoding GFP-H2B. Transfected cells were mock-infected or infected with 6 or 30 PFU per cell of HSV-1 strain KOS or KM110 as indicated. Nuclear mobility of GFP-H2B was evaluated from 4 to 5 hpi (**4**) or 7 to 8 hpi (**7**) by FRAP. Error bars, SEM; Vero, n ≥ 28, U2OS, n ≥ 32. **B)** Frequency distribution plots of the percentage of free H2B per individual cell evaluated by FRAP as described for Panel A. Dashed or solid lines, mock or HSV-1 infected cells, respectively. *, $P < 0.05$; **, $P < 0.01$.

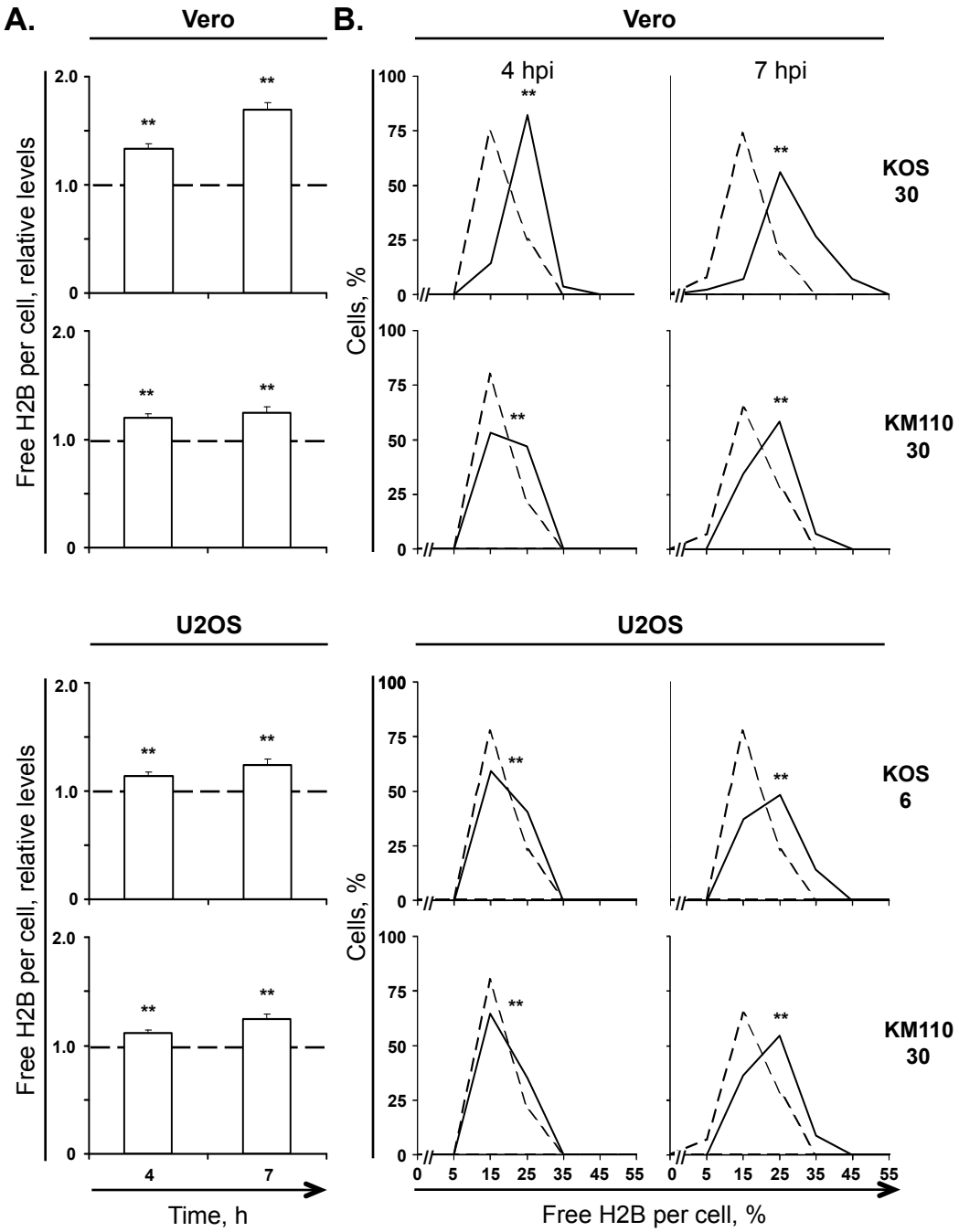
A.
Vero
B.
Vero
4 hpi
7 hpi
Free H2B per cell, relative levels
Cells, %
KOS
30
KM110
30
U2OS
U2OS
KOS
6
KM110
30
**
2.0
1.0
0
100
75
50
25
4
7
Time, h
0
5
15
25
35
45
55
Free H2B per cell, %

FIGURE 5.14: VP16 and ICP0 are not required for the decrease in the rate of initial fluorescence recovery of H2B in Vero cells. A) Bar graphs representing the average rate of initial fluorescence recovery after photobleaching in HSV-1 infected cells normalized to mock infected cells. Vero (**Vero**) and U2OS (**U2OS**) cells were transfected with plasmids encoding GFP-H2B. Transfected cells were mock-infected or infected with 6 or 30 PFU per cell of HSV-1 strain KOS or KM110 as indicated. Nuclear mobility of GFP-H2B was evaluated from 4 to 5 hpi (**4**) or 7 to 8 hpi (**7**) by FRAP. Error bars, SEM; Vero n ≥ 28, U2OS n ≥ 32. **B)** Frequency distribution plots of the rate of initial fluorescence recovery after photobleaching per individual cell evaluated by FRAP as described for Panel A. Dashed or solid lines, mock or HSV-1 infected cells, respectively. **, $P < 0.01$.

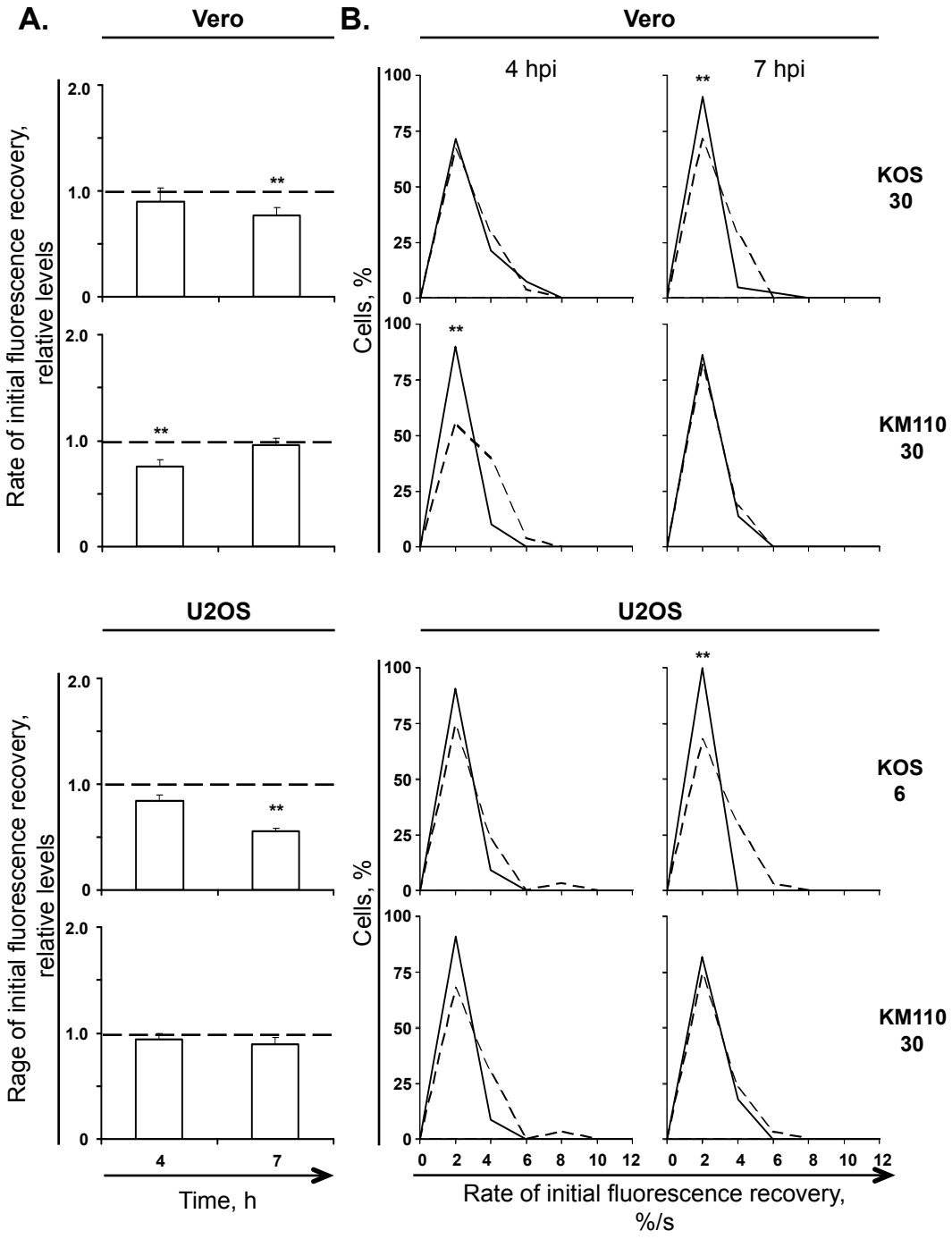
A.
Vero
B.
Vero
4 hpi
7 hpi
Rate of initial fluorescence recovery, relative levels
Cells, %
KOS 30
KM110 30
U2OS
U2OS
Rage of initial fluorescence recovery, relative levels
KOS 6
KM110 30
Time, h
Rate of initial fluorescence recovery, %/s

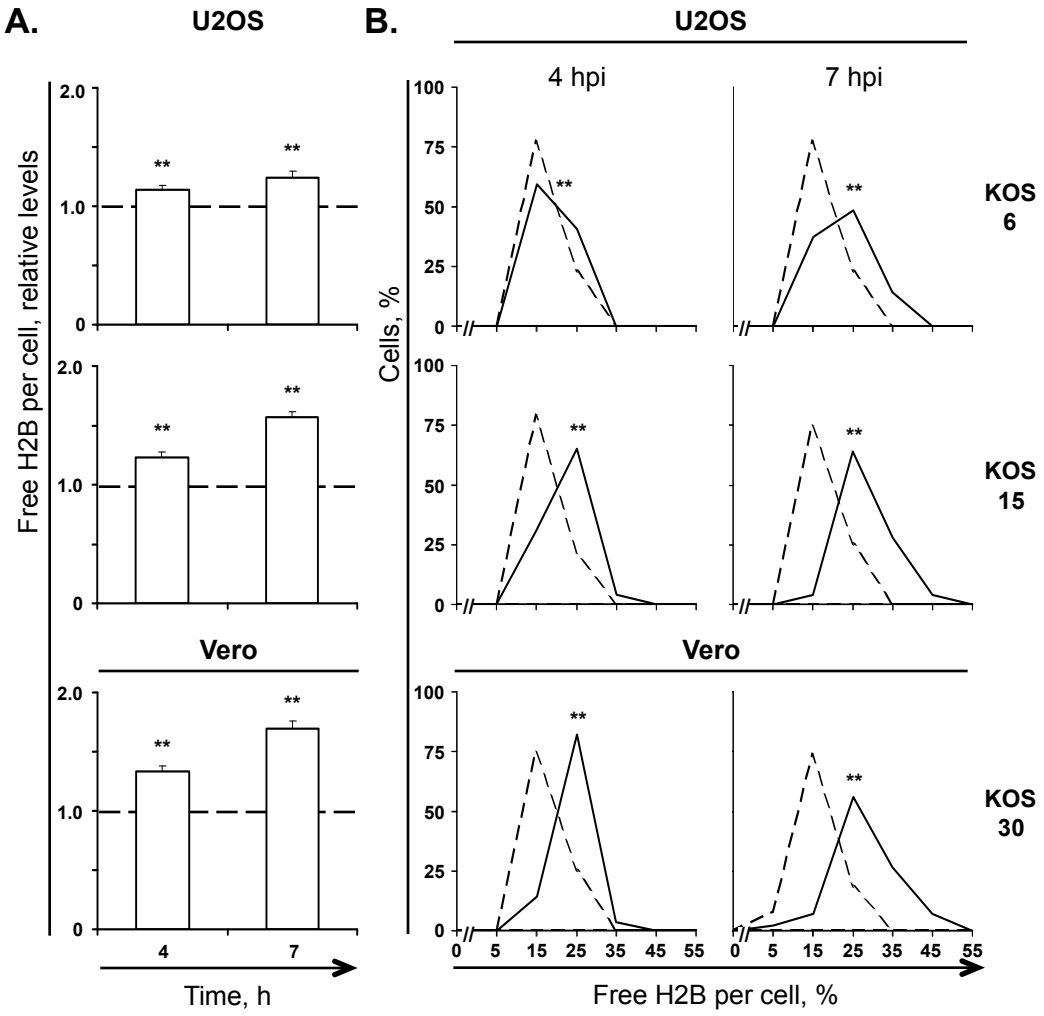

FIGURE 5.15: The level of free H2B increases with multiplicity of infection. A) Bar graphs representing the average percentage of free H2B in HSV-1 infected cells normalized to mock infected cells. U2OS (**U2OS**) and Vero (**Vero**) cells were transfected with plasmids encoding GFP-H2B. Transfected cells were mock-infected or infected with 6, 15 (U2OS), or 30 (Vero) PFU per cell of HSV-1 strain KOS as indicated. Nuclear mobility of GFP-H2B was evaluated from 4 to 5 hpi (**4**) or 7 to 8 hpi (**7**) by FRAP. Error bars, SEM; n ≥ 28. KOS 6 and KOS 30 data replotted from Figure 5.13, for comparison. **B)** Frequency distribution plots of the percentage of free H2B per individual cell evaluated by FRAP as described for Panel A. Dashed or solid lines, mock or HSV-1 infected cells, respectively. **, P <0.01.

Parameter	Histone Variant	PAA	Virus Strain	(avg ± SEM) Absolute	(avg ± SEM) Relative	% Cells with large: Increase[a]	% Cells with large: Decrease[b]
Free Pool	H2B	+	-	0.17 ± 0.01	1.19 ± 0.06	52*	4**
		-	-	0.16 ± 0.01	1.00 ± 0.03	11*	13**
		+	KOS 30	0.23 ± 0.01	1.58 ± 0.07	93*	0**
		-	KOS 30	0.27 ± 0.01	1.69 ± 0.07	88*	2**
	H3.3	+	-	0.21 ± 0.02	1.02 ± 0.08	35*	30**
		-	-	0.18 ± 0.01	1.00 ± 0.02	11*	15**
		+	KOS 30	0.30 ± 0.01	1.37 ± 0.06	64*	4**
		-	KOS 30	0.30 ± 0.01	1.55 ± 0.05	84*	1**
Rate of Recovery	H2B	+	-	1.88 ± 0.26	1.13 ± 0.17	26*	17**
		-	-	1.62 ± 0.10	1.00 ± 0.06	20*	15**
		+	KOS 30	1.48 ± 0.10	0.88 ± 0.07	7*	7**
		-	KOS 30	1.22 ± 0.11	0.77 ± 0.07	2*	34**
	H3.3	+	-	2.43 ± 0.25	1.01 ± 0.13	5*	0**
		-	-	2.31 ± 0.13	1.00 ± 0.05	14*	11**
		+	KOS 30	3.25 ± 0.34	1.40 ± 0.18	32*	4**
		-	KOS 30	2.99 ± 0.19	1.27 ± 0.07	20*	1**

TABLE 5.1: Mobilization of H2B and H3.3 in Vero cells infected with 30 PFU/cell of HSV-1 KOS and treated with PAA.

[a]*, percentage of cells in which the level of free histone was >1 SD above the average level in mock-infected cells; **, percentage of cells in which level of free histone was >1 SD lower than the average level in mock-infected cells.

[b]*, percentage of cells in which the rate of initial fluorescence recovery was >1 SD above the average rate of initial fluorescence recovery in mock-infected cells, **, percentage of cells in which the rate of initial fluorescence recovery was >1 SD lower than the average rate of initial fluorescence recovery in mock-infected cells.

			Localization (avg ± SEM) at:					
			4 hpi			7 hpi		
Cell Type	Virus Strain	PFU / cell	% Not detected	%Nuclear dispersed	% Replication compartment	% Not detected	%Nuclear dispersed	% Replication compartment
Vero	KOS	30	5 ± 2	24 ± 4	71 ± 5	3 ± 2	7 ± 1	90 ± 3
	n212	30	7 ± 2	57 ± 5	36 ± 5	5 ± 2	27 ± 5	68 ± 5
	KM110	30	95 ± 1	5 ± 1	0	80 ± 4	16 ± 3	4 ± 1
U2OS	KOS	6	9 ± 2	9 ± 3	82 ± 2	5 ± 1	5 ± 1	90 ± 2
	n212	30	1 ± 1	6 ± 1	93 ± 1	1 ± 1	5 ± 1	94 ± 2
	KM110	30	20 ± 4	49 ± 4	32 ± 7	14 ± 3	40 ± 1	46 ± 4

TABLE 5.2: Nuclear ICP4 localization in cells expressing or not GFP-H3.3 and infected with wild-type or mutant HSV-1 strains.

			4hpi			
			Free H3.3		% Cells with	Mock
Cell	Virus	PFU/	(avg ± SEM)		large increase	(avg ± SEM)
Type	Strain	cell	Absolute	Relative	in free[a]	Absolute
Vero	-	-	0.19 ± 0.01*	1.00 ± 0.02	15	-
	KOS	10	0.26 ± 0.01	1.49 ± 0.06	76	0.18 ± 0.01
		30	0.33 ± 0.01	1.71 ± 0.07	89	0.19 ± 0.01
	n212	30	0.27 ± 0.01	1.31 ± 0.06	61	0.21 ± 0.01
	KM110	30	0.21 ± 0.01	1.11 ± 0.03	25	0.19 ± 0.01
	UV	30	0.18 ± 0.01	0.93 ± 0.03	0	0.19 ± 0.01
U2OS	-	-	0.20 ± 0.01*	1.00 ± 0.02	13	-
	KOS	6	0.31 ± 0.01	1.94 ± 0.07	100	0.16 ± 0.01
	n212	30	0.28 ± 0.01	1.63 ± 0.07	88	0.17 ± 0.01
	KM110	30	0.23 ± 0.02	1.26 ± 0.06	50	0.18 ± 0.01
	UV	30	0.20 ± 0.01	1.00 ± 0.05	22	0.20 ± 0.01

TABLE 5.3 (A): Level of free H3.3 in Vero and U2OS cells infected with wild-type or mutant HSV-1 strains.

[a] Percentage of cells in which the level of free H3.3 was >1 SD above the average level in mock-infected cells.

* Average of all mock.

Cell Type	Virus Strain	PFU/ cell	7hpi Free H3.3 (avg ± SEM) Absolute	7hpi Free H3.3 (avg ± SEM) Relative	7hpi % Cells with large increase in free[a]	Mock (avg ± SEM) Absolute
Vero	-	-	0.18 ± 0.01*	1.00 ± 0.02	11	-
	KOS	10	0.30 ± 0.01	1.75 ± 0.07	94	0.17 ± 0.01
		30	0.30 ± 0.01	1.55 ± 0.05	84	0.20 ± 0.01
	n212	30	0.31 ± 0.02	1.80 ± 0.10	89	0.17 ± 0.01
	KM110	30	0.21 ± 0.01	1.21 ± 0.05	37	0.17 ± 0.01
	UV	30	0.22 ± 0.01	1.21 ± 0.05	40	0.18 ± 0.01
U2OS	-	-	0.20 ± 0.01*	1.00 ± 0.03	14	-
	KOS	6	0.31 ± 0.01	1.64 ± 0.05	96	0.19 ± 0.01
	n212	30	0.37 ± 0.01	1.83 ± 0.06	100	0.20 ± 0.02
	KM110	30	0.28 ± 0.02	1.56 ± 0.07	85	0.18 ± 0.01
	UV	30	0.20 ± 0.01	0.99 ± 0.04	11	0.20 ± 0.01

TABLE 5.3 (B): Level of free H3.3 in Vero and U2OS cells infected with wild-type or mutant HSV-1 strains.

[a] Percentage of cells in which the level of free H3.3 was >1 SD above the average level in mock-infected cells.

* Average of all mock

				4hpi				
				Rate of initial fluorescence recovery, %/s (avg ± SEM)		Fast chromatin exchange, % of cells		Mock (avg ± SEM)
Histone Variant	Cell Type	Virus Strain	PFU/ cell	Absolute	Relative	Increased [a]	Decreased [b]	Absolute
H3.3	Vero	-	-	2.05 ± 0.13*	1.00 ± 0.06	14	13	-
		KOS	10	3.66 ± 0.36	2.43 ± 0.21	82	0	1.56 ± 0.14
			30	4.12 ± 0.37	2.50 ± 0.22	70	0	1.75 ± 0.19
		n212	30	2.11 ± 0.23	1.29 ± 0.16	14	4	1.61 ± 0.27
		KM110	30	2.09 ± 0.13	1.08 ± 0.09	15	5	2.14 ± 0.22
		UV	30	1.86 ± 0.18	1.10 ± 0.12	19	13	1.81 ± 0.20
	U2OS	-	-	2.61 ± 0.17*	1.00 ± 0.06	13	7	-
		KOS	6	3.78 ± 0.38	1.55 ± 0.16	33	0	2.50 ± 0.33
		n212	30	2.56 ± 0.29	1.12 ± 0.13	15	4	2.31 ± 0.22
		KM110	30	3.38 ± 0.56	1.29 ± 0.25	19	0	2.79 ± 0.35
		UV	30	3.52 ± 0.47	1.31 ± 0.20	19	0	2.82 ± 0.44

TABLE 5.4 (A): Rate of initial fluorescence recovery of H3.3 in Vero and U2OS cells infected with wild-type or mutant HSV-1 strains.

[a] Percentage of cells in which the rate of initial fluorescence recovery was >1 SD above the average rate of initial fluorescence recovery in mock-infected cells.

[b] Percentage of cells in which the rate of initial fluorescence recovery was >1 SD lower than the average rate of initial fluorescence recovery in mock-infected cells.

* Average of all mock.

				7hpi				
				Rate of initial fluorescence recovery, %/s (avg ± SEM)		Fast chromatin exchange, % of cells		Mock (avg ± SEM)
Histone Variant	Cell Type	Virus Strain	PFU/ cell	Absolute	Relative	Increased [a]	Decreased [b]	Absolute
H3.3	Vero	-	-	2.31 ± 0.13*	1.00 ± 0.05	14	11	-
		KOS	10	3.16 ± 0.37	2.06 ± 0.30	63	0	1.62 ± 0.15
			30	2.99 ± 0.19	1.27 ± 0.07	20	1	2.53 ± 0.26
		n212	30	2.37 ± 0.22	1.31 ± 0.13	36	4	1.84 ± 0.24
		KM110	30	2.53 ± 0.26	1.10 ± 0.12	15	17	2.32 ± 0.19
		UV	30	2.30 ± 0.34	1.31 ± 0.16	29	14	1.70 ± 0.21
	U2OS	-	-	2.77 ± 0.16*	1.00 ± 0.05	14	13	-
		KOS	6	3.09 ± 0.33	1.37 ± 0.18	33	7	2.42 ± 0.29
		n212	30	2.38 ± 0.22	1.05 ± 0.10	19	19	2.33 ± 0.26
		KM110	30	3.55 ± 0.36	1.16 ± 0.12	22	7	3.06 ± 0.28
		UV	30	3.56 ± 0.43	1.11 ± 0.14	26	22	3.25 ± 0.31

TABLE 5.4 (B): Rate of initial fluorescence recovery of H3.3 in Vero and U2OS cells infected with wild-type or mutant HSV-1 strains.

[a] Percentage of cells in which the rate of initial fluorescence recovery was >1 SD above the average rate of initial fluorescence recovery in mock-infected cells.

[b] Percentage of cells in which the rate of initial fluorescence recovery was >1 SD lower than the average rate of initial fluorescence recovery in mock-infected cells.

* Average of all mock.

			Localization (avg ± SEM) at:					
			4 hpi			7 hpi		
Cell Type	Virus Strain	PFU / cell	% Not detected	%Nuclear dispersed	% Replication compartment	% Not detected	%Nuclear dispersed	% Replication compartment
Vero	KOS	30	4 ± 1	21 ± 4	75 ± 4	2 ± 1	6 ± 2	92 ± 3
	KM110	30	86 ± 7	12 ± 6	1 ± 1	39 ± 13	48 ± 7	13 ± 7
U2OS	KOS	6	17 ± 5	3 ± 2	80 ± 6	10 ± 3	1 ± 1	89 ± 4
	KM110	30	10 ± 2	30 ± 5	60 ± 4	6 ± 1	18 ± 1	76 ± 2

TABLE 5.5: Nuclear ICP4 localization in cells expressing or not GFP-H2B and infected with wild-type or mutant HSV-1 strains.

			4hpi			
			Free H2B		% Cells with	Mock
Cell	Virus	PFU/	(avg ± SEM)		large increase	(avg ± SEM)
Type	Strain	cell	Absolute	Relative	in free[a]	Absolute
Vero	-	-	0.17 ± 0.01*	1.00 ± 0.03	16	-
	KOS	30	0.24 ± 0.01	1.33 ± 0.05	79	0.18 ± 0.01
	KM110	30	0.20 ± 0.01	1.20 ± 0.04	50	0.17 ± 0.01
U2OS	-	-	0.18 ± 0.01*	1.00 ± 0.02	11	-
	KOS	6	0.20 ± 0.01	1.14 ± 0.04	41	0.18 ± 0.01
		15	0.22 ± 0.01	1.23 ± 0.04	77	0.18 ± 0.01
	KM110	30	0.19 ± 0.01	1.11 ± 0.03	35	0.17 ± 0.01

TABLE 5.6 (A): Level of free H2B in Vero and U2OS cells infected with wild-type or mutant HSV-1 strains.

[a] Percentage of cells in which the level of free H2B was >1 SD above the average level in mock-infected cells.

* Average of all mock.

			7hpi			
			Free H2B		% Cells with	Mock
Cell	Virus	PFU/	(avg ± SEM)		large increase	(avg ± SEM)
Type	Strain	cell	Absolute	Relative	in free[a]	Absolute
Vero	-	-	0.16 ± 0.01*	1.00 ± 0.03	11	-
	KOS	30	0.27 ± 0.01	1.69 ± 0.07	88	0.16 ± 0.01
	KM110	30	0.22 ± 0.01	1.25± 0.05	48	0.18 ± 0.01
U2OS	-	-	0.18 ± 0.01*	1.00± 0.02	15	-
	KOS	6	0.23 ± 0.01	1.24 ± 0.05	66	0.19 ± 0.01
		15	0.29 ± 0.01	1.57 ± 0.05	96	0.18 ± 0.01
	KM110	30	0.22 ± 0.01	1.24 ± 0.05	64	0.18 ± 0.01

TABLE 5.6 (B): Level of free H2B in Vero and U2OS cells infected with wild-type or mutant HSV-1 strains.

[a] Percentage of cells in which the level of free H2B was >1 SD above the average level in mock-infected cells.

* Average of all mock.

				4hpi				
				Rate of initial fluorescence recovery, %/s (avg ± SEM)		Fast chromatin exchange, % of cells		Mock (avg±SEM)
Histone Variant	Cell Type	Virus Strain	PFU/ cell	Absolute	Relative	Increased[a]	Decreased[b]	Absolute
H2B	Vero	-	-	1.87 ± 0.15*	1.00 ± 0.07	19	16	-
		KOS	30	1.63 ± 0.22	0.90 ± 0.12	18	32	1.84 ± 0.19
		KM110	30	1.44 ± 0.11	0.76 ± 0.06	3	20	1.94 ± 0.18
	U2OS	-	-	1.59 ± 0.12*	1.00 ± 0.06	9	15	-
		KOS	6	1.34 ± 0.07	0.85 ± 0.05	0	13	1.62 ± 0.18
			15	1.19 ± 0.08	0.79 ± 0.06	8	42	1.51 ± 0.10
		KM110	30	1.52 ± 0.08	0.94 ± 0.05	3	9	1.65 ± 0.18

TABLE 5.7 (A): Rate of initial fluorescence recovery of H2B in Vero and U2OS cells infected with wild-type or mutant HSV-1 strains.

[a] Percentage of cells in which the rate of initial fluorescence recovery was >1 SD above the average rate of initial fluorescence recovery in mock-infected cells.

[b] Percentage of cells in which the rate of initial fluorescence recovery was >1 SD lower than the average rate of initial fluorescence recovery in mock-infected cells.

* Average of all mock.

				7hpi				
				Rate of initial fluorescence recovery, %/s (avg ± SEM)		Fast chromatin exchange, % of cells		Mock (avg ± SEM)
Histone Variant	Cell Type	Virus Strain	PFU/ cell	Absolute	Relative	Increased[a]	Decreased [b]	Absolute
H2B	Vero	-	-	1.62 ± 0.10*	1.00 ± 0.06	20	15	-
		KOS	30	1.22 ± 0.11	0.77 ± 0.07	2	34	1.62 ± 0.12
		KM110	30	1.48 ± 0.10	0.96 ± 0.07	10	17	1.54 ± 0.09
	U2OS	-	-	1.70 ± 0.12*	1.00 ± 0.06	15	15	-
		KOS	6	1.01 ± 0.05	0.55 ± 0.03	0	54	1.83 ± 0.16
			15	1.08 ± 0.11	0.63 ± 0.06	4	60	1.70 ± 0.16
		KM110	30	1.45 ± 0.12	0.90 ± 0.07	9	24	1.62 ± 0.14

TABLE 5.7 (B): Rate of initial fluorescence recovery of H2B in Vero and U2OS cells infected with wild-type or mutant HSV-1 strains.

[a] Percentage of cells in which the rate of initial fluorescence recovery was >1 SD above the average rate of initial fluorescence recovery in mock-infected cells.

[b] Percentage of cells in which the rate of initial fluorescence recovery was >1 SD lower than the average rate of initial fluorescence recovery in mock-infected cells.

* Average of all mock.

CHAPTER 6: MOBILIZATION OF H2A.Z ISOFORMS DURING HSV-1 INFECTION.

This Chapter contains unpublished data.

ABSTRACT

H2A and H2B form dimers. However, H2A and H2B were differentially mobilized I HSV-1 infected cells. Whereas the fast chromatin exchange rate of H2A was increased, that of H2B was decreased. Therefore, most of the mobilized H2B cannot be paired in dimers with H2A. Most likely, this pool is paired with H2A variants. H2A has several variants, H2A.X, H2A.Z, H2A.Bbd, and MacroH2A. H2A.Z-containing nucleosomes that also contain H3.3 are highly unstable. Therefore, H2A.Z and H3.3 may be components of the unstable nucleosomes that are associated with HSV-1 genomes. I therefore first evaluated the mobility of H2A.Z. H2A.Z was mobilized at early and late times, increasing its free pool and decreasing its rate of fast chromatin exchange. H2A.Z mobilization is therefore similar to that of H2B rather than that of H3.3. These data indicate that the population of H2A.Z that is mobilized during HSV-1 infection is likely not associated in unstable nucleosomes with H3.3. The mobilization of H2A.Z, in contrast, supports the alternative hypothesis that most of the mobilized H2B is paired in dimers with H2A.Z variants.

6.1 INTRODUCTION.

During lytic HSV-1 infection, both canonical (H2A, H2B, H4) and variant (H3.3) core histones are mobilized. The mobilization of core histones and the requirements for H2B and H3.3 mobilization have indicated that different mechanisms may contribute to core histone mobilization during infection. The mobilization of H3.3 increased its free pool and the rate of fast H3.3 chromatin exchange. Conversely, mobilization of H2B increased its free pool but decreased the rate of fast H2B chromatin exchange. Surprisingly, the mobilization of H2A, which forms nucleosome dimers with H2B, was different than the mobilization of H2B. This suggests that the detected mobilization of H2B reflects dimers of H2B and an H2A variant.

HSV-1 genomes and associated histones are likely associated in unstable nucleosome complexes. Nucleosomes that contain H3.3 are relatively unstable. The stability of such nucleosomes is decreased even further if they also contain the H2A variant H2A.Z (Jin & Felsenfeld, 2007). I therefore next tested whether H2A.Z was mobilized as H3.3 during HSV-1 infection.

H2A.Z is a variant core histone with 61% sequence identity with canonical H2A (Eirin-Lopez et al., 2009). Like H3.3, H2A.Z is expressed throughout the cell cycle and is incorporated into chromatin in a DNA replication-independent manner. H2A.Z is distributed throughout chromatin, being found in peri-centromeric, hetero-, and euchromatin. The functions of H2A.Z are controversial. It is proposed to have multiple roles in regulation of gene expression. Therefore, it is not surprising that

it is associated with regions of active transcription, repressed transcription, heterochromatin boundaries, and of silenced genes at the nuclear periphery.

Two H2A.Z isoforms, H2A.Za (H2A.Z-2, formerly H2A.F/Z or H2A.V) and H2A.Zv (H2A.Z-1, formerly H2A.Z), have recently been identified. They share a high degree of amino acid sequence identity, differing in only 3 residues (Figure 6.1) (Hatch & Bonner, 1990). Both are expressed in a variety of fetal and adult tissues. There are, however, specific differences in the relative levels of H2A.Za and H2A.Zv transcripts in certain adult tissues, such as the liver and the brain, and between fetal and adult tissues (Dryhurst et al., 2009). The functional differences of these isoforms, if any, are still largely unknown. The H2A.Za and H2A.Zv promoters are different (Dryhurst et al., 2009). Consistently, they may have different developmental and functional expression. H2A.Za was not able to functionally replace H2A.Zv to overcome the lethality of H2A.Zv knockout in mice. Moreover, chicken cells with H2A.Za or H2A.Zv knocked down had different phenotypes (Matsuda et al., 2010). H2A.Za had approximately a 30% reduction in cell numbers, which was attributed to increased apoptosis (Matsuda et al., 2010). H2A.Zv knock down cells, on the other hand, had similar growth and apoptosis rates as wild-type cells (Matsuda et al., 2010). Taken together, these data suggest that the H2A.Z isoforms may have different roles. Because such differences are not yet fully characterized, I analyzed the mobility of both isoforms.

6.2 RESULTS.

6.2.1 H2A.Za and H2A.Zv have larger free pools and faster low-affinity chromatin exchange than H2A.

Histone tails influence nucleosome stability, protein-protein interactions, and chromatin condensation. Therefore, they also affect histone chromatin exchange. H2A and the different H2A variants, such as H2A.Z and H2A.X, have different rates of chromatin exchange (Higashi et al., 2007). I therefore first analyzed the inherent differences between H2A, H2A.Za, and H2A.Zv chromatin exchange.

The pools of free H2A.Za and H2A.Zv were higher than those of H2A in mock-infected cells. At 4 hours after mock-infection of Vero cells, the pool of free H2A.Zv was 127 ± 8% that of H2A ($P<0.01$) (Figure 6.2, Table 6.1). The pool of free H2A.Za also tended to be higher than that of H2A at 4h after mock-infection (113 ± 5%), although this difference was not statistically significant. At 7 hours after mock-infection, the free pools of H2A.Za or H2A.Zv were both higher than those of H2A (135 ± 8% or 168 ± 6%, respectively) ($P<0.01$, Student's T-test; 1-tail) (Figure 6.2, Table 6.1). Furthermore, the pool of free H2A.Zv was larger than that of H2A.Za at this time ($P<0.01$, Student's T-test; 1-tail). At either time analyzed, the population of cells that had a level of free H2A.Za or H2A.Zv higher than that of H2A by a large degree was at least 2-, and up to 5-, fold what would be expected (16%) in a normal population distribution (Table 6.1).

The difference in the chromatin exchange of H2A.Za relative to H2A was not a cell type-specific effect. In U2OS cells, the pool of free H2A.Za was also higher than that of H2A, 128 ± 6% or 136 ± 5% at 4 or 7 hours after mock-infection, respectively ($P<0.01$, Student's T-test; 1-tail) (Figure 6.2, Table 6.1). At both times evaluated, the population of U2OS cells with a level of free H2A.Za greater than that of H2A was at least 5-fold larger than that expected for a normal population distribution (Table 6.1). The chromatin exchange of H2A.Za and H2A.Zv is therefore different than that of H2A at 4 and 7h after mock-infection. Such different chromatin exchange results in higher levels of free H2A.Za and H2A.Zv at 4 or 7h after mock infection. However, the higher levels of free H2A.Za and H2A.Zv relative to H2A in Vero and U2OS cells may be the result of increased expression of the H2A.Z isoforms. I therefore analyzed whether the level of H2A.Za or H2A.Zv expression, evaluated by relative nuclear fluorescence, correlated with the level available in the free pool. The level of H2A.Za or H2A.Zv expression did not correlate with the level of H2A.Za or H2A.Zv available in the free pool at early or later times in Vero or U2OS cells (Figures 6.3 and 6.4). Therefore, the differences in the levels of free H2A, H2A.Za, and H2A.Zv reflect differences in chromatin exchange and not differences in expression levels. The chromatin exchange of H2A.Za and H2A.Zv are therefore different than that of H2A at 4 or 7 hours after mock-infection.

In addition to higher levels in the free pool, the H2A.Z isoforms had higher rates of fast chromatin exchange relative to H2A. The fast chromatin exchange rate of H2A.Za and H2A.Zv in Vero cells were more

than 1.5 and 2 fold higher at early and late times after mock-infection, respectively ($P<0.05$, $P<0.01$, respectively, Student's T-test; 1-tail) (Figure 6.5, Table 6.2). The fast chromatin exchange rate of H2A.Zv also was higher than that of H2A.Za ($P<0.01$ at 7 hpi, Student's T-test; 1-tail) (Figure 6.5 Panel C, Table 6.2). At either time analyzed, greater than 60% of cells had high rates of fast H2A.Za and H2A.Zv chromatin exchange, larger than one SD above the average rate of H2A (Table 6.2). The high rate of low-affinity chromatin exchange of H2A.Za was not a cell type-specific occurrence. The rate of fast chromatin exchange of H2A.Za in U2OS cells was approximately 2-fold higher than that of H2A ($P<0.01$, Student's T-test; 1-tail) (Figure 6.5, Table 6.2). The H2A.Z isoforms may, therefore, have inherently higher rates of low-affinity chromatin exchange than H2A. Alternatively, mock-infection may differentially affect the chromatin exchange of H2A and H2A.Z isoforms.

Taken together, these data demonstrate that the H2A.Z isoforms have higher rates of low-affinity chromatin binding and unbinding than H2A. Furthermore, the differences in the relative rates of H2A.Z chromatin binding and unbinding result in higher levels of H2A.Z available in the free pool at any given time. These data also indicate that the chromatin exchange of the H2A.Z isoforms differs after mock-infection. H2A.Zv tends to have a higher rate of low-affinity chromatin exchange, as well as higher levels available in the free pool, than H2A.Za does. The different levels of free H2A.Za and H2A.Zv relative to H2A, and the higher rates of H2A.Za and H2A.Zv fast chromatin exchange, suggest

that mock-infection differentially alters the chromatin exchange of the H2A.Z isoforms and H2A.

6.2.2 The pools of free H2A.Za and H2A.Zv are increased during HSV-1 infection.

The chromatin exchange of H2A.Za and H2A.Zv was increased at both early and late times after infection with HSV-1 strain KOS, as demonstrated by faster fluorescence recovery after photobleaching (Figure 6.6). During HSV-1 infection, the rates of H2A.Za and H2A.Zv chromatin association and disassociation were altered such that the free pools were increased (Figure 6.7, Table 6.3). The increase in free H2A.Za and H2A.Zv could, however, reflect changes in their expression during infection, rather than altered chromatin exchanges. Therefore, I first analyzed whether the expression of H2A.Za and H2A.Zv in infected cells, measured by relative nuclear fluorescence, correlated with the level of H2A.Za and H2A.Zv in the free pool.

The level of GFP-H2A.Za and GFP-H2A.Zv expression did not correlate with the level available in the free pool at 4 or 7h after infection with 30 PFU per cell of KOS (Figure 6.8). Therefore, the increases in the pools of free H2A.Za and H2A.Zv reflect changes in chromatin exchange and not changes in expression levels.

The pools of free H2A.Za or H2A.Zv were increased to 136 ± 6% or 127 ± 7%, respectively, at 4h after infection of Vero cells with 30 PFU per cell of KOS, ($P<0.01$, Student's T-test; 1-tail) (Figure 6.7, Table 6.3). The absolute percentages of free H2A.Za or H2A.Zv tended to be higher than

that of H2A, approximately 17 or 20% compared to approximately 14%, respectively. Nonetheless, the pools of free H2A, H2A.Za, and H2A.Zv were increased by a similar magnitude at early times during HSV-1 infection ($P>0.05$, Tukey's HSD) (Figure 6.7 Panel C 4 hpi). The pools of free H2A.Za and H2A.Zv were increased throughout the population of infected cells. At 4h after infection, more that 50% of infected cells had increased their pools of free H2A.Za or H2A.Zv by more than one SD (Table 6.3). At 7h after infection of Vero cells with 30 PFU per cell of KOS, the pools of free H2A.Za or H2A.Zv were still increased, to 158 ± 8% or 132 ± 65%, respectively ($P<0.01$, Student's T-test; 1-tail) (Figure 6.7, Table 6.3). At this time, the pool of free H2A.Za was increased by a similar magnitude as that of H2A ($P>0.05$, Tukey's HSD) (Figure 6.7 Panel C 7hpi, Table 6.3). The relative increase in free H2A.Zv, however, was to a lesser degree than that of H2A.Za and H2A ($P<0.05$ and $P<0.01$, respectively, Tukey's HSD) (Figure 6.7 Panel C 7hpi). Thus, H2A.Za and H2A may be more susceptible to the factors that alter the rates of chromatin association and dissociation relative to each other to increase the level available in the free pool. However, the absolute level of H2A.Zv available in the free pool in mock-infected cells is higher than that of H2A.Za and H2A. Therefore, the population of H2A.Zv available to be mobilized during HSV-1 infection could be limited, resulting in a smaller magnitude of relative increase (0.20 ± 0.01, 0.17 ± 0.01, and 0.15 ± 0.01, respectively) (Table 6.3). Alternatively, only a certain level of H2A.Za or H2A.Zv may need to be mobilized. In this latter scenario, the relative mobilization would be lower for the variant tat has the higher percentage

of free histone before infection. Consistent with these alternative models, the absolute levels of H2A.Za and H2A.Zv that are available in the free pool at later times after infection are similar, 0.27 ± 0.01% and 0.28 ± 0.01%, respectively (Table 6.3).

6.2.3 H2A.Zv has a decreased rate of fast chromatin exchange at later times after infection.

HSV-1 infection altered H2A.Za and H2A.Zv chromatin exchange, such that there was an increase in the level of H2A.Za and H2A.Zv available in the free pools. I next analyzed the effects of HSV-1 infection on the rate of fast chromatin exchange, or low-affinity chromatin binding, of the H2A.Z isoforms.

The fast chromatin exchange rate of H2A.Za was not significantly altered after infection of Vero cells with 30 PFU per cell of HSV-1 strain KOS, although it tended to be decreased at later times after infection (1.04 ± 0.09 or 0.92 ± 0.09 fold at 4 or 7hpi, respectively) (Figure 6.9, Table 6.4). In contrast, the fast chromatin exchange rate of H2A had a tendency to be increased during HSV-1 infection (Figure 6.9, Table 6.4). As for H2A, the fast chromatin exchange rate of H2A.Zv had a tendency to be increased at early times after infection of Vero cells with 30 PFU per cell of HSV-1 strain KOS (Figure 6.9, Table 6.4). Although not statistically significant, the rate of H2A.Zv fast chromatin exchange in HSV-1 infected cells was 1.18 ± 0.18 fold of that in mock-infected cells ($P>0.05$, Student's T-test; 1-tail) (Figure 6.8, Table 6.4). Surprisingly, the fast chromatin exchange rate of H2A.Zv was decreased, to 0.61 ± 0.08

fold, at later times after infection ($P<0.01$, Student's T-test; 1-tail) (Figure 6.9, Table 6.4). A large degree of decrease in the rate of H2A.Zv fast chromatin exchange occurred in more than 50% of cells, indicating that such a decrease occurred throughout the population of HSV-1 infected cells (Table 6.4). The rates of H2A, H2A.Za, and H2A.Zv fast chromatin exchange are therefore differentially affected during HSV-1 infection.

6.2.4 H2A and H2A.Za are mobilized during HSV-1 infection of U2OS cells.

H2A and both H2A.Z isoforms, H2A.Za and H2A.Zv, were mobilized during HSV-1 infection of Vero cells. Such mobilization altered the rate of chromatin association relative to that of chromatin dissociation such that the pools of free H2A, H2A.Za, and H2A.Zv were increased. The fast chromatin exchange rates of H2A, H2A.Za, and H2A.Zv, however, were differentially altered. That of H2A.Za was not substantially different than that in mock-infected cells, that of H2A had a tendency to be increased, and that of H2A.Zv was decreased at later times after infection.

The different mobilizations of H2A and H2A.Z during HSV-1 infection may be due to variant-specific differences in chromatin exchange. I therefore next analyzed H2A and H2A.Z mobilization during HSV-1 infection of U2OS cells. I focused on H2A.Za because the relative increase in the chromatin exchange of this isoform during HSV-1 infection of Vero cells was larger than that of H2A.Zv, as evaluated by the relative increase to the free pool.

I first evaluated the chromatin exchange of H2A.Za relative to that of H2A in mock-infected U2OS cells. As in Vero cells, the chromatin

exchange of H2A.Za was different from that of H2A, which resulted in a larger pool of free H2A.Za than H2A (Figure 6.2 U2OS). At either time analyzed, the level of GFP-H2A or GFP-H2A.Za expression did not correlate with the level available in the free pool (Figure 6.4). The differences in the levels of free H2A.Za and H2A are not the result of different expression levels and therefore reflect differences in the chromatin exchange of H2A.Za and H2A. In addition to the different levels available in the free pool, the fast chromatin exchange rate of H2A.Za had a tendency to be greater than that of H2A (Figure 6.5 U2OS). Thus, the chromatin exchange of H2A.Za differs from that of H2A. H2A.Za has a faster rate of low-affinity chromatin exchange and higher levels are available in the free pool.

The chromatin exchange of H2A and H2A.Za was increased in U2OS cells infected with 6 PFU per cell of HSV-1 strain KOS, as demonstrated by faster fluorescence recovery after photobleaching (Figure 6.10). Such mobilization altered the rates of H2A and H2A.Za chromatin association and disassociation such that the free pools of H2A and H2A.Za were increased (Figure 6.11, Table 6.3). At early and late times after infection, the levels of H2A or H2A.Za available in the free pools did not correlate with their levels of expression, measured as relative nuclear fluorescence intensity (Figure 6.12). Thus, the increase in the levels of H2A and H2A.Za available in the free pools during HSV-1 infection reflect changes in H2A and H2A.Za chromatin exchange and not increased expression.

The pool of free H2A was increased to 110 ± 3% at 4h after infection with 6 PFU per cell of HSV-1 strain KOS, whereas that of H2A.Za was increased to 135 ± 6% ($P<0.01$, Student's T-test; 1-tail) (Figure 6.11, Table 6.3). The pool of free H2A.Za was increased by a larger degree than that of H2A ($P<0.01$, Student's T-test; 1-tail) (Figure 6.11 Panel C 4 hpi, Table 6.3). H2A.Za chromatin association and disassociation may be altered relative to each other by a greater degree such that the pool of free H2A.Za was increased by a greater degree. Alternatively, the difference in the levels of free H2A and H2A.Za may reflect the population of cells that have large increases in the pools of free H2A or H2A.Za. At 4hpi, 68% of infected cells had increases in the level of free H2A.Za larger than one SD, whereas only 39% had such large increases in the levels of free H2A (Table 6.3). At later times after infection, the free pools of H2A and H2A.Za were increased by a similar magnitude (Figure 6.11 Panel C 7hpi, Table 6.3). The pool of H2A was increased to 147 ± 5% and that of H2A.Za, to 142 ± 6% (Figure 6.11, Table 6.3). A similar relative increase in the pools of free H2A and H2A.Za occurred despite the fact that the pool of free H2A.Za is intrinsically larger than that of H2A (0.33 compared to 0.25, respectively).

The free pools of H2A and H2A.Za are both increased during HSV-1 infection. Their rates of fast chromatin exchange, however, were differentially changed. The rate of fast chromatin exchange of H2A had a tendency to be decreased at early times after infection, by 0.87 ± 0.05 fold, and was decreased at later times after infection, by 0.78 ± 0.05 fold

(P<0.01 at 7hpi, Student's T-test; 1-tail) (Figure 6.13, Table 6.4). The average rate of fast chromatin exchange of H2A.Za, however, was not substantially different from that of mock-infected cells at early or late times after infection (0.87 ± 0.11 and 1.04 ± 0.14 fold, respectively) (Figure 6.13, Table 6.4). Cell-to-cell analysis of the rates of fast H2A.Za chromatin exchange at later times after infection, however, shows a wide dispersion. Two populations of HSV-1 infected cells my therefore exist with different rates of H2A.Za fast chromatin exchange, one in which the rate of fast chromatin exchange has a tendency to be increased and one in which it has a tendency to be decreased (Figure 6.13 Panel B H2A.Za 7 hpi).

Taken together, these data demonstrate that the chromatin exchange of H2A and H2A.Za is altered during HSV-1 infection of U2OS cells. The rates of H2A and H2A.Za chromatin association and dissociation are altered relative to each other such that the pools of free H2A and H2A.Za are increased at early and late times after infection. The rates of H2A and H2A.Za low-affinity chromatin exchange are differentially affected during HSV-1 infection. The rate of low-affinity chromatin exchange of H2A has a tendency to be decreased. The low-affinity chromatin exchange rate of H2A.Za also has a tendency to be decreased at early times after infection. At later times after infection, however, there is a widespread variability in the rate of fast chromatin exchange. Alternatively, two populations with different rates of low-affinity H2A.Za chromatin exchange may exist. One in which the rate of

low-affinity chromatin exchange tends to be increased and one in which it tends to be decreased.

6.3 DISCUSSION.

The H2A.Z isoforms and canonical H2A have intrinsically different chromatin exchanges. The steady-state levels of H2A.Za and H2A.Zv in the free pool were higher, and the rates of H2A.Za and H2A.Zv fast chromatin exchange faster, than those of H2A in all cells analyzed. Additionally, the chromatin exchanges of H2A.Za and H2A.Zv are intrinsically different. H2A.Zv tends to have higher levels available in the free pool and a faster rate of fast chromatin exchange than H2A.Za. The three-residue difference in H2A.Za and H2A.Zv amino acid sequence therefore provides some distinction that is evident in their chromatin exchange. Differences in the chromatin exchange of H2A.Za and H2A.Zv support a model in which they have some distinct functions or respond to different stimuli. The same rates of fast chromatin exchange and levels in the free pools would be expected if the H2A.Z isoforms were involved only in the same mechanisms of chromatin exchange and mobilized by the same stimuli.

HSV-1 infection mobilized H2A.Za and H2A.Zv, as it did canonical H2A. The rates of H2A.Za and H2A.Zv chromatin association and dissociation were altered relative to each other during infection such that the pools of free H2A.Za and H2A.Zv were increased. At early times after infection of Vero cells, the pools of free H2A.Za and H2A.Zv were increased by the same magnitude as that of H2A. Thus, even though the absolute levels of the H2A.Z isoforms are intrinsically higher than H2A,

their free pools were still increased by the same degree. At later time after infection, the pools of free H2A and H2A.Za were increased by a larger degree than that of H2A.Zv. This could reflect differences in the inherent levels of the free histones. The level of H2A.Zv in the free pool is already higher than that of H2A.Za or H2A. Cells may not tolerate as much of an increase of this variant in the free pool, or there may be a limit on the steady-state level of H2A.Zv that can be released from chromatin. Alternatively, only mobilization of a certain percentage of H2A or H2A.Z isoforms may be required (approximately 20%).

The rates of fast chromatin exchange of H2A.Za and H2A.Zv were also altered during HSV-1 infection. In contrast to H2A, which had an increased rate of fast chromatin exchange at early times after infection, the rates of H2A.Za and H2A.Zv fast chromatin exchange were unchanged from those in mock-infected cells. To allow for the increase in the pools of free H2A.Za and H2A.Zv, the rate of chromatin association must be relatively decreased, or that of chromatin disassociation must be relatively increased. However, as the overall rate of fast chromatin exchange was not substantially altered, any relative changes in H2A.Za and H2A.Zv low-or high-affinity chromatin association and disassociation are likely marginal. The increase in the levels of free H2A.Za and H2A.Zv may therefore result from changes to the rates H2A.Za and H2A.Zv high-affinity chromatin association and dissociation (slow-chromatin exchange). At later times after infection, the rate of H2A.Zv fast chromatin exchange was decreased (Figure 6.9). To accommodate the increase in the free pool of H2A.Zv, the rates of H2A.Zv low-affinity

chromatin association may be decreased by a larger degree than that of disassociation. H2A.Zv may, for example, be more likely (or even only able) to re-bind chromatin through slow, or high-affinity, chromatin exchange.

As for Vero cells, U2OS cells have an inherently higher level of free H2A.Za than H2A (Figure 6.2). The absolute percentage of free H2A.Za is higher than that of H2A at early and late times after infection (Table 6.3). At early times after infection of U2OS cells, the relative increase to the level of free H2A.Za is greater than that of H2A (135 vs 110% respectively, Figure 6.11 Panel C). At later times, however, the relative increases to the levels of free H2A.Za and H2A are similar (142 and 147%, Figure 6.11 Panel C). These data suggest that H2A.Za chromatin exchange in U2OS cells may be more responsive to, or affected by, the mechanisms that mobilize histones early during HSV-1 infection.

The rates of H2A and H2A.Za fast chromatin exchange tended to be decreased during infection of U2OS cells. However, there was a wide dispersion in the rates of fast H2A.Za chromatin exchange at later times after infection (Figure 6.13). To accommodate the increases in free H2A and H2A.Za with the decreases in their rates of fast chromatin exchange, the rates of low-affinity chromatin association should be decreased more than the rates of disassociation. Alternatively, the rates of low-affinity chromatin unbinding could remain similar, with largely decreased or inhibited low-affinity chromatin binding. This situation would force H2A or H2A.Za to re-bind chromatin by the slow, high-affinity, chromatin exchange mechanism.

The requirements for H2A.Za and H2A.Zv mobilization during HSV-1 infection remain to be characterized. H2A.Z forms most unstable nucleosomes with H3.3. The mobility of H2A.Za and H2A.Zv during HSV-1 infection was initially analyzed to test whether H2A.Z had similar mobilization as H3.3 during infection. Similar mobilization would suggest that H3.3 and H2A.Z are mobilized by similar mechanisms. However, this was not the case. Mobilization of H2A.Z decreased its rate of fast chromatin exchange, whereas mobilization of H3.3 increased its rate of fast chromatin exchange. Mobilization of H3.3 during HSV-1 infection could be strictly related to HSV-1 transcription. Then the mobilization of H2A.Za and H2A.Zv would suggest that most H2A.Z is not in the unstable nucleosomes associated with the HSV-1 genomes.

The mobilization of H2A.Z was similar to that of H2B. As for H2B, the free pools of H2A.Za and H2A.Zv were increased with a relative tendency for a decrease in the rates of low-affinity chromatin exchange. H2B forms dimers with canonical and variant H2A. The different mobilizations of H2A and H2B during HSV-1 infection suggested that most of the mobilized H2B was not in dimers with canonical H2A, but rather in dimers with H2A variants. The similar mobilizations of H2B and H2A.Z support this model. During HSV-1 infection, cellular transcription is inhibited. The relative decrease in the rates of H2B and H2A.Z fast chromatin exchange is consistent with mobilization of H2A.Z/H2B dimers from cellular chromatin.

The data presented in this chapter demonstrates that the H2A.Z isoforms are mobilized, resulting in increases to their free pools at early

and late times after infection. HSV-1 gene transcription, expression of specific HSV-1 proteins, or cellular responses to them may induce this increase. The similarities in H2B and H2A.Z mobilization during infection suggest that they are mobilized by similar factors, probably as components of the same mobilized nucleosomes. This model remains yet to be tested.

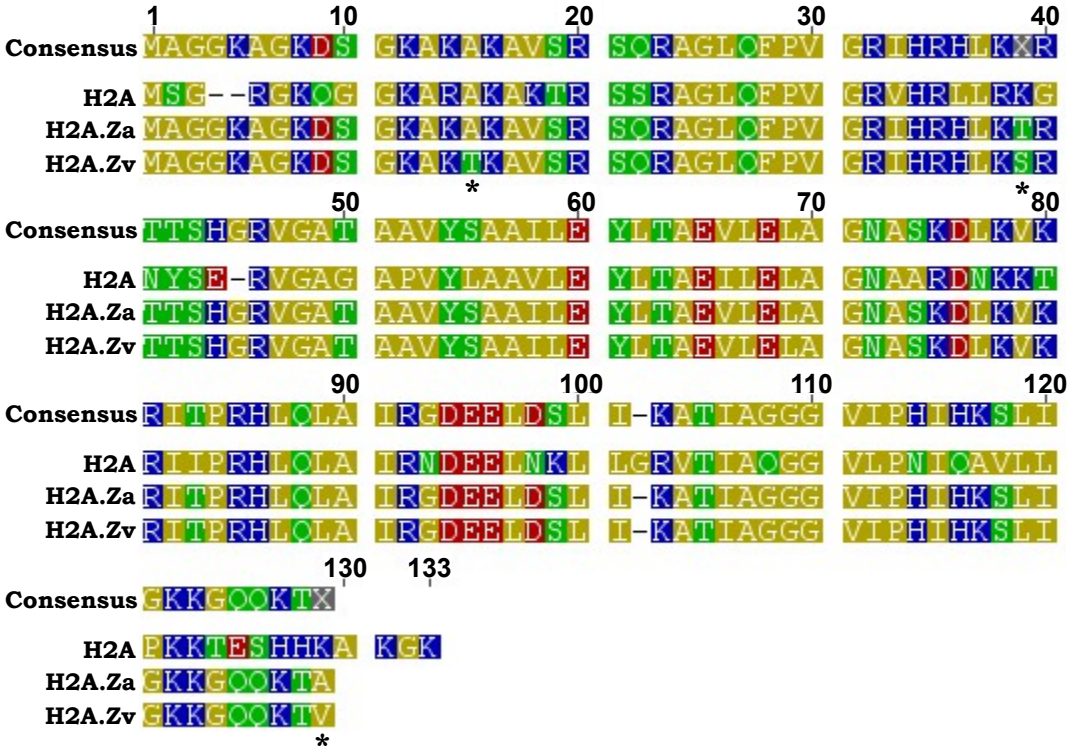

FIGURE 6.1: Sequence Alignment of H2A, H2A.Za and H2A.Zv. Alignment of the amino acid sequences of H2A (BAC28337), H2A.Za (NM_012412), and H2A.Zv (NM_002106). The amino acids are coloured based on polarity. H2A.Za and H2A.Zv share 98% sequence identity and are 61% identical to H2A. *, amino acid differences between H2A.Za and H2A.Zv.

FIGURE 6.2: The pools of free H2A.Za and H2A.Zv are larger than those of H2A in mock-infected cells. A) Bar graphs representing the average level of free H2A.Za and H2A.Zv normalized to the average level of free H2A. Vero (**Vero**) and U2OS (**U2OS**) cells were transfected with plasmids encoding GFP-H2A (**H2A**), GFP-H2A.Za (**H2A.Za**), or GFP-H2A.Zv (**H2A.Zv**). Transfected cells were mock-infected and nuclear mobility of the GFP-H2A variants was evaluated from 4 to 5 hpi (**4**) or 7 to 8 hpi (**7**) by FRAP. Error bars, SEM; n ≥ 19. **B)** Frequency distribution plots of the percentage of free H2A, H2A.Za, and H2A.Zv per individual cell evaluated by FRAP as described for Panel A. Dashed or solid lines, H2A or H2A.Z variant expressing cells, respectively. Mock H2A data replotted from Figure 4.8 for comparison. **C)** Data from Panel A replotted for comparison. *, $P < 0.05$; **, $P < 0.01$.

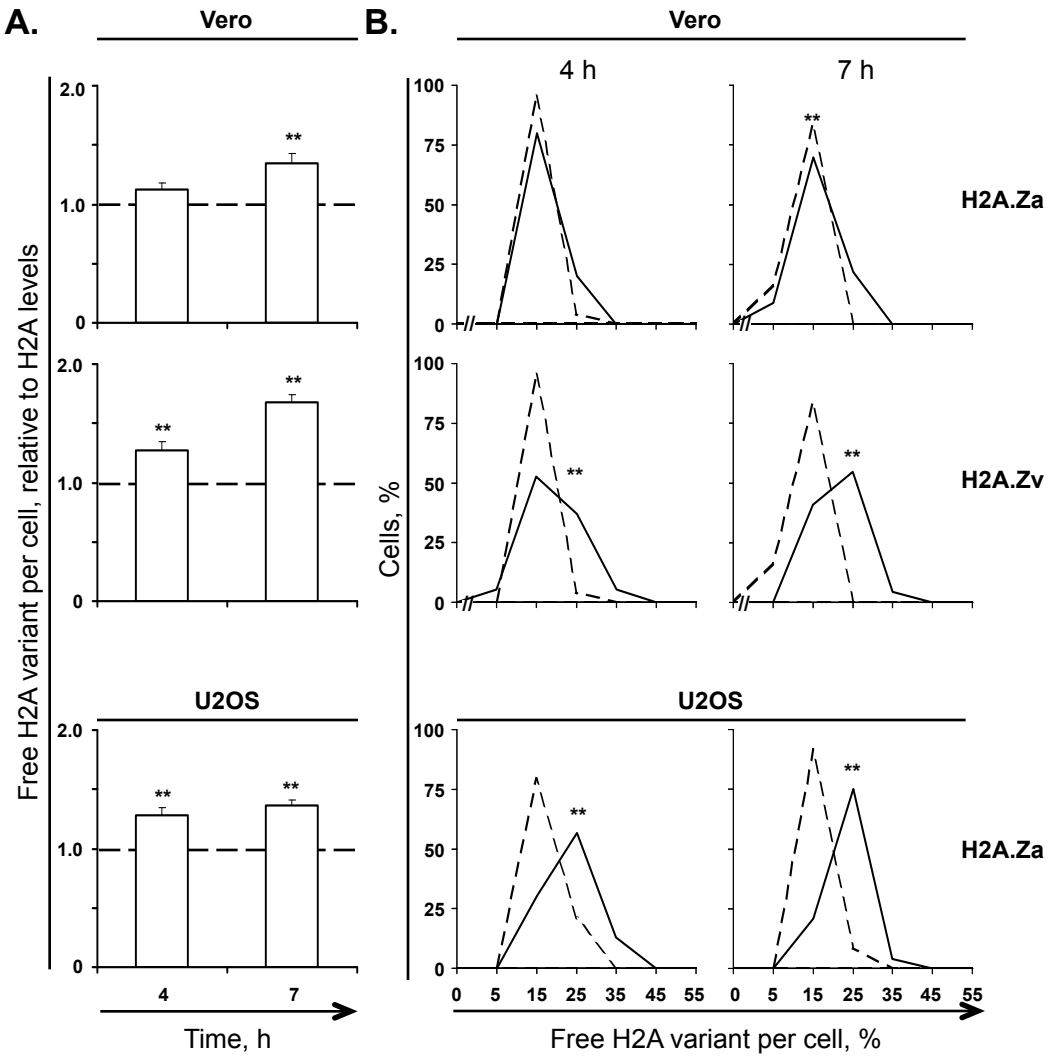
A.
Vero
B.
Vero
4 h
7 h
H2A.Za
H2A.Zv
U2OS
U2OS
H2A.Za
Free H2A variant per cell, relative to H2A levels
Cells, %
Time, h
Free H2A variant per cell, %
**

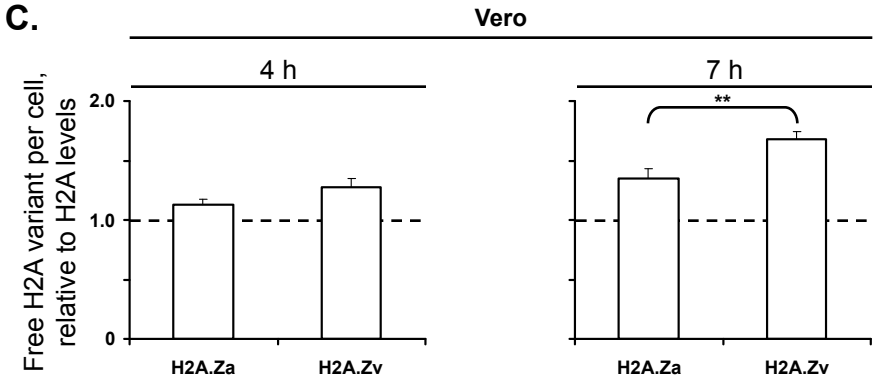
C.
Vero
4 h
7 h
Free H2A variant per cell, relative to H2A levels
H2A.Za
H2A.Zv
H2A.Za
H2A.Zv
**

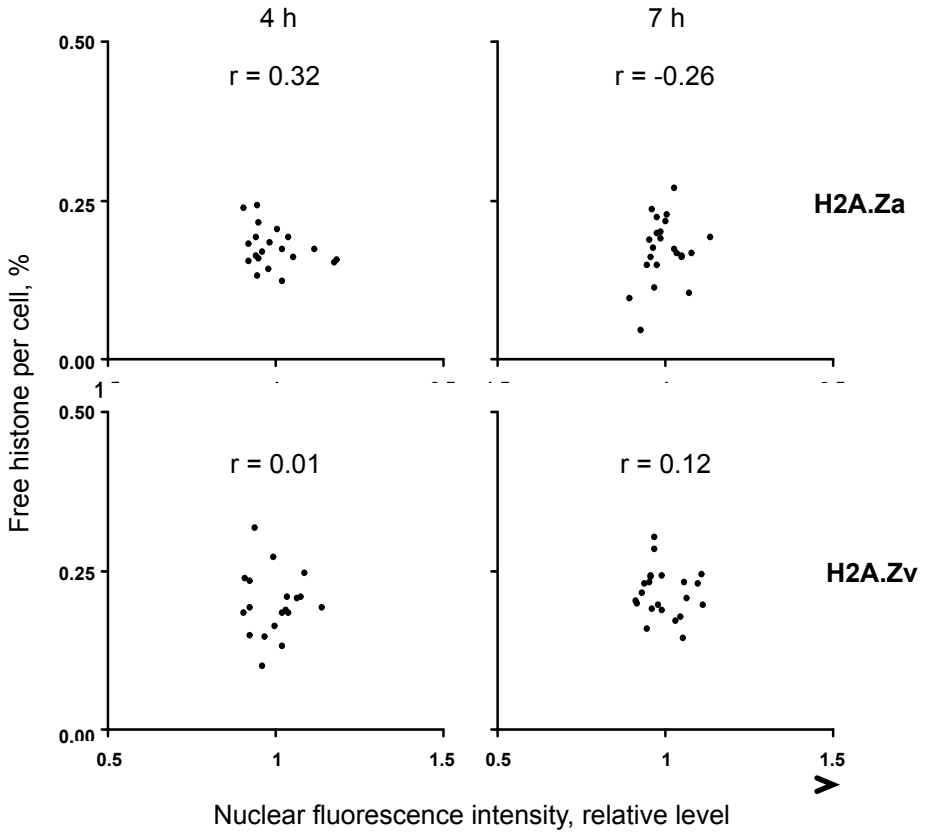

FIGURE 6.3: The percent of free GFP-H2A.Za or GFP-H2A.Zv per cell does not correlate with the level GFP-H2A.Za or GFP-H2A.Zv expression. Dot plots representing the level of GFP-H2A.Za or GFP-H2A.Zv in the free pool of each individual cell against its normalized fluorescence intensity. Vero cells were transfected with plasmids encoding GFP-H2A.Za or GFP-H2A.Zv. Transfected cells were mock-infected and nuclear mobility of GFP-H2A.Za or GFP-H2A.Zv was evaluated from 4 to 5 h (**4 h**) or 7 to 8 h (**7 h**) by FRAP.

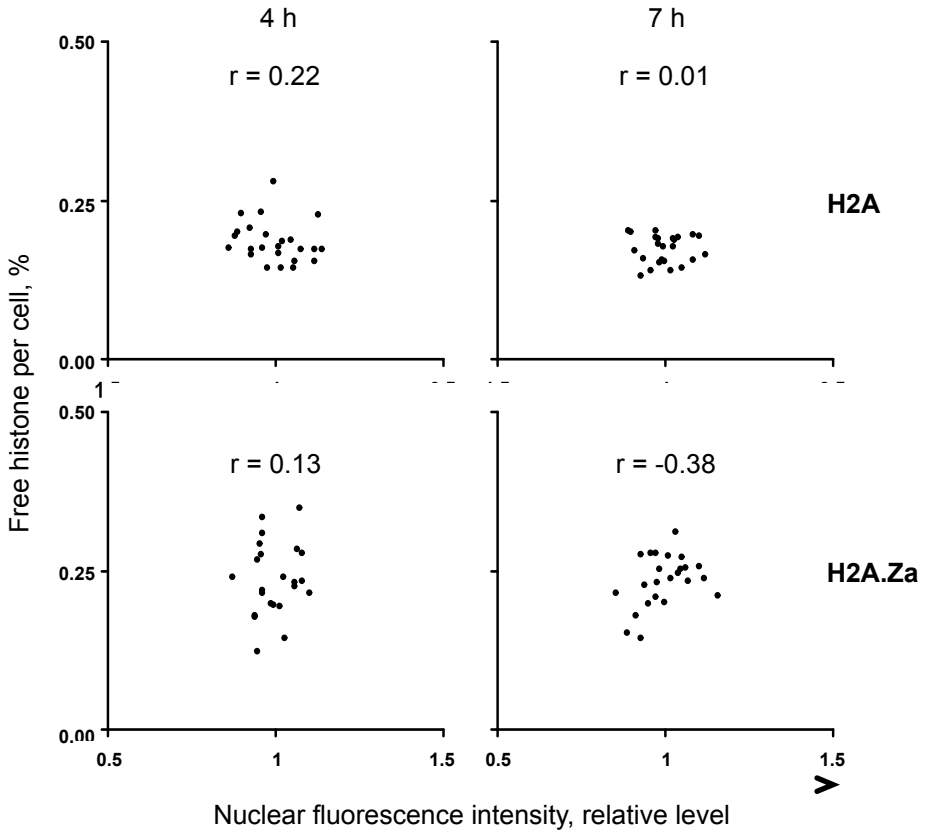

FIGURE 6.4: The percent of free GFP-H2A or GFP-H2A.Za per cell does not correlate with the level GFP-H2A or GFP-H2A.Za expression. Dot plots representing the level of GFP-H2A or GFP-H2A.Za in the free pool of each individual cell against its normalized fluorescence intensity. U2OS cells were transfected with plasmids encoding GFP-H2A or GFP-H2A.Za. Transfected cells were mock-infected and nuclear mobility of GFP-H2A or GFP-H2A.Za was evaluated from 4 to 5 h (**4 h**) or 7 to 8 h (**7 h**) by FRAP.

FIGURE 6.5: H2A.Z variants have increased rates of initial fluorescence recovery relative to H2A in mock-infected cells. A) Bar graphs representing the average rate of initial fluorescence recovery after photobleaching in cells expressing GFP-H2A.Z variants normalized to GFP-H2A expressing cells. Vero (**Vero**) and U2OS (**U2OS**) cells were transfected with plasmids encoding GFP-H2A (**H2A**), GFP-H2A.Za (**H2A.Za**), or GFP-H2A.Zv (**H2A.Zv**). Transfected cells were mock-infected and nuclear mobility of the GFP-H2A variants was evaluated from 4 to 5 hpi (**4**) or 7 to 8 hpi (**7**) by FRAP. Error bars, SEM; n ≥ 19. **B)** Frequency distribution plots of the rate of initial fluorescence recovery after photobleaching per individual cell evaluated by FRAP as described for Panel A. Dashed or solid lines, GFP-H2A or GFP-H2A.Z variant expressing cells, respectively. Mock H2A data replotted from Figure 4.9 for comparison. **C)** Data from Panel A replotted for comparison. *, $P < 0.05$; **, $P < 0.01$.

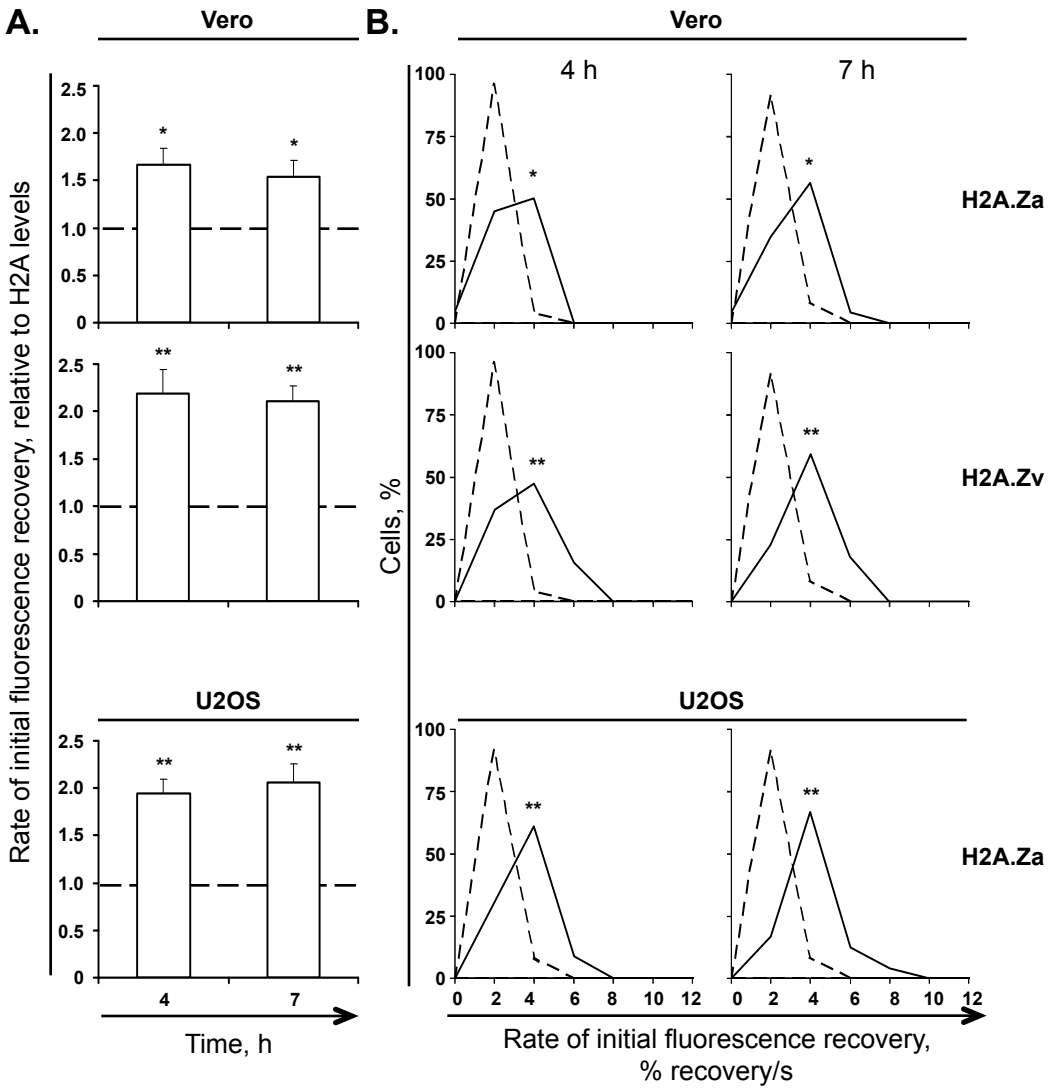
A.
Vero
B.
Vero
4 h
7 h
H2A.Za
H2A.Zv
U2OS
U2OS
H2A.Za
Rate of initial fluorescence recovery, relative to H2A levels
Cells, %
Time, h
Rate of initial fluorescence recovery,
% recovery/s

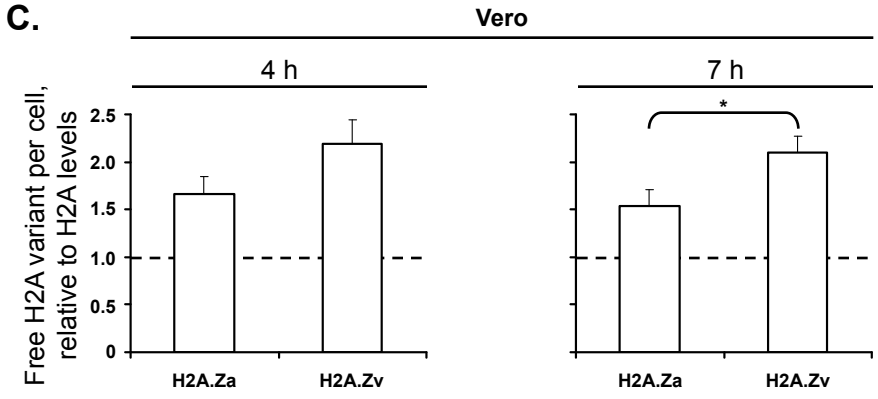
C.
Vero
4 h
7 h
Free H2A variant per cell,
relative to H2A levels
H2A.Za
H2A.Zv
H2A.Za
H2A.Zv

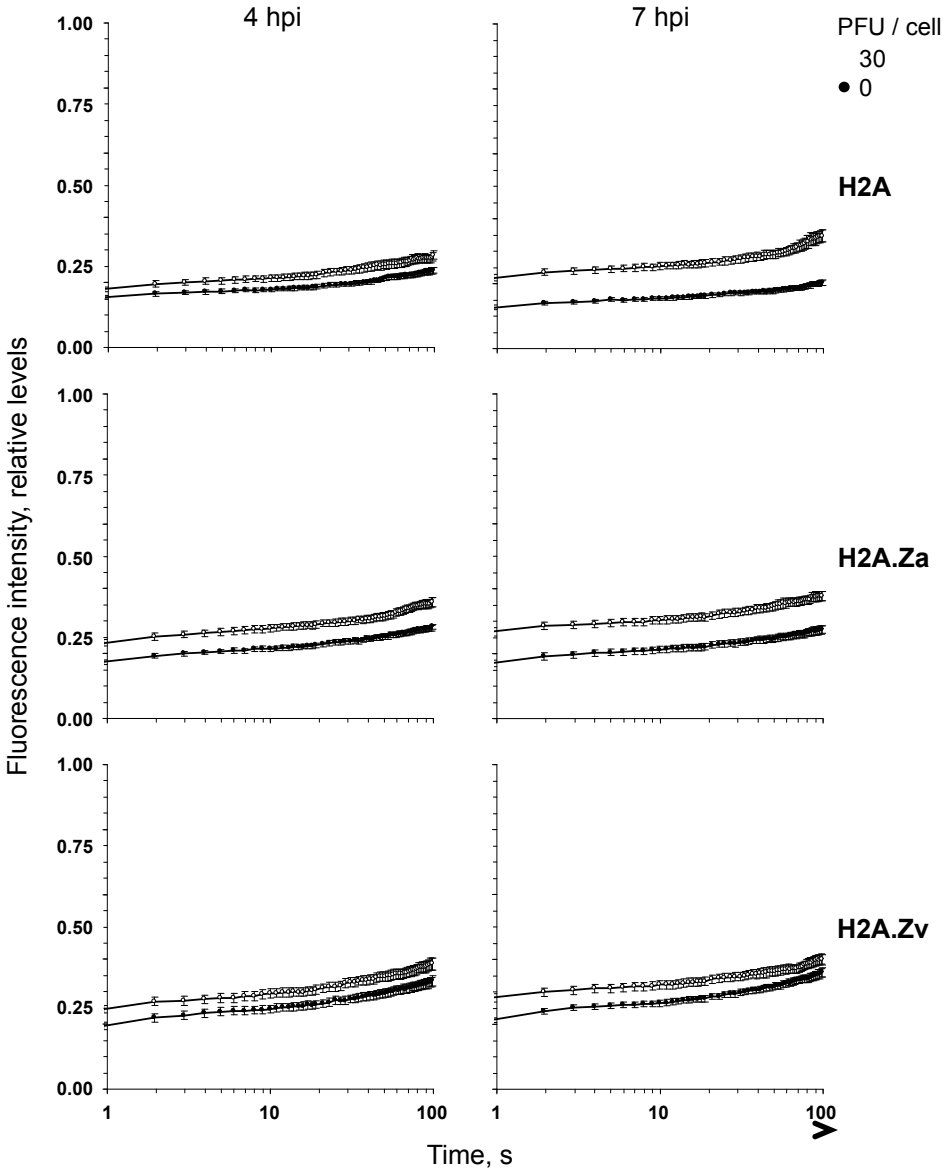

FIGURE 6.6: H2A.Za and H2A.Zv are mobilized during HSV-1 infection of Vero cells. Line graphs representing the normalized fluorescence intensity of the photobleached nuclear region against time. Vero cells were transfected with plasmids expressing GFP-H2A (**H2A**), GFP-H2A.Za (**H2A.Za**), or GFP-H2A.Zv (**H2A.Zv**). Transfected cells were mock-infected (**filled**) or infected with 30 (**open**) PFU per cell of HSV-1 strain KOS. Nuclear mobility of each GFP-core histone was evaluated from 4 to 5 hpi (**4 hpi**) or 7 to 8 hpi (**7 hpi**) by FRAP. Error bars, SEM; n ≥ 19. Time plotted on a semi-logarithmic scale. H2A data from Figure 4.6 replotted for comparison.

FIGURE 6.7: The pools of free H2A.Z variants are differentially increased at later times after HSV-1 infection of Vero cells. A) Bar graphs representing the average percentage of free H2A, H2A.Za, and H2A.Zv in HSV-1 infected cells normalized to mock infected cells. Vero cells were transfected with plasmids encoding GFP-H2A (**H2A**), GFP-H2A.Za (**H2A.Za**), or GFP-H2A.Zv (**H2A.Zv**). Transfected cells were mock-infected or infected with 30 PFU per cell of HSV-1 strain KOS. Nuclear mobility of the GFP-H2A variants was evaluated from 4 to 5 hpi (**4**) or 7 to 8 hpi (**7**) by FRAP. Error bars, SEM; n ≥ 19. H2A data replotted from Figure 4.8 for comparison. **B)** Frequency distribution plots of the percentage of free H2A variant per individual cell evaluated by FRAP as described for Panel A. Dashed or solid lines, mock or HSV-1 infected cells, respectively. **C)** Data from Panel A replotted for comparison. *, $P < 0.05$; **, $P < 0.01$.

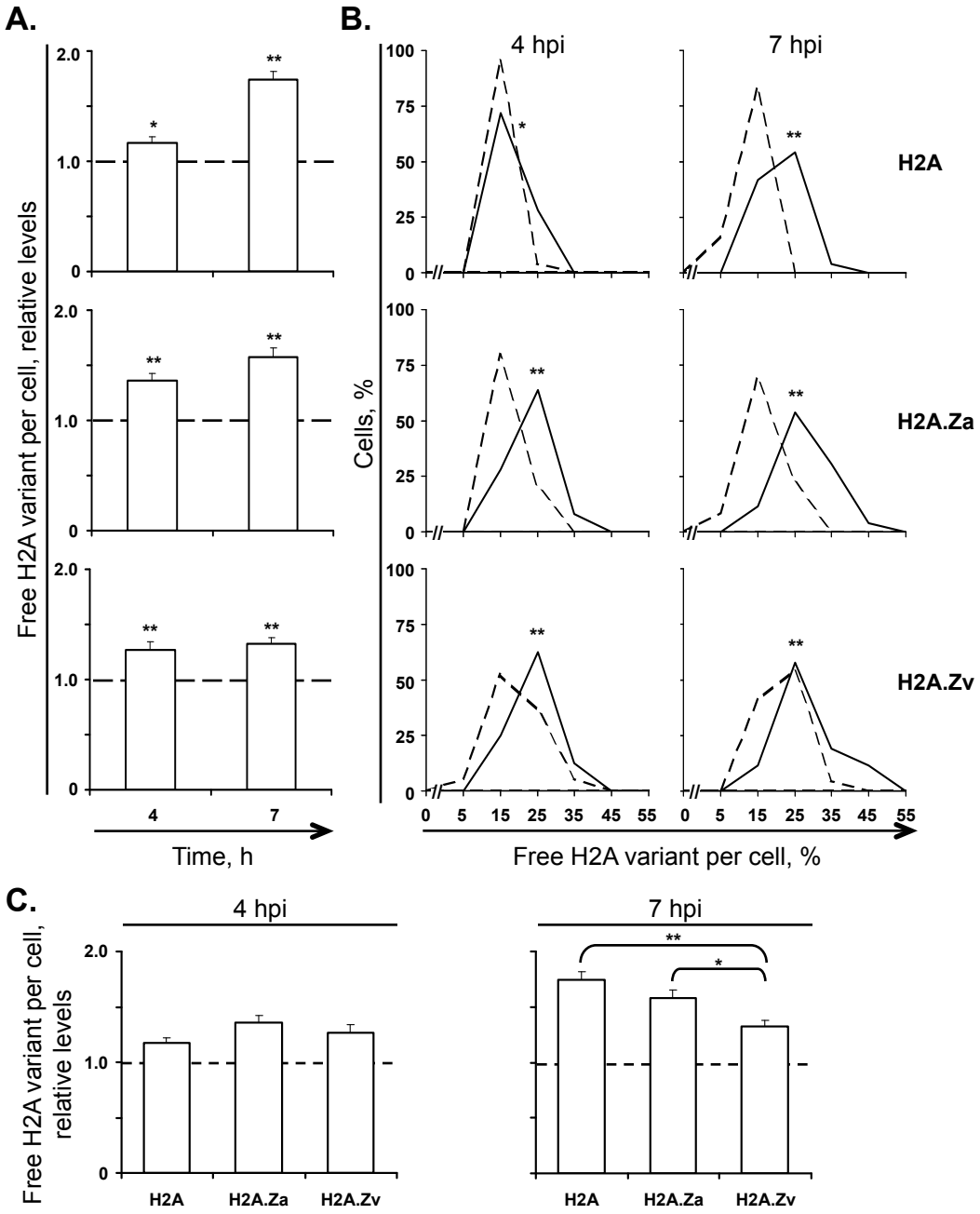
A.
B.
C.
Free H2A variant per cell, relative levels
Time, h
4
7
Cells, %
4 hpi
7 hpi
H2A
H2A.Za
H2A.Zv
Free H2A variant per cell, %
Free H2A variant per cell, relative levels
H2A
H2A.Za
H2A.Zv

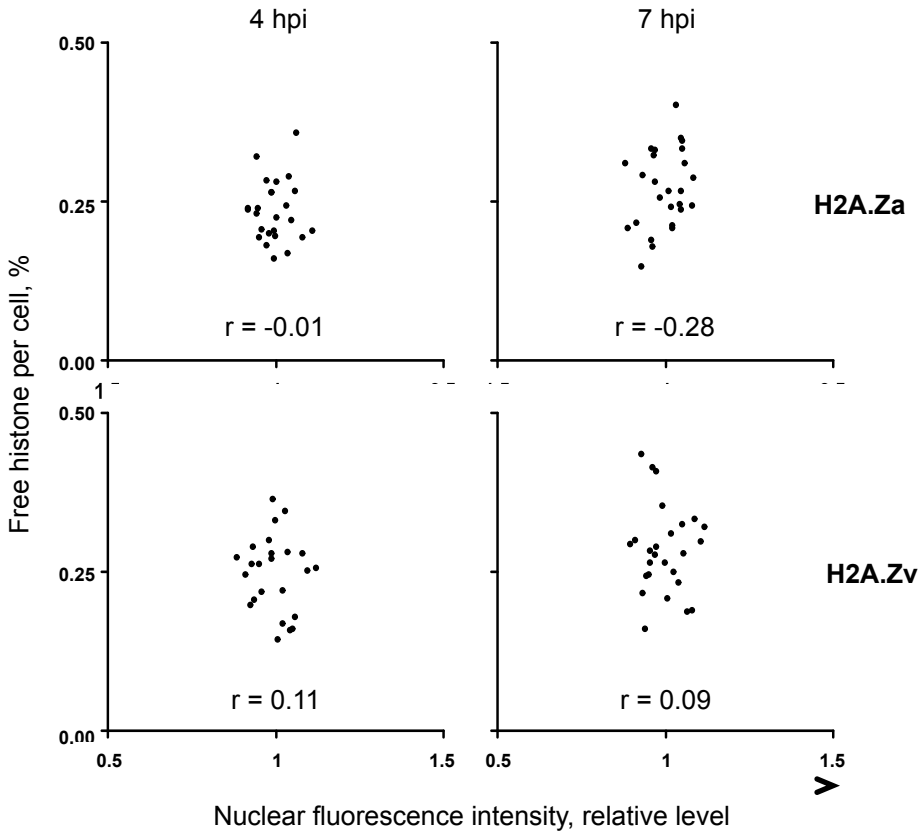

FIGURE 6.8: The percent of free GFP-H2A.Za or GFP-H2A.Zv per cell does not correlate with the level GFP-H2A.Za or GFP-H2A.Zv expression. Dot plots representing the level of GFP-H2A.Za or GFP-H2A.Zv in the free pool of each individual cell against its normalized fluorescence intensity. Vero cells were transfected with plasmids encoding GFP-H2A.Za or GFP-H2A.Zv. Transfected cells were infected with 30 PFU per cell of HSV-1 strain KOS. Nuclear mobility of GFP-H2A.Za or GFP-H2A.Zv was evaluated from 4 to 5 hpi (**4 hpi**) or 7 to 8 hpi (**7 hpi**) by FRAP.

FIGURE 6.9: H2A.Zv has a decreased rate of initial fluorescence recovery at later times after HSV-1 infection. A) Bar graphs representing the average rate of initial fluorescence recovery after photobleaching in HSV-1 infected cells normalized to mock-infected cells. Vero cells were transfected with plasmids encoding GFP-H2A (**H2A**), GFP-H2A.Za (**H2A.Za**), or GFP-H2A.Zv (**H2A.Zv**). Transfected cells were mock-infected or infected with 30 PFU per cell of HSV-1 strain KOS. Nuclear mobility of the GFP-H2A variants was evaluated from 4 to 5 hpi (**4**) or 7 to 8 hpi (**7**) by FRAP. Error bars, SEM; n ≥ 19. H2A data replotted from Figure 4.9 for comparison. **B)** Frequency distribution plots of the rate of initial fluorescence recovery after photobleaching per individual cell evaluated by FRAP as described for Panel A. Dashed or solid lines, mock or HSV-1 infected cells, respectively. **C)** Data from Panel A replotted for comparison. *, $P < 0.05$, **, $P < 0.01$.

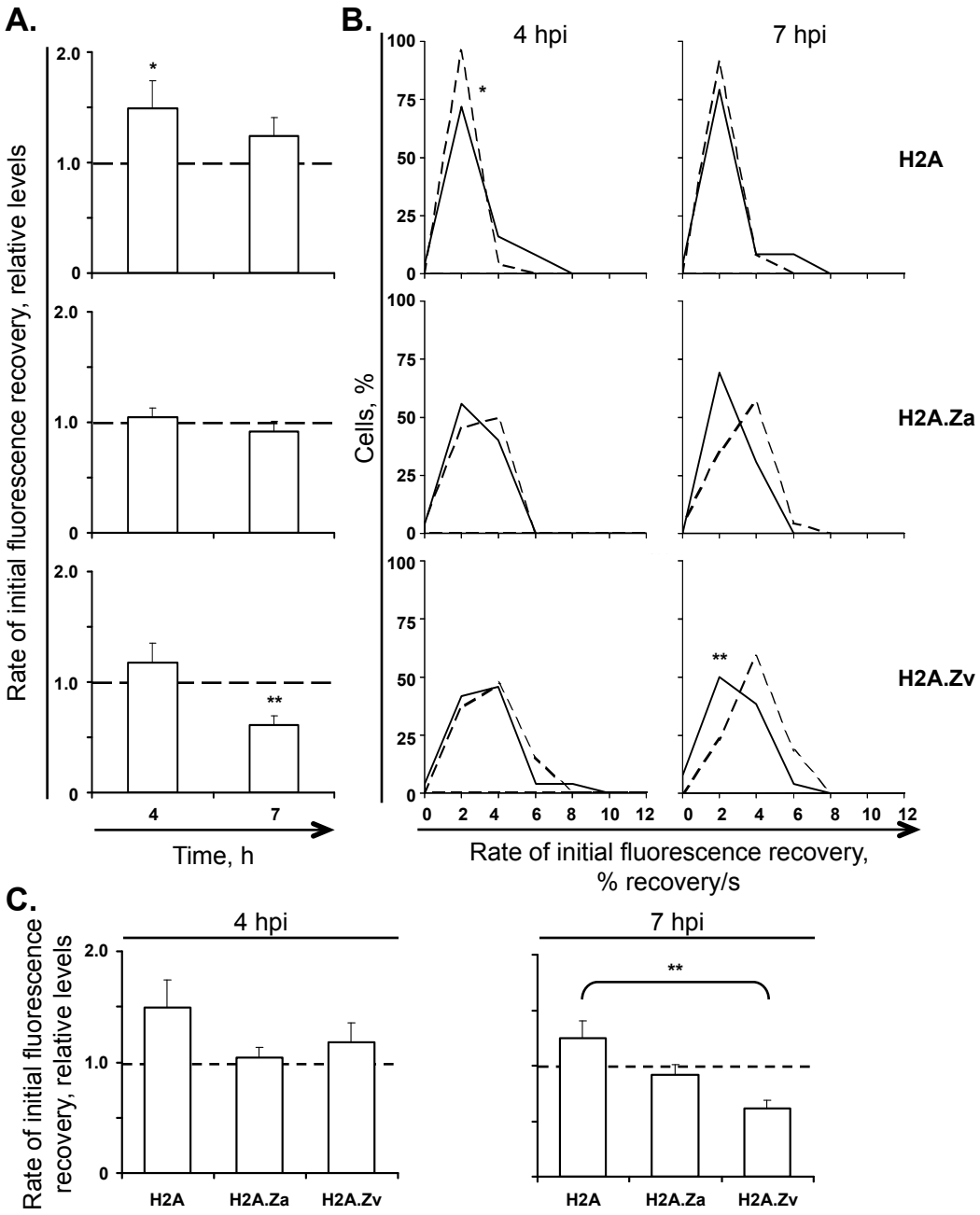
A.
B.
C.
4 hpi
7 hpi
H2A
H2A.Za
H2A.Zv
Rate of initial fluorescence recovery, relative levels
Cells, %
Time, h
Rate of initial fluorescence recovery, % recovery/s
2.0
1.0
0
100
75
50
25
4
7
0 2 4 6 8 10 12
*
**

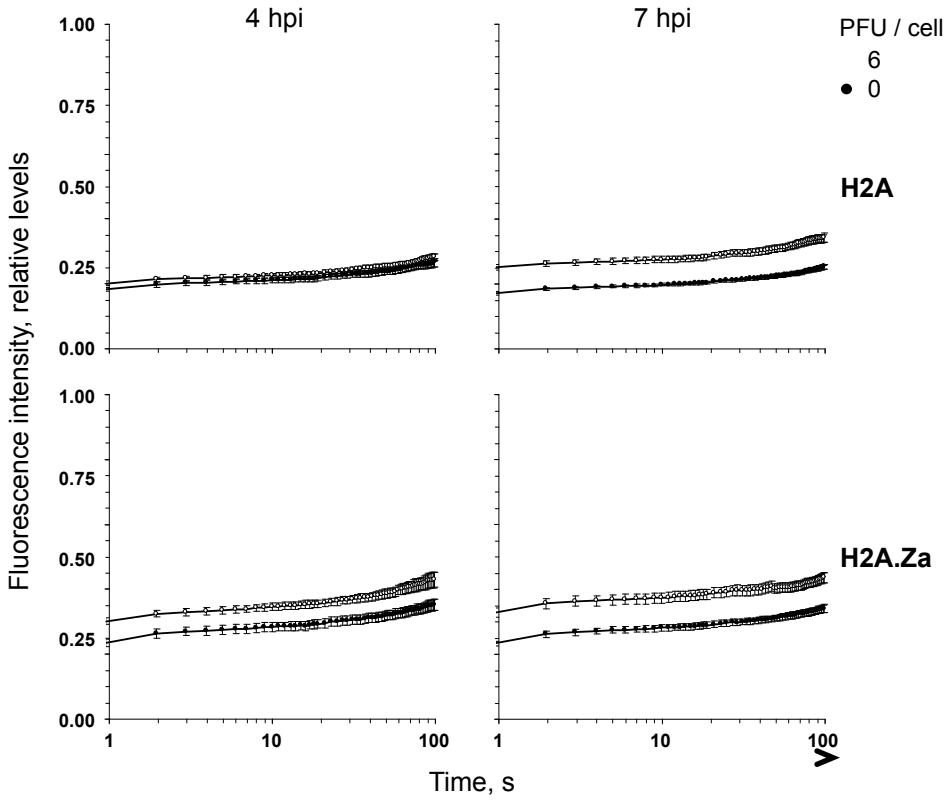

FIGURE 6.10: H2A.Za is mobilized during HSV-1 infection of U2OS cells. Line graphs representing the normalized fluorescence intensity of the photobleached nuclear region against time. U2OS cells were transfected with plasmids expressing GFP-H2A (**H2A**) or GFP-H2A.Za (**H2A.Za**). Transfected cells were mock-infected (**filled**) or infected with 6 (**open**) PFU per cell of HSV-1 strain KOS. Nuclear mobility of each GFP-core histone was evaluated from 4 to 5 hpi (**4 hpi**) or 7 to 8 hpi (**7 hpi**) by FRAP. Error bars, SEM; n ≥ 23. Time plotted on a semi-logarithmic scale.

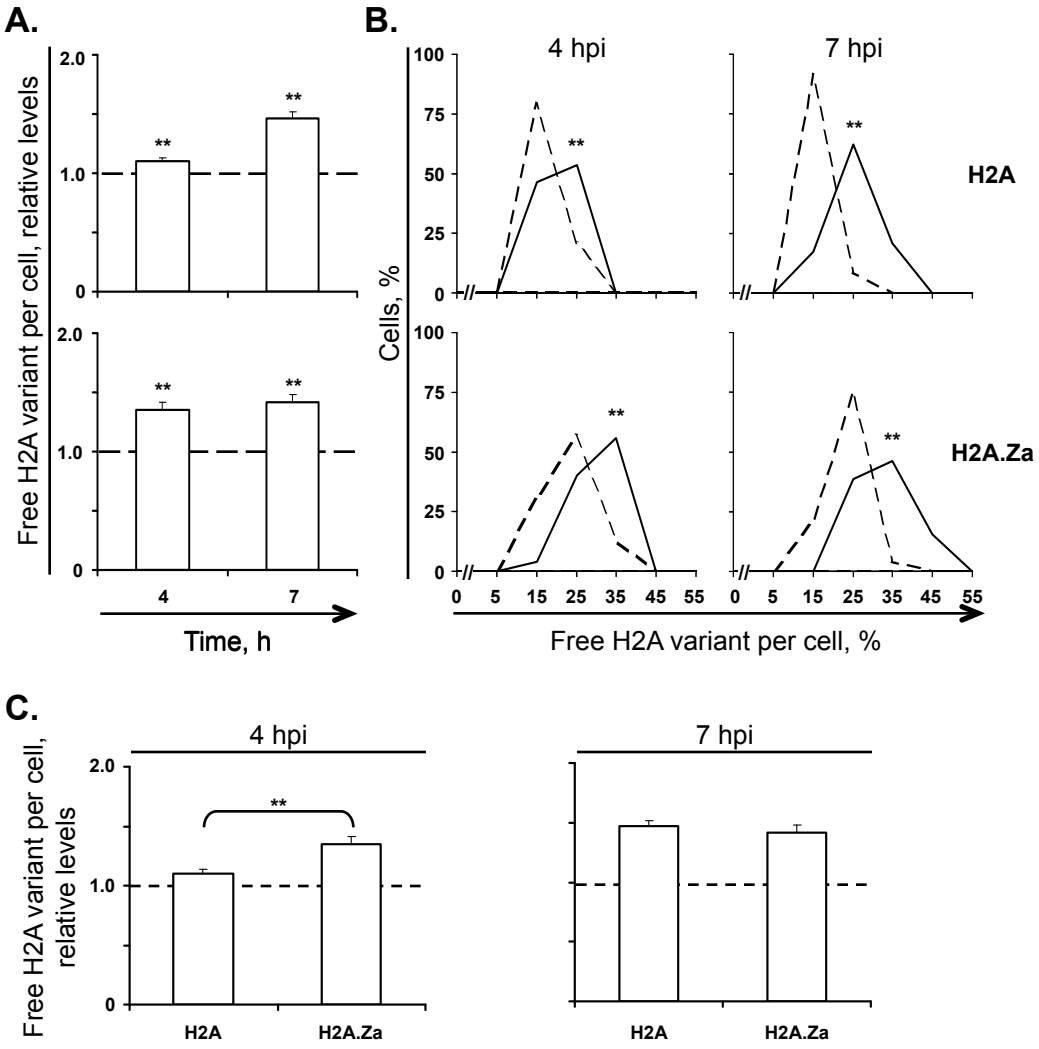

FIGURE 6.11: The pools of free H2A and H2A.Za are increased during HSV-1 infection of U2OS cells. A) Bar graphs representing the average percentage of free H2A and H2A.Za in HSV-1 infected cells normalized to mock infected cells. U2OS cells were transfected with plasmids encoding GFP-H2A (**H2A**) or GFP-H2A.Za (**H2A.Za**). Transfected cells were mock-infected or infected with 6 PFU per cell of HSV-1 strain KOS. Nuclear mobility of the GFP-H2A variants was evaluated from 4 to 5 hpi (**4**) or 7 to 8 hpi (**7**) by FRAP. Error bars, SEM; n ≥ 23). **B)** Frequency distribution plots of the percentage of free H2A variant per individual cell evaluated by FRAP as described for Panel A. Dashed or solid lines, mock or HSV-1 infected cells, respectively. **C)** Data from Panel A replotted for comparison. **, P <0.01.

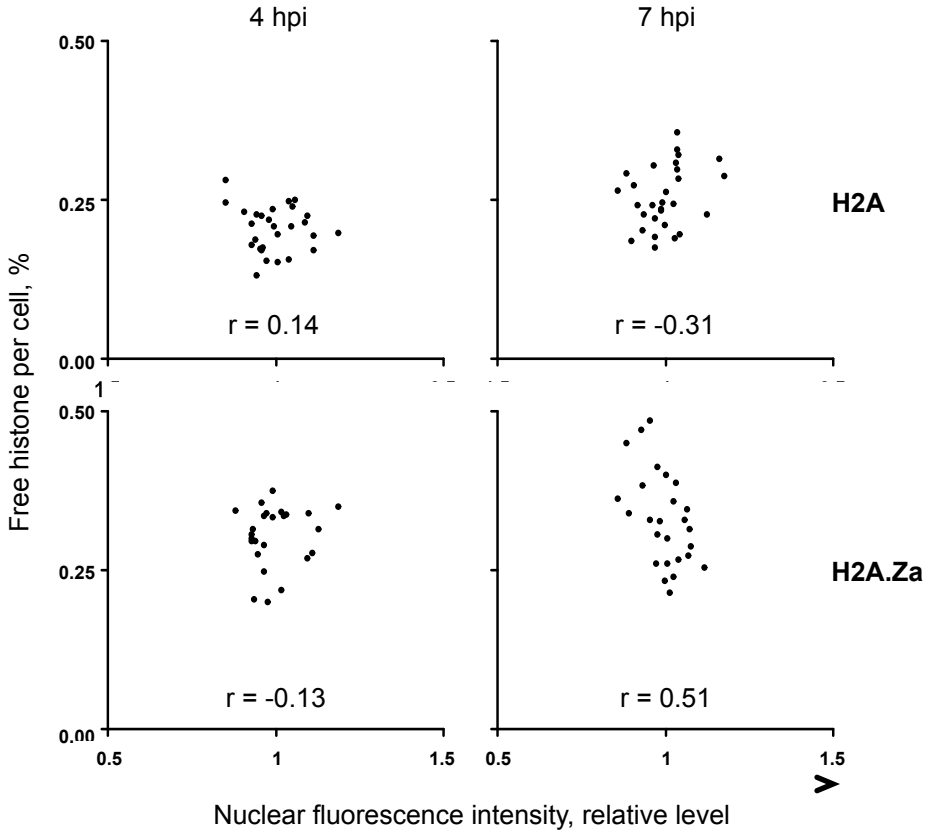

FIGURE 6.12: The percent of free GFP-H2A or GFP-H2A.Za per cell does not correlate with the level of GFP-H2A or GFP-H2A.Za expression in transiently transfected U2OS cells. Dot plots representing the level of GFP-H2A or GFP-H2A.Za in the free pool of each individual cell against its normalized fluorescence intensity. U2OS cells were transfected with plasmids encoding GFP-H2A or GFP-H2A.Za. Transfected cells were infected with 6 PFU per cell of HSV-1 strain KOS. Nuclear mobility of GFP-H2A or GFP-H2A.Za was evaluated from 4 to 5 hpi (**4 hpi**) or 7 to 8 hpi (**7 hpi**) by FRAP.

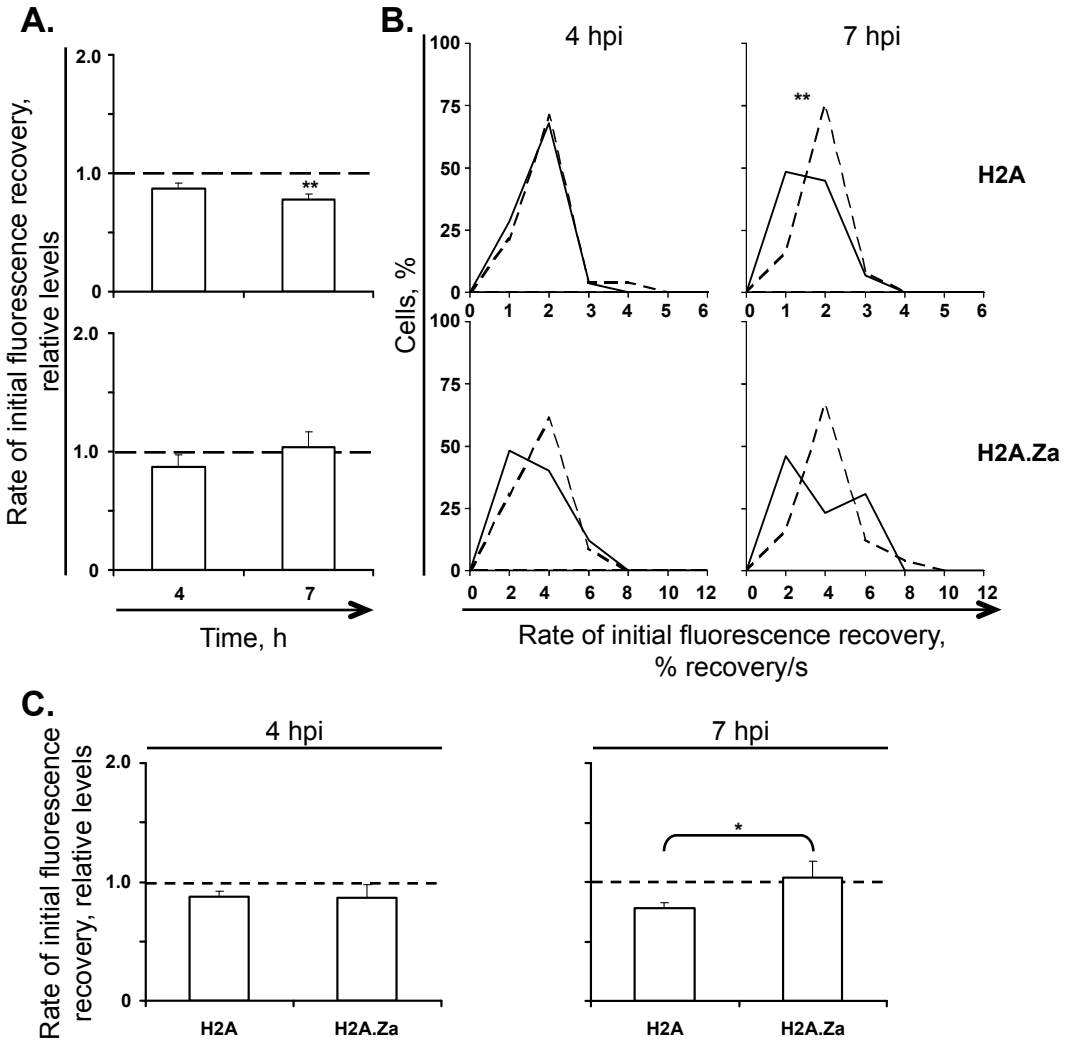

FIGURE 6.13: The rate of initial fluorescence recovery for H2A, but not H2A.Za,has a tendency to decrease during HSV-1 infection of U2OS cells. **A)** Bar graphs representing the average rate of initial fluorescence recovery after photobleaching in HSV-1 infected cells normalized to mock-infected cells. U2OS cells were transfected with plasmids encoding GFP-H2A (**H2A**), or GFP-H2A.Za (**H2A.Za**). Transfected cells were mock-infected or infected with 6 PFU per cell of HSV-1 strain KOS. Nuclear mobility of the GFP-H2A variants was evaluated from 4 to 5 hpi (**4**) or 7 to 8 hpi (**7**) by FRAP. Error bars, SEM; n ≥ 23. **B)** Frequency distribution plots of the rate of initial fluorescence recovery after photobleaching per individual cell evaluated by FRAP as described for Panel A. Dashed or solid lines, mock or HSV-1 infected cells, respectively. **C)** Data from Panel A replotted for comparison. **, P < 0.01.

Cell type	Time, h	Histone Variant	Relative Free histone (avg ± SEM)	% Cells with large increase in free[a]
Vero	4	H2A	1.00 ± 0.04	13
		H2A.Za	1.13 ± 0.05	30
		H2A.Zv	1.27 ± 0.08	58
	7	H2A	1.00 ± 0.05	17
		H2A.Za	1.35 ± 0.08	70
		H2A.Zv	1.68 ± 0.06	91
U2OS	4	H2A	1.00 ± 0.04	17
		H2A.Za	1.28 ± 0.06	61
	7	H2A	1.00 ± 0.03	17
		H2A.Za	1.36 ± 0.05	88

TABLE 6.1: Levels of free H2A.Za and H2A.Zv relative to H2A in mock-infected cells Vero or U2OS.

[a] Percentage of cells in which the level of free histone was >1 SD above the average level of free H2A in mock-infected cells.

Cell type	Time, h	Histone Variant	Relative rate of initial fluorescence recovery, %,s (avg ± SEM)	% Cells with large increase [a] in fast chromatin exchange
Vero	4	H2A	1.00 ± 0.08	17
		H2A.Za	1.67 ± 0.18	80
		H2A.Zv	2.19 ± 0.26	68
	7	H2A	1.00 ± 0.09	13
		H2A.Za	1.53 ± 0.18	61
		H2A.Zv	2.10 ± 0.16	77
U2OS	4	H2A	1.00 ± 0.09	8
		H2A.Za	1.95 ± 0.15	70
	7	H2A	1.00 ± 0.06	17
		H2A.Za	2.06 ± 0.19	92

TABLE 6.2: Rate of initial fluorescence recovery of H2A.Za and H2A.Zv relative to H2A in mock-infected cells Vero or U2OS.

[a] Percentage of cells in which the rate of initial fluorescence recovery was >1 SD above the average rate of initial fluorescence recovery of H2A in mock-infected cells.

Cell Type	Histone Variant	Virus Strain	PFU/ cell	4hpi Free histone (avg ± SEM) Absolute	4hpi Free histone (avg ± SEM) Relative	4hpi % Cells with large increase in free[a]	7hpi Free histone (avg ± SEM) Absolute	7hpi Free histone (avg ± SEM) Relative	7hpi % Cells with large increase in free[a]
Vero	H2A	-	-	0.15 ± 0.01	1.00 ± 0.04	17	0.13 ± 0.01	1.00 ± 0.05	17
		KOS	30	0.18 ± 0.01	1.17 ± 0.05	40	0.22 ± 0.01	1.74 ± 0.07	96
	H2A.Za	-	-	0.17 ± 0.01	1.00 ± 0.04	20	0.17 ± 0.01	1.00 ± 0.06	17
		KOS	30	0.23 ± 0.01	1.36 ± 0.06	68	0.27 ± 0.01	1.58 ± 0.08	73
	H2A.Zv	-	-	0.20 ± 0.01	1.00 ± 0.06	16	0.21 ± 0.01	1.00 ± 0.04	14
		KOS	30	0.25 ± 0.01	1.27 ± 0.07	50	0.28 ± 0.01	1.32 ± 0.06	65
U2OS	H2A	-	-	0.18 ± 0.01	1.00 ± 0.03	17	0.17 ± 0.01	1.00 ± 0.03	21
		KOS	30	0.20 ± 0.01	1.10 ± 0.03	39	0.25 ± 0.01	1.47 ± 0.05	83
	H2A.Za	-	-	0.23 ± 0.01	1.00 ± 0.04	17	0.23 ± 0.01	1.00 ± 0.03	13
		KOS	30	0.30 ± 0.01	1.35 ± 0.06	68	0.33 ± 0.01	1.42 ± 0.06	81

TABLE 6.3: Level of free H2A variants in Vero and U2OS cells infected with HSV-1 strain KOS.

[a] Percentage of cells in which the level of free histone was >1 SD above the average level in mock-infected cells.

				4hpi				7hpi			
				Rate of initial fluorescence recovery, %/s (avg ± SEM)		Fast chromatin exchange, % of cells		Rate of initial fuorescence recovery, %/s (avg ± SEM)		Fast chromatin exchange, % of cells	
Cell Type	Histone Variant	Virus Strain	PFU/ cell	Absolute	Relative	Increased [a]	Decreased [b]	Absolute	Relative	Increased [a]	Decreased [b]
Vero	H2A	-	-	1.12 ± 0.09	1.00 ± 0.08	17	8	1.34 ± 0.12	1.00 ± 0.08	8	13
		KOS	30	1.65 ± 0.27	1.49 ± 0.25	28	12	1.09 ± 0.22	1.25 ± 0.16	33	8
	H2A.Za	-	-	1.87 ± 0.20	1.00 ± 0.12	10	15	2.06 ± 0.24	1.00 ± 0.12	17	13
		KOS	30	1.97 ± 0.17	1.04 ± 0.09	12	8	1.81 ± 0.14	0.92 ± 0.09	12	4
	H2A.Zv	-	-	2.45 ± 0.29	1.00 ± 0.10	16	16	2.82 ± 0.22	1.00 ± 0.08	18	14
		KOS	30	2.40 ± 0.30	1.18 ± 0.18	33	29	1.72 ± 0.22	0.61 ± 0.08	4	54
U2OS	H2A	-	-	1.44 ± 0.13	1.00 ± 0.08	17	13	1.39 ± 0.08	1.00 ± 0.06	13	13
		KOS	30	1.24 ± 0.01	0.87 ± 0.05	4	11	1.08 ± 0.07	0.78 ± 0.05	7	41
	H2A.Za	-	-	2.81 ± 0.22	1.00 ± 0.07	22	17	2.85 ± 0.27	1.00 ± 0.09	8	4
		KOS	30	2.29 ± 0.26	0.87 ± 0.11	28	40	2.75 ± 0.30	1.04 ± 0.14	31	35

TABLE 6.4: Rate of initial fluorescence recovery of H2A variants in Vero and U2OS cells infected with HSV-1 strain KOS.

[a] Percentage of cells in which the rate of initial fluorescence recovery was >1 SD above the average rate of initial fluorescence recovery in mock-infected cells.

[b] Percentage of cells in which the rate of initial fluorescence recovery was >1 SD lower than the average rate of initial fluorescence recovery in mock-infected cells.

CHAPTER 7: THE MOBILIZATION OF H1.2, AND LARGE INCREASES IN ITS FREE POOL, REQUIRE FUNCTIONAL ICP4, NUCLEAR ICP0, OR E PROTEINS.

This Chapter contains unpublished data.

ABSTRACT

The results discussed in Chapter 3 indicate that HSV-1 gene transcription or expression of specific HSV-1 IE or E proteins is required to enhance H1.2 mobilization and to increase its levels in the free pool. I therefore evaluated H1.2 mobility during infection with the mutant HSV-1 strain n12. This strain expresses a truncated form of ICP4, which does not activate expression of early proteins or repress that of IE ones. During n12 infection IE proteins (with the exception of ICP4) are overexpressed, ICP0 is mislocalized to the cytoplasm, and E proteins are not expressed. Under such conditions, the pool of free H1.2 was increased by a basal degree. However, H1.2 mobility was surprisingly decreased. Truncated ICP4, cytoplasmic ICP0, or overexpression of ICP22, ICP27, or less likely ICP47 therefore inhibits the chromatin exchange of H1.2. Inhibition of H1.2 mobilization during n12 infections also demonstrates that HSV-1 IE gene transcription is not required for H1.2 mobilization nor is H1.2 mobilization required for HSV-1 IE gene transcription.

7.1 INTRODUCTION.

Basal mobilization of H1.2 required only nuclear, transcription competent, HSV-1 genomes. In contrast, enhanced H1.2 mobilization, and increases in the level of free H1.2, required HSV-1 transcription or expression of IE or E proteins. VP16, ICP0, HSV-1 DNA replication, or strictly L proteins were not required to further mobilize H1.2 or to increase the pool of free H1.2. Thus, HSV-1 transcription, an HSV-1 IE protein (other than ICP0), or an HSV-1 E protein is required to enhance H1.2 mobilization and increase the pool of free H1.2. Alternatively, further mobilization of H1.2 and the increase in the free pool of H1.2 may be the result of HSV-1 gene transcription.

I first analyzed whether ICP4 was required to enhance H1.2 mobility, or to increase the level of H1.2 available in the free pool. ICP4 is an essential IE protein required to transactivate E gene expression. To test the potential requirement for ICP4 to enhance H1.2 mobilization and increase the pool of free H1.2, I evaluated H1.2 mobility during infections with the HSV-1 ICP4 mutant strain n12. This strain expresses a truncated form of ICP4 (stop codon at codon 251) lacking the transcription transactivation domain and a nuclear localization signal (DeLuca & Schaffer, 1988). E proteins are therefore not expressed. Moreover, this truncated form of ICP4 is unable to repress IE protein expression. Consequently, IE genes are transcribed and IE proteins are expressed to high levels during n12 infections. The high levels of ICP27 expression during n12 infection result in mislocalization of ICP0 to the cytoplasm (Zhu, Cai, & Schaffer, 1994; Zhu, DeLuca, & Schaffer, 1996).

7.2 RESULTS.

7.2.1 H1.2 chromatin exchange is decreased in the absence of functional ICP4 and E proteins.

During HSV-1 infection, the rate of linker histone H1.2 chromatin exchange was increased. The increase in chromatin exchange resulted in a decrease in T_{50}, the time required for 50% of the original fluorescence to be recovered, as well as the T_{90}, the time required for 90% or the original fluorescence to be recovered (Figure 3.4). Thus, the low- and high- affinity chromatin binding of H1.2, as analyzed by the T_{50} and the T_{90}, respectively, were destabilized during HSV-1 infection. Surprisingly, H1.2 mobility was decreased at 4 or 7hpi during infection of Vero cells with 30 PFU per cell of n12 (Figure 7.1 Panel A). The decreased mobility resulted in an increase in H1.2 T_{50} to 116 ± 5% or 123 ± 6% at 4 or 7h, respectively (19.2 ± 1s or 19.3 ± 1s, respectively) ($P<0.05$ or $P<0.01$ at 4 or 7hpi, respectively, Student's T-test; 1-tail) (Figure 7.2 Vero n12, Table 7.1).

The increase in H1.2 T_{50} occurred throughout the population of n12-infected cells. At early and late times after infection, 26 and 45% of cells, respectively, had an increase in H1.2 T_{50} that was larger than one SD (Table 7.1), in comparison to the expected 16% for a normal population distribution. The increase in H1.2 T_{50} during n12 infections contrasts to KOS infections, in which H1.2 T_{50} was decreased (Figure 7.1 Panel A KOS) to 62 ± 5% or 42 ± 3% at 4 or 7h after infection ($P<0.01$, Student's T-test; 1-tail) (Figure 7.2 Vero KOS, Table 3.3). Thus,

expression of HSV-1 IE proteins, other than ICP4 or nuclear ICP0, decreases the rate of H1.2 low-affinity chromatin exchange, increasing its T_{50}. These data suggest that the transactivation activity of ICP4, nuclear ICP0, or E protein expression, is required to increase the rate of low-affinity chromatin exchange of H1.2. Furthermore, transcription of HSV-1 genomes is not sufficient to increase the rate of H1.2 low-affinity chromatin exchange, neither is an increase in the rate of H1.2 low-affinity chromatin exchange required for HSV-1 IE gene transcription.

The rate of low-affinity H1.2 chromatin exchange was decreased during n12 infection. I next analyzed whether high-affinity H1.2 chromatin binding was affected. As with H1.2 T_{50}, the T_{90} was increased. At 4h after infection with 30 PFU per cell of HSV-1 strain n12, H1.2 T_{90} was increased to 123 ± 6% (142.9 ± 5.9s) ($P<0.01$, Student's T-test; 1-tail) (Table 7.1). At 7h, H1.2 T_{90} still tended to be increased, to 116 ± 5% (131.9 ± 5.1s). However, statistical significance was not achieved ($P>0.05$, Student's T-test; 1-tail) (Table 7.1). H1.2 T_{90} was increased in a larger population of cells than would be expected from a normal frequency distribution, however, approximately 40% versus 16%, respectively (Table 7.1). The tendency to increase H1.2 T_{90} during n12 infections was also in contrast to KOS infections, in which H1.2 T_{90} was decreased to 63 ± 6% or 58 ± 5% at 4 or 7h after infection with 30 PFU per cell ($P<0.01$, Student's T-test; 1-tail) (Table 3.3). Thus, expression of HSV-1 IE proteins, in the absence of ICP4 transactivation activity, nuclear ICP0, and E proteins, decreases the rate of high-affinity chromatin exchange of H1.2, increasing its T_{90}. HSV-1 E proteins,

nuclear ICP0, or functional ICP4 are therefore required to increase the rate of high-affinity chromatin exchange of H1.2. Taken together, these data demonstrate that the affinity of H1.2 for chromatin is increased in infected cells when functional ICP4 and E proteins are not expressed, or ICP0 is mislocalized to the cytoplasm. Furthermore, these data demonstrate that HSV-1 gene transcription is not sufficient to mobilize H1.2, nor is H1.2 mobilization required for HSV-1 IE gene transcription.

The decrease in the rates of H1.2 fast and slow chromatin exchange during n12 infections of Vero cells was unexpected. During previous infections with wild-type or mutant HSV-1 strains, H1.2 low- and high-affinity chromatin exchange were either increased or unchanged from that of mock-infected cells, but never decreased. If functional ICP4 or E proteins were required to increase H1.2 chromatin exchange, then the chromatin exchange of H1.2 would be expected to be unchanged in cells infected with such mutants.

The decrease in H1.2 mobility during n12 infection may be due to the mutation in ICP4 or may be due to secondary mutations in the n12 genome. Therefore, to test whether such mobilization is indeed due to ICP4 mutation, I evaluated H1.2 mobility during n12 infection of n-33 cells. n-33 cells are derived from Vero cells and stably express full length HSV-2 ICP4 from a VP16 inducible promoter. Expression of functional HSV-2 ICP4 from the cellular genome complements the replication of ICP4 mutant strains, such as n12. During n12 infection of n-33 cells, H1.2 mobilization was restored. At 4 or 7h after infection of n-33 cells with 30 PFU per cell of n12, H1.2 T_{50} was decreased to 67 ± 5% or 59 ±

5%, respectively (12.7 ± 1.0 or 11.7 ± 1.1s, respectively) (P<0.01, Student's T-test; 1-tail) (Figure 7.2 n-33, Table 7.2). Greater that 60% of n-33 cells had a large decrease in H1.2 T_{50} at either time after infection (Table 7.2). Thus, H1.2 T_{50} was decreased throughout the population of infected cells. The decrease in H1.2 T_{50} was to a similar degree as that during wild-type KOS infections of n-33 cells (P<0.01, Tukey's HSD). H1.2 T_{50} was decreased to 72 ± 5% or 54 ± 5% at 4 or 7h after infection with 30 PFU per cell of KOS (9.4 ± 0.7 or 7.5 ± 0.6s, respectively) (P<0.01, Student's T-test; 1-tail) (Figure 7.2 n-33, Table 7.2). As during n12 infections, H1.2 T_{50} was decreased by a large degree in more than 60% of cells at any time after infection (Table 7.2). These data show that ICP4 transactivation activity, nuclear ICP0, or E proteins are required to increase the rate of low-affinity H1.2 chromatin exchange.

As with H1.2 low-affinity chromatin exchange, the rate of H1.2 high-affinity chromatin exchange was also increased during n12 infections (resulting in decreased T_{90}). H1.2 T_{90} was decreased to 73 ± 5% or 82 ± 7% at 4 or 7h after infection of n-33 cells with 30 PFU per cell of n12 (P<0.01, Student's T-test; 1-tail) (Table 7.2). A similar decrease was observed in KOS infected cells (T_{90} of 63 ± 5% or 58 ± 7% at 4 or 7h, respectively) (Table 7.2). Greater than 50% of cells had large decreases in T_{90} at either time after infection of n-33 cells with n12 or KOS, indicating that H1.2 T_{90} was decreased throughout the cell population (Table 7.2). These data show that the increased rate of H1.2 high-affinity chromatin exchange (and decreased T_{90}) requires the transactivation activity of ICP4, nuclear ICP0, or E protein expression.

To test whether the unexpected de-mobilization of H1.2 during n12 infection of Vero cells was a cell-type specific effect, I evaluated H1.2 mobilization during n12 infection of U2OS cells. During infection of U2OS cells with 30 PFU per cell of HSV-1 strain n12, H1.2 mobility was not substantially changed (Figure 7.1 Panel B U2OS). At early or late times after infection of U2OS cells with n12, H1.2 T_{50} was similar to that of mock-infected cells (106 ± 9% or 94 ± 7%, respectively) ($P>0.05$, Student's T-test; 1-tail) (Figure 7.2 U2OS, Table 7.1). This is in contrast to infections of U2OS cells with wild-type KOS, in which H1.2 mobility was increased relative to mock-infected cells (T_{50} of 66 ± 5% or 40 ± 3% at 4 or 7h after infection with 6 PFU per cell of KOS, respectively) ($P<0.01$, Student's T-test; 1-tail) (Figure 7.1, Figure 7.2 U2OS KOS, Table 3.6). The rate of H1.2 high-affinity chromatin exchange was also unchanged from that of mock-infected cells (T_{90} of 113 ± 9% or 91 ± 7% at 4 or 7hpi with n12) ($P>0.05$, Student's T-test; 1-tail) (Table 7.1). These data show that, unlike n12 infections of Vero cells, H1.2 low- and high-affinity chromatin exchange are not significantly altered during n12 infection of U2OS cells. U2OS and Vero cells may therefore have different requirements for, or mechanisms of, H1.2 mobilization during infection. However, like in Vero cells, HSV-1 genome transcription is not sufficient to mobilize H1.2 in U2OS cells, nor is H1.2 mobilization required for HSV-1 IE gene transcription in these cells.

Taken together, these data demonstrate that HSV-1 genome transcription and IE proteins, other than ICP4 or nuclear ICP0, are not sufficient to increase the rates of H1.2 low- and high-affinity chromatin

exchange. Moreover, they show that the transactivation activity of ICP4, nuclear ICP0, or E protein expression is required to increase the chromatin exchange of H1.2 during HSV-1 infection.

7.2.2 ICP4 transactivation activity or E proteins are required to substantially increase the pool of free H1.2.

In the absence of functional ICP4, nuclear ICP0, or E proteins, H1.2 was not mobilized. In Vero cells, the rates of H1.2 low- and high- chromatin exchange were decreased, which was reflected by increases in its T_{50} and T_{90}. In U2OS cells, however, the rates of H1.2 low- and high- chromatin exchange were unchanged. Although H1.2 mobilization during infections with n12 decreased its chromatin exchange relative to that which occurred during wild-type infections, the pool of free H1.2 was nonetheless marginally increased in both Vero and U2OS cells at early times after infection (Figure 7.3). At 4h after infection of Vero cells with 30 PFU per cell of HSV-1 strain n12, the pool of free H1.2 was increased to 119 ± 5% ($P<0.05$, Student's T-test; 1-tail) (Figure 7.3 Vero, Table 7.3). Free H1.2 was increased by an extreme degree in 35% of infected cells, indicating that this increase in free H1.2 occurred throughout a larger population than would be expected from a normal distribution (Table 7.3). By 7h, however, the pool of free H1.2 was not changed relative to mock-infected cells (102 ± 4%) (Figure 7.3, Table 7.3). At this time, the pool of free H1.2 was increased by a large degree in only 19% of infected cells, as expected for a normal population distribution (16%) (Table 7.3).

As with Vero cells, the pool of free H1.2 in U2OS cells was marginally increased at early times after infection with 30 PFU per cell of n12 (Figure 7.3, Table 7.3). At 4h after infection, the pool of free H1.2 was increased to 114 ± 4% ($P<0.05$, Student's T-test; 1-tail) (Figure 7.3, Table 7.3). Fifty-two percent of n12-infected cells had an increase in free H1.2 greater than one SD above the average level in mock-infected cells, (Table 7.3), larger than expected for a normal population distribution (16%). At 7h after infection, the pool of free H1.2 still appeared to be marginally increased, to 109 ± 5%, but statistical significance was not achieved ($P>0.05$, Student's T-test; 1-tail) (Figure 7.3, Table 7.3). Nonetheless, 43% of n12 infected U2OS cells had an increase in free H1.2 greater than one SD above the average in mock-infected cells (Table 7.3).

Taken together, these data indicate that HSV-1 infection, gene transcription, or expression of IE proteins other than ICP4 and nuclear ICP0 are sufficient to marginally increase the pool of free H1.2 at early times after infection. However, functional ICP4, nuclear ICP0, or E proteins are required to increase the pool of free H1.2 at later times after infection and to increase it by a large degree. Even in the absence of functional ICP4, nuclear ICP0, and E proteins, which are required to increase the rates of H1.2 chromatin exchange (lowering its T_{50} and T_{90}), the rates of H1.2 chromatin association and disassociation (or displacement) are altered relative to each other such that the pool of free H1.2 is increased.

To test whether the basal increase in free H1.2 was a consequence of the ICP4 mutation in n12, I evaluated the level of free H1.2 during n12 infections of n-33 cells. Complementation of the n12 replication defect in n-33 cells increased the pool of free H1.2 to the larger degree. The pools of free H1.2 were increased to the same degree whether n-33 cells were infected with HSV-1 strain n12 or KOS ($P>0.05$, Tukey's HSD) (Figure 7.4, Table 7.4). The pool of free H1.2 was increased to 136 ± 8% or 137 ± 6%, respectively ($P<0.01$, Student's T-test; 1-tail) at 4h after infection with 30 PFU per cell of n12 or KOS, (Figure 7.4, Table 7.4). At 7h, the pools of free H1.2 were increased to 178 ± 10% or 170 ± 7% in n12 or KOS infected cells, respectively ($P<0.01$, Student's T-test; 1-tail) (Figure 7.4, Table 7.4). Greater than 65% or 90% of the cells at early or late times, respectively, had large increases to their pools of free H1.2. The increase in free H1.2 therefore occurred throughout the infected cell populations (Table 7.4). ICP4 transactivation activity, nuclear ICP0, or E proteins are required to increase the pool of free H1.2 by a large degree. Alternatively (but not exclusively) a large increase in free H1.2 may be required for E protein expression.

Taken together, these data show that HSV-1 genome transcription or expression of IE proteins (other than ICP4 or nuclear ICP0) is sufficient to increase the pool of free H1.2 by a marginal degree at early times after infection, but not to increase the pool of free H1.2 by a large degree. The large increase in the level of free H1.2 required the transactivation activity of ICP4 or E protein expression. Alternatively, a large increase in free H1.2 may be required for E protein expression.

7.3 DISCUSSION.

Infections of Vero or U2OS cells with HSV-1 mutant strains have demonstrated that HSV-1 genome transcription and expression of IE proteins (other than ICP4 or nuclear ICP0) are not sufficient to increase the rates of H1.2 low- or high- affinity chromatin exchange or to substantially increase the pool of free H1.2. Expression of functional ICP4, nuclear ICP0, or E proteins is therefore required to increase the rates of H1.2 chromatin exchange and to increase the pool of free H1.2 by a large degree.

In the absence of functional ICP4, nuclear ICP0, and E proteins, the rates of H1.2 chromatin association and dissociation are altered relative to each other, such that the pool of free H1.2 is marginally increased at early times after infection. In Vero cells, however, the rates of low- and high-affinity H1.2 chromatin exchange are decreased. The rates of chromatin association and dissociation could therefore both be decreased, with a larger decrease in the rate of chromatin association. Alternatively, the rate of H1.2 low-affinity chromatin association could be decreased to an extreme degree. Then, H1.2 would have to rebind chromatin only through high-affinity, and slow, chromatin exchange mechanisms. This scenario would also result in an increase in the pool of free H1.2.

The alterations in the chromatin exchange of H1.2 during n12 infections were unexpected. If functional ICP4 or E proteins were required to mobilize H1.2, then H1.2 mobility would be expected to be unchanged in their absence. However, H1.2 chromatin exchange was

actually decreased in Vero cells. H1.2 appears to have a higher affinity for chromatin in n12 infected cells than in non-infected cells, as H1.2 chromatin exchange decreases during n12 infection. If ICP4 directly or indirectly increases H1.2 chromatin exchange, then the truncated ICP4 protein expressed from n12 genomes could act in a dominant negative manner to inhibit H1.2 chromatin exchange. Alternatively, the overexpression of IE proteins could inhibit chromatin exchange of H1.2. High levels of IPC27 or cytoplasmic ICP0 could inhibit H1.2 mobility. Cellular proteins involved in mobilizing H1.2 may also be mislocalized to the cytoplasm with ICP0.

In U2OS cells, the pool of free H1.2 increased without substantial changes to the rates of H1.2 low- or high-affinity chromatin exchange. Such results indicate that any changes in H1.2 chromatin association and disassociation resulting in higher levels of free H1.2 in U2OS cells are not appreciably large. Moreover, the inhibition of H1.2 chromatin exchange observed during n12 infections of Vero cells does not occur in U2OS cells. U2OS cells tend to have faster rates of low- and high-affinity chromatin exchange than Vero cells (Table 7.1). H1.2 in U2OS cells may already be mobilized to such a degree that H1.2 chromatin exchange is not susceptible to inhibition as in Vero cells, or that any such inhibition is not detectable.

The increase in the pool of free H1.2 was only observed at early times after n12 infection. Therefore, the rates of H1.2 chromatin association and disassociation are differentially altered relative to each other only at early times after infection with n12. The viral or cellular

factors that alter H1.2 chromatin exchange to increase the free pool of H1.2 during n12 infection may therefore be most active at early times after infection.

The enhanced mobilization of H1.2 and large increase in free H1.2 is independent of HSV-1 IE gene transcription. Furthermore, transcription of IE genes does not require such mobilization. Rather, functional ICP4, nuclear ICP0, or expression of specific E proteins is required to mobilize H1.2 above a basal degree (Chapter 3) and to increase its free pool by a large degree. These data indicate that specific HSV-1 proteins are required to enhance H1.2 mobilization. Further mobilization of histones by specific HSV-1 proteins is consistent with a model in which HSV-1 enhances histone mobilization to counteract or prevent cellular silencing attempts.

ICP4 is required to activate HSV-1 E gene expression. Therefore, ICP4, rather than an E protein, is likely required to enhance H1.2 mobilization. The mechanisms of ICP4 or ICP0 transactivation of E gene expression are yet unclear. The data presented herein demonstrate that ICP4, nuclear ICP0, or E proteins are required to substantially mobilize H1.2, increasing its free pool. In the presence of a truncated form of ICP4 and cytoplasmic ICP0, H1.2 mobility is decreased, the pool of free H1.2 is only marginally increased, and E proteins are not expressed, indicating that ICP4 or nuclear ICP0 are most likely involved in H1.2 mobilization. Chromatin is a physical barrier that can impede the access of transcription complexes to DNA sequences. Functional ICP4 or nuclear ICP0 may therefore be required to enhance H1.2 mobility to

decrease such a barrier and allow transcription complexes to access E genes.

FIGURE 7.1: H1.2 is differentially mobilized in the absence of functional ICP4. Line graphs representing the normalized fluorescence intensity of the photobleached nuclear region against time. Vero (**A**) and U2OS (**B**) cells were transfected with plasmids expressing GFP-H1.2. Transfected cells were mock-infected (**filled circle**) or infected with 6 (**open triangle**) or 30 (**open circle**) PFU per cell of HSV-1 strain n12 or KOS. Nuclear mobility of GFP-H1.2 was evaluated from 4 to 5 hpi (**4 hpi**) or 7 to 8 hpi (**7 hpi**) by FRAP. Error bars, SEM; n ≥ 23 for Vero, n ≥ 17 for U2OS cells. Time plotted on a semi-logarithmic scale. Solid or dashed lines, times when 50% (T_{50}) of the original relative fluorescence was recovered in mock or HSV-1 infected cells, respectively. Vero KOS 30 data was replotted from Figure 3.6 for comparison.

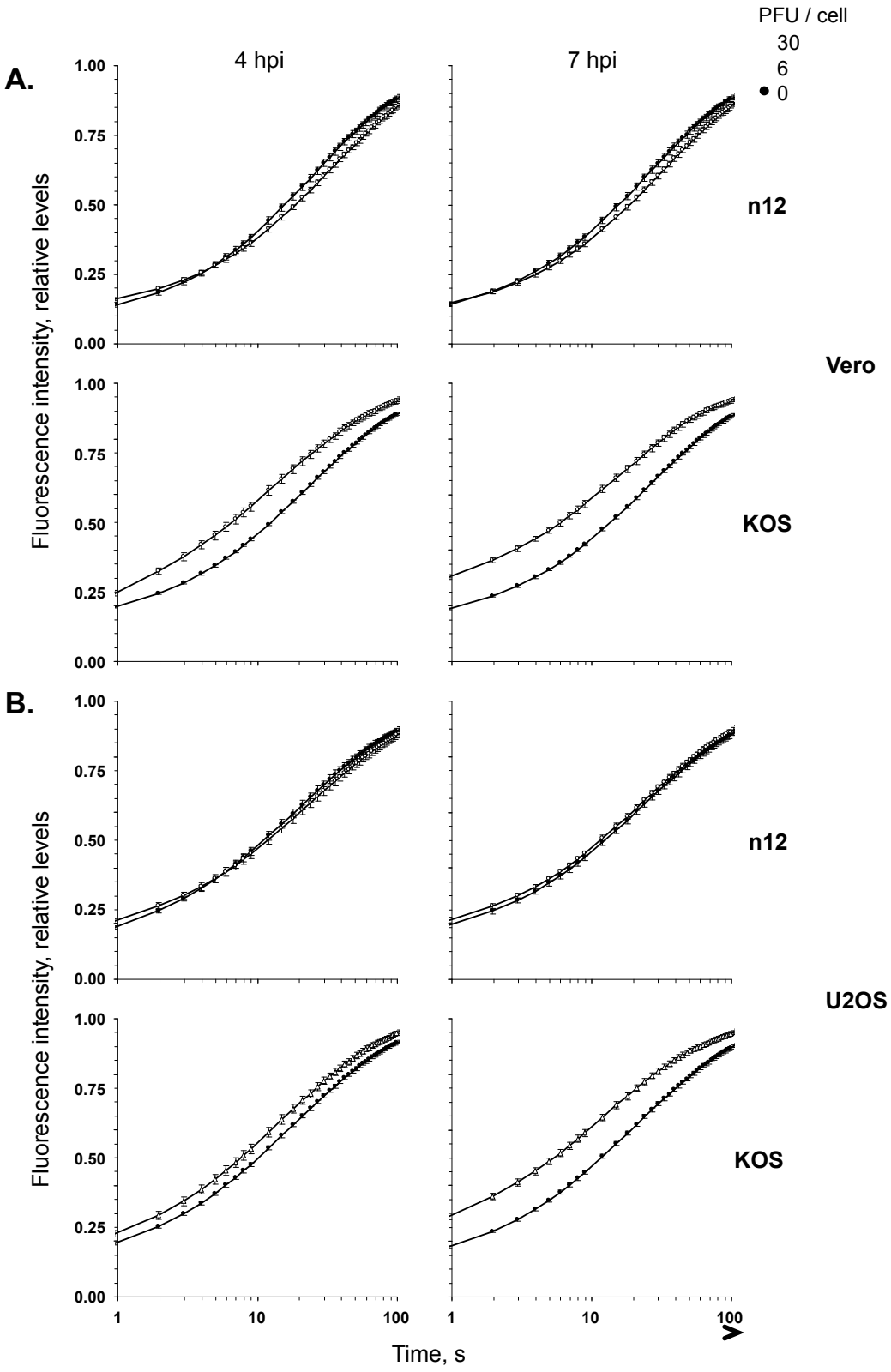
A.
B.
4 hpi
7 hpi
PFU / cell
30
6
0
n12
KOS
Vero
U2OS
Fluorescence intensity, relative levels
1.00
0.75
0.50
0.25
0.00
1
10
100
Time, s

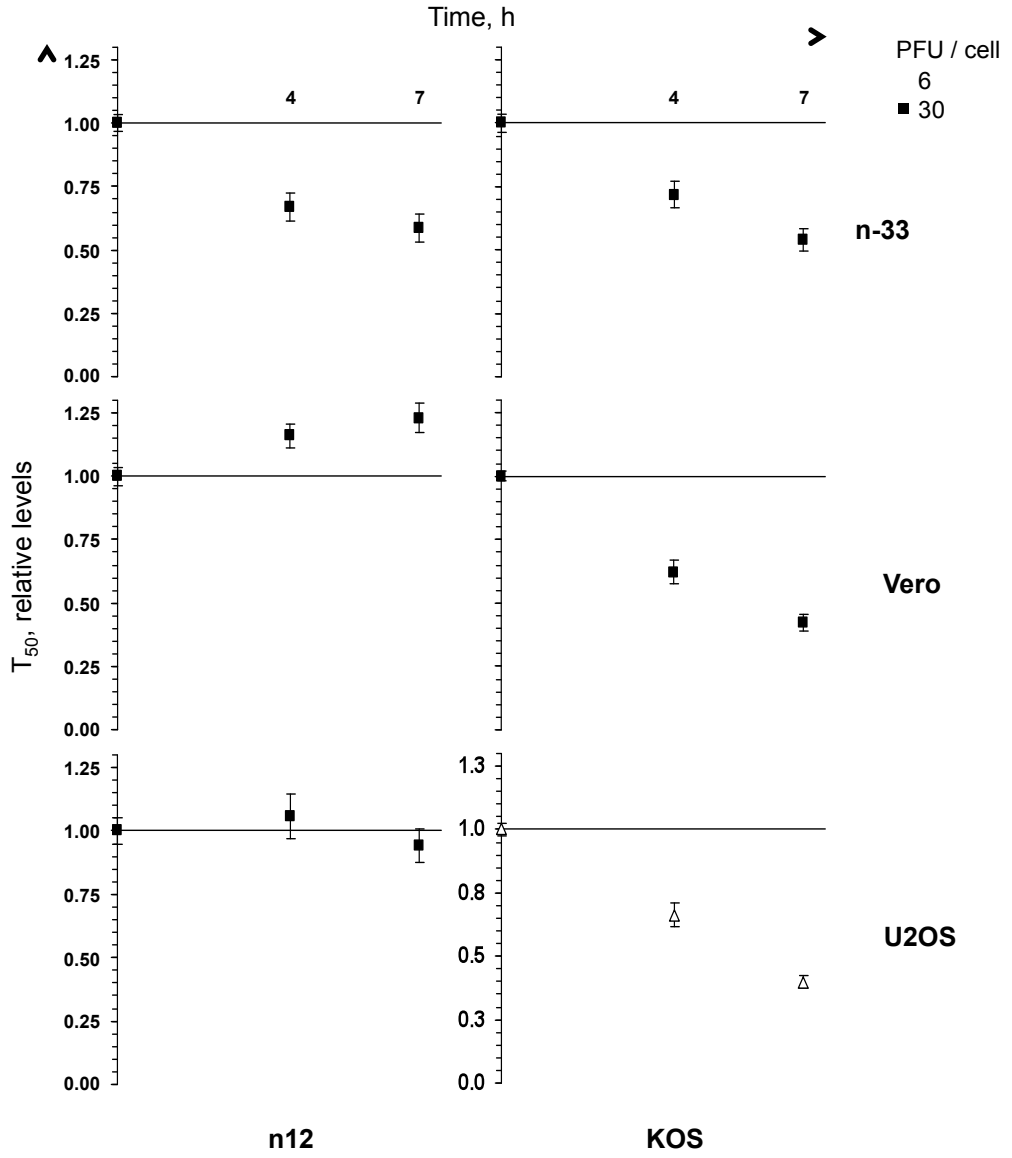

FIGURE 7.2: ICP4 or E proteins are required for enhanced mobilization of H1.2. Line graphs representing the average H1.2 T_{50} in HSV-1-infected cells normalized to mock-infected cells and plotted against time postinfection. **n-33**, **Vero,** and **U2OS** cells were transfected with plasmids expressing GFP-H1.2. Transfected cells were mock infected or infected with 6 or 30 PFU per cell of HSV-1 strain **KOS** or **n12** as indicated. Nuclear mobility of GFP-H1.2 was examined from 4 to 5 hpi (**4**) or 7 to 8 hpi (**7**) by FRAP. Error bars, SEM; n ≥ 22 for n-33, n ≥ 23 for Vero, n ≥ 17 for U2OS cells. Vero and U2OS KOS data replotted from Figure 3.9 for comparison.

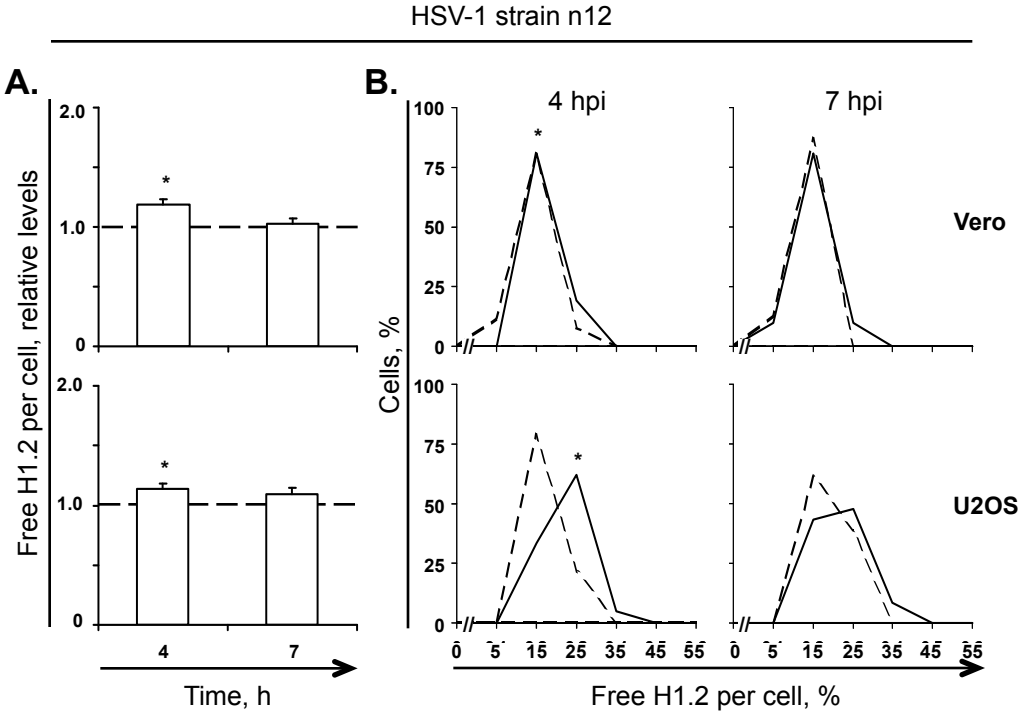

FIGURE 7.3: The increase in free H1.2 at later times requires functional ICP4 or Early proteins. A) Bar graphs representing the average percentage of free H1.2 in HSV-1 infected cells normalized to mock-infected cells and plotted against time postinfection. Vero (**Vero**) or U2OS (**U2OS**) cells were transfected with plasmids expressing GFP-H1.2. Transfected cells were mock infected or infected 30 PFU per cell of HSV-1 strain n12. Free GFP-H1.2 was evaluated from 4 to 5 hpi (**4 hpi**) or 7 to 8 hpi (**7 hpi**) by FRAP. Error bars, SEM; n ≥ 23 for Vero, n ≥ 18 for U2OS cells. **B)** Frequency distribution plots of the level of free H1.2 per individual cell evaluated by FRAP as described for Panel A. Dashed or solid lines, mock-infected or HSV-1 strain n12 infected cells, respectively. *, $P < 0.05$.

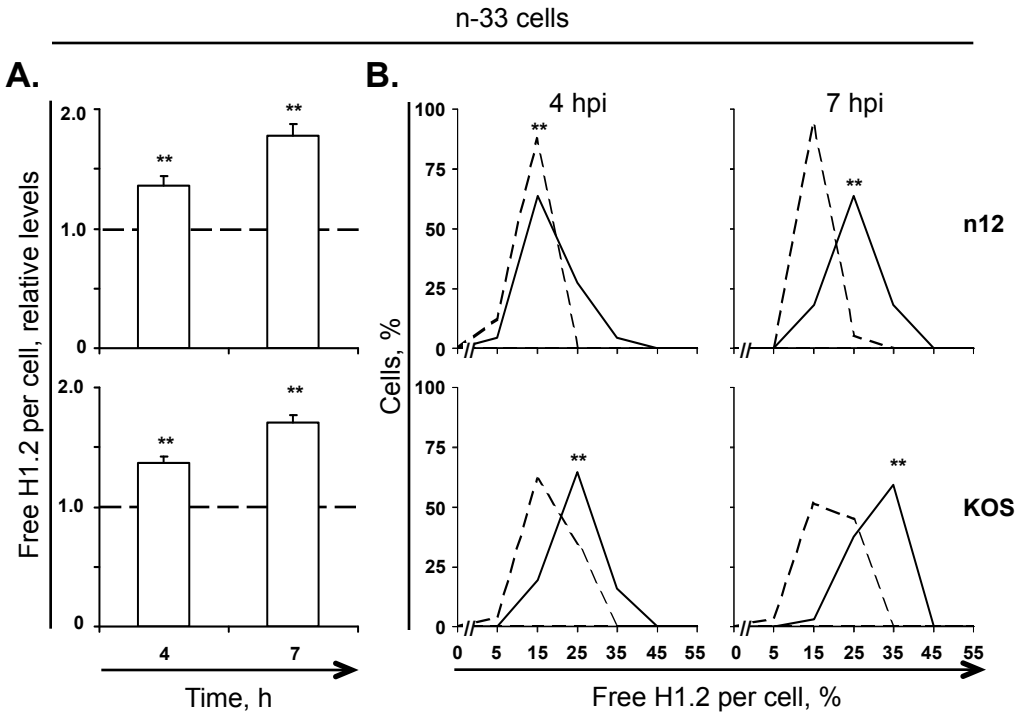

FIGURE 7.4: ICP4 or E proteins are required for the large increase in free H1.2 in n-33 cells. A) Bar graphs representing the average percentage of free H1.2 in HSV-1 infected cells normalized to mock-infected cells and plotted against time postinfection. n33 cells were transfected with plasmids expressing GFP-H1.2. Transfected cells were mock infected or infected 30 PFU per cell of HSV-1 strain KOS (**KOS**) or n12 (**n12**). Free GFP-H1.2 was evaluated from 4 to 5 hpi (**4 hpi**) or 7 to 8 hpi (**7 hpi**) by FRAP. Error bars, SEM; n ≥ 22. **B)** Frequency distribution plots of the level of free H1.2 per individual cell evaluated by FRAP as described for Panel A. Dashed or solid lines, mock-infected or HSV-1 infected cells, respectively. **, P > 0.01.

Hour Post Infection	Cell Type	Virus Strain	PFU/ cell	T_{50} (avg ± SEM)		% Cells with high H1.2 mobilization, T_{50}[a]	T_{90} (avg ± SEM)		% Cells with high H1.2 mobilization, T_{50}[b]
				Absolute (s)	Relative (%)		Absolute (s)	Relative (%)	
4	Vero	-	-	16.3 ± 1.0	100 ± 6	19	116.2 ± 6.3	100 ± 6	17
		n12	30	19.2 ± 1.0	116 ± 5	26	142.9 ± 5.9	123 ± 6	41
	U2OS	-	-	12.0 ± 0.9	100 ± 7	10	105.8 ± 10.0	100 ± 8	11
		n12	30	12.8 ± 1.1	106 ± 9	24	119.9 ± 9.4	113 ± 9	11
7	Vero	-	-	16.0 ± 0.7	100 ± 4	9	113.8 ± 7.2	100 ± 5	18
		n12	30	19.3 ± 0.9	123 ± 6	45	131.9 ± 5.1	116 ± 5	38
	U2OS	-	-	12.9 ± 0.7	100 ± 5	22	117.2 ± 8.1	100 ± 5	17
		n12	30	11.9 ± 0.7	94 ± 7	17	106.8 ± 6.4	91 ± 7	23

TABLE 7.1: Mobilization of H1.2 in Vero and U2OS cells infected with HSV-1 strain n12.

[a] Percentage of cells in which the T_{50} was >1 SD lower than the average T_{50} in mock-infected cells.

[b] Percentage of cells in which the T_{90} was >1 SD lower than the average T_{90} in mock-infected cells.

Hour Post Infection	Virus Strain	PFU/ cell	T_{50} (avg ± SEM)		% Cells with high H1.2 mobilization, T_{50}[a]	T_{90} (avg ± SEM)		% Cells with high H1.2 mobilization, T_{50}[b]
			Absolute (s)	Relative (%)		Absolute (s)	Relative (%)	
4	-	-	16.2 ± 0.8	100 ± 3	14	132.6 ± 5.6	100 ± 4	19
	KOS	30	9.4 ± 0.7	72 ± 5	65	82.9 ± 5.7	63 ± 5	56
	n12	30	12.7 ± 1.0	67 ± 5	68	97.4 ± 7.3	73 ± 5	60
7	-	-	17.1 ± 1.1	100 ± 4	11	143.7 ± 4.7	100 ± 3	10
	KOS	30	7.5 ± 0.6	54 ± 5	72	83.8 ± 7.2	58 ± 7	62
	n12	30	11.7 ± 1.1	59 ± 5	64	118.3 ± 8.2	82 ± 7	53

TABLE 7.2: Mobilization of H1.2 in n-33 cells infected with HSV-1 strains KOS or n12.

[a] Percentage of cells in which the T_{50} was >1 SD lower than the average T_{50} in mock-infected cells.

[b] Percentage of cells in which the T_{90} was >1 SD lower than the average T_{90} in mock-infected cells.

Cell Type	Virus Strain	PFU/ cell	4hpi Free H1.2 (avg ± SEM) Absolute	4hpi Free H1.2 (avg ± SEM) Relative	4hpi % Cells with large increase in free[a]	7hpi Free H1.2 (avg ± SEM) Absolute	7hpi Free H1.2 (avg ± SEM) Relative	7hpi % Cells with large increase in free[a]
Vero	-	-	0.14 ± 0.01	1.00 ± 0.04	19	0.14 ± 0.01	1.00 ± 0.04	13
	n12	30	0.16 ± 0.01	1.19 ± 0.05	35	0.15 ± 0.01	1.02 ± 0.04	19
U2OS	-	-	0.19 ± 0.01	1.00 ± 0.02	11	0.19 ± 0.01	1.00 ± 0.04	17
	n12	30	0.21 ± 0.01	1.14 ± 0.04	52	0.21 ± 0.01	1.09 ± 0.05	43

TABLE 7.3: Level of free H1.2 in Vero and U2OS cells infected with HSV-1 strain n12.

[a] Percentage of cells in which the level of free H1.2 was >1 SD above the average level in mock-infected cells.

Virus Strain	PFU/ cell	4hpi Free H1.2 (avg ± SEM) Absolute	4hpi Free H1.2 (avg ± SEM) Relative	4hpi % Cells with large increase in free[a]	7hpi Free H1.2 (avg ± SEM) Absolute	7hpi Free H1.2 (avg ± SEM) Relative	7hpi % Cells with large increase in free[a]
-	-	0.17 ± 0.01	1.00 ± 0.03	10	0.17 ± 0.01	1.00 ± 0.03	15
KOS	30	0.25 ± 0.01	1.37 ± 0.06	71	0.31 ± 0.01	1.70 ± 0.07	91
n12	30	0.18 ± 0.01	1.36 ± 0.08	68	0.26 ± 0.01	1.78 ± 0.10	91

TABLE 7.4: Level of free H1.2 in n-33 cells infected with HSV-1 strains KOS or n12.

[a] Percentage of cells in which the level of free H1.2 was >1 SD above the average level in mock-infected cells.

CHAPTER 8: FUNCTIONAL IPC4, NUCLEAR ICP0, OR EXPRESSION OF E PROTEINS IS REQUIRED TO INCREASE THE FREE POOLS OF H2B OR H3.3 TO A LARGE DEGREE, BUT NOT TO ALTER THE RATES OF H2B OR H3.3 FAST CHROMATIN EXCHANGE.

This Chapter contains unpublished data.

ABSTRACT

HSV-1 infection induced mobilization of H2B and H3.3 through common and unique mechanisms. The early mobilization of H2B is independent of HSV-1 gene transcription and protein expression, and therefore likely represents cellular responses to infection. In contrast, mobilization of H3.3 involves VP16, and like the late mobilization of H2B, requires expression of HSV-1 IE or E proteins. To test whether HSV-1 IE or E proteins were required for such mobilization, I evaluated the mobility of H2B and H3.3 during infection with n12. n12 expresses truncated, non-functional, ICP4. As a result, E protein expression is not activated, IE proteins (with the exception of ICP4) are overexpressed, and ICP0 is mislocalized to the cytoplasm. During n12 infection, the pools of free H3.3 and H2B were increased to a basal degree and their fast chromatin exchange rate was altered. IE gene transcription or expression of IE proteins other than ICP4 or nuclear ICP0 is sufficient to alter the fast chromatin exchange rates of H2B and H3.3, therefore mobilizing them

and increasing their free pools, but only by a basal degree. Further increases to the pools of free H2B and H3.3, however, still required expression of functional ICP4, nuclear ICP0, or E proteins.

8.1 INTRODUCTION.

Core histone mobilization during HSV-1 infection likely occurs through more than one mechanism. The increase to the pools of free H2B and H3.3 did not require HSV-1 DNA replication or strictly L proteins. The early increase in the pool of free H2B did not require or correlate with HSV-1 transcription or protein expression either. In contrast, free H3.3 was only increased by a marginal degree under conditions of little to no HSV-1 transcription or protein expression.

The pools of free H2B and H3.3, however, were both increased by a greater degree when HSV-1 genes were transcribed and IE and E proteins were expressed. The magnitude of increase in free H3.3 correlated with the degree of HSV-1 gene transcription and protein expression. HSV-1 gene transcription or expression of an HSV-1 IE or E protein may therefore contribute to the changes in core histone chromatin exchange that result in the higher levels in the free pool. Alternatively, the altered core histone chromatin exchange that increases the levels available in the free pool may be required for HSV-1 transcription to occur.

The increase in the fast chromatin exchange rate of H3.3 in Vero cells required HSV-1 gene transcription or expression of IE or E proteins. Mobilization of H3.3 during infections with an HSV-1 strain mutant in ICP0 suggested that ICP0 may also contribute to the increase in the fast

chromatin exchange rate of H3.3. Conversely, HSV-1 gene transcription was not sufficient to increase the rate of fast H3.3 chromatin exchange in U2OS cells. However, the absolute rates of H3.3 low-affinity chromatin exchange in U2OS cells are already high (Table 5.4). Therefore, the rate of H3.3 fast chromatin exchange may not be able to be further increased. Alternatively, the biochemical activities of ICP0 may be required. The decrease in the rate of H2B fast chromatin exchange, however, did not require HSV-1 transcription or expression of IE or E proteins in either Vero or U2OS cells. The rate of H2B low affinity chromatin exchange is therefore independent of HSV-1 transcription and protein expression, whereas that of H3.3 is not.

To further characterize the requirements for H2B and H3.3 mobilization, I evaluated the chromatin exchange of H2B and H3.3 during n12 infections. The loci encoding IE genes are transcribed and IE proteins are expressed to high levels during n12 infections (DeLuca & Schaffer, 1988). Such overexpression of IE proteins results in ICP0 mislocalization to the cytoplasm (Zhu et al., 1994; Zhu et al., 1996). Additionally, the truncated ICP4 expressed lacks transactivation activity and the nuclear localization domain. Therefore, during n12 infection E gene expression is not activated (DeLuca & Schaffer, 1988).

8.2 RESULTS.

8.2.1 HSV-1 IE gene transcription is not sufficient to mobilize H2B or H3.3.

The mobilization of H2B and H3.3 during n12 infection was tested in Vero and U2OS cells. During n12 infection of non-complementary cell lines, IE proteins are expressed to high levels. However, ICP4 is non-functional, and consequently E gene expression is not activated. In Vero cells infected with 30 PFU per cell of n12, H2B chromatin exchange was only marginally increased at later times, as demonstrated by slightly faster fluorescence recovery after photobleaching (Figure 8.1 Vero). In U2OS cells infected with 30 PFU per cell of n12, however, H2B chromatin exchange tended to be slightly decreased at later times, as demonstrated by slightly slower fluorescence recovery after photobleaching (Figure 8.1 U2OS). H3.3 chromatin exchange was not substantially altered during infection of Vero or U2OS cells with 30 PFU per cell of n12 (Figure 8.2). These data demonstrate that HSV-1 IE gene expression is not sufficient to substantially alter H2B or H3.3 chromatin exchange. Functional ICP4 or E proteins are therefore required.

To test whether the defects in Vero and U2OS cell mobilization of H2B or H3.3 were indeed a consequence of the ICP4 mutation in n12, I analyzed n12 infections of n-33 cells. Infection of n-33 cells with 30 PFU per cell of n12 increased H2B and H3.3 chromatin exchange at 4 and 7hpi, as demonstrated by faster fluorescence recovery after photobleaching (Figures 8.3 and 8.4, respectively). The overall chromatin exchange of H2B and H3.3 was increased to a similar degree as during

infection with wild-type KOS (Figures 8.3 and 8.4, respectively). Thus, complementation of the transactivation function of ICP4 such that E proteins are expressed altered the chromatin exchange of core histones H2B and H3.3 to a similar degree as during wild-type infection. The overexpression of IE proteins largely excludes ICP0 from the nucleus during n12 infection. Therefore, functional ICP4, nuclear ICP0, or E proteins are required to increase the chromatin exchange of H2B and H3.3 during HSV-1 infection. Alternatively, increased chromatin exchange of H2B or H3.3 may be required for E, but not IE, gene transcription. Taken together, these data demonstrate that HSV-1 IE gene transcription, cytoplasmic ICP0, and expression of IE proteins other than ICP4 are not sufficient to increase the chromatin exchange of H2B or H3.3.

8.2.2 ICP4, nuclear ICP0, or E proteins are required to substantially increase the pools of free H2B and H3.3.

The chromatin exchange of H2B or H3.3 was not significantly altered during infections with n12, in which ICP4 does not transactivate expression of E genes. Under such conditions, the free pools of H2B were not increased (Figure 8.5). At early times after infection of Vero cells, and early or late times after infection of U2OS cells with 30 PFU per cell of HSV-1 strain n12, the pools of free H2B were similar to those in mock-infected cells ($P>0.05$, Student's T-test; 1-tail) (Figure 8.5, Table 8.1). Whereas at late times after infection of Vero cells with 30 PFU per cell of n12, the pool of free H2B was marginally increased to 115 ± 5%

(P<0.05, Student's T-Test; 1-tail) (Figure 8,5, Table 8.). Thus, transcription of IE genes or expression of IE proteins other than ICP4 or nuclear ICP0 is sufficient to marginally increase the pool of free H2B, but only at late times after infection. Complementation of the replication defects of n12 increased the pools of free H2B. In n-33 cells infected with 30 PFU per cell of n12, the pool of free H2B was increased to 158 ± 5% or 142 ± 7% at 4 or 7h (P<0.01, Student's T-test; 1-tail) (Figure 8.6, Table 8.2). The increase in free H2B was to the same degree as that which occurred during wild-type KOS infection (160 ± 6% or 157 ± 9% at 4 or 7hpi with 30 PFU per cell of KOS) (P>0.05, Student's T-test; 1-tail) (Figure 8.6, Table 8.2). The population of n12 or KOS infected cells with the pool of free H2B increased to a degree larger than one SD was at least 4 fold higher than that which would be expected (16%) for a normal distribution (Table 8.2). These data show that HSV-1 IE gene transcription and expression of IE proteins (other than ICP4 and nuclear ICP0) are not sufficient to alter H2B chromatin exchange such that the pools of free H2B are increased. Functional ICP4, nuclear ICP0, or E proteins are required to increase the pool of free H2B.

In contrast to H2B, the pool of free H3.3 was marginally increased at early or late times in Vero cells in the absence of functional ICP4, nuclear ICP0, and E proteins (Figure 8.7). At 4 or 7h after infection with 30 PFU per cell of n12, the pool of free H3.3 was increased to 116 ± 4% or 117 ± 5%, respectively. (P<0.05 or P<0.01 at 4 or 7h, respectively, Student's T-test; 1-tail) (Figure 8.7, Table 8.1). The population of n12 infected cells with an increase in free H3.3 greater than one SD above the

average level of free H3.3 in mock-infected cells was approximately 2-fold larger than would be expected for a normal frequency distribution (Table 8.1). Thus, HSV-1 transcription or expression of IE proteins other than ICP4 or nuclear ICP0 is sufficient to marginally increase the pool of free H3.3 in Vero cells. Functional ICP4, nuclear ICP0, or E proteins, however, are required to increase the pool of free H3.3 in Vero cells to a larger extent.

Unlike in Vero cells, the pool of free H3.3 was not increased in U2OS cells (Figure 8.7). At early and late times after infection of U2OS cells with 30 PFU per cell of n12, the pools of free H3.3 were similar to those in mock-infected cells (Figure 8.7, Table 8.1). Thus, HSV-1 gene transcription and IE proteins other than ICP4 or nuclear ICP0 are not sufficient to increase the pool of free H3.3 in U2OS cells. ICP4, nuclear ICP0, or E proteins are required.

To test whether only ICP4, nuclear ICP0, or E proteins were required to increase the pool of free H3.3 by a large degree, I analyzed the levels of free H3.3 during n12 infections of n-33 cells. The pool of free H3.3 was again increased by a large degree ($P<0.01$, Student's T-test; 1-tail) at early and late times after infection of n-33 cells with 30 PFU of n12, (Figure 8.8). It was increased to 188 ± 6% at 4 or 203 ± 8% at 7hpi (Figure 8.8, Table 8.2). The pool of free H3.3 was increased by a large degree in over 90% of cells, at either time evaluated, indicating that the increase in free H3.3 occurred throughout the population of infected cells (Table 8.2). Somewhat surprisingly, the pool of free H3.3 was increased to a lower degree during KOS infection of n-33 cells ($P<0.05$, Tukey's

HSD). The pool of free H3.3 was increased to only 162 ± 5% or 169 ± 8% at 4 or 7h after infection with 30 PFU per cell of wild-type KOS (in comparison to 188 ± 6% at 4 or 203 ± 8% at 7hpi with n12) (Figure 8.8, Table 8.2). As during n12 infections, however, the increase in free H3.3 occurred throughout the population of KOS infected n-33 cells. At 4 and 7hpi, greater than 90% of cells had large increases in their pools of free H3.3 (Table 8.2).

HSV-1 transcription or expression of IE proteins other than ICP4 or nuclear ICP0 is sufficient to increase the pool of free H3.3 in Vero cells, but only by a marginal degree. To substantially increase the pools of free H2B and H3.3 in Vero and U2OS cells the transactivation activity of ICP4, nuclear ICP0, or expression of E proteins is required.

8.2.3 The fast chromatin exchange rates of H2B and H3.3 have a tendency to be altered even in the absence of functional ICP4, nuclear ICP0, and E proteins.

Functional ICP4, nuclear ICP0, or E proteins were required to alter the rates of H2B chromatin association and dissociation relative to each other, in order to increase the pool of free H2B during infection. Functional ICP4, nuclear ICP0, or E proteins are not required, however, to alter the rate of fast H2B chromatin exchange. The fast chromatin exchange rate of H2B had a tendency to be decreased (to 0.76 ± 0.12 or 0.82 ± 0.11 fold, respectively) at 4 or 7h after infection of Vero cells with 30 PFU per cell of HSV-1 strain n12 (Figure 8.9, Table 8.3). Although statistical significance was not achieved, the population of n12 infected

cells with a large decrease in the rate of H2B fast chromatin exchange was approximately 1.5 or 3 fold larger at early and late times, respectively, than would be expected based on a normal population distribution (Table 8.3). These data are in agreement with previous data from KM110 and KOS infections, which demonstrated that the decrease in the fast chromatin exchange rate of H2B is independent of HSV-1 transcription and protein expression (Chapter 5). As in Vero cells, the fast chromatin exchange rate of H2B in n12-infected U2OS cells was decreased at early and late times ($P<0.05$ and $P<0.01$, respectively, Student's T-test; 1-tail) (Figure 8.9). The fast chromatin exchange rate of H2B was decreased to 0.77 ± 0.03 or 0.74 ± 0.03 fold at 4 or 7h after infection of U2OS with 30 PFU per cell of n12, respectively (Figure 8.9, Table 8.3). Thus, the transactivation activity of ICP4, nuclear ICP0, or E proteins are not required to decrease the fast chromatin exchange rate of H2B either. The data presented here, in combination with the data presented in Chapter 5, indicate that the rate of H2B low-affinity chromatin exchange is largely independent of HSV-1 function. That is, transcription of HSV-1 genes or HSV-1 protein expression is not required to decrease the rate of H2B low-affinity chromatin exchange. Such a decrease may therefore be a cellular response to infection, result from inhibition of cellular transcription by HSV-1 structural proteins, or potentially be the result of the process of infection (for example virion fusion, virion tegument proteins, nuclear entry of naked HSV-1 genomes, etc.).

Complementation of n12 replication defects during infection of n-33 cells differentially altered the fast chromatin exchange rate of H2B (Figure 8.10). At early times after infection with 30 PFU per cell of n12, the rate of fast H2B chromatin exchange tended to be decreased (to 0.89 ± 0.10 fold) (Figure 8.10, Table 8.4). At later times after n12 infection, however, the fast chromatin exchange rate of H2B appeared to be increased to 1.37 ± 0.17 fold ($P<0.05$, Student's T-test; 1-tail) (Figure 8.10, Table 8.4). A similar trend was observed during KOS infection of n-33 cells. The fast chromatin exchange rate of H2B was decreased to 0.72 ± 0.08 fold at 4h after infection with 30 PFU per cell of KOS ($P<0.01$, Student's T-test; 1-tail), and appeared to be increased at 7h (to 1.26 ± 0.17 fold) (Figure 8.10, Table 8.4). However, the absolute rate of H2B fast chromatin exchange at late times in mock-infected n-33 cells was abnormally low (1.18 compared to 1.98 at 4h). Such a low value may lead to apparent altered relative rates of H2B fast chromatin exchange at later times after KOS or n12 infection. Consistent with such a possibility, the absolute rate of H2B fast chromatin exchange in KOS-infected cells was similar at 4 and 7hpi, 1.36 ± 0.12 and 1.34 ± 0.17, respectively (Table 8.4). In n12-infected cells, the absolute rate of H2B fast chromatin exchange was actually decreased at 7hpi relative to 4hpi, 1.42 ± 0.17 and 1.76 ± 0.23, respectively (Table 8.4). Further analyses of the rate of H2B fast chromatin exchange in mock-infected n-33 cells is required to analyze whether the low rate of exchange at later times is indeed real, or just an artifact of these experiments.

In the absence of functional ICP4, nuclear ICP0, and E proteins, the fast chromatin exchange rate of H3.3 tended to be increased in Vero cells at early times after infection (Figure 8.11). The fast chromatin exchange rate of H3.3 was increased to 1.47 ± 0.21 fold at 4h after infection with 30 PFU per cell of n12. However, statistical significance was not achieved (Figure 8.11, Table 8.3). At 7h, the fast chromatin exchange rate of H3.3 tended to be similar to that of mock-infected cells (1.15 ± 0.10 fold) (Figure 8.11, Table 8.3). Thus, HSV-1 transcription or expression of IE proteins other than ICP4 or nuclear ICP0 are sufficient to increase the rate of H3.3 low-affinity chromatin exchange at early times after infection of Vero cells. Expression of ICP4, nuclear ICP0, and E protein expression is therefore not required. The fast chromatin exchange rate of H3.3 tended to be decreased during n12 infection of U2OS cells, but statistical significance was not achieved (to 0.85 ± 0.09 or 0.91 ± 0.13 fold at 4 or 7h after infection with 30 PFU per cell of n12) (Figure 8.11, Table 8.3). This tendency towards a decrease was somewhat surprising given that the H3.3 fast chromatin exchange rate tended to be increased during infections of U2OS (or Vero) cells with wild-type HSV-1. HSV-1 transcription or expression of IE proteins other than ICP4 or nuclear ICP0 is not sufficient to increase the rate of H3.3 low-affinity chromatin exchange in U2OS cells to the same extent as during wild-type infections.

To test whether this phenotype was indeed specific for the ICP4 mutation, I evaluated the rate of H3.3 fast chromatin exchange during n12 infections of n-33 cells. The fast chromatin exchange rate of H3.3

was increased to a similar degree during infections of n-33 cells with n12 or KOS (Figure 8.12). At 4h after infection with 30 PFU per cell of n12 or KOS, the fast chromatin exchange rate of H3.3 was increased to 2.15 ± 0.18 or 1.78 ± 0.25 fold, respectively ($P<0.01$ or $P<0.05$, respectively, Student's T-test; 1-tail) (Figure 8.12, Table 8.4). At 7h after infection with n12 or KOS, the fast chromatin exchange rate of H3.3 remained increased, to 1.48 ± 0.11 or 1.40 ± 0.14 fold, respectively ($P<0.01$ or $P<0.05$, respectively, Student's T-test; 1-tail) (Figure 8.12, Table 8.4).

The decrease in the rate of H2B low-affinity chromatin exchange during infection is independent of HSV-1 IE gene transcription and protein expression. Conversely, HSV-1 IE gene transcription or expression of IE proteins other than ICP4 or nuclear ICP0 is sufficient to increase the rate of H3.3 low affinity chromatin exchange in Vero cells. ICP4, nuclear ICP0, or E protein expression is required, however, to increase the rate of H3.3 low-affinity chromatin exchange in U2OS cells. The difference in the requirements to increase the rate of H3.3 low-affinity chromatin exchange in Vero and U2OS cells implies that they may have different mechanisms of H3.3 mobilization during infection, or that they respond differently to HSV-1 infection. Alternatively, as the absolute rate of H3.3 fast chromatin exchange is higher in U2OS cells than in Vero cells, further mobilization of H3.3 during HSV-1 infection of U2OS cells may not be required.

8.3 DISCUSSION.

Infection with the ICP4 mutant strain n12 has demonstrated that HSV-1 gene transcription or expression of IE proteins other than ICP4 or nuclear ICP0 is not sufficient to increase the pool of free H2B at early times, but is sufficient to increase its free pool by a basal degree at late times after infection. The transactivation activity of ICP4, nuclear ICP0, or E protein expression is therefore required to increase the pool of free H2B by a large degree. Conversely, the decrease in the rate of H2B fast chromatin exchange still occurred in the absence of functional ICP4, nuclear ICP0, and E proteins. These results are consistent with the previous ones demonstrating that the decrease in H2B fast chromatin exchange was independent of HSV-1 gene transcription or protein expression (Chapter 5). The decrease in the fast chromatin exchange rate of H2B during HSV-1 infection therefore occurs regardless of whether infection is productive or not. The decrease in the rate of H2B fast chromatin exchange could therefore reflect a cellular response to infection. Alternatively, it may result from the decrease in cellular transcription. In cellular chromatin, the fast component of H2B chromatin exchange is transcription associated. Therefore, a decrease in the rate of cellular transcription would result in a decrease in H2B chromatin exchange. The inhibition of cellular transcription during infection could therefore result in decreased H2B chromatin exchange.

The pool of free H3.3 was still marginally increased in the absence of functional ICP4, nuclear ICP0, and E proteins. Thus, HSV-1 transcription and expression of IE proteins other than ICP4 or nuclear

ICP0 are sufficient to increase the pool of free H3.3, but only by a basal degree. Expression of ICP4, nuclear ICP0, or E proteins is required, however, to increase the pool of free H3.3 to a larger degree. In the absence of functional ICP4, nuclear ICP0, and E proteins, the pool of free H3.3 was increased to a similar degree as during conditions of little to no HSV-1 protein expression (in KM110 infections). The marginal increase in free H3.3 could therefore reflect a cellular response to HSV-1 infection. The degree of increase in the level of free H3.3, however, was closely associated with the degree of HSV-1 transcription and IE or E protein expression (see Chapter 5). During n12 infection, a truncated form of ICP4 is expressed and IE proteins are expressed to high levels, but ICP0 is mislocalized to the cytoplasm. The large increase in the pool of free H3.3 may be inhibited under such conditions. Alternatively, a large increase in the pool of free H3.3 may be a consequence of E protein transcription. Consistently, U2OS cells did not have an increase in the pool of free H3.3 in the absence of functional ICP4, nuclear ICP0, or E protein expression. Thus, HSV-1 transcription and expression of IE proteins other than ICP4 were not sufficient to increase the pool of free H3.3 in U2OS cells. Instead, ICP4, nuclear ICP0, or E proteins are required.

HSV-1 transcription or expression of IE proteins other than ICP4 or nuclear ICP0 was sufficient to increase the fast chromatin exchange rate of H3.3 in Vero cells in the absence of functional ICP4, nuclear ICP0, or E proteins. The fast chromatin exchange rate of H3.3 was not altered during infection of Vero cells with KM110, in which there was little to no

HSV-1 transcription or protein expression. HSV-1 transcription of IE genes may therefore increase the rate of fast H3.3 chromatin exchange. Alternatively, an increased rate of H3.3 fast chromatin exchange may be required for HSV-1 IE gene transcription. U2OS cells did require functional ICP4, nuclear ICP0, or E proteins, however, to increase the rate of fast H3.3 chromatin exchange. In this cell type, HSV-1 genes may be transcribed in the absence of H3.3 mobilization. However, U2OS cells have an inherently high rate of fast H3.3 chromatin exchange. The rate of H3.3 fast chromatin exchange may therefore be sufficiently fast enough in U2OS cells, such that further mobilization is not required. Alternatively, the rate of fast H3.3 exchange may not be able to be increased any further. Taken together, these data demonstrate that a further increase in rate of H3.3 low-affinity chromatin exchange is not required for HSV-1 gene transcription in U2OS cells. Moreover, HSV-1 gene transcription does not further increase the rate of H3.3 low-affinity chromatin exchange in U2OS cells.

That HSV-1 transcription or expression of IE proteins other than ICP4 or nuclear ICP0 was not sufficient to increase the rate of H3.3 low-affinity chromatin exchange in U2OS cells was very surprising. Analysis of the rate of H3.3 fast chromatin exchange during infection with HSV-1 strains mutant in ICP0 (n212) had indicated that ICP0 may be required to increase the rate of H3.3 fast chromatin exchange in U2OS cells (Chapter 5). During n212 infections, HSV-1 E genes were transcribed. Thus, transcription and expression of E proteins was not sufficient to increase the rate of H3.3 fast chromatin exchange during infection of

U2OS cells with ICP0 null HSV-1. However, expression of ICP0 in the absence of functional ICP4 and E protein expression, as during n12 infection, was also not sufficient to increase the rate of H3.3 low-affinity chromatin exchange. Under such conditions, ICP0 is largely excluded from the nucleus. The fast chromatin exchange rate of H3.3 in U2OS cells may therefore already be fast enough such that further mobilization is not required. Alternatively, these data indicate that ICP0 and ICP4 may act in concert to increase the rate of H3.3 low-affinity chromatin exchange in U2OS cells. If nuclear ICP0 is required to increase the rate of H3.3 fast chromatin exchange in U2OS cells, then the mislocalization of overexpressed ICP0 during n12 infections may adversely affect the mechanisms that increase the rate of H3.3 fast chromatin exchange.

The data presented in this chapter demonstrate that the changes to the rates of H2B and H3.3 fast chromatin exchange do not require functional ICP4, nuclear ICP0, or E proteins, whereas the large increases to the pools of free H3.3 and H2B do. ICP4 and ICP0 are transcription transactivators that activate expression of E proteins. The data presented in Chapter 5 demonstrated that ICP0 is not required for the large increase in free H3.3, however, mislocalization of ICP0 to the cytoplasm could still negatively regulate core histone mobility. Therefore, I propose that functional ICP4 and nuclear ICP0, rather than E proteins, are required to enhance H2B and H3.3 mobilization during infection. These data also indicate that the same groups of HSV-1 proteins enhance the mobilization of H2B and H3.3. However, whereas the enhanced mobilization of H3.3 occurs already at early times, that of H2B

occurs only later. Although the enhanced mobilization of H3.3 may be required for HSV-1 E gene expression, therefore, that of H2B is not.

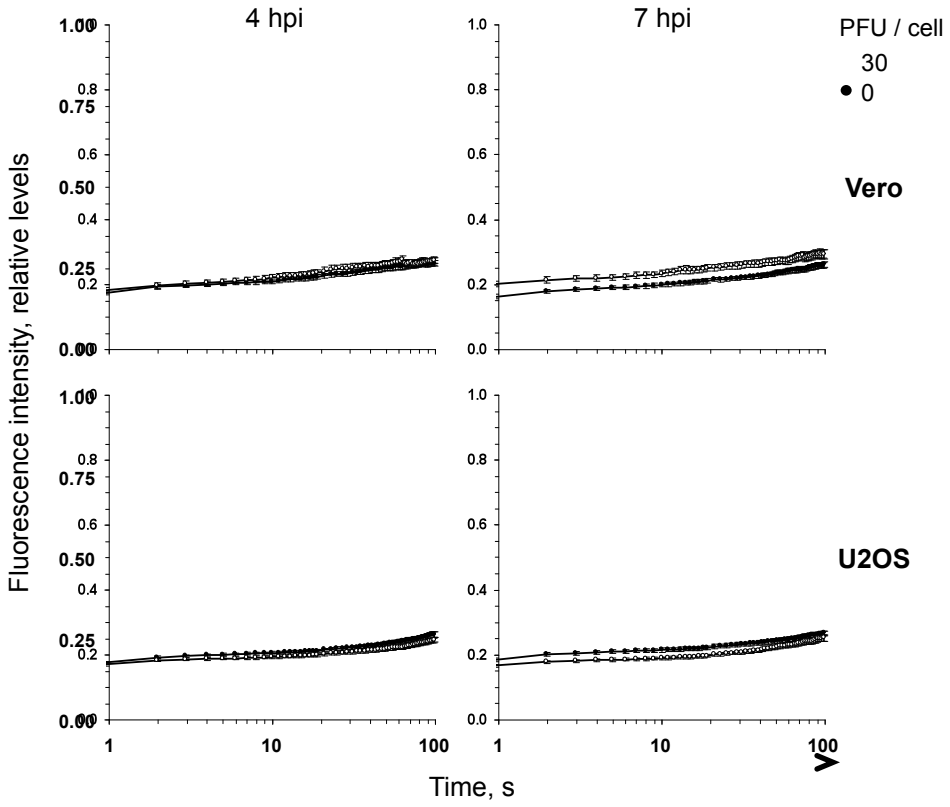

FIGURE 8.1: H2B mobilization requires E proteins or ICP4 transactivation activity. Line graphs representing the normalized fluorescence intensity of the photobleached nuclear region against time. Vero (**Vero**) and U2OS (**U2OS**) cells were transfected with plasmids expressing GFP-H2B. Transfected cells were mock-infected (**filled**) or infected with 30 (**open**) PFU per cell of HSV-1 strain n12. Nuclear mobility of GFP-H2B was evaluated from 4 to 5 hpi (**4 hpi**) or 7 to 8 hpi (**7 hpi**) by FRAP. Error bars, SEM; n ≥ 32 for U2OS and n ≥ 20 for Vero cells. Time plotted on a semi-logarithmic scale.

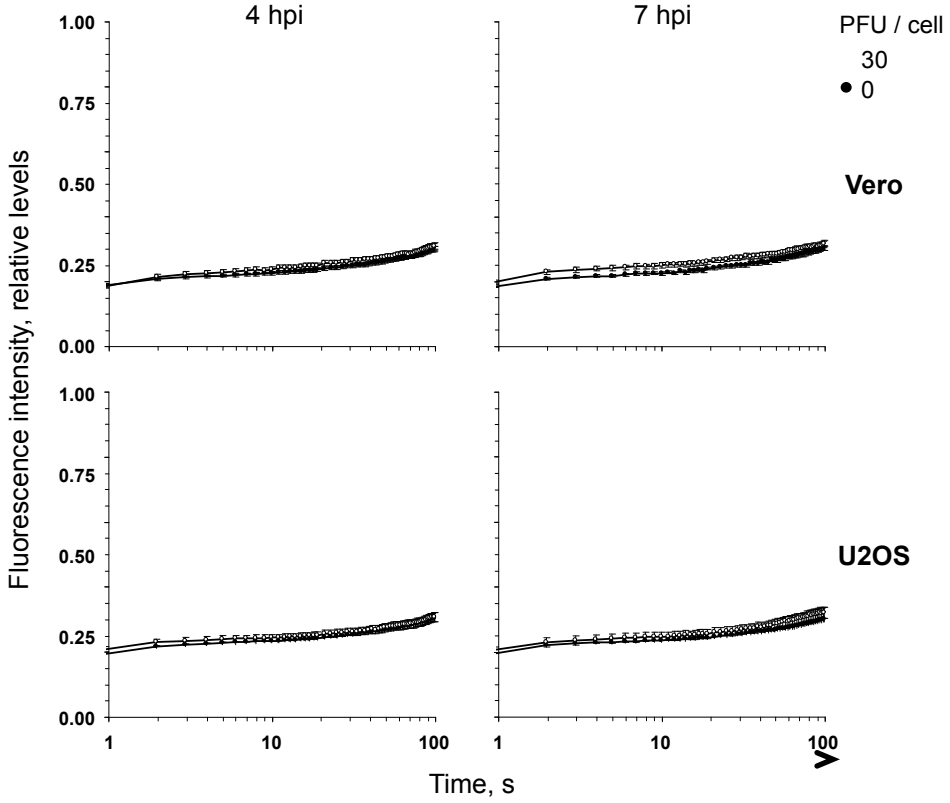

FIGURE 8.2: H3.3 mobilization requires E proteins or ICP4 transactivation activity. Line graphs representing the normalized fluorescence intensity of the photobleached nuclear region against time. Vero (**Vero**) and U2OS (**U2OS**) cells were transfected with plasmids expressing GFP-H3.3. Transfected cells were mock-infected (**filled**) or infected with 30 (**open**) PFU per cell of HSV-1 strain n12. Nuclear mobility of GFP-H3.3 was evaluated from 4 to 5 hpi (**4 hpi**) or 7 to 8 hpi (**7 hpi**) by FRAP. Error bars, SEM; n ≥ 32 except for U2OS n12 30 at 7 hpi n = 24. Time plotted on a semi-logarithmic scale.

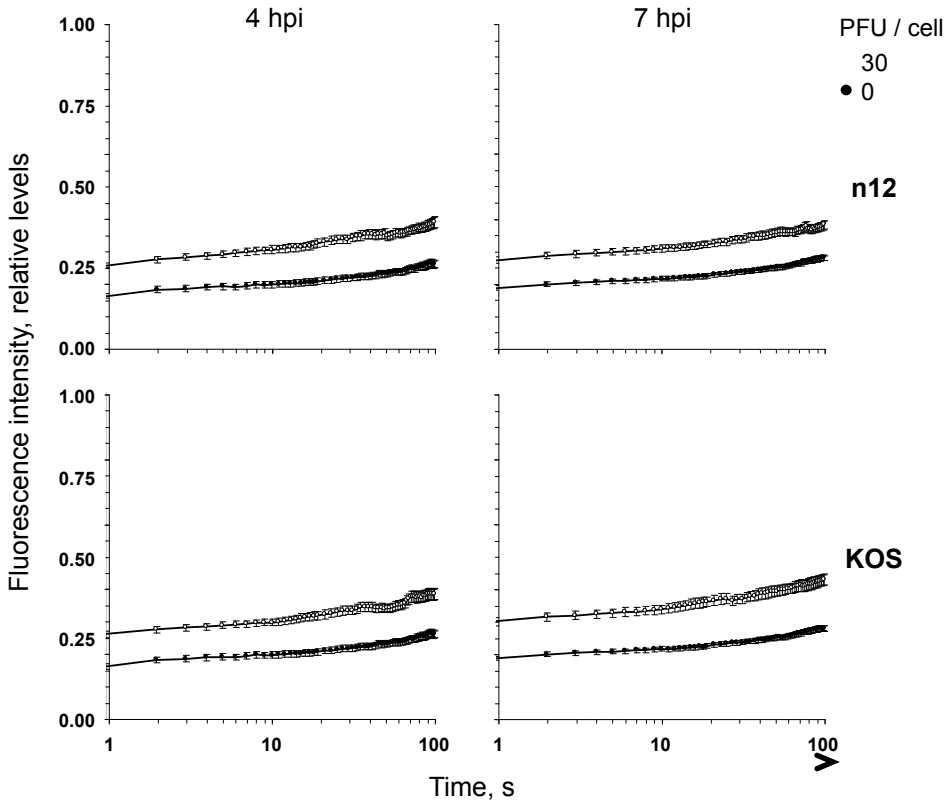

FIGURE 8.3: H2B is mobilized when wild-type ICP4 and E proteins are expressed. Line graphs representing the normalized fluorescence intensity of the photobleached nuclear region against time. n-33 cells were transfected with plasmids expressing GFP-H2B. Transfected cells were mock-infected (**filled**) or infected with 30 (**open**) PFU per cell of HSV-1 strain n12 (**n12**) or KOS (**KOS**). Nuclear mobility of GFP-H2B was evaluated from 4 to 5 hpi (**4 hpi**) or 7 to 8 hpi (**7 hpi**) by FRAP. Error bars, SEM; n ≥ 23. Time plotted on a semi-logarithmic scale.

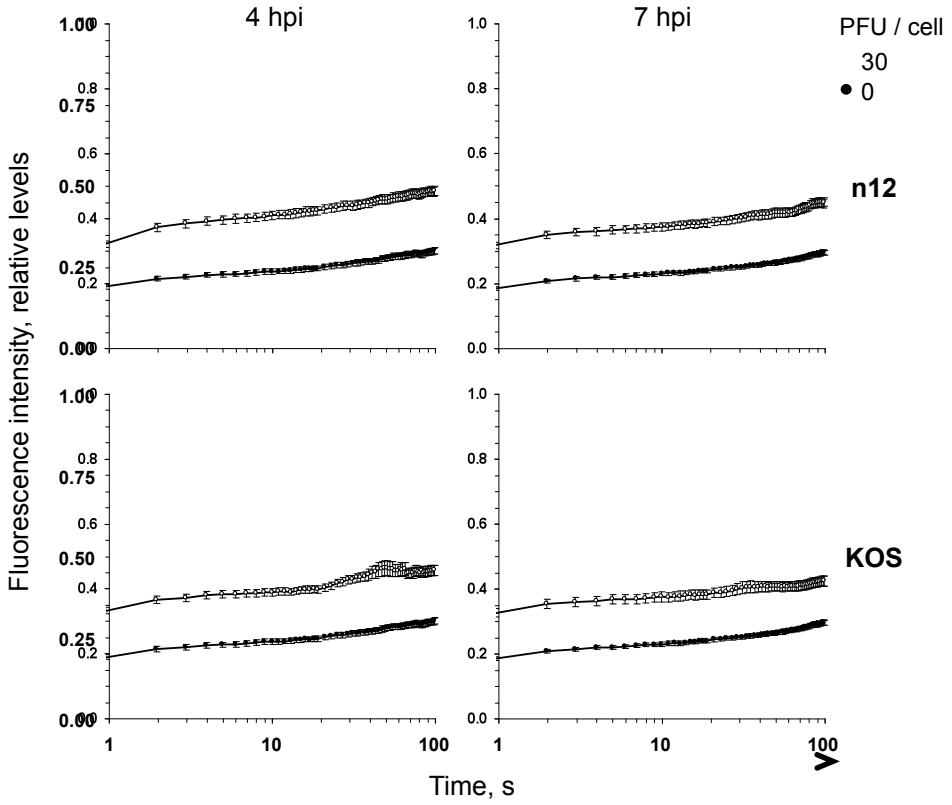

FIGURE 8.4: H3.3 is mobilized when wild-type ICP4 and E proteins are expressed. Line graphs representing the normalized fluorescence intensity of the photobleached nuclear region against time. n-33 cells were transfected with plasmids expressing GFP-H3.3. Transfected cells were mock-infected (**filled**) or infected with 30 (**open**) PFU per cell of HSV-1 strain n12 (**n12**) or KOS (**KOS**). Nuclear mobility of GFP-H3.3 was evaluated from 4 to 5 hpi (**4 hpi**) or 7 to 8 hpi (**7 hpi**) by FRAP. Error bars, SEM; n ≥ 35, except for KOS at 4 and 7 hpi, n ≥ 24. Time plotted on a semi-logarithmic scale.

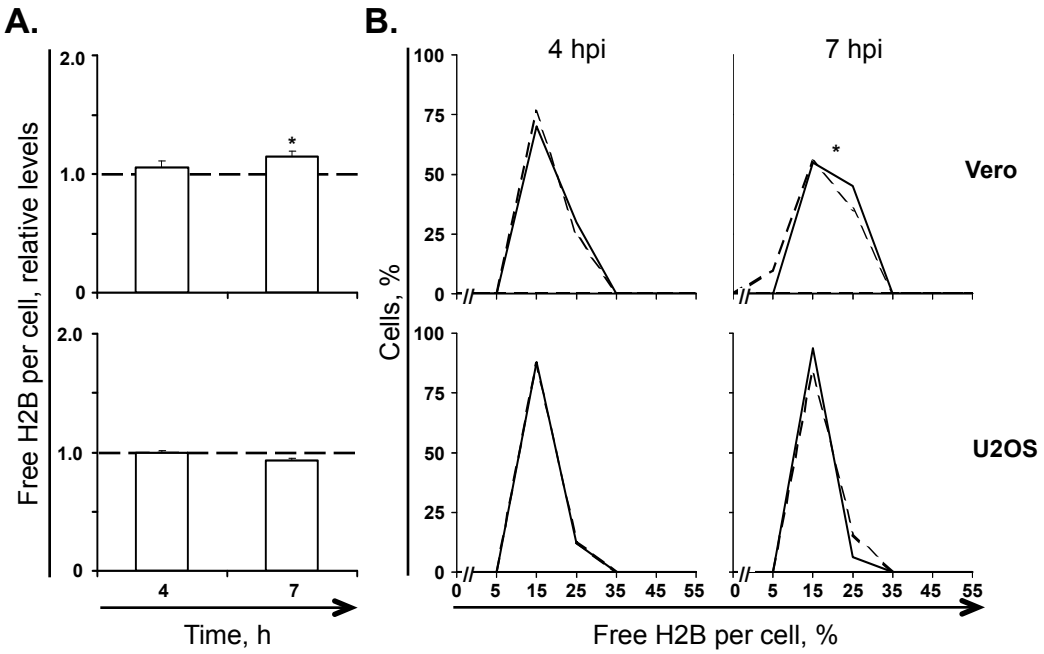

FIGURE 8.5: The increase in free H2B requires ICP4 transactivation activity or E proteins. A) Bar graphs representing the average percentage of free H2B in HSV-1 infected cells normalized to mock infected cells. Vero (**Vero**) and U2OS (**U2OS**) cells were transfected with plasmids encoding GFP-H2B. Transfected cells were mock-infected or infected with 30 PFU per cell of HSV-1 strain n12. Nuclear mobility of GFP-H2B was evaluated from 4 to 5 hpi (**4**) or 7 to 8 hpi (**7**) by FRAP. Error bars, SEM; n ≥ 32 for U2OS and n ≥ 20 for Vero. **B)** Frequency distribution plots of the percentage of free H2B per individual cell evaluated by FRAP as described for Panel A. Dashed or solid lines, mock or HSV-1 infected cells, respectively. *, P<0.05.

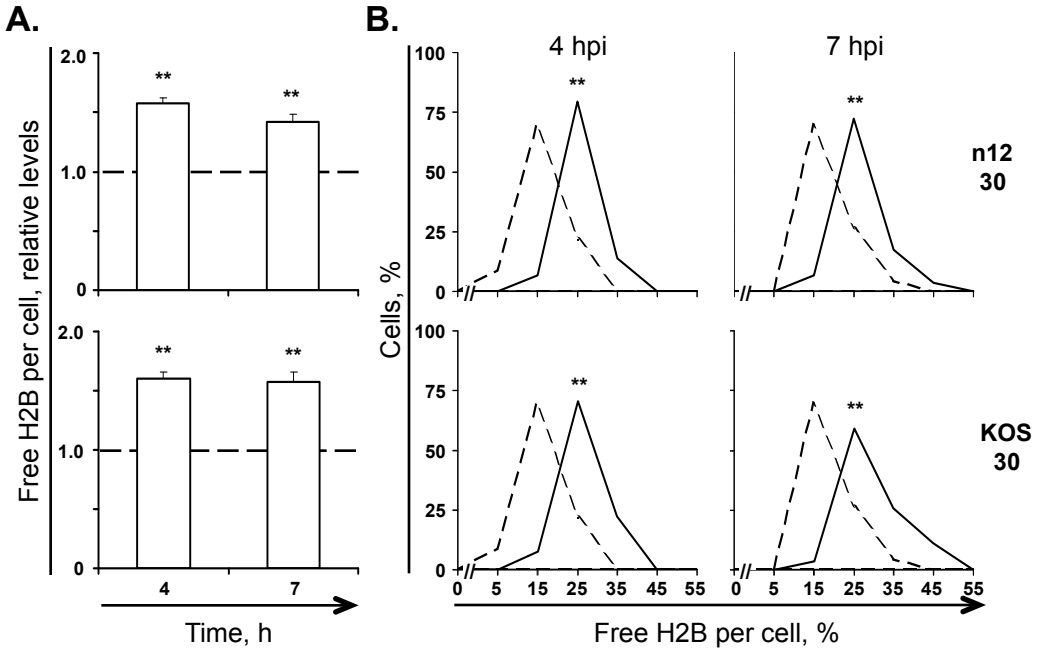

FIGURE 8.6: The pool of free H2B is increased to the same degree during n12 or KOS infections of n-33 cells. A) Bar graphs representing the average percentage of free H2B in HSV-1 infected cells normalized to mock infected cells. n-33 cells were transfected with plasmids encoding GFP-H2B. Transfected cells were mock-infected or infected with 30 PFU per cell of HSV-1 strain n12 (**n12 30**) or KOS (**KOS 30**). Nuclear mobility of GFP-H2B was evaluated from 4 to 5 hpi (**4**) or 7 to 8 hpi (**7**) by FRAP. Error bars, SEM; n ≥ 23. **B)** Frequency distribution plots of the percentage of free H2B per individual cell evaluated by FRAP as described for Panel A. Dashed or solid lines, mock or HSV-1 infected cells, respectively. **, P <0.01.

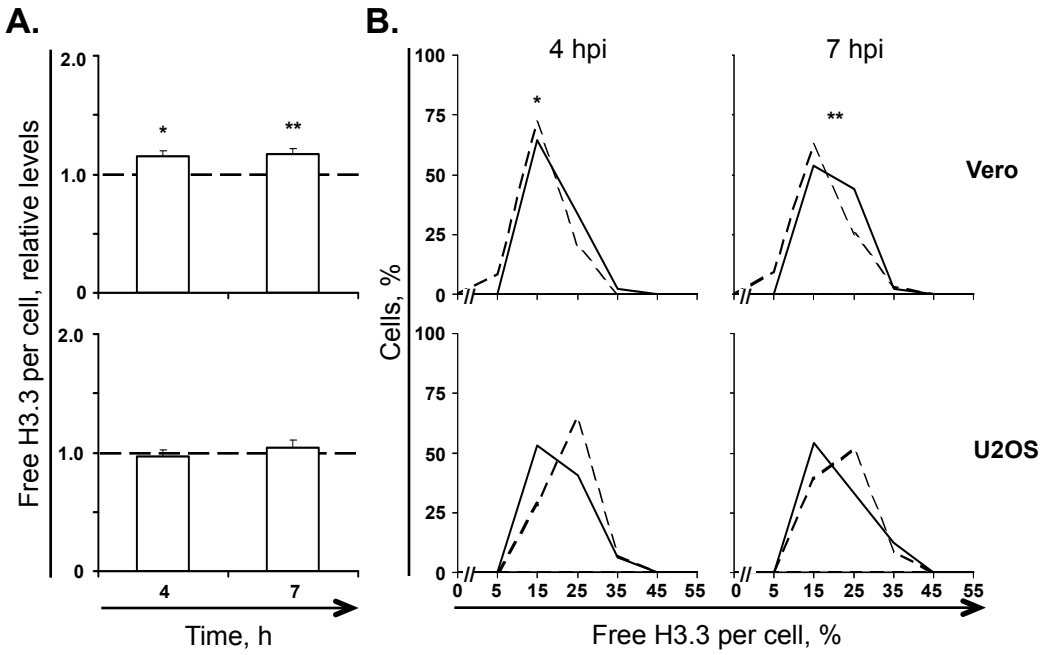

FIGURE 8.7: The pool of free H3.3 is marginally increased in Vero, but not U2OS, cells in the absence of ICP4 transactivation activity or E protein expression. A) Bar graphs representing the average percentage of free H3.3 in HSV-1 infected cells normalized to mock infected cells. Vero (**Vero**) and U2OS (**U2OS**) cells were transfected with plasmids encoding GFP-H3.3. Transfected cells were mock-infected or infected with 30 PFU per cell of HSV-1 strain n12. Nuclear mobility of GFP-H3.3 was evaluated from 4 to 5 hpi (**4**) or 7 to 8 hpi (**7**) by FRAP. Error bars, SEM; n ≥ 32, except for U2OS n12 30 at 7 hpi, n = 24. **B)** Frequency distribution plots of the percentage of free H3.3 per individual cell evaluated by FRAP as described for Panel A. Dashed or solid lines, mock or HSV-1 infected cells, respectively. *, $P < 0.05$; **, $P < 0.01$.

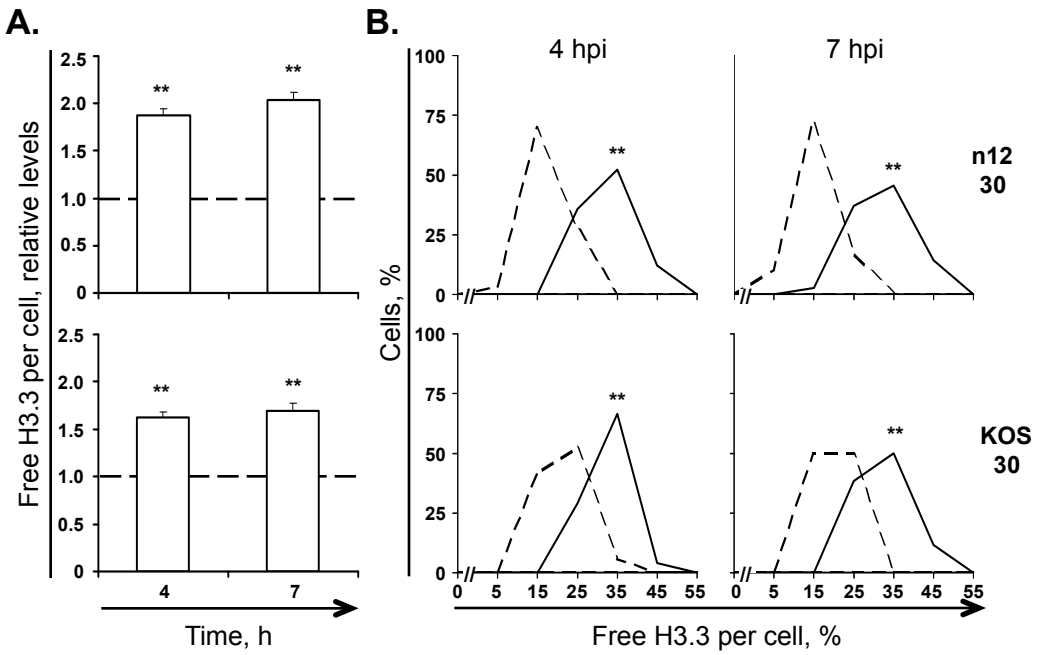

FIGURE 8.8: The pool of free H3.3 is increased to a large degree during n12 or KOS infections of n-33 cells. A) Bar graphs representing the average percentage of free H3.3 in HSV-1 infected cells normalized to mock infected cells. n-33 cells were transfected with plasmids encoding GFP-H3.3. Transfected cells were mock-infected or infected with 30 PFU per cell of HSV-1 strain n12 (**n12 30**) or KOS (**KOS 30**). Nuclear mobility of GFP-H3.3 was evaluated from 4 to 5 hpi (**4**) or 7 to 8 hpi (**7**) by FRAP. Error bars, SEM; n ≥ 35, except for KOS 30 at 4 and 7 hpi, n ≥ 24. **B)** Frequency distribution plots of the percentage of free H3.3 per individual cell evaluated by FRAP as described for Panel A. Dashed or solid lines, mock or HSV-1 infected cells, respectively. **, P <0.01.

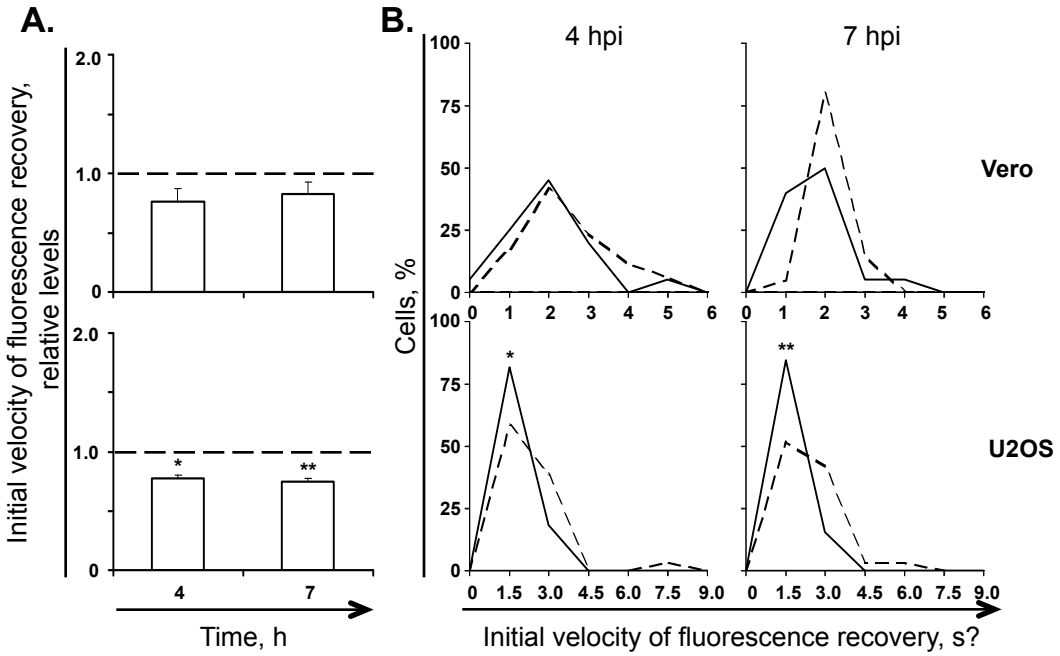

FIGURE 8.9: The rate of initial fluorescence recovery of H2B is tends to decrease in the absence of functional ICP4 and E proteins. A) Bar graphs representing the average rate of initial fluorescence recovery after photobleaching in HSV-1 infected cells normalized to mock infected cells. Vero (**Vero**) and U2OS (**U2OS**) cells were transfected with plasmids encoding GFP-H2B. Transfected cells were mock-infected or infected with 30 PFU per cell of HSV-1 strain n12. Nuclear mobility of GFP-H2B was evaluated from 4 to 5 hpi (**4**) or 7 to 8 hpi (**7**) by FRAP. Error bars, SEM; n ≥ 32 for U2OS and n ≥ 20 for Vero. **B)** Frequency distribution plots of the rate of initial fluorescence recovery after photobleaching per individual cell evaluated by FRAP as described for Panel A. Dashed or solid lines, mock or HSV-1 infected cells, respectively. *, $P < 0.05$; **, $P < 0.01$.

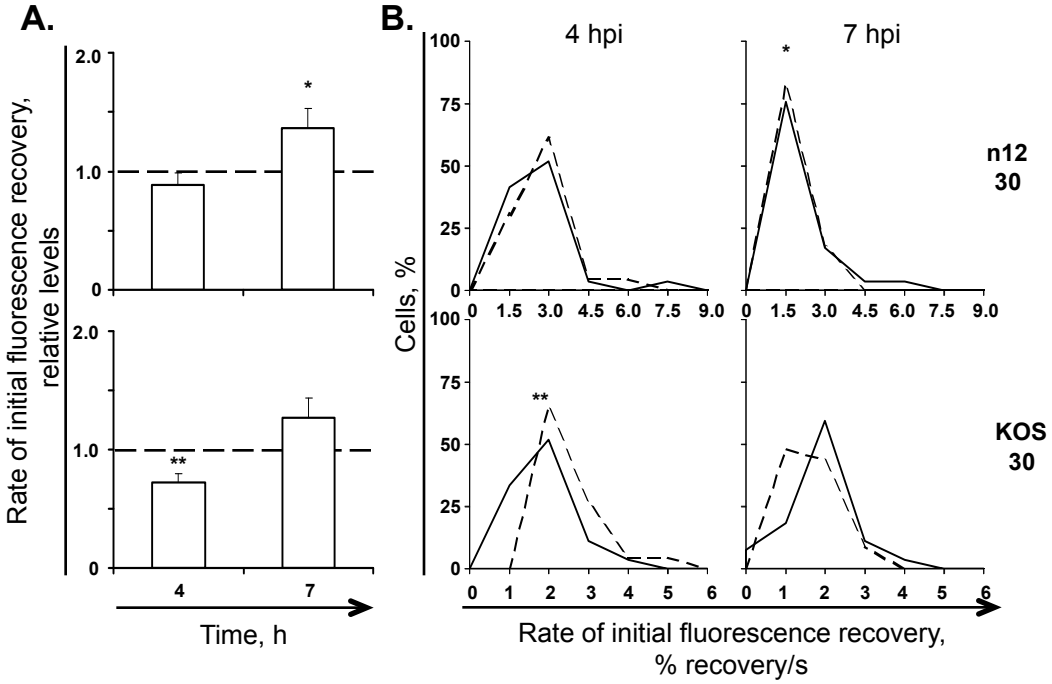

FIGURE 8.10: The rate of initial fluorescence recovery of H2B tends to decrease at early times and increase at later times during infection of n-33 cells with HSV-1. A) Bar graphs representing the average rate of initial fluorescence recovery after photobleaching in HSV-1 infected cells normalized to mock infected cells. n-33 cells were transfected with plasmids encoding GFP-H2B. Transfected cells were mock-infected or infected with 30 PFU per cell of HSV-1 strain n12 (**n12 30**) or KOS (**KOS 30**). Nuclear mobility of GFP-H2B was evaluated from 4 to 5 hpi (**4**) or 7 to 8 hpi (**7**) by FRAP. Error bars, SEM; n ≥ 23. **B)** Frequency distribution plots of the rate of initial fluorescence recovery after photobleaching per individual cell evaluated by FRAP as described for Panel A. Dashed or solid lines, mock or HSV-1 infected cells, respectively. *, $P < 0.05$; **, $P < 0.01$.

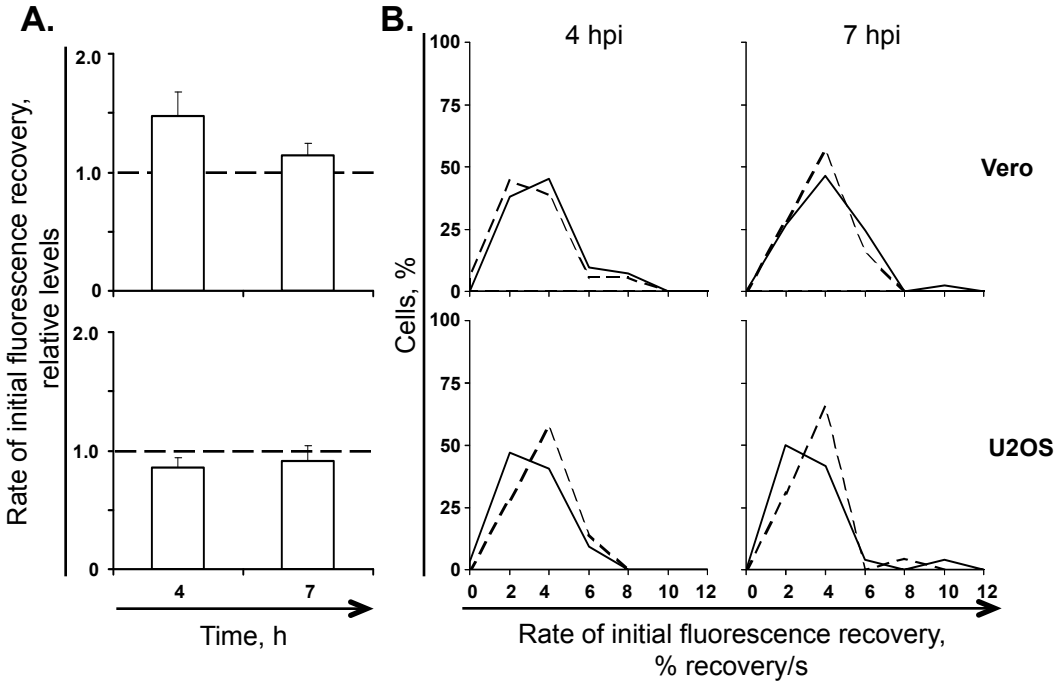

FIGURE 8.11: In the absence of functional ICP4 and E proteins, the rate of initial fluorescence recovery of H3.3 tends to increase in Vero cells but decrease in U2OS cells. A) Bar graphs representing the average rate of initial fluorescence recovery after photobleaching in HSV-1 infected cells normalized to mock infected cells. Vero (**Vero**) and U2OS (**U2OS**) cells were transfected with plasmids encoding GFP-H3.3. Transfected cells were mock-infected or infected with 30 PFU per cell of HSV-1 strain n12. Nuclear mobility of GFP-H3.3 was evaluated from 4 to 5 hpi (**4**) or 7 to 8 hpi (**7**) by FRAP. Error bars, SEM; n ≥ 32, except for U2OS n12 30 at 7 hpi, n = 24. **B)** Frequency distribution plots of the rate of initial fluorescence recovery after photobleaching per individual cell evaluated by FRAP as described for Panel A. Dashed or solid lines, mock or HSV-1 infected cells, respectively.

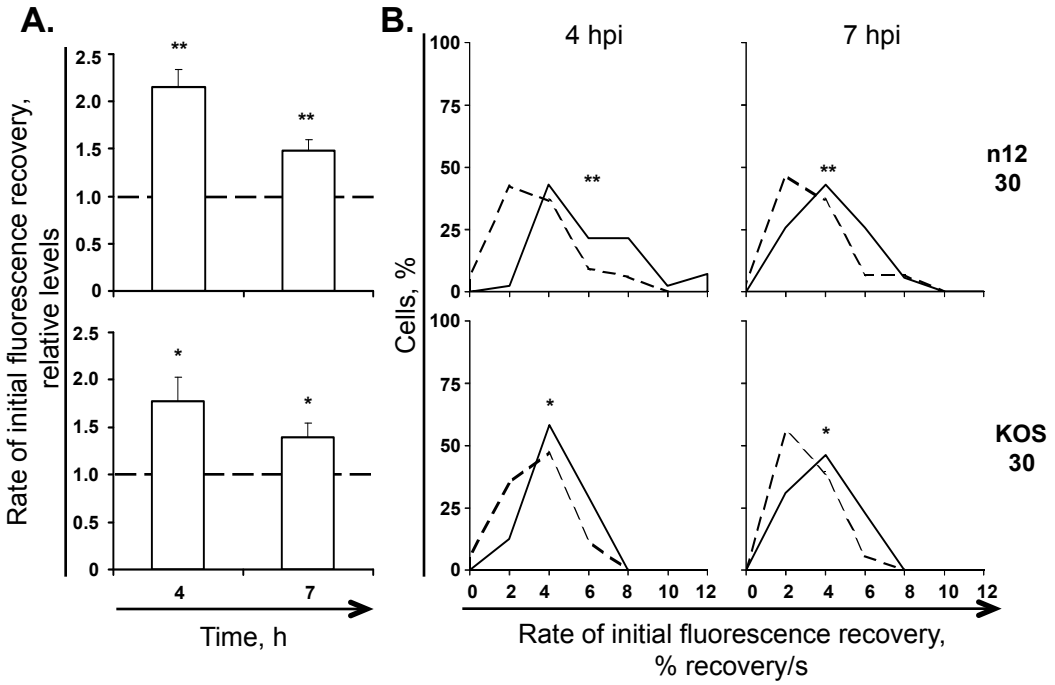

FIGURE 8.12: The rate of initial fluorescence recovery of H3.3 is increased during n12 or KOS infection of n-33 cells. A) Bar graphs representing the average rate of initial fluorescence recovery after photobleaching in HSV-1 infected cells normalized to mock infected cells. n-33 cells were transfected with plasmids encoding GFP-H3.3. Transfected cells were mock-infected or infected with 30 PFU per cell of HSV-1 strain n12 (**n12 30**) or KOS (**KOS 30**). Nuclear mobility of GFP-H3.3 was evaluated from 4 to 5 hpi (**4**) or 7 to 8 hpi (**7**) by FRAP. Error bars, SEM; n ≥ 35, except for KOS 30 at 4 and 7 hpi, n ≥ 24). **B)** Frequency distribution plots of the rate of initial fluorescence recovery after photobleaching per individual cell evaluated by FRAP as described for Panel A. Dashed or solid lines, mock or HSV-1 infected cells, respectively. *, $P < 0.05$; **, $P < 0.01$.

Histone Variant	Cell Type	Virus Strain	PFU/ cell	4hpi Free core histone (avg ± SEM) Absolute	Relative	Free Pool, % Cells with large: Increase[a]	Decrease[b]	Mock (avg ± SEM) Absolute
H2B	Vero	-	-	0.17 ± 0.01*	1.00 ± 0.03	16	19	-
		KOS	30	0.24 ± 0.01	1.33 ± 0.05	79	4	0.18 ± 0.01
		n12	30	0.18 ± 0.01	1.06 ± 0.06	20	15	0.17 ± 0.01
	U2OS	-	-	0.18 ± 0.01*	1.00 ± 0.02	11	13	-
		KOS	6	0.20 ± 0.01	1.14 ± 0.04	41	0	0.18 ± 0.01
			15	0.22 ± 0.01	1.23 ± 0.04	77	12	0.18 ± 0.01
		n12	30	0.17 ± 0.01	0.99 ± 0.02	15	6	0.17 ± 0.01
H3.3	Vero	-	-	0.19 ± 0.01*	1.00 ± 0.02	15	15	-
		KOS	30	0.33 ± 0.01	1.71 ± 0.07	89	0	0.19 ± 0.01
		n12	30	0.19 ± 0.01	1.16 ± 0.04	33	5	0.16 ± 0.01
	U2OS	-	-	0.20 ± 0.01*	1.00 ± 0.02	13	13	-
		KOS	6	0.31 ± 0.01	1.94 ± 0.07	100	0	0.16 ± 0.01
		n12	30	0.21 ± 0.01	0.97 ± 0.05	28	34	0.22 ± 0.01

TABLE 8.1 (A): Levels of free H2B and H3.3 in Vero and U2OS cells infected with HSV-1 strains KOS or n12.

[a] Percentage of cells in which the level of free H2B or H3.3 was >1 SD above the average level in mock-infected cells.

[b] Percentage of cells in which the level of free H2B or H3.3 was >1 SD lower than the average level in mock-infected cells.

* Average of all mock.

Histone Variant	Cell Type	Virus Strain	PFU/ cell	7hpi: Free core histone (avg ± SEM) Absolute	7hpi: Free core histone (avg ± SEM) Relative	7hpi: Free Pool, % Cells with large: Increase[a]	7hpi: Free Pool, % Cells with large: Decrease[b]	Mock (avg ± SEM) Absolute
H2B	Vero	-	-	0.16 ± 0.01*	1.00 ± 0.03	11	13	-
		KOS	30	0.27 ± 0.01	1.69 ± 0.07	88	2	0.16 ± 0.01
		n12	30	0.20 ± 0.01	1.15 ± 0.05	25	5	0.18 ± 0.01
	U2OS	-	-	0.18 ± 0.01*	1.00± 0.02	15	21	-
		KOS	6	0.23 ± 0.01	1.24 ± 0.05	66	11	0.19 ± 0.01
			15	0.29 ± 0.01	1.57 ± 0.05	96	0	0.28 ± 0.01
		n12	30	0.17 ± 0.01	0.93 ± 0.02	3	28	0.18 ± 0.01
H3.3	Vero	-	-	0.18 ± 0.01*	1.00 ± 0.02	11	15	-
		KOS	30	0.30 ± 0.01	1.55 ± 0.05	84	1	0.20 ± 0.01
		n12	30	0.20 ± 0.01	1.17 ± 0.05	29	2	0.17 ± 0.01
	U2OS	-	-	0.20 ± 0.01*	1.00 ± 0.03	14	14	-
		KOS	6	0.31 ± 0.01	1.64 ± 0.05	96	0	0.19 ± 0.01
		n12	30	0.21 ± 0.01	1.05 ± 0.06	25	8	0.20 ± 0.01

TABLE 8.1 (B): Levels of free H2B and H3.3 in Vero and U2OS cells infected with HSV-1 strains KOS or n12.

[a] Percentage of cells in which the level of free H2B or H3.3 was >1 SD above the average level in mock-infected cells.

[b] Percentage of cells in which the level of free H2B or H3.3 was >1 SD lower than the average level in mock-infected cells.

* Average of all mock.

Histone Variant	Virus Strain	PFU/ cell	4hpi Free histone (avg ± SEM) Absolute	4hpi Free histone (avg ± SEM) Relative	4hpi % Cells with large increase in free[a]	Mock (avg ± SEM) Absolute
H2B	-	-	0.16 ± 0.01*	1.00 ± 0.05	17	-
	KOS	30	0.26 ± 0.01	1.60 ± 0.06	96	0.16 ± 0.01
	n12	30	0.26 ± 0.01	1.58 ± 0.05	93	0.16 ± 0.01
H3.3	-	-	0.19 ± 0.11*	1.00 ± 0.03	16	-
	KOS	30	0.33 ± 0.01	1.62 ± 0.05	92	0.21 ± 0.01
	n12	30	0.32 ± 0.01	1.88 ± 0.06	98	0.17 ± 0.01

TABLE 8.2 (A): Levels of free H2B and H3.3 in n-33 cells infected with HSV-1 strains KOS or n12.

[a] Percentage of cells in which the level of free H2B or H3.3 was >1 SD above the average level in mock-infected cells.

* Average of all mock.

Histone Variant	Virus Strain	PFU/ cell	7hpi Free histone (avg ± SEM) Absolute	Relative	% Cells with large increase in free[a]	Mock (avg ± SEM) Absolute
H2B	-	-	0.19 ± 0.01*	1.00 ± 0.03	13	-
	KOS	30	0.30 ± 0.01	1.57 ± 0.09	85	0.19 ± 0.01
	n12	30	0.27 ± 0.01	1.42 ± 0.07	69	0.19 ± 0.01
H3.3	-	-	0.19 ± 0.01*	1.00 ± 0.02	15	-
	KOS	30	0.33 ± 0.01	1.69 ± 0.08	96	0.20 ± 0.01
	n12	30	0.32 ± 0.01	2.03 ± 0.08	94	0.16 ± 0.01

TABLE 8.2 (B): Levels of free H2B and H3.3 in n-33 cells infected with HSV-1 strains KOS or n12.

[a] Percentage of cells in which the level of free H2B or H3.3 was >1 SD above the average level in mock-infected cells.

* Average of all mock.

				4hpi				
				Rate of initial fluorescence recovery, %/s (avg ± SEM)		Fast chromatin exchange, % of cells		Mock (avg ±SEM)
Histone Variant	Cell Type	Virus Strain	PFU/ cell	Absolute	Relative	Increased[a]	Decreased[b]	Absolute
H2B	Vero	-	-	1.87 ± 0.15*	1.00 ± 0.07	19	16	-
		KOS	30	1.63 ± 0.22	0.90 ± 0.12	18	32	1.84 ± 0.19
		n12	30	1.43 ± 0.21	0.76 ± 0.12	5	25	1.94 ± 0.25
	U2OS	-	-	1.59 ± 0.12*	1.00 ± 0.06	9	15	-
		KOS	6	1.34 ± 0.07	0.85 ± 0.05	0	13	1.62 ± 0.18
			15	1.19 ± 0.08	0.79 ± 0.06	8	42	1.51 ± 0.10
		n12	30	1.26 ± 0.05	0.77 ± 0.03	0	6	1.65 ± 0.18
H3.3	Vero	-	-	2.05 ± 0.13*	1.00 ± 0.06	14	13	-
		KOS	30	4.12 ± 0.37	2.50 ± 0.22	70	0	1.75 ± 0.19
		n12	30	2.83 ± 0.25	1.47 ± 0.21	24	7	2.38 ± 0.28
	U2OS	-	-	2.61 ± 0.17*	1.00 ± 0.06	13	7	-
		KOS	6	3.78 ± 0.38	1.55 ± 0.16	33	0	2.50 ± 0.33
		n12	30	2.13 ± 0.22	0.85 ± 0.09	13	19	2.53 ± 0.21

TABLE 8.3 (A): Rate of initial fluorescence recovery of H2B and H3.3 in Vero and U2OS cells infected with HSV-1 strains KOS and n12.

[a] Percentage of cells in which the rate of initial fluorescence recovery was >1 SD above the average rate of initial fluorescence recovery in mock-infected cells.

[b] Percentage of cells in which the rate of initial fluorescence recovery was >1 SD lower than the average rate of initial fluorescence recovery in mock-infected cells.

* Average of all mock.

				7hpi				
				Rate of initial fluorescence recovery, %/s (avg ± SEM)		Fast chromatin exchange, % of cells		Mock (avg ± SEM)
Histone Variant	Cell Type	Virus Strain	PFU/ cell	Absolute	Relative	Increased[a]	Decreased[b]	Absolute
H2B	Vero	-	-	1.62 ± 0.10*	1.00 ± 0.06	20	15	-
		KOS	30	1.22 ± 0.11	0.77 ± 0.07	2	34	1.62 ± 0.12
		n12	30	1.26 ± 0.16	0.82 ± 0.11	10	45	1.53 ± 0.11
	U2OS	-	-	1.70 ± 0.12*	1.00 ± 0.06	15	15	-
		KOS	6	1.01 ± 0.05	0.55 ± 0.03	0	54	1.83 ± 0.16
			15	1.08 ± 0.11	0.63 ± 0.06	4	60	1.70 ± 0.16
		n12	30	1.20 ± 0.05	0.74 ± 0.03	0	9	1.62 ± 0.14
H3.3	Vero	-	-	2.31 ± 0.13*	1.00 ± 0.056	14	11	-
		KOS	30	2.99 ± 0.19	1.27 ± 0.07	20	1	2.53 ± 0.26
		n12	30	3.07 ± 0.26	1.15 ± 0.10	31	17	2.72 ± 0.21
	U2OS	-	-	2.77 ± 0.16*	1.00 ± 0.05	14	13	-
		KOS	6	3.09 ± 0.33	1.37 ± 0.18	33	7	2.42 ± 0.29
		n12	30	2.40 ± 0.36	0.91 ± 0.13	8	33	2.58 ± 0.23

TABLE 8.3 (B): Rate of initial fluorescence recovery of H2B and H3.3 in Vero and U2OS cells infected with HSV-1 strains KOS and n12.

[a] Percentage of cells in which the rate of initial fluorescence recovery was >1 SD above the average rate of initial fluorescence recovery in mock-infected cells.

[b] Percentage of cells in which the rate of initial fluorescence recovery was >1 SD lower than the average rate of initial fluorescence recovery in mock-infected cells.

* Average of all mock.

			4hpi				
			Rate of initial fluorescence recovery, %/s (avg ± SEM)		Fast chromatin exchange, % of cells		Mock (avg ± SEM)
Histone Variant	Virus Strain	PFU/ cell	Absolute	Relative	Increased [a]	Decreased [b]	Absolute
H2B	-	-	1.98 ± 0.17*	1.00 ± 0.07	13	9	-
	KOS	30	1.36 ± 0.12	0.72 ± 0.08	7	52	1.98 ± 0.17
	n12	30	1.76 ± 0.23	0.89 ± 0.10	10	31	1.98 ± 0.17
H3.3	-	-	2.52 ± 0.20*	1.00 ± 0.09	13	7	-
	KOS	30	3.34 ± 0.25	1.78 ± 0.25	33	0	2.30 ± 0.38
	n12	30	5.11 ± 0.41	2.15 ± 0.18	50	0	2.48 ± 0.31

TABLE 8.4 (A): Rate of initial fluorescence recovery of H2B and H3.3 in n-33 cells infected with HSV-1 strains KOS or n12.

[a] Percentage of cells in which the rate of initial fluorescence recovery was >1 SD above the average rate of initial fluorescence recovery in mock-infected cells.

[b] Percentage of cells in which the rate of initial fluorescence recovery was >1 SD lower than the average rate of initial fluorescence recovery in mock-infected cells.

* Average of all mock.

			7hpi				
			Rate of initial fluorescence recovery, %/s (avg ± SEM)		Fast chromatin exchange, % of cells		Mock (avg ±SEM)
Histone Variant	Virus Strain	PFU/ cell	Absolute	Relative	Increased [a]	Decreased [b]	Absolute
H2B	-	-	1.18 ± 0.08	1.00 ± 0.06	13	16	-
	KOS	30	1.34 ± 0.17	1.26 ± 0.17	33	11	1.06 ± 0.10
	n12	30	1.42 ± 0.17	1.37 ± 0.17	28	3	1.06 ± 0.01
H3.3	-	-	2.29 ± 0.18	1.00 ± 0.07	16	9	-
	KOS	30	2.80 ± 0.26	1.40 ± 0.14	35	4	2.80 ± 0.26
	n12	30	3.28 ± 0.26	1.48 ± 0.11	31	0	2.21 ± 0.33

TABLE 8.4 (B): Rate of initial fluorescence recovery of H2B and H3.3 in n-33 cells infected with HSV-1 strains KOS or n12.

[a] Percentage of cells in which the rate of initial fluorescence recovery was >1 SD above the average rate of initial fluorescence recovery in mock-infected cells.

[b] Percentage of cells in which the rate of initial fluorescence recovery was >1 SD lower than the average rate of initial fluorescence recovery in mock-infected cells.

* Average of all mock.

CHAPTER 9: DISCUSSION.

In this thesis, I demonstrate that linker and core histones are mobilized during HSV-1 infection. Mobilization of H1.2 resulted from changes to low-and high-affinity chromatin binding and led to a net increase in its free pool. H1.2 was mobilized to a basal degree under conditions of little to no HSV-1 gene expression (KM110 infection of Vero cells). This mobilization only required transcription competent (i.e. non-cross-linked) nuclear HSV-1 genomes. Basal mobilization of H1.2, however, did not result in a net increase in the level of free H1.2. Mobilization was further increased above the basal degree and the pool of free H1.2 increased only if IE and E HSV-1 proteins were expressed. Such increases were independent of HSV-1 genome replication or L proteins. Surprisingly, H1.2 mobility was inhibited under conditions of overexpression of all IE proteins, except for ICP4, in the absence of E proteins (n12 infection of Vero and U2OS cells). This inhibition of H1.2 mobility, however, still resulted in a marginal net increase in its free pool.

As with linker histones, core histones H2A, H2A.Z, H2B, H3.3, and H4 were mobilized during HSV-1 infection. This mobilization resulted in net increases in their free pools. The low-affinity chromatin exchange of these core histones, however, was differently affected by infection. The requirements for core histone mobilization indicate that at least two mechanisms mobilize core histones during infection (discussed below). These mechanisms have requirements similar to, as well as distinct from, those that result in H1 mobilization (discussed below).

HSV-1 genomes associate with histones during lytic infection in complexes that have the properties of unstable nucleosomes (Lacasse & Schang, 2010). However, HSV-1 genomes are not associated with histones when they first enter the nucleus (Oh & Fraser, 2008). Therefore, this association would require synthesis of new histones or the movement of pre-existing ones from domains containing cellular chromatin to those containing HSV-1 genomes. The later depletion of histones from replication compartments subsequently requires histone degradation, or movement of histones away from the domains containing the HSV-1 genomes. Histone synthesis is tightly regulated at transcriptional and post-transcriptional levels. Most histones are synthesized only during S-phase, whereas HSV-1 infects cells in any phase of the cell cycle and inhibits histone synthesis (Yager & Bachenheimer, 1988; Sorenson et al., 1991; Marzluff & Duronio, 2002; Kamakaka & Biggins, 2005; Gunjan et al., 2005; Jaeger, Barends, Giege, Eriani, & Martin, 2005). Histone levels consequently remain relatively constant during HSV-1 infection (Kent et al., 2004; Huang et al., 2006). Therefore, it is unlikely that the histones that bind to HSV-1 genomes are synthesized de novo in infected cells. Consistent with such conclusion, I found that linker and core histones are instead mobilized during infection.

The observed mobility of each somatic H1 variant in mock-infected Vero cells was consistent with previous reports (Th'ng et al., 2005). Based on average T_{50}, the H1 variants were classified into two groups. H1.4 and H1.5, which tend to associate with heterochromatin and have

longer C-terminal domains (CTDs), had significantly slower mobility than $H1^0$, H1.1, H1.2, and H1.3, which tend to associate with euchromatin ($H1^0$, H1.1, H1.2, and H1.3) or have shorter CTDs ($H1^0$, H1.1, H1.2) (Th'ng et al., 2005). Such consistency with previous results supports the suitability of my FRAP approach to evaluate H1 mobilization during HSV-1 infection.

H1 mobilization occurs through modulation of its binding to, and dissociation or displacement from, chromatin. Mobilization during infection may have resulted from promoting dissociation of H1.2 from chromatin, decreasing its affinity for chromatin binding, or competition for its binding sites. Posttranslational modifications (to H1 or core histones) and competition for binding sites both promote the dissociation of H1 from chromatin and decrease its rebinding affinity. Such modifications or competitions could therefore increase H1.2 free pools in infected cells.

Although H1.2 has not yet been directly shown to bind to HSV-1 genomes, it has a high affinity for naked DNA (Talasz, Sapojnikova, Helliger, Lindner, & Puschendorf, 1998). If H1.2 did bind to HSV-1 genomes, then the passage of transcription complexes could displace bound H1.2, increasing its free pool. However, transcription of HSV-1 IE genes (during n12-infections) resulted in only a marginal increase in free H1.2 only at early times (119 ± 5% at 4hpi vs. 102 ± 4% at 7hpi). In both Vero and U2OS cells, this increase was to the same degree as that which occurred during infection with KM110 ($P>0.05$, Tukey's HSD). Transcription is severely restricted during KM110 infection of Vero cells,

whereas it is only delayed during infection of U2OS cells. Therefore, high levels of HSV-1 genome transcription and overexpression of IE proteins (except for ICP4) during n12 infection did not suffice to further increase the pool of free H1.2 above the level which occurred under conditions of little to no HSV-1 gene transcription or protein expression. Passage of transcription complexes along IE genes is therefore not sufficient to displace H1.2 to an extent that results in a net increase in its free pool. However, IE loci represent a small percentage of the HSV-1 genome. Transcription of all HSV-1 genes, as during productive infection, may therefore still contribute to a net increase in the pool of free H1.2.

HSV-1 proteins may also directly affect the interactions between histones and HSV-1 genomes. For example, VP16 recruits histone acetyltransferases and promotes removal of H3 from IE gene promoters (Tumbar et al., 1999; Memedula & Belmont, 2003; Herrera & Triezenberg, 2004). Both acetylation and removal of core histones promote dissociation of linker histone H1 from chromatin. VP16 may therefore inhibit binding of mobilized H1.2 to HSV-1 genomes and promote the disassociation of H3.3 bound to HSV-1 genomes. Consistent with such a model, free H1.2 did not increase and free H3.3 was only marginally increased in the absence of VP16 (and HSV-1 transcription). Also consistent with such a model, H1.2 was not mobilized by infection with UV-inactivated HSV-1 virions, and the VP16 in the input virions did not induce increases in free H1.2 or free H3.3 (at early times). VP16 was not essential to increase the levels of free H1.2 or H3.3 in U2OS cells. However, the increases in free H1.2 and H3.3 were

still significantly greater in n212- than in KM110- infections (1.84 and 1.49 fold, respectively, for H1.2; 1.83 and 1.56 fold, respectively for H3.3; $P<0.01$). These strains only differ in the inactivation of VP16 in the latter. VP16 may therefore contribute to the increases in free H1.2 or H3.3, even in U2OS cells.

H1.2 low and high-affinity chromatin binding was increased during n12 infections. Overexpression of all IE proteins except for ICP4 in the absence of E proteins decreased the rates of low- and high-affinity H1.2 chromatin exchange. These results suggest that the truncated ICP4 expressed during n12 infection, or mislocalization of ICP0 to the cytoplasm, inhibits H1.2 chromatin exchange. ICP0 interacts with many proteins. The proteins that mediate H1.2 chromatin exchange, or alter H1.2 chromatin affinity through posttranslational modifications (to H1 or to core histones), may also be mislocalized to the cytoplasm due to direct or indirect interaction with ICP0. Alternatively, such inhibition may be due to direct or indirect interactions with truncated ICP4. If ICP0 or ICP4 were to promote H1.2 mobilization through interactions with chromatin modifying proteins that mobilize H1.2, then mislocalization of ICP0 and any associated chromatin modifying proteins to the cytoplasm, or binding to truncated ICP4, could inhibit H1.2 mobility.

ICP0 is not required for H1.2 mobilization, however, which suggests that it does not positively regulate H1.2 mobility. Nonetheless, ICP0 could still negatively affect H1.2 mobilization. The potential regulation of H1.2 mobility by ICP4 has yet to be determined. Alternatively, high levels of ICP27 expressed during n12 infection could

negatively regulate H1.2 chromatin exchange or proteins that mediate H1.2 chromatin exchange.

Productive HSV-1 infection activates the cellular DNA damage response (Wilkinson & Weller, 2004; Shirata et al., 2005; Wilkinson & Weller, 2006). H1.2 has been reported to translocate to the cytoplasm following double-strand breaks (Konishi et al., 2003; Okamura, Yoshida, Amorim, & Haneji, 2008). Mobilization of H1.2 during HSV-1 infection could therefore be the result of activation of DNA damage responses and subsequent release of H1.2. However, GFP-H1.2 fusion proteins were undetectable in the cytoplasm at any time post infection. GFP-H1.2 was still strictly nuclear even at late times after infection in cells in which ICP4 was detected in the cytoplasm. Moreover, the late enhanced mobilization of H1.2 and the increase in its free pool were not affected by PAA, whereas only NBS1 has been reported activated during HSV-1 infection in the presence or absence of PAA (Wilkinson & Weller, 2004; Shirata et al., 2005; Wilkinson & Weller, 2005). It is therefore unlikely that the mobilization of H1.2 during HSV-1 infection is the result of activation of DNA damage responses.

H1.2 T_{50} was decreased up to less than half (42%) of that in mock-infected cells. Such degree of mobilization has previously been reported in cells treated with tricostatin A (TSA), a histone deacetlyase (HDAC) inhibitor (Yoshida, Kijima, Akita, & Beppu, 1990). TSA globally increases the levels of core histone acetylation, which in turn promotes the dissociation of H1 from chromatin. $H1^0$-GFP and H1.1-GFP were mobilized in TSA treated cells, such that their recovery of fluorescence

occurred in 45-60% of the time required in untreated cells (Misteli et al., 2000). However, H1 mobilization in HSV-1 infected cells is unlikely to be due to a global increase in core histone acetylation. Although the global levels of histone acetylation (of H3K9 and H3K14) are elevated up to 1.5 fold at 10hpi, they are not changed (or perhaps even modestly decreased) at 4 and 7hpi, when H1 was already significantly mobilized (Kent et al., 2004). Moreover, even though ICP0 inhibits HDACs, such inhibition does not increase the global level of core histone acetylation (Lomonte et al., 2004), neither was ICP0 required for H1.2 mobilization.

Like acetylation of core histones, phosphorylation of H1 destabilizes its binding to chromatin and therefore results in its mobilization. The binding of H1.1 phosphomimetic mutants to chromatin is destabilized such that their T_{50} is decreased up to 50% of wild-type (Hendzel, Lever, Crawford, & Th'ng, 2004). Competition for H1 binding sites is yet another mechanism of H1 mobilization. High mobility group (HMG) proteins compete for H1 binding sites and thus mobilize H1 (Catez et al., 2002; Catez et al., 2004). Microinjection of different HMG proteins decreased GFP-$H1^0$ T_{40} to 36-56% of control, depending on the specific HMG type (Catez et al., 2004). Changes in HMG function or nuclear localization during HSV-1 infection could therefore affect H1 mobilization.

H1 binding to chromatin promotes the formation of higher order, more compact, structures. Late in infection, cellular chromatin becomes marginalized (Monier et al., 2000; Simpson-Holley et al., 2004; Simpson-Holley et al., 2005). It is therefore particularly surprising that H1.2 and

core histones are mobilized, and their free pools are increased, precisely at these at late times. Even at these late times, however, cellular chromatin remains accessible. Consistently, J. Lacasse demonstrated that cellular chromatin remains accessible to MCN digestion even at late times during HSV-1 infection (Lacasse & Schang, 2010). In fact, cellular chromatin from HSV-1 infected cells is digested faster than that from mock-infected cells. Such faster digestion is consistent with increased core histone exchange and chromatin accessibility. The marginalization of cellular chromatin therefore does not likely involve the formation of more compact chromatin structures at seven to eight hours after infection.

The nuclear morphological changes during HSV-1 infection could affect histone mobilization. The nuclear volume expands to up to twice its original size during approximately the first ten hours of infection (Monier et al., 2000; Simpson-Holley et al., 2005). Viral replication compartments form and occupy additional volume during this expansion. Histone mobilization involves diffusion through the nucleoplasm to new potential binding sites. Changing the distance between binding sites would therefore affect histone mobilization. If the increases in nuclear volume were greater than the volume occupied by replication compartments, then the relative distance between histone binding sites would increase. Histones could thus be mobilized just because of the increased diffusion time between binding events. This hypothesis, however, is not well supported by the kinetics of histone diffusion, approximately $25\mu m^2 \times sec^{-1}$, which is too fast to be affected by the

relatively small changes in distance between binding sites in infected cells. Neither was this hypothesis supported by my experimental results. For example, H1.2 mobilization did not correlate with the formation of replication compartments. Less than 2% of Vero cells infected with KM110 had replication compartments at early or late times post infection, whereas approximately 30 to 40% of them had a high degree of H1.2 mobilization. A similar trend was observed in infections with n212 at early times after infection. Whereas 44% of Vero cells had a high degree of H1.2 mobilization, and 35% a large increase in free H1.2, only 11% had replication compartments. Furthermore, replication compartments were formed in a similar percentage of Vero cells at late times post infection with n212 as at early times post infection with KOS (56% and 52%, respectively). However, a greater percentage of n212-infected cells had a high degree of H1.2 mobilization (83%) and large increase in free H1.2 (75%) at late times than KOS-infected cells at early times (61% and 52%, respectively). The altered nuclear morphology is therefore not a major contributing factor to H1.2 mobilization, although it may still affect it. A similar analysis was not possible for core histone mobilization because I only evaluated mobilization of the populations of histones that would be available to bind to HSV-1 genomes, namely those in the free pool and those undergoing fast chromatin exchange.

All core histones evaluated (H2A, H2A.Z, H2B, H3.3, and H4) were mobilized during HSV-1 infection. Although I did not attempt to assess the mechanisms for such mobilization, posttranslational modifications alter histone affinity for DNA. For example, acetylation of core histones

decreases their positive charges and thus decreases their affinity for negatively charged DNA. Reduced affinity between histones and DNA contributes to increase the chromatin exchange of core histones (Ito et al., 2000). Core histone acetylation is associated with non-condensed chromatin structures (euchromatin) and processes that require chromatin exchange, such as transcription or DNA replication. Acetylation could therefore contribute to core histone mobilization during HSV-1 infection. Consistent with such a model, ICP0 disrupts HDAC complexes and ICP0 and VP16 interact with HATs (Tumbar et al., 1999; Memedula & Belmont, 2003; Lomonte et al., 2004; Herrera & Triezenberg, 2004; Gu et al., 2005; Gu & Roizman, 2007; Cliffe & Knipe, 2008). Such interactions, however, do not alter the global levels of acetylation. At 10h after infection, acetylation levels are increased up to 1.5 fold (Kent et al., 2004). In contrast, they are modestly decreased at earlier times, when linker and core histones are already mobilized (Kent et al., 2004). If acetylation is a contributing factor to core histone mobilization, then the basal acetylation levels are sufficient for such mobilization. Alternatively, if a subset of histones were differentially acetylated during infection, such changes may contribute to histone mobilization. Such specific changes would likely not be detected by examining global levels of histone acetylation. Acetylation of different histone residues has different functional significance. Evaluation of the global acetylation levels wouldn't detect any residue-specific changes in acetylation during infection. On the other hand, evaluation of potential changes to acetylation of specific residues requires the previous

identification of the relevant ones. Therefore, changes in acetylation or acetylation of specific residues that mobilize histones during infection may have yet to be analyzed.

The recruitment of HATs to HSV-1 promoters was proposed to be required for gene expression early during infection (Tumbar et al., 1999; Memedula & Belmont, 2003; Herrera & Triezenberg, 2004). However, HSV-1 gene expression was not decreased, it was rather marginally increased, in cells in which HATs were knocked down by siRNAs (Kutluay et al., 2009). Depletion of HATs, however, would decrease the acetylation of any histones associated with HSV-1 genomes and also of all the histones associated with cellular chromatin. Knocking down HATs would therefore be expected to decrease the mobilization of core histones from cellular chromatin. Such an effect would result in less core histones available to bind to HSV-1 genomes. The consequent decrease in histone occupancy on HSV-1 genes would then result in less-condensed chromatin structures. Such overtly accessible chromatin would permit access of transcription proteins, even in absence of chromatin modifying proteins (such as HATs or chromatin remodeling proteins) that would otherwise be required to open the chromatin structure of the HSV-1 promoters. Therefore, manipulation of global histone acetylation may not be an appropriate approach to evaluate the local effects of histone acetylation at HSV-1 promoters.

HSV-1 genomes likely enter the nucleus associated with polyamines (Gibson & Roizman, 1971). When and how polyamines are removed is unclear, but removal must occur before HSV-1 transcription

starts. The association of HSV-1 genomes with histones could involve replacement of polyamines with histones. It could also involve assembly of nucleosomes on naked DNA following polyamine removal. Usually, nucleosome assembly is coupled with processes such as transcription or DNA replication. However, nucleosomes are apparently associated with HSV-1 genomes prior to HSV-1 gene transcription or DNA replication. How histones are initially assembled into nucleosomes on input HSV-1 genomes is unclear. Replacement of polycations such as polyamines with nucleosomes and assembly of nucleosomes with naked DNA are not common processes in somatic nuclei. However, a somewhat similar process occurs in germ cells during fertilization. The sperm DNA released into the egg is condensed with protamines, small basic proteins with structural similarities to polyamines. Prior to DNA replication, the male DNA requires decondensation, removal of protamines, and assembly into chromatin. The histone chaperone HIRA is essential for this chromatin assembly on the male DNA during decondensation (Loppin et al., 2005). In contrast to transcription associated chromatin assembly, HIRA assembles H3.3 into nucleosomes on male DNA independent of ASF1 (Bonnefoy, Orsi, Couble, & Loppin, 2007). HIRA mediates chromatinization of the sperm DNA, but it is not required for removal of associated protamines (Bonnefoy et al., 2007). The assembly of nucleosomes and removal of protamines are therefore two distinct processes. The potential for HIRA mediated nucleosome assembly on input HSV-1 genomes is therefore also likely independent of whether the genomes enter the nucleus associated with polyamines or not. HIRA is

also expressed in somatic cells. However, the mechanisms by which HIRA assembles nucleosomes during sperm decondensation may be different from those that normally occur during replication independent chromatin assembly. Consistent with a model postulating HIRA mediated deposition of H3.3 containing nucleosomes onto parental HSV-1 genomes, H3.3 is associated with HSV-1 genomes at early times post infection (Placek et al., 2009). Such association is proposed to contribute to HSV-1 replication, in that depletion of HIRA inhibits HSV-1 gene expression (Placek et al., 2009). However, HIRA depletion globally affects H3.3 chromatin exchange. Such knockdown therefore also indirectly affects cellular transcription. Global HIRA depletion is therefore not likely a suitable approach to study the localized assembly of nucleosomes on input HSV-1 genomes.

The data presented in this thesis suggests that there are at least two mechanisms of chromatin exchange that mobilize core histones during HSV-1 infection. Mobilization of core histones H2A, H2A.Z, H2B, H3.3, and H4 led to a net increase in their free pools. The low-affinity chromatin exchange of these core histones, however, was differently affected by infection. H2A and H3.3 tended to have increased rates of low-affinity chromatin exchange, whereas H2A.Z and H2B tended to have decreased rates of low-affinity chromatin exchange, and the low-affinity chromatin exchange of H4 was not obviously affected by infection.

H3.3 was mobilized to a basal degree under conditions of little to no HSV-1 protein expression (KM110 infection of Vero cells) or under conditions of overexpression of all IE proteins except for ICP4 in the

absence of E proteins (n12 infections of Vero cells). Such mobilization resulted in only a marginal net increase in the pool of free H3.3. This marginal increase in free H3.3 therefore required only nuclear, transcription competent (i.e. non-cross-linked) HSV-1 genomes. The low-affinity chromatin exchange of H3.3 tended to be differentially altered whether HSV-1 proteins were expressed or not. Under conditions of little to no HSV-1 protein expression, the relative rate of H3.3 low-affinity chromatin exchange was not significantly altered. When all IE proteins except for ICP4 were overexpressed in the absence of E proteins, however, the relative rate of H3.3 low-affinity chromatin exchange had a tendency to be increased at early times after infection. Nonetheless, the apparent differences in the relative rates of low-affinity H3.3 chromatin exchange under these conditions were not statistically significant. Like H1.2, H3.3 was mobilized to a greater degree when HSV-1 IE and E proteins were expressed. This enhanced mobility led to a net increase in the pool of free H3.3 and increased the rate of H3.3 low-affinity chromatin exchange. Perhaps surprisingly, the enhanced mobility of H3.3 was independent of HSV-1 DNA replication or L proteins. Neither ICP0 nor VP16 were required to increase the pool of free H3.3. The pool of free H3.3 was increased to a large degree during infections with n212. However its rate of fast chromatin exchange was not. These results suggest that ICP0 may alter the fast chromatin exchange of H3.3.

The mobilization of H2B was largely independent of HSV-1 transcription. The pool of free H2B was increased even in under conditions of little to no HSV-1 gene expression (KM110 infection of Vero

cells). This increase was to the same degree as that which occurred during infections in which all HSV-1 IE proteins except for ICP4 are overexpressed in the absence of E proteins ($P>0.05$, Tukey's HSD). Thus, HSV-1 transcription or protein expression is not required to increase the pool of free H2B. The increase to the pool of free H2B was larger, however, when HSV-1 IE or E proteins were expressed. As for H3.3, this larger increase to the level of free H2B was independent of HSV-1 DNA replication or L proteins.

Mobilization of H2B during HSV-1 infection resulted in a decreased rate of H2B fast chromatin exchange. Under conditions in which all IE proteins except ICP4 are overexpressed in the absence of E proteins, the rate of H2B fast chromatin exchange was also decreased. This suggests that HSV-1 transcription or IE proteins other than ICP4 could be sufficient for such mobilization. However, the fast chromatin exchange rate of H2B was also decreased to a similar extent during KM110 infection of Vero cells, in which there is little to no HSV-1 transcription or protein expression. Moreover, the fast chromatin exchange rate of H2B in U2OS cells was decreased to a similar degree during n12 and KM110 infections. These results indicate that the rate of H2B fast chromatin exchange is actually independent of HSV-1 transcription, or of ICP0. Taken together, these data suggest that transcription competent HSV-1 genomes are sufficient to decrease the rate of fast H2B chromatin exchange. Alternatively, HSV-1 virion binding and fusing to the host cell, capsid or tegument proteins, or HSV-1 genome delivery to the nucleus may be sufficient.

The fast chromatin exchange of H3.3 and its free pool were increased already at early times. The fast chromatin exchange of H2B, in contrast, was decreased at later times and the pool of free H2B tended to be increased to a greater degree also at later times. Thus, the substantial changes in H2B chromatin exchange are more evident at later times after infection. However, the substantial changes in H3.3 chromatin exchange peaked at early times after infection, and tended to diminish at later times. Thus, different mechanisms appear to mobilize H3.3 or H2B.

Nucleosomes that contain H2A.Z and H3.3 are most unstable (Jin & Felsenfeld, 2007). I therefore proposed that unstable H3.3 containing nucleosomes mobilized during HSV-1 infection might also contain H2A.Z. However, my data did not support this hypothesis. The mobilization of H2A.Z during HSV-1 infection was most similar to that of H2B, whereas that of H2A was most similar to H3.3. As for H2B, the free pool of H2A.Z was increased with a tendency for the rate of fast H2A.Z chromatin exchange to be decreased. These results are consistent with mobilization of H2B/H2A.Z dimers during HSV-1 infection. The fast chromatin exchange of H2B is associated with transcription. The decreased rate of H2B/H2A.Z fast chromatin exchange during infection suggests that the majority of these dimers are mobilized from cellular chromatin, in which transcription is inhibited. Considering this new model, I would test in the future whether the mobilization of H2A.Z has similar requirements as that of H2B.

Histone exchange typically occurs during DNA replication, transcription, or DNA repair. The mobilization of linker histone H1.2 and core histones H2B and H3.3 during HSV-1 infection was independent of HSV-1 DNA replication. An alternative, if unlikely, scenario is that the cellular DNA damage responses activated by inhibition of HSV-1 DNA replication with PAA mobilizes histones to the same degree as they would have been mobilized by HSV-1 DNA replication in the absence of PAA. The increase in the chromatin exchange of linker and core histones during HSV-1 infection is therefore most likely not due to mechanisms of chromatin exchange associated with DNA replication. Cellular transcription is inhibited during HSV-1 infection, and basal mobilization of linker and core histones is independent of HSV-1 gene transcription. Therefore, transcription associated mechanisms of chromatin exchange are also not likely major contributing factors to histone mobilization during HSV-1 infection. Furthermore, typical DNA damage signaling cascades are disrupted during infection with HSV-1. Taken together, this evidence strongly suggests that histone mobilization also does not occur through mechanisms of chromatin exchange associated with DNA repair. Mobilization of linker and core histones during HSV-1 infection therefore likely represents a new mechanism of chromatin exchange.

Chromatin exchange in non-infected cells is a balance between nucleosome assembly and disassembly. The equilibrium of chromatin exchange maintains a steady state level of free core histones. Non-chromatinized DNA, such as HSV-1 genomes, would initially interact with histones in the free pool and therefore deplete the levels of free

histones. Such depletion may shift the balance between chromatin assembly and disassembly towards disassembly to replenish the free pools. A shift in the equilibrium of chromatin exchange would thus mobilize histones. Depletion of the levels of free core histones could also trigger a "foreign DNA response". Mobilization of histones may replenish, and even increase, the levels available in the free pool to maintain a population of histones available to bind foreign DNA.

During HSV-1 infection, the chromatin exchange of each core histone evaluated (H2A, H2A.Z, H2B, H3.3, and H4) was increased. This increase was maintained even at later times after infection when core histones are depleted from HSV-1 replication compartments (Monier et al., 2000; Simpson-Holley et al., 2004; Simpson-Holley et al., 2005). Furthermore, only HSV-1 genomes that are not associated with histones are packaged into capsids (Oh & Fraser, 2008). Even at late times, however, histone chromatin exchange continues to occur. Chromatin exchange is a balance of histone binding and unbinding. If binding or unbinding were completely prevented, this would be detected as changes to the steady state levels of histone available in the free pool. Inhibition of free histone re-binding would be detected as an increase in the free pool with no measureable chromatin exchange. Conversely, inhibition of histone unbinding would be detected as a decrease in the free pool with no measureable chromatin exchange. Thus, mobilized histones continue to bind and unbind chromatin even at late times after infection. Nonetheless, depletion of histones from replication compartments suggests that unbound histones are less likely to re-bind DNA in this

nuclear domain. What prevents histones from rebinding to HSV-1 genomes, or removes them if already bound is presently unknown.

HSV-1 gene transcription and DNA replication are actively proceeding at late times after infection. Moreover, replication compartments contain DNA binding proteins, including ICP4. High genome occupancy of non-histone proteins, transcription and DNA replication complexes, and passage of transcription or DNA replication complexes along HSV-1 genomes may all promote the removal of associated histones and block re-association of unbound histones. The tegument protein VP22 inhibits TAF-1 mediated histone deposition onto naked DNA (van Leeuwen et al., 2003). VP22 localizes to nuclear foci at late times after infection, even though it is assembled into progeny virions in the cytoplasm (Morrison, Stevenson, Wang, & Meredith, 1998; Mettenleiter, 2006). These data suggest that nuclear VP22 may inhibit reassembly of nucleosomes on HSV-1 genomes at late times after infection.

HSV-1 genomes within the capsid are associated with polyamines (Gibson & Roizman, 1971). Although it is not yet known when HSV-1 genomes first become associated with polyamines, such association would also preclude their association with histones.

At late times after infection, enhanced histone mobilization in combination with reduced affinity for binding to HSV-1 genomes would decrease the retention of histones in replication compartments. A decrease in the affinity of histones for binding to HSV-1 genomes would increase the likelihood that free histones would instead associate with

cellular chromatin. The preferential association of unbound histones with cellular chromatin, rather than HSV-1 genomes, may therefore contribute to the relative depletion of free histones from replication compartments at late times.

Why histones are mobilized, how are they mobilized, and the viral or cellular factors that mobilize them remain unclear. Chromatinization of HSV-1 genomes may be beneficial to viral replication. Cellular transcription proteins and the process of transcription are closely associated with chromatin. Transcriptionally active genes are identified by posttranslational modifications to associated histones, and transcription proteins are recruited to these loci through interactions with such modifications. The cellular transcription proteins normally transcribe through chromatin, which involves chromatin disassembly and reassembly. Therefore, adoption of the host transcriptionally active gene structure may promote recruitment of the host transcription proteins and therefore transcription of HSV-1 genes. HSV-1 proteins may therefore mobilize histones to increase the population available for assembling nucleosomes with HSV-1 genomes. Alternatively, infected cells may attempt to silence HSV-1 gene expression through assembly of repressive chromatin on HSV-1 genomes. Then cellular factors would mobilize histones to increase the population of histones available to assemble into nucleosomes on HSV-1 genomes in an attempt to silence the viral gene expression. In such a scenario, HSV-1 proteins may further mobilize histones to prevent or inhibit cellular silencing attempts.

The data presented in this thesis supports the mobilization of histones by both cellular and viral factors. Basal mobilization of linker and core histones is independent of HSV-1 protein expression and HSV-1 proteins in virions are not sufficient to induce it. These data suggest that basal mobilization of histones is a cellular response to transcription competent HSV-1 genomes. Enhanced mobilization of histones, in contrast, requires expression of HSV-1 IE or E proteins. Thus, HSV-1 IE or E proteins, or a cellular response to them, further mobilize histones. The requirements for linker and core histone mobilization support the existence of several mechanisms that mobilize histones during HSV-1 infection. The differential mobilization of H1, H2B, and H3.3, as well as their different requirements for mobilization, suggest that they likely represent such different mobilization mechanisms.

Based on the data presented in this thesis, I propose the following model. Immediately after nuclear entry of HSV-1 genomes and prior to HSV-1 gene expression, the chromatin exchange rate of H1 and the pools of free H2B and H3.3 are slightly increased by cellular mechanisms (Figure 9.1 Panel B). This "basal" mobilization of histones would be a cellular response to infection to silence gene expression from foreign DNA. However, such basal mobilization of histones is not sufficient to silence HSV-1 IE gene expression because IE genes are still expressed when histones are mobilized to this degree. HSV-1 IE gene transcription is initiated soon after HSV-1 genomes enter the nucleus. Therefore, the establishment of repressive chromatin structures on HSV-1 IE promoters or genes would be precluded or prevented by the occupancy of

transcription factors and proteins at such loci. Consequently, HSV-1 IE proteins are expressed, inducing expression of E genes and resulting in further histone mobilization (Figure 9.1 Panel C), increasing the pools of free H1.2 and H3.3, and the fast chromatin exchange rate of H3.3. This further mobilization of H1.2 likely requires VP16 or ICP4, whereas that of H3.3 likely also requires ICP0. Such requirements are consistent with a model in which further mobilization of H1.2 and H3.3 is required for E gene expression. No enhanced mobilization of H1.2 and H3.3 correlated with no E gene expression. The enhanced histone mobilization may counteract or prevent the cellular attempts to silence HSV-1 gene expression. When all HSV-1 proteins are expressed HSV-1 DNA replication is highly active, histones are further mobilized. The chromatin exchange and free pool of H1.2, and the pools of free H2B and H3.3, are all further increased (Figure 9.1 Panel D). This later mobilization requires expression of ICP4 or E proteins, and may promote the removal of histones from HSV-1 genomes prior to their encapsidation. Alternatively, the enhanced mobility of histones at later times may be the result of high levels of ICP4 expression at such times.

Regardless of the effects of histone mobilization during HSV-1 infection, such mobilization is a novel consequence of cell-virus interactions. Mobilization of histones was a surprising, and unpredicted, discovery. Histone mobilization has never been described during infections with any other viruses. Therefore, this observation was unanticipated. Such mobilization of histones during HSV-1 infection represents a novel cellular response to viral infection. Moreover, the

discovery of histone mobilization addresses a previously unexplored aspect of HSV-1 infection. It was known that histones associated with HSV-1 genomes during infection. However, the source of the histones that associate with HSV-1 genomes was not considered. My discovery that histones are mobilized during HSV-1 infection provides an explanation for the source of histones that associate with HSV-1 genomes.

The data presented in this thesis suggest that the chromatin exchange mechanisms that mobilize histones during HSV-1 infection are likely different from the classical mechanisms associated with transcription, DNA replication, and DNA repair in non-infected cells. Chromatin exchange involves the dynamic transfer of histones between nucleosomes and histone chaperones. The likely novel mechanism of chromatin exchange during HSV-1 infection may or may not involve the transfer of histones to novel complexes containing histone chaperones. I would first evaluate the sizes of the freely diffusing complexes containing histones during HSV-1 infection. This would determine whether or not they are similar to the freely diffusing histone-chaperone complexes in uninfected cells.

Several histone chaperones typically bind to certain histones. For example, CAF-1 binds to H3.1/H4 dimers, whereas HIRA binds to H3.3/H4 dimers. Other histone chaperones bind to several different histones. For example ASF-1 binds to H3.1/H4 or H3.3/H4 dimers, and NAP-1 binds to linker histone H1, H2A/H2B dimers, or H3/H4 dimers. I would immunoprecipitate histones to identify the proteins that interact

with the mobilized histones, including histone chaperones, during HSV-1 infection.

I would next evaluate the mobility of histone chaperones identified by immunoprecipitation. If the histone chaperones are indeed complexed with mobilized histones, they should have similar mobilization and similar requirements for mobilization. Identification of the histone chaperones and other proteins associated with mobilized histones is a first step towards identification of the proteins that increase chromatin assembly and disassembly to mobilize histones during HSV-1 infection.

The data presented in this thesis demonstrates that expression of HSV-1 IE or E proteins enhances the mobilization of H1, H2B, and H3.3. I would next aim to identify the HSV-1 proteins required for this enhanced mobilization. HSV-1 encodes only five IE proteins, four of which (ICP0, ICP4, ICP22, and ICP27) regulate HSV-1 gene expression. As an initial step to identify the HSV-1 proteins required, I would evaluate whether transient expression of IE proteins is sufficient to mobilize histones. I would first evaluate the IE proteins known to regulate HSV-1 gene expression, ICP0, ICP4, ICP22, and ICP27. If these proteins were not sufficient I would then test whether ICP47, which is not implicated in regulating HSV-1 gene expression, mobilizes histones in a last effort prior to evaluating E proteins. If E proteins are required for histone mobilization, I would then take a rational approach to identify such proteins.

FIGURE 9.1: A model for the mobilization of linker and core histones during HSV-1 infection. A) Histone incorporation in cellular chromatin is dynamic. Those histones already associated with chromatin normally disassociate, diffuse through the nucleoplasm, and reassociate at a different site. **B)** Early after HSV-1 genome nuclear entry and prior to HSV-1 protein expression, linker histones, for example H1.2, and core histones, for example H2B and H3.3, are mobilized to a basal degree, increasing the chromatin exchange rate of H1.2 and the pools of free H2B and H3.3. This mobilization is the result of cellular mechanisms, and may be a cellular antiviral response aimed at silencing input HSV-1 genomes. **C)** When HSV-1 IE proteins are expressed, linker histone H1.2 and core histone H3.3 are further mobilized, increasing the pools of free H1.2 and H3.3, and the rate of H3.3 fast chromatin exchange. This enhanced mobilization of H1.2 requires VP16 or ICP4, and that of H3.3 likely also ICP0. Enhanced histone mobilization may counteract cellular silencing attempts. Consistently, it may be required to activate HSV-1 E gene expression. **D)** At late times after infection when all HSV-1 proteins are expressed and HSV-1 DNA replication is actively ongoing, linker histone H1.2 and core histones H2B and H3.3 are even further mobilized, increasing the fast chromatin exchange of H1.2 and the pools of free H1.2, H2B, and H3.3. This later histone mobilization requires ICP4 or expression of E proteins. Late histone mobilization may promote the removal of histones associated with HSV-1 genomes such that they can be encapsidated.

A.

Normal cell

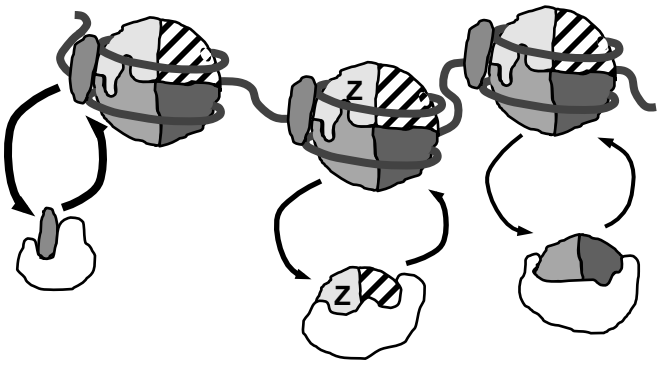

B.

Immediately after nuclear entry (prior to IE protein expression)

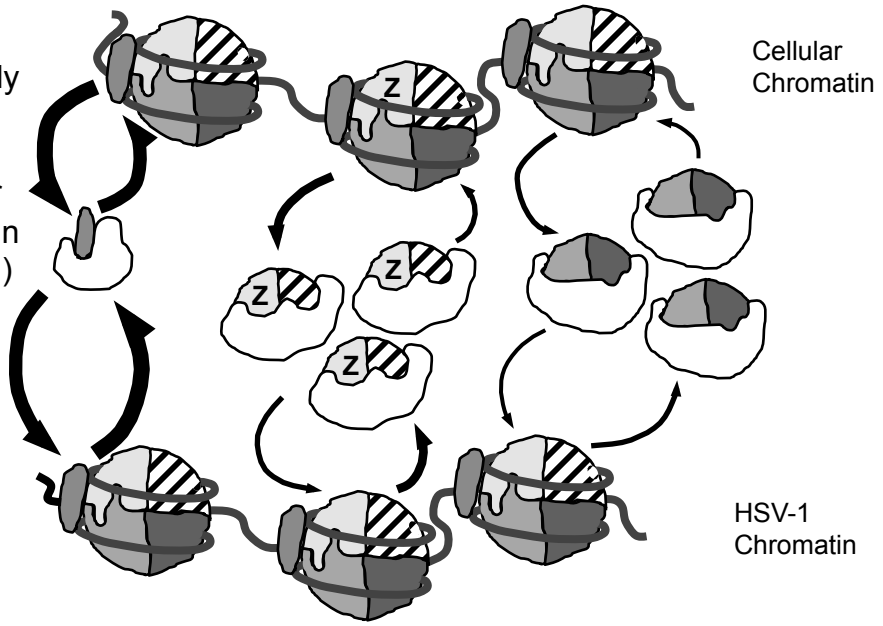

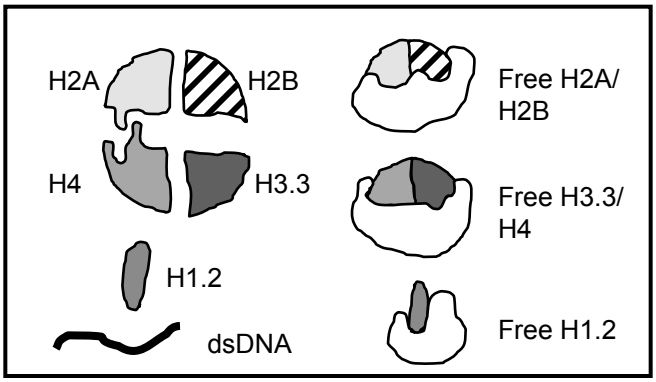

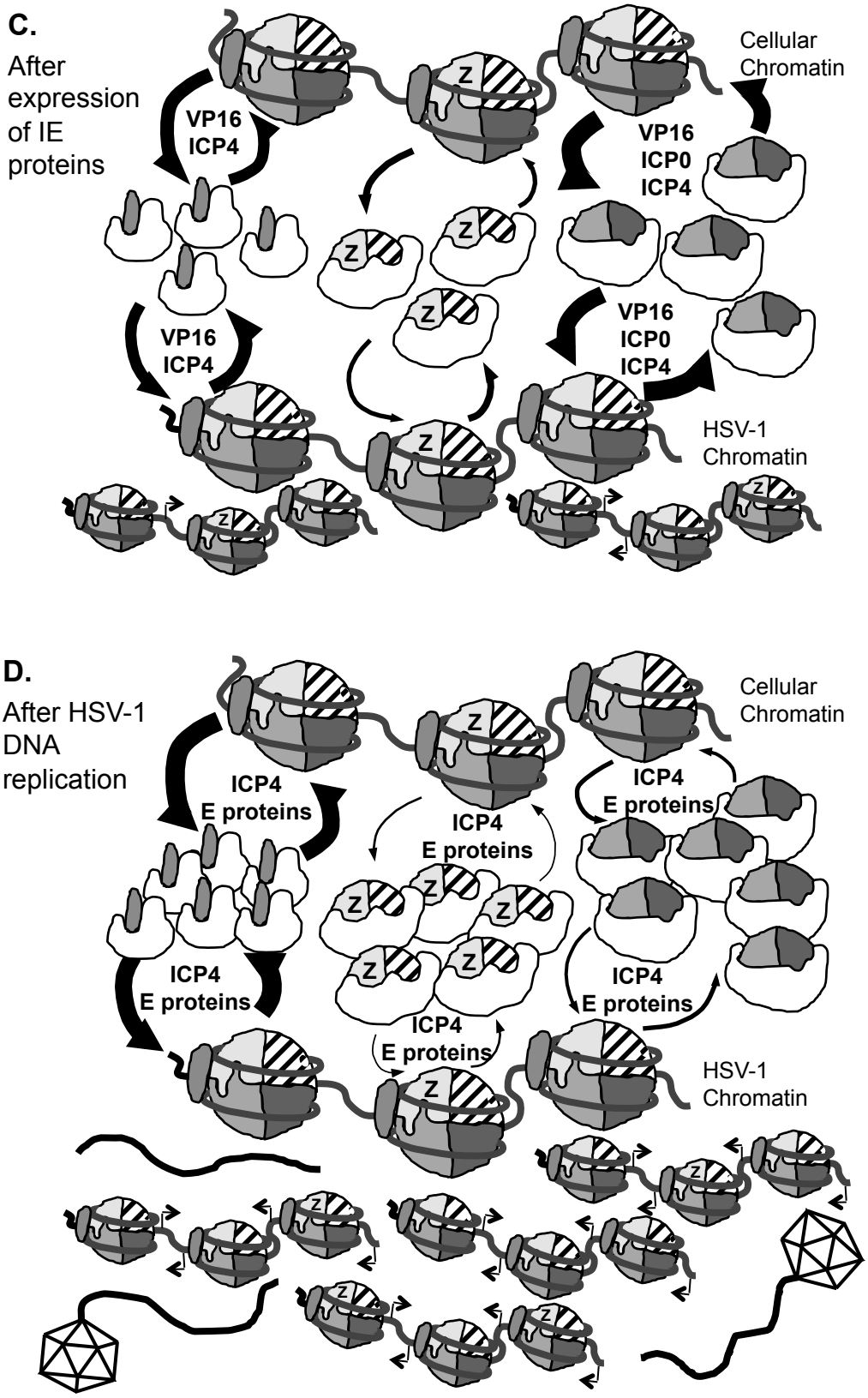
C.
After expression of IE proteins
Cellular Chromatin
VP16
ICP4
VP16
ICP0
ICP4
VP16
ICP4
VP16
ICP0
ICP4
HSV-1 Chromatin
Z
D.
After HSV-1 DNA replication
Cellular Chromatin
ICP4
E proteins
ICP4
E proteins
ICP4
E proteins
ICP4
E proteins
ICP4
E proteins
ICP4
E proteins
HSV-1 Chromatin
Z

REFERENCES

Abbott, D. W., Laszczak, M., Lewis, J. D., Su, H., Moore, S. C., Hills, M. et al. (2004). Structural characterization of macroH2A containing chromatin. *Biochemistry*, *43*(5), 1352-1359.

Adkins, M. W., & Tyler, J. K. (2004). The histone chaperone Asf1p mediates global chromatin disassembly in vivo. *J Biol Chem*, *279*(50), 52069-52074.

Albig, W., Kioschis, P., Poustka, A., Meergans, K., & Doenecke, D. (1997). Human histone gene organization: nonregular arrangement within a large cluster. *Genomics*, *40*(2), 314-322.

Alekseev, O. M., Bencic, D. C., Richardson, R. T., Widgren, E. E., & O'Rand, M. G. (2003). Overexpression of the Linker histone-binding protein tNASP affects progression through the cell cycle. *J Biol Chem*, *278*(10), 8846-8852.

Alvelo-Ceron, D., Niu, L., & Collart, D. G. (2000). Growth regulation of human variant histone genes and acetylation of the encoded proteins. *Mol Biol Rep*, *27*(2), 61-71.

Amelio, A. L., McAnany, P. K., & Bloom, D. C. (2006). A chromatin insulator-like element in the herpes simplex virus type 1 latency-associated transcript region binds CCCTC-binding factor and displays enhancer-blocking and silencing activities. *J Virol*, *80*(5), 2358-2368.

Angelov, D., Molla, A., Perche, P. Y., Hans, F., Cote, J., Khochbin, S. et al. (2003). The histone variant macroH2A interferes with transcription factor binding and SWI/SNF nucleosome remodeling. *Mol Cell*, *11*(4), 1033-1041.

Arthur, J. L., Scarpini, C. G., Connor, V., Lachmann, R. H., Tolkovsky, A. M., & Efstathiou, S. (2001). Herpes simplex virus type 1 promoter activity during latency establishment, maintenance, and reactivation in primary dorsal root neurons in vitro. *J Virol*, *75*(8), 3885-3895.

Ascoli, C. A., & Maul, G. G. (1991). Identification of a novel nuclear domain. *J Cell Biol*, *112*(5), 785-795.

Bao, Y., Konesky, K., Park, Y. J., Rosu, S., Dyer, P. N., Rangasamy, D. et al. (2004). Nucleosomes containing the histone variant H2A.Bbd organize only 118 base pairs of DNA. *EMBO J*, *23*(16), 3314-3324.

Bastian, T. W., Livingston, C. M., Weller, S. K., & Rice, S. A. (2010). Herpes simplex virus type 1 immediate-early protein ICP22 is required for VICE domain formation during productive viral infection. *J Virol*, *84*(5), 2384-2394.

Batterson, W., Furlong, D., & Roizman, B. (1983). Molecular genetics of herpes simplex virus. VIII. further characterization of a temperature-sensitive mutant defective in release of viral DNA and in other stages of the viral reproductive cycle. *J Virol*, *45*(1), 397-407.

Belotserkovskaya, R., Oh, S., Bondarenko, V. A., Orphanides, G., Studitsky, V. M., & Reinberg, D. (2003). FACT facilitates

transcription-dependent nucleosome alteration. *Science*, *301*(5636), 1090-1093.
Bertrand, L., Leiva-Torres, G. A., Hyjazie, H., & Pearson, A. (2010). Conserved residues in the UL24 protein of herpes simplex virus 1 are important for dispersal of the nucleolar protein nucleolin. *J Virol*, *84*(1), 109-118.
Bertrand, L., & Pearson, A. (2008). The conserved N-terminal domain of herpes simplex virus 1 UL24 protein is sufficient to induce the spatial redistribution of nucleolin. *J Gen Virol*, *89*(Pt 5), 1142-1151.
Bloom, D. C., Giordani, N. V., & Kwiatkowski, D. L. (2010). Epigenetic regulation of latent HSV-1 gene expression. *Biochim Biophys Acta*, *1799*(3-4), 246-256.
Bonnefoy, E., Orsi, G. A., Couble, P., & Loppin, B. (2007). The essential role of Drosophila HIRA for de novo assembly of paternal chromatin at fertilization. *PLoS Genet*, *3*(10), 1991-2006.
Booy, F. P., Trus, B. L., Newcomb, W. W., Brown, J. C., Conway, J. F., & Steven, A. C. (1994). Finding a needle in a haystack: detection of a small protein (the 12-kDa VP26) in a large complex (the 200-MDa capsid of herpes simplex virus). *Proc Natl Acad Sci U S A*, *91*(12), 5652-5656.
Brown, D. T., Alexander, B. T., & Sittman, D. B. (1996). Differential effect of H1 variant overexpression on cell cycle progression and gene expression. *Nucleic Acids Res*, *24*(3), 486-493.
Brush, D., Dodgson, J. B., Choi, O. R., Stevens, P. W., & Engel, J. D. (1985). Replacement variant histone genes contain intervening sequences. *Mol Cell Biol*, *5*(6), 1307-1317.
Burch, A. D., & Weller, S. K. (2004). Nuclear sequestration of cellular chaperone and proteasomal machinery during herpes simplex virus type 1 infection. *J Virol*, *78*(13), 7175-7185.
Burch, A. D., & Weller, S. K. (2005). Herpes simplex virus type 1 DNA polymerase requires the mammalian chaperone hsp90 for proper localization to the nucleus. *J Virol*, *79*(16), 10740-10749.
Cai, W., & Schaffer, P. A. (1992). Herpes simplex virus type 1 ICP0 regulates expression of immediate-early, early, and late genes in productively infected cells. *J Virol*, *66*(5), 2904-2915.
Cai, W. Z., & Schaffer, P. A. (1989). Herpes simplex virus type 1 ICP0 plays a critical role in the de novo synthesis of infectious virus following transfection of viral DNA. *J Virol*, *63*(11), 4579-4589.
Calle, A., Ugrinova, I., Epstein, A. L., Bouvet, P., Diaz, J. J., & Greco, A. (2008). Nucleolin is required for an efficient herpes simplex virus type 1 infection. *J Virol*, *82*(10), 4762-4773.
Carozzi, N., Marashi, F., Plumb, M., Zimmerman, S., Zimmerman, A., Coles, L. S. et al. (1984). Clustering of human H1 and core histone genes. *Science*, *224*(4653), 1115-1117.
Catez, F., Brown, D. T., Misteli, T., & Bustin, M. (2002). Competition between histone H1 and HMGN proteins for chromatin binding sites. *EMBO Rep*, *3*(8), 760-766.
Catez, F., Yang, H., Tracey, K. J., Reeves, R., Misteli, T., & Bustin, M. (2004). Network of dynamic interactions between histone H1 and

high-mobility-group proteins in chromatin. *Mol Cell Biol*, *24*(10), 4321-4328.
Chakravarthy, S., & Luger, K. (2006). The histone variant macro-H2A preferentially forms "hybrid nucleosomes". *J Biol Chem*, *281*(35), 25522-25531.
Chen, D. H., Jakana, J., McNab, D., Mitchell, J., Zhou, Z. H., Dougherty, M. et al. (2001). The pattern of tegument-capsid interaction in the herpes simplex virus type 1 virion is not influenced by the small hexon-associated protein VP26. *J Virol*, *75*(23), 11863-11867.
Cheng, G. H., Nandi, A., Clerk, S., & Skoultchi, A. I. (1989). Different 3'-end processing produces two independently regulated mRNAs from a single H1 histone gene. *Proc Natl Acad Sci U S A*, *86*(18), 7002-7006.
Cheung, P., Panning, B., & Smiley, J. R. (1997). Herpes simplex virus immediate-early proteins ICP0 and ICP4 activate the endogenous human alpha-globin gene in nonerythroid cells. *J Virol*, *71*(3), 1784-1793.
Cliffe, A. R., Garber, D. A., & Knipe, D. M. (2009). Transcription of the herpes simplex virus latency-associated transcript promotes the formation of facultative heterochromatin on lytic promoters. *J Virol*, *83*(16), 8182-8190.
Cliffe, A. R., & Knipe, D. M. (2008). Herpes simplex virus ICP0 promotes both histone removal and acetylation on viral DNA during lytic infection. *J Virol*, *82*(24), 12030-12038.
Coleman, H. M., Connor, V., Cheng, Z. S., Grey, F., Preston, C. M., & Efstathiou, S. (2008). Histone modifications associated with herpes simplex virus type 1 genomes during quiescence and following ICP0-mediated de-repression. *J Gen Virol*, *89*(Pt 1), 68-77.
Collart, D., Romain, P. L., Huebner, K., Pockwinse, S., Pilapil, S., Cannizzaro, L. A. et al. (1992). A human histone H2B.1 variant gene, located on chromosome 1, utilizes alternative 3' end processing. *J Cell Biochem*, *50*(4), 374-385.
Conn, K. L., Hendzel, M. J., & Schang, L. M. (2008). Linker histones are mobilized during infection with herpes simplex virus type 1. *J Virol*, *82*(17), 8629-8646.
Copeland, A. M., Newcomb, W. W., & Brown, J. C. (2009). Herpes simplex virus replication: roles of viral proteins and nucleoporins in capsid-nucleus attachment. *J Virol*, *83*(4), 1660-1668.
Dai-Ju, J. Q., Li, L., Johnson, L. A., & Sandri-Goldin, R. M. (2006). ICP27 interacts with the C-terminal domain of RNA polymerase II and facilitates its recruitment to herpes simplex virus 1 transcription sites, where it undergoes proteasomal degradation during infection. *J Virol*, *80*(7), 3567-3581.
Das, C., Tyler, J. K., & Churchill, M. E. (2010). The histone shuffle: histone chaperones in an energetic dance. *Trends Biochem Sci*.
Davison, A. J., Eberle, R., Ehlers, B., Hayward, G. S., McGeoch, D. J., Minson, A. C. et al. (2009). The order Herpesvirales. *Arch Virol*, *154*(1), 171-177.

Dellaire, G., & Bazett-Jones, D. P. (2004). PML nuclear bodies: dynamic sensors of DNA damage and cellular stress. *Bioessays*, *26*(9), 963-977.

DeLuca, N. A., & Schaffer, P. A. (1988). Physical and functional domains of the herpes simplex virus transcriptional regulatory protein ICP4. *J Virol*, *62*(3), 732-743.

Deshmane, S. L., & Fraser, N. W. (1989). During latency, herpes simplex virus type 1 DNA is associated with nucleosomes in a chromatin structure. *J Virol*, *63*(2), 943-947.

Doenecke, D., Albig, W., Bouterfa, H., & Drabent, B. (1994). Organization and expression of H1 histone and H1 replacement histone genes. *J Cell Biochem*, *54*(4), 423-431.

Dohner, K., Wolfstein, A., Prank, U., Echeverri, C., Dujardin, D., Vallee, R. et al. (2002). Function of dynein and dynactin in herpes simplex virus capsid transport. *Mol Biol Cell*, *13*(8), 2795-2809.

Drane, P., Ouararhni, K., Depaux, A., Shuaib, M., & Hamiche, A. (2010). The death-associated protein DAXX is a novel histone chaperone involved in the replication-independent deposition of H3.3. *Genes Dev*, *24*(12), 1253-1265.

Dryhurst, D., Ishibashi, T., Rose, K. L., Eirin-Lopez, J. M., McDonald, D., Silva-Moreno, B. et al. (2009). Characterization of the histone H2A.Z-1 and H2A.Z-2 isoforms in vertebrates. *BMC Biol*, *7*, 86.

Eilers, A., Bouterfa, H., Triebe, S., & Doenecke, D. (1994). Role of a distal promoter element in the S-phase control of the human H1.2 histone gene transcription. *Eur J Biochem*, *223*(2), 567-574.

Eirin-Lopez, J. M., Gonzalez-Romero, R., Dryhurst, D., Ishibashi, T., & Ausio, J. (2009). The evolutionary differentiation of two histone H2A.Z variants in chordates (H2A.Z-1 and H2A.Z-2) is mediated by a stepwise mutation process that affects three amino acid residues. *BMC Evol Biol*, *9*, 31.

Eskiw, C. H., Dellaire, G., & Bazett-Jones, D. P. (2004). Chromatin contributes to structural integrity of promyelocytic leukemia bodies through a SUMO-1-independent mechanism. *J Biol Chem*, *279*(10), 9577-9585.

Everett, R. D. (1984). Trans activation of transcription by herpes virus products: requirement for two HSV-1 immediate-early polypeptides for maximum activity. *EMBO J*, *3*(13), 3135-3141.

Everett, R. D. (2001). DNA viruses and viral proteins that interact with PML nuclear bodies. *Oncogene*, *20*(49), 7266-7273.

Everett, R. D., & Chelbi-Alix, M. K. (2007). PML and PML nuclear bodies: implications in antiviral defence. *Biochimie*, *89*(6-7), 819-830.

Everett, R. D., Earnshaw, W. C., Findlay, J., & Lomonte, P. (1999). Specific destruction of kinetochore protein CENP-C and disruption of cell division by herpes simplex virus immediate-early protein Vmw110. *EMBO J*, *18*(6), 1526-1538.

Everett, R. D., Murray, J., Orr, A., & Preston, C. M. (2007). Herpes simplex virus type 1 genomes are associated with ND10 nuclear substructures in quiescently infected human fibroblasts. *J Virol*, *81*(20), 10991-11004.

Everett, R. D., Orr, A., & Elliott, M. (1991). High level expression and purification of herpes simplex virus type 1 immediate early polypeptide Vmw110. *Nucleic Acids Res*, *19*(22), 6155-6161.
Everett, R. D., Sourvinos, G., Leiper, C., Clements, J. B., & Orr, A. (2004). Formation of nuclear foci of the herpes simplex virus type 1 regulatory protein ICP4 at early times of infection: localization, dynamics, recruitment of ICP27, and evidence for the de novo induction of ND10-like complexes. *J Virol*, *78*(4), 1903-1917.
Everett, R. D., Sourvinos, G., & Orr, A. (2003). Recruitment of herpes simplex virus type 1 transcriptional regulatory protein ICP4 into foci juxtaposed to ND10 in live, infected cells. *J Virol*, *77*(6), 3680-3689.
Finn, R. M., Browne, K., Hodgson, K. C., & Ausio, J. (2008). sNASP, a histone H1-specific eukaryotic chaperone dimer that facilitates chromatin assembly. *Biophys J*, *95*(3), 1314-1325.
Frank, D., Doenecke, D., & Albig, W. (2003). Differential expression of human replacement and cell cycle dependent H3 histone genes. *Gene*, *312*, 135-143.
Gibson, W., & Roizman, B. (1971). Compartmentalization of spermine and spermidine in the herpes simplex virion. *Proc Natl Acad Sci U S A*, *68*(11), 2818-2821.
Goto, H., Motomura, S., Wilson, A. C., Freiman, R. N., Nakabeppu, Y., Fukushima, K. et al. (1997). A single-point mutation in HCF causes temperature-sensitive cell-cycle arrest and disrupts VP16 function. *Genes Dev*, *11*(6), 726-737.
Groth, A., Corpet, A., Cook, A. J., Roche, D., Bartek, J., Lukas, J. et al. (2007). Regulation of replication fork progression through histone supply and demand. *Science*, *318*(5858), 1928-1931.
Gu, H., Liang, Y., Mandel, G., & Roizman, B. (2005). Components of the REST/CoREST/histone deacetylase repressor complex are disrupted, modified, and translocated in HSV-1-infected cells. *Proc Natl Acad Sci U S A*, *102*(21), 7571-7576.
Gu, H., & Roizman, B. (2007). Herpes simplex virus-infected cell protein 0 blocks the silencing of viral DNA by dissociating histone deacetylases from the CoREST-REST complex. *Proc Natl Acad Sci U S A*, *104*(43), 17134-17139.
Gunjan, A., & Brown, D. T. (1999). Overproduction of histone H1 variants in vivo increases basal and induced activity of the mouse mammary tumor virus promoter. *Nucleic Acids Res*, *27*(16), 3355-3363.
Gunjan, A., Paik, J., & Verreault, A. (2005). Regulation of histone synthesis and nucleosome assembly. *Biochimie*, *87*(7), 625-635.
Hake, S. B., Garcia, B. A., Duncan, E. M., Kauer, M., Dellaire, G., Shabanowitz, J. et al. (2006). Expression patterns and post-translational modifications associated with mammalian histone H3 variants. *J Biol Chem*, *281*(1), 559-568.
Harris, R. A., & Preston, C. M. (1991). Establishment of latency in vitro by the herpes simplex virus type 1 mutant in1814. *J Gen Virol*, *72(*Pt 4), 907-913.
Hatch, C. L., & Bonner, W. M. (1990). The human histone H2A.Z gene. Sequence and regulation. *J Biol Chem*, *265*(25), 15211-15218.

Heldwein, E. E., & Krummenacher, C. (2008). Entry of herpesviruses into mammalian cells. *Cell Mol Life Sci*, *65*(11), 1653-1668.
Hendzel, M. J., & Davie, J. R. (1990). Nucleosomal histones of transcriptionally active/competent chromatin preferentially exchange with newly synthesized histones in quiescent chicken erythrocytes. *Biochem J*, *271*(1), 67-73.
Hendzel, M. J., Lever, M. A., Crawford, E., & Th'ng, J. P. (2004). The C-terminal domain is the primary determinant of histone H1 binding to chromatin in vivo. *J Biol Chem*, *279*(19), 20028-20034.
Herrera, F. J., & Triezenberg, S. J. (2004). VP16-dependent association of chromatin-modifying coactivators and underrepresentation of histones at immediate-early gene promoters during herpes simplex virus infection. *J Virol*, *78*(18), 9689-9696.
Higashi, M., Inoue, S., & Takashi, I. (2010). Core histone H2A ubiquitylation and transcriptional regulation. *Experimental Cell Research*.
Higashi, T., Matsunaga, S., Isobe, K., Morimoto, A., Shimada, T., Kataoka, S. et al. (2007). Histone H2A mobility is regulated by its tails and acetylation of core histone tails. *Biochem Biophys Res Commun*, *357*(3), 627-632.
Huang, J., Kent, J. R., Placek, B., Whelan, K. A., Hollow, C. M., Zeng, P. Y. et al. (2006). Trimethylation of histone H3 lysine 4 by Set1 in the lytic infection of human herpes simplex virus 1. *J Virol*, *80*(12), 5740-5746.
ICTV. (2009). Virus Taxonomy: 2009 Release. 2010, from http://www.ictvonline.org/virusTaxonomy.asp?bhcp=1.
Ishov, A. M., & Maul, G. G. (1996). The periphery of nuclear domain 10 (ND10) as site of DNA virus deposition. *J Cell Biol*, *134*(4), 815-826.
Ito, T., Ikehara, T., Nakagawa, T., Kraus, W. L., & Muramatsu, M. (2000). p300-mediated acetylation facilitates the transfer of histone H2A-H2B dimers from nucleosomes to a histone chaperone. *Genes Dev*, *14*(15), 1899-1907.
Jaeger, S., Barends, S., Giege, R., Eriani, G., & Martin, F. (2005). Expression of metazoan replication-dependent histone genes. *Biochimie*, *87*(9-10), 827-834.
Jamai, A., Imoberdorf, R. M., & Strubin, M. (2007). Continuous histone H2B and transcription-dependent histone H3 exchange in yeast cells outside of replication. *Mol Cell*, *25*(3), 345-355.
Jasencakova, Z., Scharf, A. N., Ask, K., Corpet, A., Imhof, A., Almouzni, G. et al. (2010). Replication stress interferes with histone recycling and predeposition marking of new histones. *Mol Cell*, *37*(5), 736-743.
Jin, C., & Felsenfeld, G. (2007). Nucleosome stability mediated by histone variants H3.3 and H2A.Z. *Genes Dev*, *21*(12), 1519-1529.
Jordan, R., & Schaffer, P. A. (1997). Activation of gene expression by herpes simplex virus type 1 ICP0 occurs at the level of mRNA synthesis. *J Virol*, *71*(9), 6850-6862.
Jovasevic, V., Liang, L., & Roizman, B. (2008). Proteolytic cleavage of VP1-2 is required for release of herpes simplex virus 1 DNA into the nucleus. *J Virol*, *82*(7), 3311-3319.

Kamakaka, R. T., & Biggins, S. (2005). Histone variants: deviants? *Genes Dev*, *19*(3), 295-310.
Kanda, T., Sullivan, K. F., & Wahl, G. M. (1998). Histone-GFP fusion protein enables sensitive analysis of chromosome dynamics in living mammalian cells. *Curr Biol*, *8*(7), 377-385.
Kent, J. R., Zeng, P. Y., Atanasiu, D., Gardner, J., Fraser, N. W., & Berger, S. L. (2004). During lytic infection herpes simplex virus type 1 is associated with histones bearing modifications that correlate with active transcription. *J Virol*, *78*(18), 10178-10186.
Kepert, J. F., Mazurkiewicz, J., Heuvelman, G. L., Toth, K. F., & Rippe, K. (2005). NAP1 modulates binding of linker histone H1 to chromatin and induces an extended chromatin fiber conformation. *J Biol Chem*, *280*(40), 34063-34072.
Kieff, E. D., Bachenheimer, S. L., & Roizman, B. (1971). Size, composition, and structure of the deoxyribonucleic acid of herpes simplex virus subtypes 1 and 2. *J Virol*, *8*(2), 125-132.
Kim, H. J., Seol, J. H., Han, J. W., Youn, H. D., & Cho, E. J. (2007). Histone chaperones regulate histone exchange during transcription. *EMBO J*, *26*(21), 4467-4474.
Kimura, H., & Cook, P. R. (2001). Kinetics of core histones in living human cells: little exchange of H3 and H4 and some rapid exchange of H2B. *J Cell Biol*, *153*(7), 1341-1353.
Kireeva, M. L., Walter, W., Tchernajenko, V., Bondarenko, V., Kashlev, M., & Studitsky, V. M. (2002). Nucleosome remodeling induced by RNA polymerase II: loss of the H2A/H2B dimer during transcription. *Mol Cell*, *9*(3), 541-552.
Knipe, D. M., & Howley, P. M. (2007a). Herpes Simplex Viruses. In *Fields Virology (5th Edition).* Lippincott Williams & Wilkins.
Knipe, D. M., & Howley, P. M. (2007b). The Family Herpesviridae: A Brief Introduction. In *Fields Virology (5th Edition).* Lippincott Williams & Wilkins.
Kolb, G., & Kristie, T. M. (2008). Association of the cellular coactivator HCF-1 with the Golgi apparatus in sensory neurons. *J Virol*, *82*(19), 9555-9563.
Konishi, A., Shimizu, S., Hirota, J., Takao, T., Fan, Y., Matsuoka, Y. et al. (2003). Involvement of histone H1.2 in apoptosis induced by DNA double-strand breaks. *Cell*, *114*(6), 673-688.
Kubat, N. J., Tran, R. K., McAnany, P., & Bloom, D. C. (2004). Specific histone tail modification and not DNA methylation is a determinant of herpes simplex virus type 1 latent gene expression. *J Virol*, *78*(3), 1139-1149.
Kuddus, R., Gu, B., & DeLuca, N. A. (1995). Relationship between TATA-binding protein and herpes simplex virus type 1 ICP4 DNA-binding sites in complex formation and repression of transcription. *J Virol*, *69*(9), 5568-5575.
Kuddus, R. H., & DeLuca, N. A. (2007). DNA-dependent oligomerization of herpes simplex virus type 1 regulatory protein ICP4. *J Virol*, *81*(17), 9230-9237.
Kutluay, S. B., DeVos, S. L., Klomp, J. E., & Triezenberg, S. J. (2009). Transcriptional coactivators are not required for herpes simplex

virus type 1 immediate-early gene expression in vitro. *J Virol*, *83*(8), 3436-3449.
Kutluay, S. B., & Triezenberg, S. J. (2009). Regulation of histone deposition on the herpes simplex virus type 1 genome during lytic infection. *J Virol*, *83*(11), 5835-5845.
Lacasse, J. J., & Schang, L. M. (2010). During lytic infections, herpes simplex virus type 1 DNA is in complexes with the properties of unstable nucleosomes. *J Virol*, *84*(4), 1920-1933.
Lallemand-Breitenbach, V., & de The, H. (2010). PML nuclear bodies. *Cold Spring Harb Perspect Biol*, *2*(5), a000661.
Lam, Q., Smibert, C. A., Koop, K. E., Lavery, C., Capone, J. P., Weinheimer, S. P. et al. (1996). Herpes simplex virus VP16 rescues viral mRNA from destruction by the virion host shutoff function. *EMBO J*, *15*(10), 2575-2581.
Latchman, D. S., Partidge, J. F., Estridge, J. K., & Kemp, L. M. (1989). The different competitive abilities of viral TAATGARAT elements and cellular octamer motifs, mediate the induction of viral immediate-early genes and the repression of the histone H2B gene in herpes simplex virus infected cells. *Nucleic Acids Res*, *17*(21), 8533-8542.
Lees-Miller, S. P., Long, M. C., Kilvert, M. A., Lam, V., Rice, S. A., & Spencer, C. A. (1996). Attenuation of DNA-dependent protein kinase activity and its catalytic subunit by the herpes simplex virus type 1 transactivator ICP0. *J Virol*, *70*(11), 7471-7477.
Leinbach, S. S., & Summers, W. C. (1980). The structure of herpes simplex virus type 1 DNA as probed by micrococcal nuclease digestion. *J Gen Virol*, *51*(Pt 1), 45-59.
Lennox, R. W., & Cohen, L. H. (1983). The histone H1 complements of dividing and nondividing cells of the mouse. *J Biol Chem*, *258*(1), 262-268.
Lever, M. A., Th'ng, J. P., Sun, X., & Hendzel, M. J. (2000). Rapid exchange of histone H1.1 on chromatin in living human cells. *Nature*, *408*(6814), 873-876.
Lewis, P. W., Elsaesser, S. J., Noh, K. M., Stadler, S. C., & Allis, C. D. (2010). Daxx is an H3.3-specific histone chaperone and cooperates with ATRX in replication-independent chromatin assembly at telomeres. *Proc Natl Acad Sci U S A*.
Li, A., Yu, Y., Lee, S. C., Ishibashi, T., Lees-Miller, S. P., & Ausio, J. (2010). Phosphorylation of histone H2A.X by DNA-dependent protein kinase is not affected by core histone acetylation, but it alters nucleosome stability and histone H1 binding. *J Biol Chem*, *285*(23), 17778-17788.
Li, L., Johnson, L. A., Dai-Ju, J. Q., & Sandri-Goldin, R. M. (2008). Hsc70 focus formation at the periphery of HSV-1 transcription sites requires ICP27. *PLoS One*, *3*(1), e1491.
Li, W., Cun, W., Liu, L., Hong, M., Wang, L., Wang, L. et al. (2009). The transactivating effect of HSV-1 ICP0 is enhanced by its interaction with the PCAF component of histone acetyltransferase. *Arch Virol*, *154*(11), 1755-1764.
Liu, M., Rakowski, B., Gershburg, E., Weisend, C. M., Lucas, O., Schmidt, E. E. et al. (2010). ICP0 antagonizes ICP4-dependent

silencing of the herpes simplex virus ICP0 gene. *PLoS One*, *5*(1), e8837.
Livingston, C. M., DeLuca, N. A., Wilkinson, D. E., & Weller, S. K. (2008). Oligomerization of ICP4 and rearrangement of heat shock proteins may be important for herpes simplex virus type 1 prereplicative site formation. *J Virol*, *82*(13), 6324-6336.
Lomonte, P., & Morency, E. (2007). Centromeric protein CENP-B proteasomal degradation induced by the viral protein ICP0. *FEBS Lett*, *581*(4), 658-662.
Lomonte, P., Sullivan, K. F., & Everett, R. D. (2001). Degradation of nucleosome-associated centromeric histone H3-like protein CENP-A induced by herpes simplex virus type 1 protein ICP0. *J Biol Chem*, *276*(8), 5829-5835.
Lomonte, P., Thomas, J., Texier, P., Caron, C., Khochbin, S., & Epstein, A. L. (2004). Functional interaction between class II histone deacetylases and ICP0 of herpes simplex virus type 1. *J Virol*, *78*(13), 6744-6757.
Loppin, B., Bonnefoy, E., Anselme, C., Laurencon, A., Karr, T. L., & Couble, P. (2005). The histone H3.3 chaperone HIRA is essential for chromatin assembly in the male pronucleus. *Nature*, *437*(7063), 1386-1390.
Loret, S., Guay, G., & Lippe, R. (2008). Comprehensive characterization of extracellular herpes simplex virus type 1 virions. *J Virol*, *82*(17), 8605-8618.
Luciano, R. L., & Wilson, A. C. (2002). An activation domain in the C-terminal subunit of HCF-1 is important for transactivation by VP16 and LZIP. *Proc Natl Acad Sci U S A*, *99*(21), 13403-13408.
Luger, K., Mader, A. W., Richmond, R. K., Sargent, D. F., & Richmond, T. J. (1997). Crystal structure of the nucleosome core particle at 2.8 A resolution. *Nature, 389*(6648), 251-260.
Luk, E., Vu, N. D., Patteson, K., Mizuguchi, G., Wu, W. H., Ranjan, A. et al. (2007). Chz1, a nuclear chaperone for histone H2AZ. *Mol Cell*, *25*(3), 357-368.
Lukonis, C. J., Burkham, J., & Weller, S. K. (1997). Herpes simplex virus type 1 prereplicative sites are a heterogeneous population: only a subset are likely to be precursors to replication compartments. *J Virol*, *71*(6), 4771-4781.
Lymberopoulos, M. H., & Pearson, A. (2007). Involvement of UL24 in herpes-simplex-virus-1-induced dispersal of nucleolin. *Virology*, *363*(2), 397-409.
Marzluff, W. F., & Duronio, R. J. (2002). Histone mRNA expression: multiple levels of cell cycle regulation and important developmental consequences. *Curr Opin Cell Biol*, *14*(6), 692-699.
Matsuda, R., Hori, T., Kitamura, H., Takeuchi, K., Fukagawa, T., & Harata, M. (2010). Identification and characterization of the two isoforms of the vertebrate H2A.Z histone variant. *Nucleic Acids Res*, *38*(13), 4263-4273.
Matta, M. K., & Panagiotidis, C. A. (2008). High-mobility group protein A1 binds herpes simplex virus gene regulatory sequences and affects their expression. *Arch Virol*, *153*(7), 1251-1262.

Maul, G. G., Ishov, A. M., & Everett, R. D. (1996). Nuclear domain 10 as preexisting potential replication start sites of herpes simplex virus type-1. *Virology*, *217*(1), 67-75.
Maurer, U. E., Sodeik, B., & Grunewald, K. (2008). Native 3D intermediates of membrane fusion in herpes simplex virus 1 entry. *Proc Natl Acad Sci U S A*, *105*(30), 10559-10564.
Melroe, G. T., Silva, L., Schaffer, P. A., & Knipe, D. M. (2007). Recruitment of activated IRF-3 and CBP/p300 to herpes simplex virus ICP0 nuclear foci: Potential role in blocking IFN-beta induction. *Virology*, *360*(2), 305-321.
Memedula, S., & Belmont, A. S. (2003). Sequential recruitment of HAT and SWI/SNF components to condensed chromatin by VP16. *Curr Biol*, *13*(3), 241-246.
Mettenleiter, T. C. (2006). Intriguing interplay between viral proteins during herpesvirus assembly or: the herpesvirus assembly puzzle. *Vet Microbiol*, *113*(3-4), 163-169.
Misteli, T., Gunjan, A., Hock, R., Bustin, M., & Brown, D. T. (2000). Dynamic binding of histone H1 to chromatin in living cells. *Nature*, *408*(6814), 877-881.
Mocarski, E. S., & Roizman, B. (1981). Site-specific inversion sequence of the herpes simplex virus genome: domain and structural features. *Proc Natl Acad Sci U S A*, *78*(11), 7047-7051.
Monier, K., Armas, J. C., Etteldorf, S., Ghazal, P., & Sullivan, K. F. (2000). Annexation of the interchromosomal space during viral infection. *Nat Cell Biol*, *2*(9), 661-665.
Morrison, E. E., Stevenson, A. J., Wang, Y. F., & Meredith, D. M. (1998). Differences in the intracellular localization and fate of herpes simplex virus tegument proteins early in the infection of Vero cells. *J Gen Virol*, *79(*Pt 10), 2517-2528.
Mossman, K. L., & Smiley, J. R. (1999). Truncation of the C-terminal acidic transcriptional activation domain of herpes simplex virus VP16 renders expression of the immediate-early genes almost entirely dependent on ICP0. *J Virol*, *73*(12), 9726-9733.
Mouttet, M. E., Guetard, D., & Bechet, J. M. (1979). Random cleavage of intranuclear herpes simplex virus DNA by micrococcal nuclease. *FEBS Lett*, *100*(1), 107-109.
Muggeridge, M. I., & Fraser, N. W. (1986). Chromosomal organization of the herpes simplex virus genome during acute infection of the mouse central nervous system. *J Virol*, *59*(3), 764-767.
Mullen, T. E., & Marzluff, W. F. (2008). Degradation of histone mRNA requires oligouridylation followed by decapping and simultaneous degradation of the mRNA both 5' to 3' and 3' to 5'. *Genes Dev*, *22*(1), 50-65.
Narayanan, A., Nogueira, M. L., Ruyechan, W. T., & Kristie, T. M. (2005). Combinatorial transcription of herpes simplex virus and varicella zoster virus immediate early genes is strictly determined by the cellular coactivator HCF-1. *J Biol Chem*, *280*(2), 1369-1375.
Nelson, D. M., Ye, X., Hall, C., Santos, H., Ma, T., Kao, G. D. et al. (2002). Coupling of DNA synthesis and histone synthesis in S phase

independent of cyclin/cdk2 activity. *Mol Cell Biol*, *22*(21), 7459-7472.
Newcomb, W. W., Booy, F. P., & Brown, J. C. (2007). Uncoating the herpes simplex virus genome. *J Mol Biol*, *370*(4), 633-642.
Newcomb, W. W., Trus, B. L., Booy, F. P., Steven, A. C., Wall, J. S., & Brown, J. C. (1993). Structure of the herpes simplex virus capsid. Molecular composition of the pentons and the triplexes. *J Mol Biol*, *232*(2), 499-511.
Oh, J., & Fraser, N. W. (2008). Temporal association of the herpes simplex virus genome with histone proteins during a lytic infection. *J Virol*, *82*(7), 3530-3537.
Okamura, H., Yoshida, K., Amorim, B. R., & Haneji, T. (2008). Histone H1.2 is translocated to mitochondria and associates with Bak in bleomycin-induced apoptotic cells. *J Cell Biochem*, *103*(5), 1488-1496.
Okuwaki, M., Kato, K., Shimahara, H., Tate, S., & Nagata, K. (2005). Assembly and disassembly of nucleosome core particles containing histone variants by human nucleosome assembly protein I. *Mol Cell Biol*, *25*(23), 10639-10651.
Okuwaki, M., & Nagata, K. (1998). Template activating factor-I remodels the chromatin structure and stimulates transcription from the chromatin template. *J Biol Chem*, *273*(51), 34511-34518.
Osley, M. A. (2006). Regulation of histone H2A and H2B ubiquitylation. *Brief Funct Genomic Proteomic*, *5*(3), 179-189.
Panagiotidis, C. A., & Silverstein, S. J. (1999). The host-cell architectural protein HMG I(Y) modulates binding of herpes simplex virus type 1 ICP4 to its cognate promoter. *Virology*, *256*(1), 64-74.
Parkinson, J., Lees-Miller, S. P., & Everett, R. D. (1999). Herpes simplex virus type 1 immediate-early protein vmw110 induces the proteasome-dependent degradation of the catalytic subunit of DNA-dependent protein kinase. *J Virol*, *73*(1), 650-657.
Parseghian, M. H., Henschen, A. H., Krieglstein, K. G., & Hamkalo, B. A. (1994). A proposal for a coherent mammalian histone H1 nomenclature correlated with amino acid sequences. *Protein Sci*, *3*(4), 575-587.
Pasdeloup, D., Blondel, D., Isidro, A. L., & Rixon, F. J. (2009). Herpesvirus capsid association with the nuclear pore complex and viral DNA release involve the nucleoporin CAN/Nup214 and the capsid protein pUL25. *J Virol*, *83*(13), 6610-6623.
Patel, A. H., Rixon, F. J., Cunningham, C., & Davison, A. J. (1996). Isolation and characterization of herpes simplex virus type 1 mutants defective in the UL6 gene. *Virology*, *217*(1), 111-123.
Pehrson, J. R., & Cole, R. D. (1982). Histone H1 subfractions and H10 turnover at different rates in nondividing cells. *Biochemistry*, *21*(3), 456-460.
Perng, G. C., & Jones, C. (2010). Towards an understanding of the herpes simplex virus type 1 latency-reactivation cycle. *Interdiscip Perspect Infect Dis*, *2010*, 262415.
Placek, B. J., Huang, J., Kent, J. R., Dorsey, J., Rice, L., Fraser, N. W. et al. (2009). The histone variant H3.3 regulates gene expression

during lytic infection with herpes simplex virus type 1. *J Virol*, *83*(3), 1416-1421.
Preston, C. M., & Nicholl, M. J. (1997). Repression of gene expression upon infection of cells with herpes simplex virus type 1 mutants impaired for immediate-early protein synthesis. *J Virol*, *71*(10), 7807-7813.
Preston, V. G., Murray, J., Preston, C. M., McDougall, I. M., & Stow, N. D. (2008). The UL25 gene product of herpes simplex virus type 1 is involved in uncoating of the viral genome. *J Virol*, *82*(13), 6654-6666.
Ramaswamy, A., & Ioshikhes, I. (2007). Global dynamics of newly constructed oligonucleosomes of conventional and variant H2A.Z histone. *BMC Struct Biol*, *7*, 76.
Ransom, M., Dennehey, B. K., & Tyler, J. K. (2010). Chaperoning histones during DNA replication and repair. *Cell*, *140*(2), 183-195.
Raska, I., Shaw, P. J., & Cmarko, D. (2006). Structure and function of the nucleolus in the spotlight. *Curr Opin Cell Biol*, *18*(3), 325-334.
Regad, T., & Chelbi-Alix, M. K. (2001). Role and fate of PML nuclear bodies in response to interferon and viral infections. *Oncogene*, *20*(49), 7274-7286.
Reske, A., Pollara, G., Krummenacher, C., Chain, B. M., & Katz, D. R. (2007). Understanding HSV-1 entry glycoproteins. *Rev Med Virol*, *17*(3), 205-215.
Rice, S. A., Long, M. C., Lam, V., Schaffer, P. A., & Spencer, C. A. (1995). Herpes simplex virus immediate-early protein ICP22 is required for viral modification of host RNA polymerase II and establishment of the normal viral transcription program. *J Virol*, *69*(9), 5550-5559.
Rice, S. A., Long, M. C., Lam, V., & Spencer, C. A. (1994). RNA polymerase II is aberrantly phosphorylated and localized to viral replication compartments following herpes simplex virus infection. *J Virol*, *68*(2), 988-1001.
Richardson, R. T., Batova, I. N., Widgren, E. E., Zheng, L. X., Whitfield, M., Marzluff, W. F. et al. (2000). Characterization of the histone H1-binding protein, NASP, as a cell cycle-regulated somatic protein. *J Biol Chem*, *275*(39), 30378-30386.
Rufiange, A., Jacques, P. E., Bhat, W., Robert, F., & Nourani, A. (2007). Genome-wide replication-independent histone H3 exchange occurs predominantly at promoters and implicates H3 K56 acetylation and Asf1. *Mol Cell*, *27*(3), 393-405.
Samaniego, L. A., Neiderhiser, L., & DeLuca, N. A. (1998). Persistence and expression of the herpes simplex virus genome in the absence of immediate-early proteins. *J Virol*, *72*(4), 3307-3320.
Sampath, P., & Deluca, N. A. (2008). Binding of ICP4, TATA-binding protein, and RNA polymerase II to herpes simplex virus type 1 immediate-early, early, and late promoters in virus-infected cells. *J Virol*, *82*(5), 2339-2349.
Sandri-Goldin, R. M. (2008). The many roles of the regulatory protein ICP27 during herpes simplex virus infection. *Front Biosci*, *13*, 5241-5256.

Schang, L. M., Rosenberg, A., & Schaffer, P. A. (2000). Roscovitine, a specific inhibitor of cellular cyclin-dependent kinases, inhibits herpes simplex virus DNA synthesis in the presence of viral early proteins. *J Virol*, *74*(5), 2107-2120.

Schek, N., & Bachenheimer, S. L. (1985). Degradation of cellular mRNAs induced by a virion-associated factor during herpes simplex virus infection of Vero cells. *J Virol*, *55*(3), 601-610.

Seo, S. B., McNamara, P., Heo, S., Turner, A., Lane, W. S., & Chakravarti, D. (2001). Regulation of histone acetylation and transcription by INHAT, a human cellular complex containing the set oncoprotein. *Cell*, *104*(1), 119-130.

Seyedin, S. M., & Kistler, W. S. (1979). H1 histone subfractions of mammalian testes. 1. Organ specificity in the rat. *Biochemistry*, *18*(7), 1371-1375.

Shahin, V., Hafezi, W., Oberleithner, H., Ludwig, Y., Windoffer, B., Schillers, H. et al. (2006). The genome of HSV-1 translocates through the nuclear pore as a condensed rod-like structure. *J Cell Sci*, *119*(Pt 1), 23-30.

Shibahara, K., & Stillman, B. (1999). Replication-dependent marking of DNA by PCNA facilitates CAF-1-coupled inheritance of chromatin. *Cell*, *96*(4), 575-585.

Shirata, N., Kudoh, A., Daikoku, T., Tatsumi, Y., Fujita, M., Kiyono, T. et al. (2005). Activation of ataxia telangiectasia-mutated DNA damage checkpoint signal transduction elicited by herpes simplex virus infection. *J Biol Chem*, *280*(34), 30336-30341.

Shukla, A., Chaurasia, P., & Bhaumik, S. R. (2009). Histone methylation and ubiquitination with their cross-talk and roles in gene expression and stability. *Cell Mol Life Sci*, *66*(8), 1419-1433.

Simpson-Holley, M., Baines, J., Roller, R., & Knipe, D. M. (2004). Herpes simplex virus 1 U(L)31 and U(L)34 gene products promote the late maturation of viral replication compartments to the nuclear periphery. *J Virol*, *78*(11), 5591-5600.

Simpson-Holley, M., Colgrove, R. C., Nalepa, G., Harper, J. W., & Knipe, D. M. (2005). Identification and functional evaluation of cellular and viral factors involved in the alteration of nuclear architecture during herpes simplex virus 1 infection. *J Virol*, *79*(20), 12840-12851.

Smibert, C. A., & Smiley, J. R. (1990). Differential regulation of endogenous and transduced beta-globin genes during infection of erythroid cells with a herpes simplex virus type 1 recombinant. *J Virol*, *64*(8), 3882-3894.

Smiley, J. R., Smibert, C., & Everett, R. D. (1987). Expression of a cellular gene cloned in herpes simplex virus: rabbit beta-globin is regulated as an early viral gene in infected fibroblasts. *J Virol*, *61*(8), 2368-2377.

Smith, C. A., Bates, P., Rivera-Gonzalez, R., Gu, B., & DeLuca, N. A. (1993). ICP4, the major transcriptional regulatory protein of herpes simplex virus type 1, forms a tripartite complex with TATA-binding protein and TFIIB. *J Virol*, *67*(8), 4676-4687.

Smith, C. A., & Schaffer, P. A. (1987). Mutants defective in herpes simplex virus type 2 ICP4: isolation and preliminary characterization. *J Virol*, *61*(4), 1092-1097.
SMITH, K. O. (1964). RELATIONSHIP BETWEEN THE ENVELOPE AND THE INFECTIVITY OF HERPES SIMPLEX VIRUS. *Proc Soc Exp Biol Med*, *115*, 814-816.
Sodeik, B., Ebersold, M. W., & Helenius, A. (1997). Microtubule-mediated transport of incoming herpes simplex virus 1 capsids to the nucleus. *J Cell Biol*, *136*(5), 1007-1021.
Sorenson, C. M., Hart, P. A., & Ross, J. (1991). Analysis of herpes simplex virus-induced mRNA destabilizing activity using an in vitro mRNA decay system. *Nucleic Acids Res*, *19*(16), 4459-4465.
Sourvinos, G., & Everett, R. D. (2002). Visualization of parental HSV-1 genomes and replication compartments in association with ND10 in live infected cells. *EMBO J*, *21*(18), 4989-4997.
Spencer, C. A., Dahmus, M. E., & Rice, S. A. (1997). Repression of host RNA polymerase II transcription by herpes simplex virus type 1. *J Virol*, *71*(3), 2031-2040.
Spencer, C. A., Kruhlak, M. J., Jenkins, H. L., Sun, X., & Bazett-Jones, D. P. (2000). Mitotic transcription repression in vivo in the absence of nucleosomal chromatin condensation. *J Cell Biol*, *150*(1), 13-26.
Stevens, J. G., Wagner, E. K., Devi-Rao, G. B., Cook, M. L., & Feldman, L. T. (1987). RNA complementary to a herpesvirus alpha gene mRNA is prominent in latently infected neurons. *Science*, *235*(4792), 1056-1059.
Strang, B. L., & Stow, N. D. (2005). Circularization of the herpes simplex virus type 1 genome upon lytic infection. *J Virol*, *79*(19), 12487-12494.
Strom, T., & Frenkel, N. (1987). Effects of herpes simplex virus on mRNA stability. *J Virol*, *61*(7), 2198-2207.
Subramanian, R. P., & Geraghty, R. J. (2007). Herpes simplex virus type 1 mediates fusion through a hemifusion intermediate by sequential activity of glycoproteins D, H, L, and B. *Proc Natl Acad Sci U S A*, *104*(8), 2903-2908.
Szilagyi, J. F., & Cunningham, C. (1991). Identification and characterization of a novel non-infectious herpes simplex virus-related particle. *J Gen Virol*, *72(*Pt 3), 661-668.
Tagami, H., Ray-Gallet, D., Almouzni, G., & Nakatani, Y. (2004). Histone H3.1 and H3.3 complexes mediate nucleosome assembly pathways dependent or independent of DNA synthesis. *Cell*, *116*(1), 51-61.
Takami, Y., Ono, T., Fukagawa, T., Shibahara, K., & Nakayama, T. (2007). Essential role of chromatin assembly factor-1-mediated rapid nucleosome assembly for DNA replication and cell division in vertebrate cells. *Mol Biol Cell*, *18*(1), 129-141.
Talasz, H., Sapojnikova, N., Helliger, W., Lindner, H., & Puschendorf, B. (1998). In vitro binding of H1 histone subtypes to nucleosomal organized mouse mammary tumor virus long terminal repeat promotor. *J Biol Chem*, *273*(48), 32236-32243.

Tan, B. C., Chien, C. T., Hirose, S., & Lee, S. C. (2006). Functional cooperation between FACT and MCM helicase facilitates initiation of chromatin DNA replication. *EMBO J*, *25*(17), 3975-3985.
Tang, Q., Li, L., Ishov, A. M., Revol, V., Epstein, A. L., & Maul, G. G. (2003). Determination of minimum herpes simplex virus type 1 components necessary to localize transcriptionally active DNA to ND10. *J Virol*, *77*(10), 5821-5828.
Taylor, T. J., McNamee, E. E., Day, C., & Knipe, D. M. (2003). Herpes simplex virus replication compartments can form by coalescence of smaller compartments. *Virology*, *309*(2), 232-247.
Th'ng, J. P., Sung, R., Ye, M., & Hendzel, M. J. (2005). H1 family histones in the nucleus. Control of binding and localization by the C-terminal domain. *J Biol Chem*, *280*(30), 27809-27814.
Thambirajah, A. A., Dryhurst, D., Ishibashi, T., Li, A., Maffey, A. H., & Ausio, J. (2006). H2A.Z stabilizes chromatin in a way that is dependent on core histone acetylation. *J Biol Chem*, *281*(29), 20036-20044.
Tripputi, P., Emanuel, B. S., Croce, C. M., Green, L. G., Stein, G. S., & Stein, J. L. (1986). Human histone genes map to multiple chromosomes. *Proc Natl Acad Sci U S A*, *83*(10), 3185-3188.
Trus, B. L., Cheng, N., Newcomb, W. W., Homa, F. L., Brown, J. C., & Steven, A. C. (2004). Structure and polymorphism of the UL6 portal protein of herpes simplex virus type 1. *J Virol*, *78*(22), 12668-12671.
Tumbar, T., Sudlow, G., & Belmont, A. S. (1999). Large-scale chromatin unfolding and remodeling induced by VP16 acidic activation domain. *J Cell Biol*, *145*(7), 1341-1354.
Umene, K., & Nishimoto, T. (1996). Replication of herpes simplex virus type 1 DNA is inhibited in a temperature-sensitive mutant of BHK-21 cells lacking RCC1 (regulator of chromosome condensation) and virus DNA remains linear. *J Gen Virol*, *77(*Pt 9), 2261-2270.
Valyi-Nagy, T., Deshmane, S. L., Spivack, J. G., Steiner, I., Ace, C. I., Preston, C. M. et al. (1991). Investigation of herpes simplex virus type 1 (HSV-1) gene expression and DNA synthesis during the establishment of latent infection by an HSV-1 mutant, in1814, that does not replicate in mouse trigeminal ganglia. *J Gen Virol*, *72(*Pt 3), 641-649.
van Leeuwen, H., Okuwaki, M., Hong, R., Chakravarti, D., Nagata, K., & O'Hare, P. (2003). Herpes simplex virus type 1 tegument protein VP22 interacts with TAF-I proteins and inhibits nucleosome assembly but not regulation of histone acetylation by INHAT. *J Gen Virol*, *84*(Pt 9), 2501-2510.
Wadsworth, S., Jacob, R. J., & Roizman, B. (1975). Anatomy of herpes simplex virus DNA. II. Size, composition, and arrangement of inverted terminal repetitions. *J Virol*, *15*(6), 1487-1497.
Wang, Q. Y., Zhou, C., Johnson, K. E., Colgrove, R. C., Coen, D. M., & Knipe, D. M. (2005). Herpesviral latency-associated transcript gene promotes assembly of heterochromatin on viral lytic-gene promoters in latent infection. *Proc Natl Acad Sci U S A*, *102*(44), 16055-16059.
Whitfield, M. L., Zheng, L. X., Baldwin, A., Ohta, T., Hurt, M. M., & Marzluff, W. F. (2000). Stem-loop binding protein, the protein that

binds the 3' end of histone mRNA, is cell cycle regulated by both translational and posttranslational mechanisms. *Mol Cell Biol*, *20*(12), 4188-4198.
Whitlow, Z., & Kristie, T. M. (2009). Recruitment of the transcriptional coactivator HCF-1 to viral immediate-early promoters during initiation of reactivation from latency of herpes simplex virus type 1. *J Virol*, *83*(18), 9591-9595.
Wilkinson, D. E., & Weller, S. K. (2003). The role of DNA recombination in herpes simplex virus DNA replication. *IUBMB Life*, *55*(8), 451-458.
Wilkinson, D. E., & Weller, S. K. (2004). Recruitment of cellular recombination and repair proteins to sites of herpes simplex virus type 1 DNA replication is dependent on the composition of viral proteins within prereplicative sites and correlates with the induction of the DNA damage response. *J Virol*, *78*(9), 4783-4796.
Wilkinson, D. E., & Weller, S. K. (2005). Inhibition of the herpes simplex virus type 1 DNA polymerase induces hyperphosphorylation of replication protein A and its accumulation at S-phase-specific sites of DNA damage during infection. *J Virol*, *79*(11), 7162-7171.
Wilkinson, D. E., & Weller, S. K. (2006). Herpes simplex virus type I disrupts the ATR-dependent DNA-damage response during lytic infection. *J Cell Sci*, *119*(Pt 13), 2695-2703.
Wingfield, P. T., Stahl, S. J., Thomsen, D. R., Homa, F. L., Booy, F. P., Trus, B. L. et al. (1997). Hexon-only binding of VP26 reflects differences between the hexon and penton conformations of VP5, the major capsid protein of herpes simplex virus. *J Virol*, *71*(12), 8955-8961.
Woodcock, C. L., & Ghosh, R. P. (2010). Chromatin higher-order structure and dynamics. *Cold Spring Harb Perspect Biol*, *2*(5), a000596.
Wysocka, J., Myers, M. P., Laherty, C. D., Eisenman, R. N., & Herr, W. (2003). Human Sin3 deacetylase and trithorax-related Set1/Ash2 histone H3-K4 methyltransferase are tethered together selectively by the cell-proliferation factor HCF-1. *Genes Dev*, *17*(7), 896-911.
Yager, D. R., & Bachenheimer, S. L. (1988). Synthesis and metabolism of cellular transcripts in HSV-1 infected cells. *Virus Genes*, *1*(2), 135-148.
Yao, F., & Schaffer, P. A. (1994). Physical interaction between the herpes simplex virus type 1 immediate-early regulatory proteins ICP0 and ICP4. *J Virol*, *68*(12), 8158-8168.
Yao, F., & Schaffer, P. A. (1995). An activity specified by the osteosarcoma line U2OS can substitute functionally for ICP0, a major regulatory protein of herpes simplex virus type 1. *J Virol*, *69*(10), 6249-6258.
Yao, X. D., Matecic, M., & Elias, P. (1997). Direct repeats of the herpes simplex virus a sequence promote nonconservative homologous recombination that is not dependent on XPF/ERCC4. *J Virol*, *71*(9), 6842-6849.

Yoshida, M., Kijima, M., Akita, M., & Beppu, T. (1990). Potent and specific inhibition of mammalian histone deacetylase both in vivo and in vitro by trichostatin A. *J Biol Chem*, *265*(28), 17174-17179.

Zhang, Y., & McKnight, J. L. (1993). Herpes simplex virus type 1 UL46 and UL47 deletion mutants lack VP11 and VP12 or VP13 and VP14, respectively, and exhibit altered viral thymidine kinase expression. *J Virol*, *67*(3), 1482-1492.

Zhou, Z. H., Chen, D. H., Jakana, J., Rixon, F. J., & Chiu, W. (1999). Visualization of tegument-capsid interactions and DNA in intact herpes simplex virus type 1 virions. *J Virol*, *73*(4), 3210-3218.

Zhu, Z., Cai, W., & Schaffer, P. A. (1994). Cooperativity among herpes simplex virus type 1 immediate-early regulatory proteins: ICP4 and ICP27 affect the intracellular localization of ICP0. *J Virol*, *68*(5), 3027-3040.

Zhu, Z., DeLuca, N. A., & Schaffer, P. A. (1996). Overexpression of the herpes simplex virus type 1 immediate-early regulatory protein, ICP27, is responsible for the aberrant localization of ICP0 and mutant forms of ICP4 in ICP4 mutant virus-infected cells. *J Virol*, *70*(8), 5346-5356.

APPENDIX 1: MOBILIZATION OF LINKER HISTONE H1 AND CORE HISTONES H2A, H2B, H3.3, AND H4 DURING INFECTION OF N-33 CELLS WITH UV-INACTIVATED KOS.

This Appendix contains unpublished data.

A1.1 INTRODUCTION.

Analysis of H1.2 mobilization during HSV-1 infection has demonstrated that ICP4 or E protein expression is required to increase the pool of free H1.2 at later times after infection. During n12 infections of Vero cells, under conditions of high levels of IE protein expression in the absence of functional ICP4 and E proteins, the chromatin affinity of H1.2 was increased. Therefore, both the low- and high-affinity chromatin exchange of H1.2 were decreased. The decrease in H1.2 mobility during n12 infections was most surprising. H1.2 was still mobilized to a basal degree, in that its low- and high-affinity chromatin exchange was increased, under conditions of little to no HSV-1 transcription or protein expression. HSV-1 gene transcription is therefore not required to increase H1.2 chromatin exchange. The decrease in H1.2 chromatin exchange that occurred during n12 infections may be the result of high levels of IE protein expression, other than ICP4, mislocalization of IE proteins, or expression of a truncated ICP4 protein. Inhibition of H1.2 chromatin exchange as a result of high levels of IE protein (other than ICP4) expression is unlikely. If this were the case, then it would be unlikely that H1.2 chromatin exchange would be increased at early times

after infection, when IE protein expression is high. If ICP4 expression contributes to enhance H1.2 mobilization, then expression of a truncated form could act in a dominant negative manner to inhibit H1.2 mobility.

In the absence of functional ICP4 and E proteins, the pool of free H2B was not increased, and that of H3.3 was only increased by a marginal degree. This indicated that ICP4 or E proteins are required to increase the pool of free H2B and to increase the pool of free H3.3 by a large degree.

Taken together, the data discussed above suggest that ICP4 or E proteins contribute to aspects of linker and core histone mobilization. I first aimed to test the role of ICP4. One method to test this hypothesis would be to evaluate histone mobility in cells that transiently express ICP4. However, I did not have available an ICP4 expression vector and attempts to clone ICP4 into an expression vector were initially unsuccessful. Therefore, as a first step to evaluate the contribution of ICP4 expression on linker and core histone mobilization, I analyzed histone mobility during infection of n-33 cells with UV-inactivated KOS. n-33 cells express HSV-2 ICP4 under control of a VP16 responsive promoter (Smith & Schaffer, 1987). Thus VP16 within infecting virions induces HSV-2 ICP4 expression in the absence of expression of any HSV-1 proteins from the cross-linked infecting genomes.

A1.2 RESULTS.

A1.2.1 ICP4 is not expressed from input UV-inactivated HSV-1 strain KOS genomes.

I first evaluated whether I could detect ICP4 expression from the UV-inactivated genomes. To this end, ICP4 expression in n-33 cells infected with 5 PFU per cell HSV-1 strains KOS or UV-inactivated KOS was evaluated by Western-blot. ICP4 was detected in KOS infected cells at 2hpi (Figure A1.1). At 2h after infection with UV-inactivated KOS, however, the detected ICP4 expression was not above the background detected in mock-infected cells (Figure A1.1). At 4h, the level of ICP4 detected in n-33 cells infected with UV-inactivated KOS was still similar to that in mock-infected cells (Figure A1.1). Thus, ICP4 expressed from genes incorporated in the n-33 genome is not detectable by Western blot at 2 or 4h after infection with UV-inactivated HSV-1 strain KOS.

Unfortunately, induction of HSV-2 ICP4 expression from the expression vector recombined into n-33 genomes during infection with UV-inactivated KOS could not be assessed. Available ICP4 antibodies detect only HSV-1 ICP4 and do not cross-react with HSV-2 ICP4. It is presumed that ICP4 expression is induced because n-33 cells complement the replication of strains mutant in ICP4 (Smith & Schaffer, 1987). ICP4 is an essential HSV-1 protein. If ICP4 expression from the n-33 genome were not induced then replication of ICP4 mutant strains would not be complemented. However, the level of HSV-2 ICP4 expressed from the n-33 cellular genome is unknown.

A1.2.2 Infection of n-33 cells with UV-inactivated KOS is not sufficient to mobilize H1.2 above a basal level or to increase its free pool.

Infection of n-33 cells with 30 PFU per cell of UV-inactivated KOS failed to increase the fast chromatin exchange of H1.2. At 4 and 7h after infection, H1.2 T_{50} was not significantly altered from that of mock-infected cells (Figure A1.2 Panel A, Table A1.1). As with low-affinity H1.2 chromatin exchange, high-affinity H1.2 chromatin exchange was not significantly altered during infection of n-33 cells with UV-inactivated KOS. The H1.2 T_{90} at early and late times after infection was similar to that in mock-infected cells (Table A1.1). The H1.2 T_{50} and T_{90} had a tendency to be decreased at later times after infection. However, this tendency was also observed in Vero cells infected with UV-inactivated KOS. Thus, infection of n-33 cells with UV-inactivated KOS does not significantly alter the low- or high-affinity chromatin exchange rates of H1.2. ICP4 expression may not contribute to increase H1.2 chromatin exchange, or the induction of ICP4 expression during infection with UV-inactivated KOS may not have been to a high enough level to alter or detect changes in H1.2 chromatin exchange.

The pool of free H1.2 was marginally increased at early, but not late, times after infection of n-33 cells with 30 PFU per cell of UV-inactivated HSV-1 strain KOS. It was increased to 110 ± 3% at 4hpi ($P<0.05$, Student's T-test; 1-tail) (Figure A1.2 Panel B, Table A1.1). This increase in the pool of free H1.2 was not observed during infection of Vero cells with UV-inactivated KOS. Infection of n-33 cells with UV-

inactivated KOS, or potentially the induction of ICP4 expression from n-33 genomes, therefore alters the rates of H1.2 chromatin association and disassociation relative to each other to increase the pool of free H1.2 at early times after infection.

A1.2.3 The chromatin exchange of H3.3, but not H2A, H2B, or H4, is increased during infection of n-33 cells with UV-inactivated KOS.

The core histones H2A, H2B, H3.3, and H4 were differentially mobilized during infection of n-33 cells with UV-inactivated HSV-1 strain KOS. At 7h after infection with 30 PFU per cell of UV-inactivated KOS the chromatin exchange of H3.3 was increased, as demonstrated by faster fluorescence recovery after photobleaching (Figure A1.3). In contrast, the chromatin exchange of H2B tended to be slightly decreased, as demonstrated by marginally slower fluorescence recovery after photobleaching (Figure A1.3). The chromatin exchange of H2A and H4, were not substantially altered at later times after infection with 30 PFU per cell of UV-inactivated KOS (Figure A1.3).

The pools of free H2A, H2B, H3.3, and H4 were also differentially altered during infection of n-33 cells with UV-inactivated KOS. At 7h after infection with 30 PFU per cell of UV-inactivated KOS, the pool of free H3.3 was increased to 140 ± 7% ($P<001$, Student's T-test; 1-tail) (Figure A1.4, Table A1.3). The population of cells in which the pool of free H3.3 was increased by a large degree was 4-fold higher than would be expected in a normal population distribution (Table A1.3). Thus, infection of n-33 cells with UV-inactivated KOS altered the rates of H3.3

chromatin association and dissociation relative to each other such that the pool of free H3.3 was increased. The pool of free H3.3 was also increased, to 121 ± 5%, at later times after infection of Vero cells with 30 PFU per cell of UV-inactivated KOS ($P<0.01$, Student's T-test; 1-tail) (Figure A1.5, Table 5.3). This increase in free H3.3 also occurred throughout the population of infected cells. The pool of free H3.3 was increased by a large degree in 2.5 fold more cells than would be expected based on a normal population distribution (Table 5.3). The increase in free H3.3, however, was to a larger degree during UV-inactivated KOS infection of n-33 cells than Vero cells ($P<0.05$, Student's T-test; 1-tail) (Figure A1.5, Tables A1.3 and 5.3).

The pools of free H2A, H2B, and H4 were not significantly altered by infection with UV-inactivated KOS. At 7h after infection of n-33 cells with 30 PFU per cell of UV-inactivated KOS, the pools of free H2A and H2B tended to be slightly decreased, to 95 ± 4% and 95 ± 3%, respectively (Figure A1.4, Table A1.3). The pool of free H4, in contrast, tended to be slightly increased, to 104 ± 4% (Figure A1.4, Table A1.3).

The fast chromatin exchange of the core histones evaluated was differentially altered during UV-inactivated KOS infection of n-33 cells. The fast chromatin exchange rates of H2A and H4 were similar to that in mock-infected cells (Figure A1.6, Table A1.4). The fast chromatin exchange rates of H2B and H3.3, in contrast, were increased at 7h after infection of n-33 cells with 30 PFU per cell of UV-inactivated KOS (Figure A1.6, Table A1.4). The fast chromatin exchange rate of H2B was increased to 1.34 ± 0.14 fold and that of H3.3 was increased to 1.89 ±

0.25 fold ($P<0.05$ and $P<0.01$, respectively, Student's T-test; 1-tail) (Figure A1.6, Table A1.4). The rates of fast H2B and H3.3 chromatin exchange were increased by a large degree in a larger population of infected cells than would be expected in a normal population distribution, in 28 and 48% of infected cells, respectively (Table A1.4). Infection of n-33 cells with UV-inactivated KOS therefore alters the rates of H2B and H3.3 low-affinity chromatin exchange such that they are increased relative to mock-infected cells. The rate of H3.3 fast chromatin exchange also tended to be increased at 7h after infection of Vero cells with 30 PFU per cell of UV-inactivated KOS (to 1.31 ± 0.16 fold), however statistical significance was not achieved (Figure A1.7, Table 5.4). The increase in the rate of fast H3.3 chromatin exchange during infection with UV-inactivated KOS was greater in n-33 than in Vero cells ($P<0.05$, Student's T-test; 1-tail) (Figure A1.7, Tables A1.4 and 5.4).

A1.3 DISCUSSION.

Infection of n-33 cells with UV-inactivated KOS altered the chromatin exchange of H1.2 so that the pool of free H1.2 was marginally increased at early times after infection. This increase may be due to the induced expression of ICP4 from the n-33 genome, or alternatively, it may be a cellular response to infection with UV-inactivated KOS. However, the pool of free H1.2 was not increased at later times after infection of Vero cells with UV-inactivated KOS. n-33 cells are derived from Vero cells, it is therefore unlikely that a cellular response to infection with UV-inactivated KOS occurs in one cell line but not the other.

The chromatin exchange of H3.3 was altered during infection of n-33 cells with UV-inactivated KOS. At later times after infection, the rates of H3.3 chromatin association and dissociation were altered relative to each other such that the pool of free H3.3 was increased. Additionally, the rate of fast H3.3 chromatin exchange was increased. The pool of free H3.3, and the rate of fast H3.3 chromatin exchange, was also increased at later times after infection of Vero cells with UV-inactivated KOS. Thus, the increase in free H3.3 and the faster rate of H3.3 fast chromatin exchange may be cellular responses to infection with UV-inactivated KOS. If the UV-inactivation was not to a great enough degree, then HSV-1 gene transcription and expression of HSV-1 proteins could contribute to the mobilization of H3.3. However, ICP4 expression from the UV-inactivated KOS stock was not detected by western blot during n-33 infection. Infection of n-33 cells may have induced expression of ICP4 from the n-33 genome. The UV-inactivated stock used to infect Vero cells was different than that used to infect n-33 cells. ICP4 expression during infections with this stock was not analyzed.

These results are suggestive that ICP4 may contribute to histone mobilization, but are still highly inconclusive. The level of HSV-2 ICP4 induction from n-33 genomes during infection with UV-inactivated KOS is presently unknown. Moreover, if ICP4 does contribute to linker and core histone mobilization during infection, HSV-2 ICP4 may or may not be conserved in the regions that regulate histone mobility. Nonetheless, evaluation of linker and core histone mobilization in cells that transiently express HSV-1 ICP4 is likely still an avenue worth pursuing.

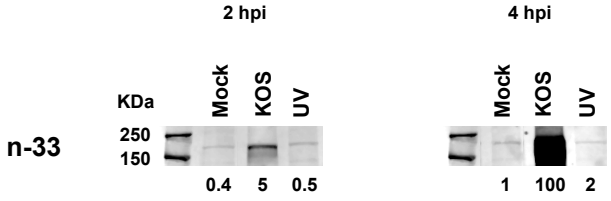

FIGURE A1.1: ICP4 expressed from UV-inactivated KOS genomes is not detected during infection of n-33 cells. HSV-1 ICP4 western blots of whole cell lysates prepared from infected n-33 cells. n-33 (**n-33**) cells were mock-infected or infected with 5 PFU per cell of HSV-1 strains KOS (**KOS**), or UV-inactivated KOS (**UV**) as indicated. At 2 (**2 hpi**) or 4 (**4hpi**) hours after infection, cells were harvested and whole cell lysates prepared. Proteins were resolved on 10% SDS-PAGE gels and transferred to PVDF membranes. Membranes were probed with monoclonal α-ICP4 antibody. Signal was detected using a Li-COR Biosciences Odyssey Infrared Imaging System and quantitated using Li-COR Odyssey version 3.0 software. Signal intensity is expressed as a percent of the signal detected for KOS at 4 hpi.

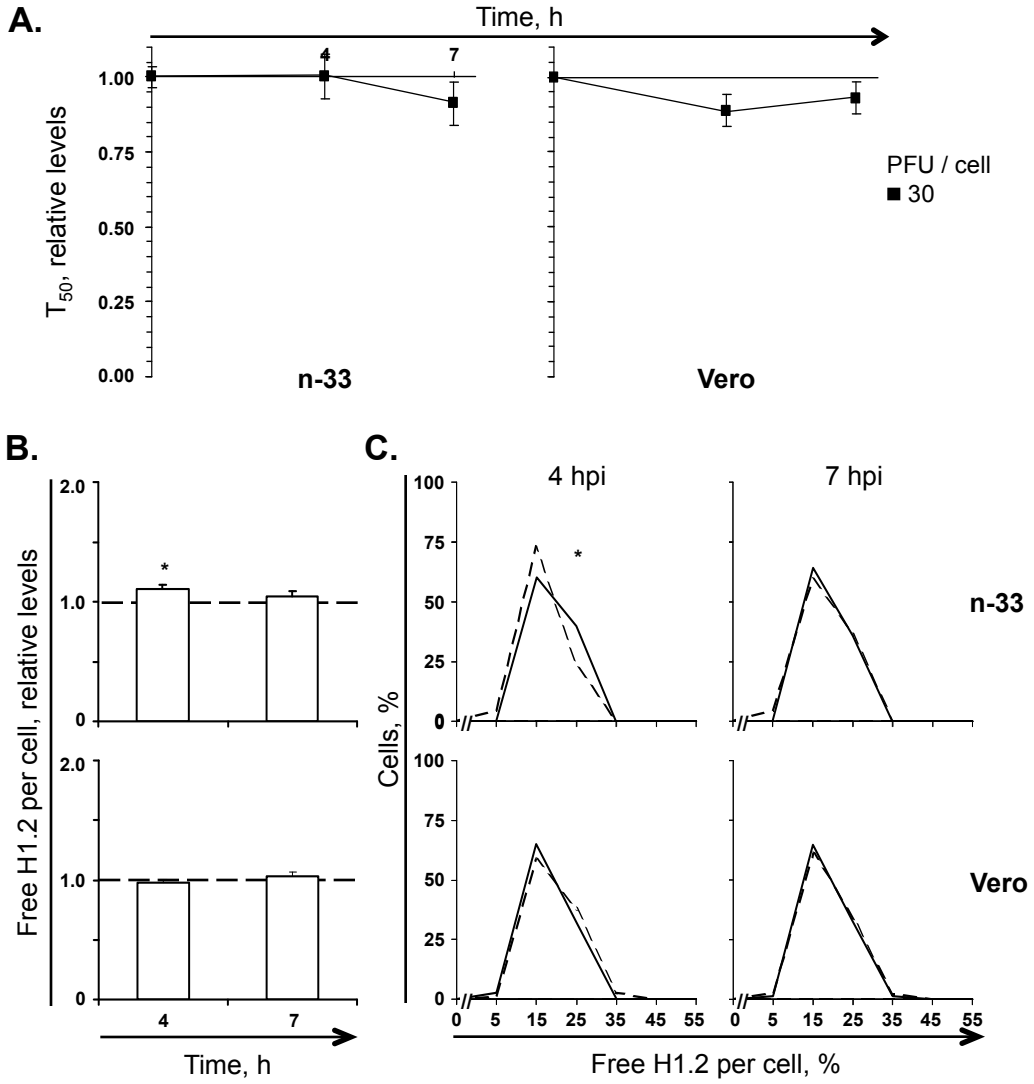

FIGURE A1.2: ICP4 does not enhance H1.2 mobilization but marginally increases the pool of free H1.2 at early times after infection. A) Line graphs representing the average H1.2 T_{50} in HSV-1-infected cells normalized to mock-infected cells and plotted against time postinfection. n-33 and Vero cells were transfected with plasmids expressing GFP-H1.2. Transfected cells were mock infected or infected with 30 PFU per cell (n-33) or 10 to 60 PFU per cell (Vero) of UV-inactivated HSV-1 strain KOS. Nuclear mobility of GFP-H1.2 was examined from 4 to 5 hpi (**4**) or 7 to 8 hpi (**7**) by FRAP. Error bars, SEM; n ≥ 22. **B)** Bar graphs representing the average percentage of free H1.2 in HSV-1 infected cells, evaluated by FRAP as described for Panel A, normalized to mock-infected cells and plotted against time postinfection. Error bars, SEM; n ≥ 22. **C)** Frequency distribution plots of the level of free H1.2 per individual cell evaluated by FRAP as described for Panel A. Dashed or solid lines, mock-infected or HSV-1 infected cells, respectively. *, P > 0.05. Vero data replotted from Figures 3.9 and 3.10 for comparison.

FIGURE A1.3: H3.3, but not H2A, H2B, or H4, is mobilized when only ICP4 is expressed. A) Line graphs representing the normalized fluorescence intensity of the photobleached nuclear region against time. n-33 cells were transfected with plasmids expressing GFP-H2A (**H2A**), GFP-H2B (**H2B**), GFP-H3.3 (**H3.3**), or GFP-H4 (**H4**). Transfected cells were mock-infected (**filled**) or infected with 30 (**open**) PFU per cell of UV inactivated HSV-1 strain KOS. Nuclear mobility of each GFP-core histone was evaluated from 7 to 8 hpi by FRAP. Error bars, SEM; n ≥ 20. Time plotted on a linear scale. **B)** Same data presented on a semi-logarithmic scale.

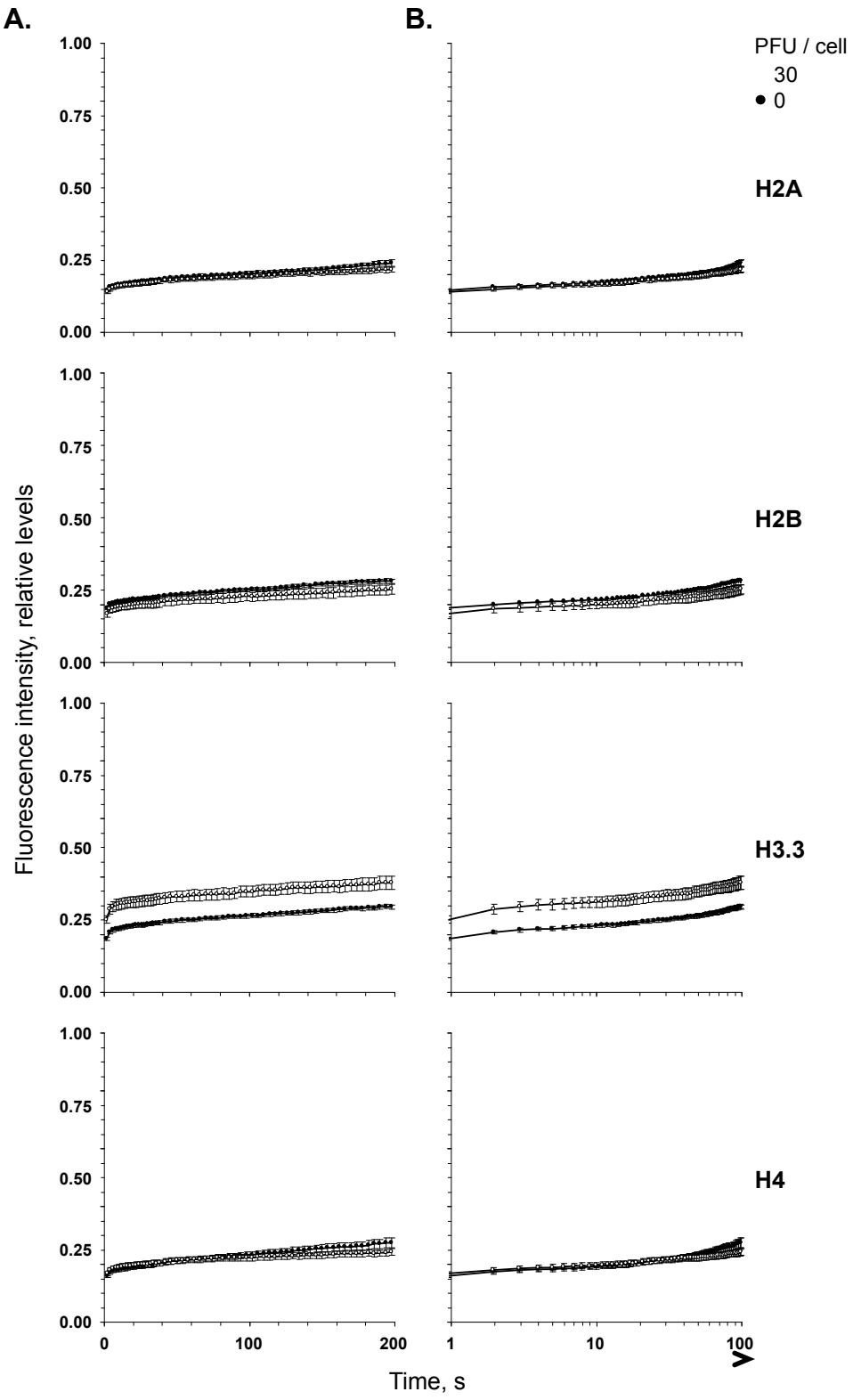
A.
B.
PFU / cell
30
0
H2A
H2B
H3.3
H4
Fluorescence intensity, relative levels
1.00
0.75
0.50
0.25
0.00
0
100
200
1
10
100
Time, s

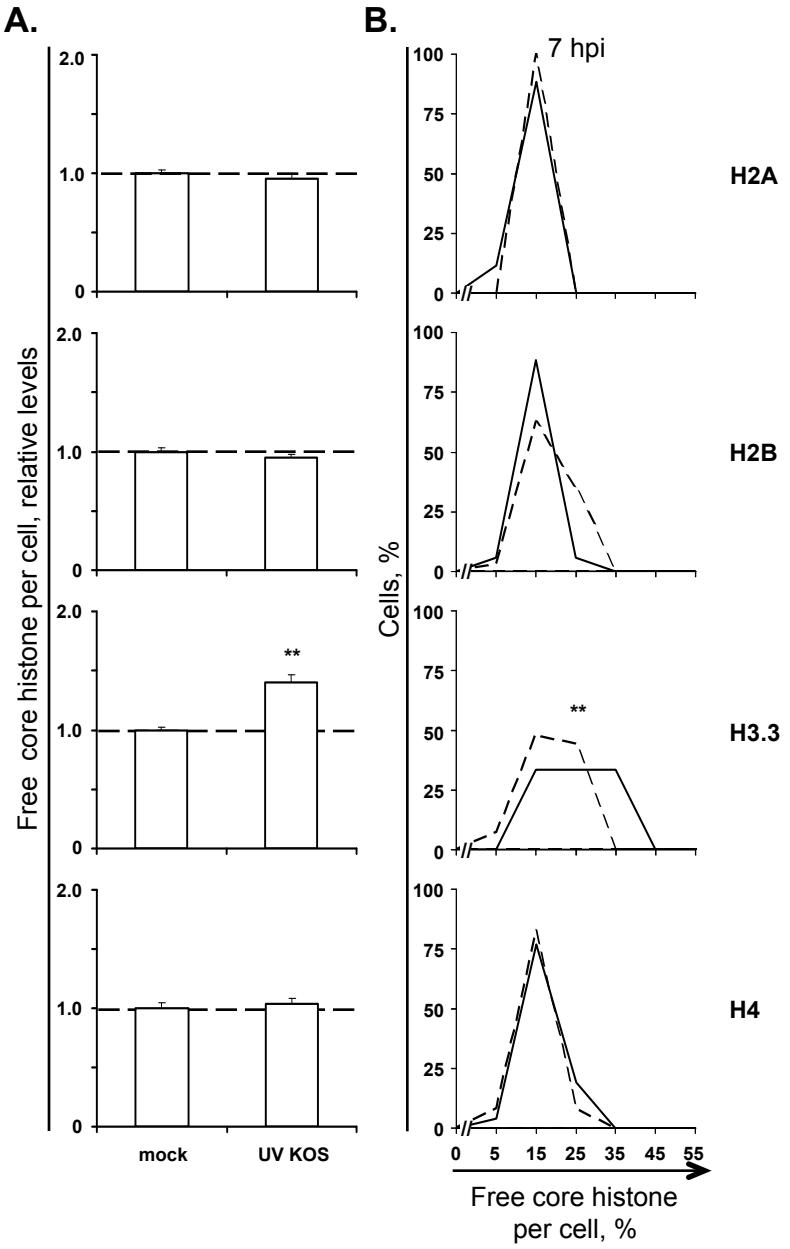

FIGURE A1.4: The pool of free H3.3, but not H2A, H2B, or H4, is increased when only ICP4 is expressed. A) Bar graphs representing the average percentage of free H2A, H2B, H3.3, and H4 in HSV-1 infected cells normalized to mock infected cells. n-33 cells were transfected with plasmids encoding GFP-H2A (**H2A**), GFP-H2B (**H2B**), GFP-H3.3 (**H3.3**), and GFP-H4 (**H4**). Transfected cells were mock-infected or infected with 30 PFU per cell of UV-inactivated HSV-1 strain KOS. Nuclear mobility of the core histones was evaluated from 7 to 8 hpi by FRAP. Error bars, SEM; n ≥ 21. **B)** Frequency distribution plots of the percentage of free core histone per individual cell evaluated by FRAP as described for Panel A. Dashed or solid lines, mock or HSV-1 infected cells, respectively. **, P <0.01.

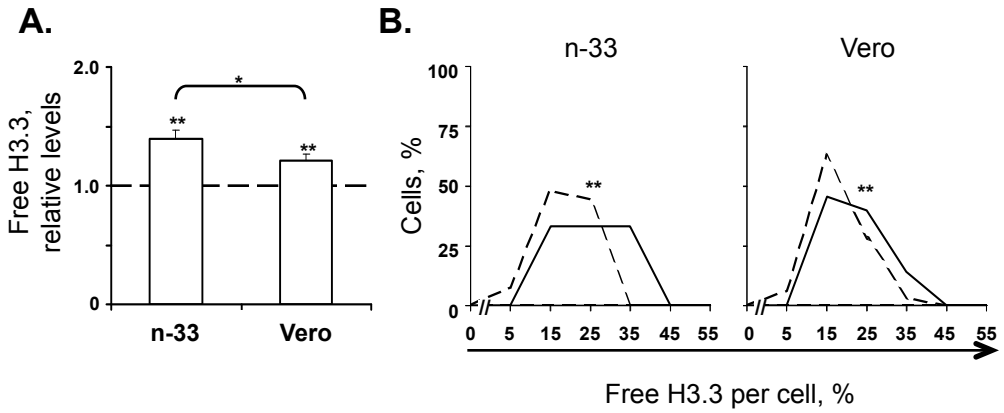

FIGURE A1.5: The pool of free H3.3 is increased to a greater degree in n-33 than in Vero cells during infection with UV-inactivated KOS. A) Bar graphs representing the average percentage of free H3.3 in HSV-1 infected cells normalized to mock-infected cells. n-33 and Vero cells were transfected with plasmids expressing GFP-H3.3. Transfected cells were mock infected or infected with 30 PFU per cell of UV-inactivated HSV-1 strain KOS. Nuclear mobility of GFP-H3.3 was examined from 7 to 8 hpi by FRAP. Error bars, SEM; n ≥ 32. **B)** Frequency distribution plots of the percentage of free H3.3 per individual cell evaluated by FRAP as described for Panel A. Dashed or solid lines, mock-infected or HSV-1 infected cells, respectively. *, $P > 0.05$; **, $P < 0.01$. n-33 data replotted from Figure A1.4 and Vero data replotted from Figures 5.5 for comparison.

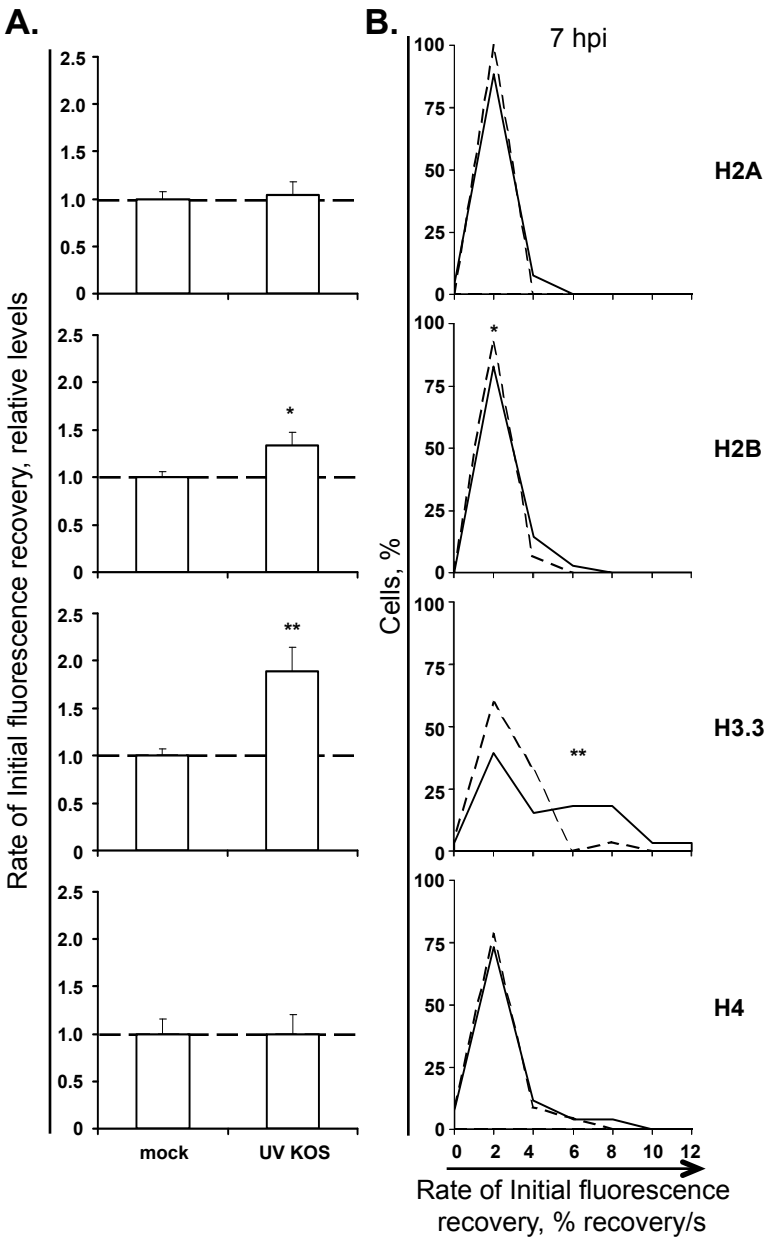

FIGURE A1.6: The rate of initial fluorescence recovery of H2B and H3.3, but not H2A or H4, is increased when only ICP4 is expressed. A) Bar graphs representing the average rate of initial fluorescence recovery after photobleaching in HSV-1 infected cells normalized to mock infected cells. n-33 cells were transfected with plasmids encoding GFP-H2A (**H2A**), GFP-H2B (**H2B**), GFP-H3.3 (**H3.3**), and GFP-H4 (**H4**). Transfected cells were mock-infected or infected with 30 PFU per cell of UV-inactivated HSV-1 strain KOS. Nuclear mobility of the core histones was evaluated from 7 to 8 hpi by FRAP. Error bars, SEM; n ≥ 21. **B)** Frequency distribution plots of the rate of initial fluorescence recovery after photobleaching per individual cell evaluated by FRAP as described for Panel A. Dashed or solid lines, mock or HSV-1 infected cells, respectively. *, $P < 0.05$; **, $P < 0.01$.

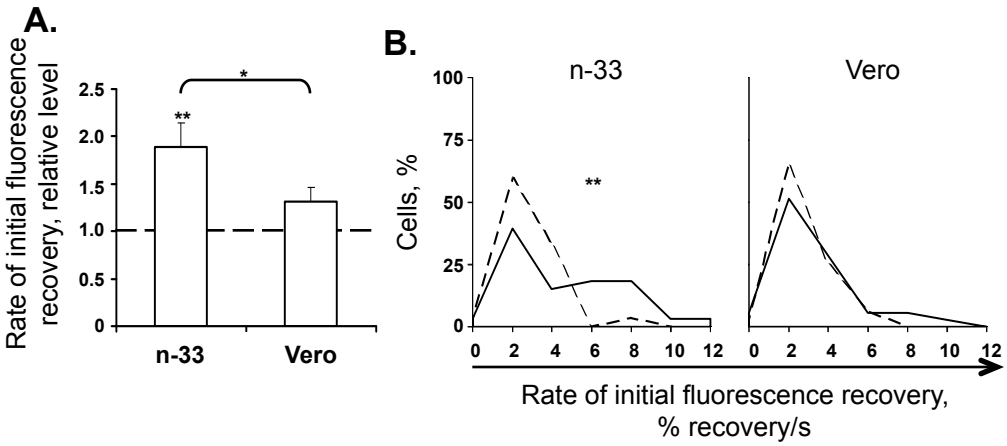

FIGURE A1.7: The rate of fluorescence recovery of H3.3 is greater in n-33 than in Vero cells during infection with UV-inactivated KOS. A) Bar graphs representing the average rate of fluorescence recovery after photobleaching of GFP-H3.3 in HSV-1 infected cells normalized to mock-infected cells. n-33 and Vero cells were transfected with plasmids expressing GFP-H3.3. Transfected cells were mock infected or infected with 30 PFU per cell of UV-inactivated HSV-1 strain KOS. Nuclear mobility of GFP-H3.3 was examined from 7 to 8 hpi by FRAP. Error bars, SEM; n ≥ 32. **B)** Frequency distribution plots of the rate of initial fluorescence recovery after photobleaching of GFP-H3.3 per individual cell evaluated by FRAP as described for Panel A. Dashed or solid lines, mock-infected or HSV-1 infected cells, respectively. *, $P > 0.05$; **, $P < 0.01$. n-33 data replotted from Figure A1.6 and Vero data replotted from Figure 5.6 for comparison.

Hour Post Infection	Virus Strain	PFU/ cell	T_{50} (avg ± SEM)		% Cells with high H1.2 mobilization, T_{50}[a]	T_{90} (avg ± SEM)		% Cells with high H1.2 mobilization, T_{50}[b]
			Absolute (s)	Relative (%)		Absolute (s)	Relative (%)	
4	-	-	16.2 ± 0.8	100 ± 3	14	132.6 ± 5.6	100 ± 4	19
	UV	30	15.1 ± 1.1	100 ± 7	28	131.3 ± 8.6	99 ± 7	22
7	-	-	17.1 ± 1.1	100 ± 4	11	143.7 ± 4.7	100 ± 3	10
	UV	30	14.1 ± 0.9	91 ± 7	16	120.5 ± 6.6	84 ± 6	7

TABLE A1.1: Mobilization of H1.2 in n-33 cells infected with UV-inactivated HSV-1 strain KOS.

[a] Percentage of cells in which the T_{50} was >1 SD lower than the average T_{50} in mock-infected cells.

[b] Percentage of cells in which the T_{90} was >1 SD lower than the average T_{90} in mock-infected cells.

Hour Post Infection	Virus Strain	PFU/ cell	Free H1.2 (avg ± SEM) Absolute	Free H1.2 (avg ± SEM) Relative	% Cells with large increase in free[a]
4	-	-	0.17 ± 0.01	1.00 ± 0.03	10
	UV	30	0.19 ± 0.01	1.10 ± 0.03	36
7	-	-	0.17 ± 0.01	1.00 ± 0.03	15
	UV	30	0.19 ± 0.01	1.05 ± 0.04	20

TABLE A1.2: Level of free H1.2 in n-33 cells infected with UV-inactivated HSV-1 strain KOS.

[a] Percentage of cells in which the level of free H1.2 was >1 SD above the average level in mock-infected cells.

			7hpi			
			Free histone		Free Pool,	
Histone	Virus	PFU/	(avg ± SEM)		% Cells with large:	
Variant	Strain	cell	Absolute	Relative	Increase[a]	Decrease[b]
H2A	-	-	0.15 ± 0.01	1.00 ± 0.03	13	7
	UV	30	0.14 ± 0.01	0.95 ± 0.04	12	27
H2B	-	-	0.19 ± 0.01	1.00 ± 0.03	13	11
	UV	30	0.17 ± 0.04	0.95 ± 0.03	9	26
H3.3	-	-	0.19 ± 0.01	1.00 ± 0.02	15	13
	UV	30	0.25 ± 0.01	1.40 ± 0.07	64	3
H4	-	-	0.16 ± 0.01	1.00 ± 0.05	9	13
	UV	30	0.17 ± 0.01	1.04 ± 0.04	23	8

TABLE A1.3: Levels of free H2A, H2B, H3.3, and H4 in n-33 cells infected with UV-inactivated HSV-1 strain KOS.

[a] Percentage of cells in which the level of free histone was >1 SD above the average level in mock-infected cells.

[b] Percentage of cells in which the level of free histone was >1 SD lower than the average level in mock-infected cells.

			7hpi			
			Rate of initial fluorescence recovery, %/s (avg ± SEM)		Fast chromatin exchange, % of cells	
Histone Variant	Virus Strain	PFU/ cell	Absolute	Relative	Increased [a]	Decreased [b]
H2A	-	-	1.03 ± 0.08	1.00 ± 0.08	17	13
	UV	30	1.07 ± 0.13	1.04 ± 0.14	27	31
H2B	-	-	1.18 ± 0.08	1.00 ± 0.06	13	16
	UV	30	1.54 ± 0.12	1.34 ± 0.14	28	3
H3.3	-	-	2.29 ± 0.18	1.00 ± 0.07	16	9
	UV	30	3.60 ± 0.50	1.89 ± 0.25	48	6
H4	-	-	1.28 ± 0.20	1.00 ± 0.16	9	9
	UV	30	1.29 ± 0.28	1.00 ± 0.21	15	12

TABLE A1.4: Rate of initial fluorescence recovery of H2A, H2B, H3.3, and H4 in n-33 cells infected with UV-inactivated HSV-1 strain KOS.

[a] Percentage of cells in which the rate of initial fluorescence recovery was >1 SD above the average rate of initial fluorescence recovery in mock-infected cells.

[b] Percentage of cells in which the rate of initial fluorescence recovery was >1 SD lower than the average rate of initial fluorescence recovery in mock-infected cells.